University of Strathclyde

National Centre for Prosthetics and Orthotics

Inter- and Intra Socket Shape and Volume Consistency Assessed Using Magnetic Resonance Imaging for Hands-on and Hands-off Casting of Amputee below Knee Sockets

By

Mohammad Reza Safari

A thesis presented in fulfilment of the requirement for the degree of Doctor of Philosophy

2010

This thesis is the result of the author's original research. It has been composed by the author and has not been previously submitted for examination which has led to the award of a degree.

Signed: **Date**

Dedication

For My parents,

sister

and

brothers

Acknowledgements

It is a pleasure to thank those who made this thesis possible

I would like to express my deep gratitude to:

My Scholarship sponsor from Iran Ministry of Health & Medical Education and the University of Social Welfare & Rehabilitation Sciences.

Dr Arjan Buis for his ongoing support, encouragement and constructive suggestions throughout the course of this thesis.

Professor Philip Rowe for his invaluable guidance and comments.

Dr Angus McFaydan for his generous statistical advice and assistance.

All staff in the National Centre for their support in particular Mr Jake Duers for his patience in making the experiments' rigs, Dr Kevin Murray for his valuable assistance in taking casts and Mrs Joyce Martin for taking photographs.

I also wish to thank staff of Institute of Neurological Science, Southern General Hospital to name a few, Professor Donald Hadley and Dr. Barrie Condon for their precious guidance and support, Mrs Maureen Waterston for taking the MRI scans, Dr David Brennan and Mr John McLean.

Finally I would like to thank my parents for their unconditional support, encouragement and giving me chance to prove and improve myself throughout my life.

Table of Contents

List of Figures

List of Tables

Abstract

Casting consistency has a great influence on the quality of socket fit. Investigations into the shape and volume of trans-tibial prosthetic sockets are complicated due to the difficulty in establishing an accurate reference grid. The use of Magnetic Resonance Imaging (MRI) presents a possible solution to this problem. However, the reliability of MRI in defining the stump/cast interface depends on the materials present not distorting the scanned image.

Volume and shape consistency of two casting concepts namely Hands-on and Hands-off were explored using MRI. Prior to this the validity and repeatability of MRI when using common socket material were also examined.

The results show that MRI is an accurate and repeatable method in dimensional measurement when using water doped with copper sulphate (CU). Controlled material tests were conducted and the experimental results indicate that the materials, silicone and wet Plaster of Paris (POP) doped with 1gr/l CU, do not distort or interfere with the scanned image. Moreover MRI accuracy was validated using controlled experiments using animal specimens with known volume and surface areas wrapped in POP and silicon liner. No significant errors were indicated.

Residual limbs were cast of twelve persons with a unilateral below the knee amputation and scanned twice for each casting concept. Subsequently, all four volume images of an amputee were registered to a common coordinate system using the tibia.

The results show that both casting methods have intra cast volume consistency and there is no significant volume difference between two methods. Additionally, inter and intra cast mean volume difference was not clinically significant based on the volume of one sock criteria. Furthermore neither Hands-off method nor Hands-on method results in a consistent residual limb shape as the coefficient of variation of intra cast shape differences were high. Although the resultant shape of the residual limb in Hands-off method was not repeatable, the intra cast shape difference was not

clinically significant. However, the Hands-on shape difference is not clinically significant but equal to the maximum acceptable limit for a poor socket fit.

1 Introduction

1.1 Rationale of Study

The ultimate goal for prosthesis replacement is the functional and cosmetic restoration of the lost limb. The shape of the socket, prosthetic alignment and simulation of the body joints are key factors influencing gait symmetry and comfort of the amputee. The socket is the only part of a prosthesis that is in close contact with the residual limb. During ambulation, the generated forces and moments are transmitted from the socket, through the soft tissue, into the weight bearing structure - the skeleton.

The quality of socket fit is dependent on the connection (coupling) stiffness of that coupling to minimise undesirable longitudinal and transverse movement between prosthesis and skeleton. Supporting body weight through a prosthetic socket will result in the generation of normal and shear stresses within the residual limb during static and dynamic situations. Considering the viscoelastic behaviour of the soft tissue, Klasson (Klasson, 1994, Klasson and Buis, 2006) developed the concept of 'surface matching' and 'volume matching' to cope with those stresses. Surface matching is "the generation of the surface which develops a uniform pressure distribution over bony areas at full load". According to the volume matching concept if the volume of the residual limb can be contained in a socket of the same volume with a shape to produce even pressure distribution, the hydrostatic weight bearing can be made if the volume of the tissue under pressure is constant. Shape capturing technique is fundamental to achieve the desired surface matching and volume matching situations.

Currently there are three shape capturing techniques in use; computer aided socket design (CASD), hand casting (Hands-on), and pressure casting (Hands-off). The so called "Hands-on" concept was developed based on residual limb anatomical features and the biomechanical principle involved in gait. In this design loads are mostly transferred to specific areas of the residual limb through a specially shaped socket. As opposed to the Hands-on design, the "Hands-off" socket uniformly

transfers loads over the entire residual limb surface based on the hydrostatic principle.

Socket manufacturing, prosthetic alignment and clinical evaluation are predominantly based on the prosthetist's skill and experience and input from an amputee. Evaluation of shape capturing consistency is important to examine the effect of variability of the socket fabrication process, such as rectification on final outcome. Consistent socket manufacturing could also increase an amputee's quality of life.

A reliable reference grid is required for inter- and intra- socket shape comparison. The tibia, the only rigid entity within the residual limb, can be used for this purpose using MRI scans (Buis et al., 2006). MRI is a high resolution and non-ionising imaging technique which can provide a clear distinction between tissues, however; the common drawback of MRI is chemical shift artefact resulting from chemical property of the tissues within a magnetic field.

The objectives of this study are firstly to validate the MRI technology when commonly used socket materials are used and secondly to investigate inter and intra casting consistency of two different transtibial socket concepts namely, Hands-on and Hands-off, using MRI reference grid.

1.2 Socket Fit

The soft tissue of the residual limb is not physiologically designed to tolerate forces and moments applied by the socket in static and dynamic conditions so that the amputee's comfort, to a great extent, depends on how the socket fits the residual limb. Socket fit is therefore the most important characteristic of a prosthesis indicated by amputees (Legro et al., 1999, Hoaglund et al., 1983, Hagberg et al., 2004).

It is common for amputees to develop residual limb skin problems. Load conditions exceeding the 'tissue load tolerance threshold' could cause discomfort and pain in the residual limb and even a reluctance to wear the prosthesis (Dudek et al., 2005,

Lyon et al., 2000). Reswick and Rogers (1978), Figure 1-1, documented the relationship between the maximum amounts of static pressure that soft tissue could tolerate for a certain period of time. Although this study reported on a continued, static, loading condition, it provides a basis for clinical management. Apart from the static stress, dynamic normal and shear stresses could result in skin breakdown (Sanders et al., 1995). Therefore, a proper socket design is an important factor in establishing a near normal gait and improving the life quality of the amputee.

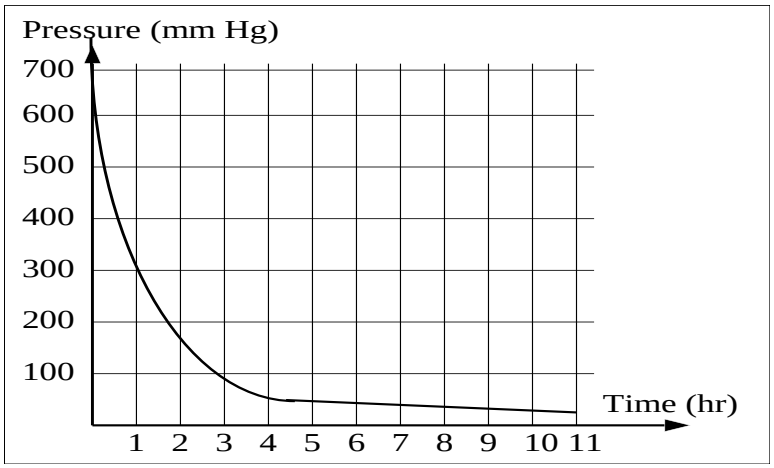

Figure 1-1: Reswick and Rogers, safe pressure diagram

Between April 2006 and March 2007, a total of 4957 new referrals to prosthetics service centres in the UK were reported, of which 53 percent was at the trans-tibial (below knee) level. According to the Amputee Statistical Report for the UK, vascular disease accounts for 74 percent, 55% of which are diabetes mellitus (NASDAB, 2009). Peripheral Vascular disease (PVD) is the narrowing or blockage of arteries mostly due to arthrosclerosis results in reduced blood supply, poor sensation and poor tissue quality which brings its challenge to prosthetic fitting. In a study of 179 amputees (23% dysvascular including diabetes and 73% traumatic) it was found that pain was associated with weight bearing most often in dysvascular amputees in which three quarters of the dysvascular below the knee amputees had pain while

walking (Hoaglund et al., 1983). In comparison with traumatic amputees, this population engaged in less daily walking and recreation activities and made more use of assistive devices for daily activities.

Dudek et al. (2005) conducted a retrospective study to investigate the frequency of and the factors related to residual limb skin problems in a cohort of 745 lower limb amputees. Besides the finding that half of the amputees had at least one skin problem, it was described that the most common skin problem was ulceration of the skin, followed by irritation, cysts and callus formation, all of which were most likely related to pressure on the skin. It was also suggested that the activity level of the amputees is related to the factors which are independently associated with the existence of skin problems. Legro et al. (1998) reported that the demand on the body-device interface pressure distribution is more critical for prosthetic users in a high activity life style. Therefore, the quality of fit of a socket is becoming more important to improve comfort in active amputees (Legro et al., 1998).

Another variable in the complexity of socket fit relates to the fact that volume fluctuation of the residual limb may negatively influence the quality of socket fit. A prosthetic socket that is too loose might cause piston movement between the prosthesis and the residual limb, resulting in skin friction and irritation. Additionally, longitudinal movement could compromise the skin over bony prominence extra stress (Yiğiter et al., 2002). A socket that is too tight might lead to difficulties in donning and might result in compromised circulation and associated numbness.

The residual limb is subject to both short and long term volume change. Board et al. (2001) measured the variations in residual limb volume in a sample size (n=11) after 30 minutes of treadmill walking, using a water displacement method to measure changes. It was noted that an average of 6.5% (52ml) in volume reduction was found when the subjects used a “normal” total surface bearing socket. Furthermore, an average of 3.7% (30ml) increase in volume of the residual limb was found when there was an active vacuum applied between the socket and the liner. They believe that the short term volume changes may happen because fluid is expelled from the residual limb.

In another study, in measuring volume change of the residual limb after doffing the prosthesis, researchers found a volume increase ranged from 2.4% to 10.9% (Med 6.0% ± 3.6) in six amputees (Zachariah et al., 2004). They also found -2.0% to 12.6% volume changes after a two week period revealing the possibility of long term residual limb volume change. Furthermore, a rapid reduction of residual limb volume occurred post-amputation. This was followed by a slow reduction (Lilja and Oberg, 1997). Early definitive prosthesis fitting may not be economically reasonable during this time because of the huge volume lost resulting in socket misfit. However, early prosthetic management would result in better rehabilitation facilitating a more independent life.

There is little quantitative information about the quality of socket fit. Measurement of the external surface counter, geometric assessment of internal structures of the residual limb and relating this information to the socket shape can provide better understanding of available socket fit and designs (Zheng et al., 2001).

1.3 Socket Design, Manufacturing and Concept

A prosthetic socket is designed to fit the skeletal structures, providing stability (coupling stiffness) and load transfer during static and dynamic conditions, whilst providing an appropriate suspension of the prosthesis during the swing phase. An understanding of the mechanical behaviour of soft tissue under load is required to understand ideal pressure distribution over the residual limb without exceeding the tissue tolerance limit while maintaining the socket-residual limb coupling stiffness.

1.3.1 Basic Principles

To enable standing and walking in a normal human, the ground reaction forces are transmitted via the sole of the feet to the weight bearing structure - the skeleton. If a total restoration of a lost limb is required, those forces have to be transferred to the skeletal structure as in a normal limb. However, the socket is attached to the residual limb in an abnormal way via connection to soft tissue and hence transfers forces through soft tissue to internal skeletal structure. Therefore, the quality of these load transfers from soft tissue to skeleton depends on the biological adaptability of soft

tissue to the prosthetic socket in a comfortable manner. The quality of the socket-limb coupling is related to the stiffness of that coupling, with the aim to minimise longitudinal and transverse movement between prosthesis and skeleton. If the stiffness with no tissue damage is maintained, the pressure symptoms on the residual limb will decrease and proprioception might increase resulting in more comfort to the amputee.

Soft tissue exhibits similarities in behaviour to that of viscoelastic material that has both viscosity and elasticity components. Elastic materials absorb energy while under load and release it after removing the applied load. The behaviour of viscous materials depends on both duration and speed of the applied load, deforming more under slow and long period loadings. There are two main forces generated in the soft tissue under load by socket including pressure and shear forces. In the following sections tissue behaviours and viscoelasticity are discussed considering these two types of stresses.

1.3.1.1 Pressure and Shear Stresses

For elastic material under load there is a relationship between stress (force per unit area) and strain (deformation in relation to the thickness). The higher the amount of stress, the more deformation or strain will occur. This rule with regard to socket-limb coupling indicates that the ideal pressure distribution over the residual limb is a uniform application of load over entire area to avoid local peak pressures. The concept of "surface matching" was developed by Klasson (1994) to address this rule in elastic perpendicular pressure distribution. Surface matching is "the generation of the surface which develops a uniform pressure distribution over bony areas at full load". There is concern as to the suitability of this theory. The stress-strain relationship is more complicated in soft tissues. The pressure in elastic materials depends on the thickness of the material where higher pressure exists when tissue thickness decreases. Varying thickness in several areas of the residual limb makes it complicated to define desirable or an even pressure over the entire surface. This would be more complicated where the tissue stiffness gradient exists over the residual limb soft tissue resulting in different elastic moduli, varying stress-strain

relationships, in different areas. Moreover the surface matching is true in a static model and oversimplification to get to a dynamic situation.

The force applied to the residual limb is not a purely perpendicular to the skin surface. The applied ground reaction force/body weight is almost in line with the longitudinal axis of the limb. Considering the residual limb as a cone this force will have two components; one perpendicular to and the other parallel with the surface of the cone: Figure 1-2.

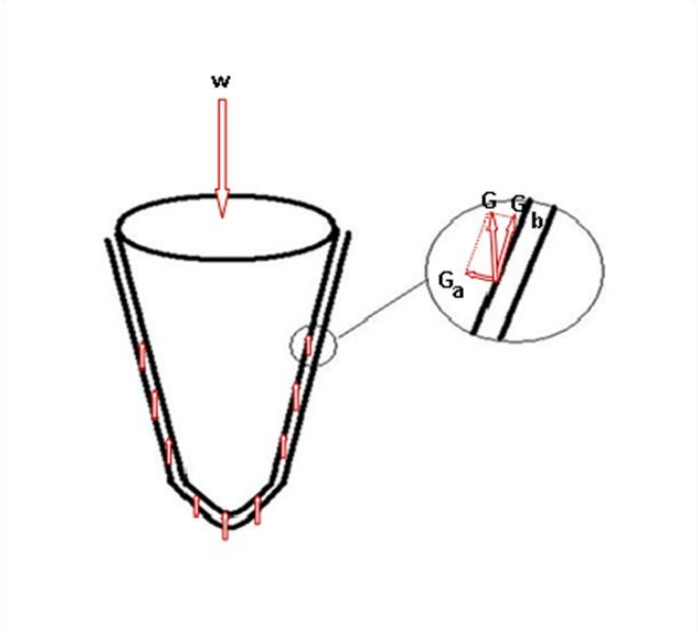

Figure 1-2: Applied body force (W) on residual limb has two components - parallel (G_b) and perpendicular (G_a) - to the skin surface.

The parallel force results in shear force within the soft tissue. These shear forces, in certain conditions, plus the perpendicular component of the vertical weight load help to transfer the weight force to the bone. Furthermore, shear force builds up if the pressure gradients, difference in perpendicular forces at adjacent areas, exist. Like

perpendicular pressure shear stresses results in skin breakdown and should be avoided.

The soft tissue responds to the shear stress as a fibre composite with a fluid viscose matrix. Pulled fibres within the soft tissue stretch and reorient themselves to counteract the shear force. In the presence of the shear stress the matrix flows and stops at the point where the force binding the matrix to fibres resists the effect of shear pressure, denoting hydrostatic pressure. In an ideal hydrostatic medium, no shear stress exists (Klasson and Buis, 2006). If the volume of the residual limb can be contained in a socket of the same volume with a shape to produce even pressure distribution, the hydrostatic weight bearing can be made if the volume of the tissue under pressure is constant. This is the concept of "volume matching" developed by Klasson.

1.3.2 Shape Capturing

Currently there are three shape capturing techniques in clinical use; computer aided socket design (CASD), hand casting (Hands-on), and pressure casting (Hands-off). These are discussed in the following sections. The Hands-on and Hands-off techniques were developed based on the principles of relating socket designs. Therefore, the principle of socket designs and corresponding shape capturing techniques are explained in the following sections.

1.3.2.1 Patella Tendon Bearing (PTB), Hands-on

Early trans-tibial prosthetic sockets had some degrees of weight bearing. Because of an inadequate design, the prosthetic socket was not capable of full body weight bearing. To address this, a thigh corset was attached to the prosthesis to transfer some of the load to the proximal part of the limb, the thigh muscles. This type of prosthesis was cumbersome and furthermore, due to the lack of total contact and the tight fastening, the thigh corset could result in chronic distal oedema and atrophy of thigh musculature (Kapp and Fergason, 2004).

It was argued that the pressure around the residual limb should be distributed according the pressure tolerant threshold of the residual limb based on the

biomechanical principle of the socket and residual limb. As a result the Patellar Tendon Bearing (PTB) socket was first introduced in the 1950s by Radcliffe. (Radcliffe and Foort, 1961). Based on PTB principles the residual limb is loaded proportionally to the load tolerance of the underlying soft tissue and bony areas.

The socket loaded the residual limb on more tolerant areas whilst relieving pressure from sensitive structures. The term 'patella tendon bearing' does not mean that the patella tendon is the only part of the residual limb tolerating the load. The anterior compartment, medial tibia flare, shaft of fibula, and posterior compartment are also involved in the load transfer. These areas were indented in the socket to allow the application of pressure while in other areas, such as anterior distal of tibia, distal of fibula, crest of tibia, and peroneal and condyles of femur, relief is provided. The medial and lateral socket walls extend proximally to the level of adductor tubercle of the femur to provide medio-lateral stability to both prosthesis and the knee and also increase the rotational stability of the socket. The posterior wall provides the anterior direction force to keep the patella tendon on the socket bar and cut proximally so that it does not apply pressure on hamstring tendons. The anterior wall ends proximally to the distance of one third of the patella.

The common practice for PTB socket fabrication is to make the socket using a plaster impression taken from an amputee's residual limb. In this technique, layers of wet Plaster of Paris (POP) bandage are wrapped around the residual limb. While still wet, prosthetist indents the POP at mid-patellar tendon and popliteal areas using a specific position of the hands and fingers until the POP is cured. Here it is called "Hands-on" casting because of the prosthetist's use of hands to pre-shape the cast. This technique requires the prosthetist's skill and dexterity to palpate and indent the underlying soft tissue, therefore, resulting in a lack of inter- and intra-prosthetist reproducibility of the captured shape of the residual limb. Then a positive plaster mould is produced. The Plaster is subsequently added to the positive mould in areas where pressure relief is required and removed from other areas to increase pressure.

1.3.2.2 Pressure Cast Socket, Hands-off

It was proposed by the total surface bearing (TBS) theory that all parts of the residual limb can bear loads to some extent so that the pressure is distributed more equally around the residual limb than the PTB designs. (Pearson et al., 1973) The TBS concept relies more on the socket-residual limb interface materials which have deformable characteristics under load. These materials include polyurethane, mineral oil gels and silicon.

The hydro-cast method was used to produce a socket to resolve some inconsistency resulting from manual dexterity of the prosthetist (Murdoch, 1968). In this method, the residual limb, while wrapped with POP, is placed in a tank of water. A membrane separates the residual limb and the water. The amputee puts weight on the residual limb and at the same time pressure is applied by water to hold the limb in place. This gives the surface and volume matching results. The concept of hydro-casting is based on Pascal's principle of fluids which states pressure applied to an enclosed fluid is transmitted evenly to every part of the fluid, as well as to the walls of the container. Equal pressure is applied as a plaster cast is obtained and socket is produced from a mould that has very little modification. Compared to the Hands-on concept, the socket does not have any identifying specific weight bearing areas. The pressure on one part of the residual limb is equally distributed over the entire residual limb.

In 1990s the Icelandic Roll on Suction Socket (ICEROSS) casting, pressure casting, system which was based on uniform pressure distribution was introduced (Kristinsson, 1993). The ICEROSS method uses air to produce equal pressure around the residual limb during casting. However, the efficiency of the hydrostatic concept depends on use of silicon liners between the socket and the residual limb. The silicon liner is pulled over the residual limb and then a plaster bandage is wrapped. A uniformly adjustable pressure is then applied over the wet POP using a pneumatic pressure bladder while it is cured. As a result the elongation of soft tissue occurs resulting in more surface matching and volume matching. The term “Hands-off” is used because no hand dexterity is required for the shape capturing process. The socket is fabricated over a positive plaster mould with very little modification.

1.3.2.3 Computer Aided Socket Design (CASD)

CASD is a way of obtaining numerical surface information of the residual limb to be used in socket fabrication. There are different ways of obtaining this computerised information. Optical scanning, including laser scanning, is the most commonly used method in residual limb scanning with good shape capturing information. Sometimes, either the interior of the negative plaster cast or surface of the plaster model is scanned using an optical scanner or a mechanical digitiser. Using a mechanical digitiser in probing the surface of the residual limb distorts the soft tissue and because of the long scanning time, errors may result due to residual limb movements. Additionally, ultra sound has been used for shape capturing. In this method there is a concern regarding the prob-socket coupling.

The CASD offers a way to do what prosthetists have been doing manually in a computerised way. The digital shape data is then saved into the computer and the prosthetist uses the computer programme to rectify the shape for the final socket fit. In some cases a plaster mould is made of the residual limb data and then a prosthetist rectifies the cast in a plaster room in the traditional way. The shape of the residual limb is taken when the shape is not deformed under load. Prosthetists are not interested only in the shape of an unloaded residual limb but are also interested in a shape which meets the fitting criteria to get to volume matching and surface matching conditions. Furthermore, the residual limb shape sensing is important only if the soft tissue stress-strain information can be incorporated into residual limb geometric data to get to the desirable socket fit. It has been stated that the CASD will save time in the socket manufacturing. However, this may not always be the case as the socket requires trial and error checking to get to the final shape.

One may consider that the repeatability, reliability and accuracy are an advantage of the CASD due to the nature of the computerised approach. Errors may occur in the shape capturing process and/or socket manufacturing from the data. Reliability, repeatability and accuracy of two common CASD shape techniques (contact method; Tracer CAD and noncontact method; T-ring) were evaluated using three models and compared to the conventional plaster shape capturing method (McGarry, 2009).

Reliability of Tracer CAD and T-ring was high (ICC>0.999 and ICC>0.984 respectively). Both CAS systems showed an inaccuracy and lack of repeatability especially at the distal deformable part of the residual limb models. Sanders et al. compared the manufactured socket shape and CAD data files shapes of three different amputees' sockets fabricated by ten different central fabrication centres in the United States with the aim of identifying differences in volume and cross sections of the sockets. The results showed variability in socket shape made by central fabrication centres. Some companies made consistently good sockets, some companies made consistently poor sockets and some companies sometimes made good sockets (Sanders et al., 2007).

1.3.3 Suspension

Suspension refers to the ability of holding the prosthesis over the limb through the gait. Secure suspension offers an amputee the confidence in ambulation and less skin friction and irritation. The common below the knee prosthetic suspensions includes Supracondylar Cuff, External Elastic Sleeve, Supracondylar, Side Joints and Corset, and Silicone Suspension (Edwards, 2000). The first four suspension systems are used in PTB (Hands-on) socket and the Silicon Suspension is inherent to the Hands-off socket type because of the use of silicon liners between the hard socket and the residual limb. The Supracondylar Cuff suspension is achieved using a cuff attached to the proximal part of the socket and tightens above the patella. The External Elastic Sleeve is commonly made of latex rubber, neoprene or silicone and covers the proximal aspect of the prosthesis and is rolled over the thigh region of the amputee's thigh and because of high friction and the coefficiency of the material provides suspension. The Supracondylar suspension is an extension of the medial and lateral brims of the socket over the femur condyls. Sometimes the anterior wall is extended above the patella to provide more suspension and knee stability, called Supracondylar-Suprapatellar suspension. The last category in hand-on suspension systems is the use of thigh corset attached to the prosthesis through side joints.

Writa et.al (1990), when comparing the effects of seven different transtibial suspensions used for Hands-on socket, used axial movement detectors and knee

electrogoniometer in twenty trans-tibial amputees. Ten amputees had conical shape residual limb and other ten cylindrical shape residual limb. They found that there is a harmonic ratio among suspension systems relating to residual limb length and shape in which the amounts of axial movement were higher for people with long cylindrical residual limbs. Axial movement was not related to speed of walking. No silicon suspension system was used and the amount of axial movement of those suspension systems used in the study was 1.91 on average (min = 0.6cm and max = 3.1cm) in which the minimum amount of axial movement was related to the Elastic Sleeve (Wirta et al., 1990).

Polyethylene foam (Pe-lite) is usually used as an interface material between the external hard socket and the residual limb, whereas in the Hands-off socket a silicone liner is worn. Often a pin-lock mechanism at the bottom of the liner is used to secure the silicone liner to the prosthesis. Because of high friction coefficient between the silicone liner and the skin, the silicone adheres to skin and minimises the amount of friction. In addition, in the Hands-off concept the residual limb soft tissue is elongated distally resulting in less piston movement of tissue (Kristinsson, 1993).

1.3.4 PTB versus Pressure Casting

There is a lack of evidence supporting both Hands-on and Hands-off socket concepts. Kristinsson believed that the PTB principle of load transfer is “in the most cases both ineffective and uncomfortable” (Kristinsson, 1993). According to him the hydrostatic principle for load transfer is the most effective socket, in which force applied to a part of the enclosed system is transferred equally to all parts of the system. Goh believes that the hydrostatic principle is based on fluid at rest while the fluid in the residual limb is not at rest (Goh et al., 2004) and Fergason and Smith reason that it is based on fluid in a closed system, whereas the limb is not (Fergason and Smith, 1999). They mentioned that the PTB socket designed is based on the dynamic forces produced in walking and since it is assumed that in a hydrostatic socket these dynamic forces are transferred to the other tissues according to fluid principles; they believe a hybrid socket might be an answer to achieve a better socket fit. Dumbleton et al. compared the dynamic interface pressure distribution of pressure in twenty four

patients wearing Hands-off sockets, and twenty four amputees wearing Hands-on sockets using a Tekscan F-scan socket transducer (Dumbleton et al., 2009). Their results show that there was no significant difference between the two concepts in the dynamic mean interface pressure distribution during gait for any regions of the prosthetic socket despite different casting concepts, but the Hands-off concept resulted in less variability in pressure distribution. This suggests that the Hands-off concept leads to a more consistent socket fit in amputees. However, there was a significant difference in the magnitude of the pressure between the two groups in which the higher pressure was recorded for the Hands-off concept despite the uniform pressure distribution of the Hands-off concept. In spite of this the pressure gradients were steeper for the Hands-on concept indicating more shear stress in the soft tissue.

In considering the hydrostatic behaviour of enclosed soft tissue, one should consider that the soft tissue within the residual limb is not a simple liquid medium. Firstly, it is comprised of tendons, ligaments, fascia, fibrous tissue, fat, synovial membranes, muscles, nerves and blood vessels which behave differently to applied load considering the fact that loads choose the stiffest path. Secondly, the fibrous tissues, like collagen fibres, behave differently in different directions. Another issue to consider is viscosity behaviour of the soft tissue which denotes that its response to load depends on both the magnitude and the timing of the load. Gait is a cycle of short time loading and unloading of the soft tissue within the socket. Lastly, blood and extracellular fluids flow from the tissue, and when loaded is more complex than a simple leaking of the fluid in a hydrostatic medium. Therefore, the soft tissue is a rather quasi-hydrostatic medium than a purely hydrostatic. The viscoelastisity and flow property of silicone material under load adds to the volume matching and surface matching of the Hands-off socket (Covey et al., 2000, Kristinsson, 1993). In general, Pe-lite foam is used in the PTB prosthesis. In a randomised control trial Selles et al. found no statistically significant difference between ICEX and PTB with silicon liner in patient satisfaction, gait characteristics, and activity of daily life after three months of prosthesis use (Selles et al., 2005) . They stated that the lack of

difference between two groups may be related to the use of the silicone liner in the PTB group.

Lack of evidence in supporting the two Hands-on and Hands-off concepts also results in a lack of consensus on absolute indication of these sockets to amputees. In a questionnaire survey sent to thirty seven doctors and thirty five prosthetists known to have experience with the ICEROSS, McCurdie et al. (1997) found that there was not a consensus on absolute/primary indication for ICEROSS for amputees. Shear sensitive skin/split skin graft, pistoning, patient unsuccessful with Supracondylar or Cuff suspension, insufficient suspension because of type or level of activity were given the grade between absolute to partial indication for ICEROSS. However, ulceration, poor amputee hygiene and lack of commitment to prosthetic rehabilitation were considered as contraindication of ICEROSS by the study population. Several factors such as long residual limb, conical residual limb, patient suitable for PTB/SC or cuff suspension, older traumatic, diabetic, peripheral vascular disease, unsatisfactory cosmesis, and general dissatisfaction with the current system was regarded as to have no significant difference between ICEROSS and other methods. Although there was a consensus on these criteria, it is predominantly based on personal experience rather than evidenced based practise e.g. diabetic or traumatic amputees (McCurdie et al., 1997). In a questionnaire survey Dasgupta et. al. considered the differences in performance of ICEROSS prosthesis between amputees in employment and those who were out of employment and also whether there was any difference in performance between ICEROSS and old prosthesis for users in employment. Apart from questionnaires, medical, physiotherapy and prosthetic records were also considered. There was a difference in ICEROSS prosthesis performance between employed and unemployed amputees. The ICEROSS was worn successfully by employed amputees and this group, which were younger and more active, were significantly satisfied with the cosmesis of the ICEROSS (Dasgupta et al., 1997). Hachisuka suggested that long residual limb, bony spurs at distal end and difficulty in donning and doffing are contraindication for TSB (Hachisuka et al., 1998) and Datta believed that ICEROSS failed in amputees with tenderness and hypersensitivity at sump, especially at distal end due to using PTB

and stated that ICEROSS might have given better results for these amputees had they not had any skin problems at the beginning (Datta et al., 1996).

Studies comparing Hands-on and Hands-off concepts mostly focus on outcome measures such as suspension, walking performance, skin problems, pain and comfort. Based on questionnaire surveys, amputees stated an improvement in suspension using the ICEROSS system (Cluitmans et al., 1994, Datta et al., 1996, Dasgupta et al., 1997). Narita et al. compared ICEROSS and PTB socket axial movement of tibia of ten residual limbs (mostly traumatic) using x-ray as well as tibia stability, measured as the angular movement of tibia in anterior posterior direction, and axial movement of tibia during walking using cineradiography in three residual limbs, five repetitions for each case. The axial movement of tibia was significantly lower for ICEROSS in the static situation, 2.53±0.9 cm and 3.6±0.56 cm for ICEROSS and PTB respectively, as well as in the dynamic situation. Tibia stability was also significantly less in PTB (Narita et al., 1997). In another study by Yiğiter, the prosthesis pistoning was 1.6±0.4 cm and 0.4±0.5 cm for PTB and TSB with liner respectively when measuring the distance between the lines on anterior superior border of the socket in the standing and swing phases of the gait (Yiğiter et al., 2002).

In a questionnaire survey of forty three amputees (twenty six of which had previously PTB prosthesis) Cluitmans et. al found that amputees walking was improved in the form of speed, distance, uneven ground walking and stair climbing (Cluitmans et al., 1994). However, the ICEROSS system did not improve walking in terms of distance, duration of walking, walking on rough grounds and using less walking aids in another questionnaire survey of fifty four amputees who had PTB before using the ICEROSS system (Datta et al., 1996). Both of these studies were based on amputees' subjective assessment. In an objective assessment of PTB and TSB with liner prosthesis Yiğiter et al. assessed weight bearing on the amputated side, ambulatory activity, suspension and temporal characteristic of gait and balance evaluation of twenty amputees using both prosthetic socket types. Results show that weight acceptance on the amputated side was more normal with Hands-off and stance balance was better with PTB prosthesis. TSB prosthesis was lighter than PTB

prosthesis. A statistical significant difference was found in ambulation activity in favour of TSB prosthesis except for sitting and standing up from a chair and crossing an obstacle. Also there was a difference in temporal-distance characteristics in favour of TSB prosthesis in terms of intact side step length, walking speed and step width (Yiğiter et al., 2002). However, in a randomised control trial of twenty one amputees (control group No. 10 and experiment group No. 11), Datta et al. found there were no statistically significant differences between two groups in gait symmetry, nor in the socket comfort score (Datta et al., 2004). Furthermore, in a crossover study Coleman et al. (2008) examined patients' satisfaction, pain, socket comfort, daily ambulatory functions, and physical changes and patients comments associated with the use of two systems of Alpha elastomic liner and PTB with sleeve suspension. Thirteen subjects used each prosthesis for three months and then ambulatory activity was monitored using an activity monitor. Their results show that subjects achieved 83% more steps with Pe-lite prosthesis and spent 82% more time wearing the Pe-lite. Subjects wore the PTB prosthesis for a full day in 86% of the days monitored compared to 55% full day wearing of the other prosthesis type. There were no differences in the intensity of activity between the two prosthesis types. Also there were no significant difference between PTB and Alpha liner prosthesis in terms of subject socket comfort score and pain. Ultimately, eight out of thirteen subjects selected the PTB mostly because of ease of donning and doffing and comfort was more consistent over time with PTB. Hygiene problems and skin irritations were caused by the Alpha liner (Coleman et al., 2004).

In Cluitman's study skin irritation in the form of creasing, soreness, itching and perspiration were experienced by the study sample using the ICEROSS socket. However, these problems markedly decreased after some weeks or months. Moreover residual limb pressure sores occurred less frequently using the ICEROSS socket. Changing to the ICEROSS socket, pressure problem disappeared in fourteen amputees previously experiencing these problems with the PTB socket, five amputees stated no difference, while one amputee felt it was worsened (Cluitmans et al., 1994). However, in Datta's study of fifty four amputees who had PTB previously, fifteen participants stopped using ICEROSS. The reasons for stopping

ICEROSS were skin problems (skin rashes, blisters, excessive sweating) in ten people, pain and discomfort at distal end in four and insecurity in one amputee (last amputee had PTB/SC previously) (Datta et al., 1996). Similar to Cluitman's study, sweating was higher in the first three weeks but decreased after this period. Skin breakdown was less in ICEROSS users. Important observations, when considering ICEROSS, are: improved suspension, reduction of skin breakdown and better overall rating of this prosthesis. Researchers believe that ICEROSS cannot be considered as a standard prosthesis for all transtibial amputees because there is no convincing clinical evidence and also because of the rejection of fifteen amputees. They suggested that ICEROSS can result in a satisfactory outcome by improving in fitting technique, availability size and type of silicone sleeve and appropriate patient selection (Datta et al., 1996).

To examine the overall satisfaction of amputees with the TSB socket with laminated silicone inner, Hachisuka et al. asked thirty two subjects to rate different individual items. Three items, i.e. "comfort to wear", "ease to swing the prosthesis" and "piston movement during walking" were significantly related to amputees' satisfaction with TSB. 75% of amputees experienced less pain during walking, and less skin irritation and preferred cosmesis and durability of TSB. Nine amputees who were asked to wear both PTB and TSB alternately for three to four days for two months all chose TSB as their first prosthesis after amputation. The main reason for dissatisfaction was difficulty in donning and doffing. Also factors such as perspiration and crease at the back of knee were problems mentioned with TSB (Hachisuka et al., 1998). They stated that pain at the distal end of the residual limb is due to inappropriate weight bearing in this area because in a residual limb with excessive soft tissue the tibia sinks in the socket in the distal direction and causes impinging of the soft tissue in this region. Fergason believes that the tibia is not held back properly in the pressure cast socket compared to the PTB socket, where posterior direction force applied to the anteromedial and anterolaterl tibial flares, resulting in pain at the antrodistal part of the residual limb (Fergason and Smith, 1999).

The time and cost of fabrication are other issues where the cost of PTB is smaller but manufacturing time is longer (Datta et al., 2004, Selles et al., 2005). PTB prosthesis

manufacturing takes two and a half times longer but is two and a half times less expensive than ICEX to complete. (Datta et al., 2004).

In addition to the above mentioned pros and cons of the Hands-off concept, it gives more consistent results in casting than the Hands-on concepts and less variation in interface pressure distribution (Buis et al., 2003, Dumbleton et al., 2009). Hands-on sockets are not reproducible by most technicians and are quite variable among practitioners since it requires dexterity and skill.

In order to achieve the optimum socket design, socket shape and volume investigation of various existing socket designs is important. Furthermore, consistency in the socket shape is the fundamental factor to investigate the socket designs and to understand differences between them. In addition, in order to achieve a consistency in prosthetic alignment, consistency in socket shape is essential.

1.3.5 Consistency

There is a lack of evidence based practise in trans-tibial prosthetic socket manufacturing and prosthetic alignment; both are subjective based on a prosthetist's past experience and input from the amputee. Despite many studies on different aspects of trans-tibial socket and residual limb there is a lack of knowledge to enable consistent manufacturing of a comfortable socket and desirable alignment without the need for several trial and error fittings.(Trower, 2006)

Regardless of different socket concepts, the consistency of the final socket fit for an individual amputee is important for two reasons. Firstly, the consistency of prosthesis manufacturing influences the quality of transtibial socket fit. If an accurate and reproducible socket can be produced then the experience of the amputee might improve and the time each amputee spends in a prosthetic centre could decrease (Klasson, 1985). Secondly, if a consistent socket shape can be made, then it will be possible to assess other factors such as the effect of the alignment of the prosthesis, component on socket fit to achieve a better understanding of the socket designs.

The socket is usually made through the process namely of shape capturing, rectification, and alignment. A consistent shape capturing process enables the team to evaluate the effect of variability of the socket fabrication process, such as rectification on final outcome. Also if consistent shape capturing and rectification is achieved then the variability of alignment, prosthetic foot characteristic, and material compliance can be assessed. This could also result in better understanding of the socket-residual limb interaction leading to a possible "good socket fit".

Currently there is an inconsistency in residual limb shape capturing results using Plaster of Paris. In the case of the hand-on concept the residual limb soft tissue is pre-shaped by prosthetists using their hands. Consistency of the results highly depends on the experience and skill of the prosthetist, but despite that, even with well experienced prosthetists there is a lack of repeatability due to the dexterity. In the Hands-off concept which is supposed to minimise the prosthetist's influence on the variability of the captured shape, the consistency of shape depends on precisely setting the air pressure in the bladder as well as the alignment of the bladder to the residual limb during POP setting. During casting, the prosthetist applies proximal force to the cast bladder to hold it over the residual limb while the POP is being cured where a subtle angular change in the direction of the force may lead to an inconsistency of the captured shape. The direction of this force in relation to the long axis of the residual limb has to be consistent in a repeated casting. One would expect that the direction of the applied force to the bladder would not change the resulted residual limb shape as based on hydrostatic principle the force applied to an enclosed fluid medium would distribute equally to the entire volume. However, in the Hands-off casting the bladder is attached to the distal pin of the silicone liner and the liner is in close contact with the skin. Any change in the direction of the proximally applied force to the bladder would result in a slight change in the force applied over the residual limb.

In the later stage, the positive plaster mould of the residual limb is made and, in the case of the Hands-on technique, then rectified by adding or removing plaster to and from some specific regions of the mould. Again the final shape of the modified plaster mould is influenced by prosthetist's dexterity.

Prior to final socket fabrication a check socket is made and the fit is checked on an amputee's residual limb. The necessary modification is then made based on the prosthetist's observation, skill, experience and input from the amputee through the repeated process of trial and error.

Regardless of the quality of the socket fit, the new socket always comes with a fear to the amputee and it takes time for an amputee to accustom himself with it. According to anecdotal information and prosthetists' observations, an amputee experiences a period of fear and discomfort after a new socket has been issued. Over time the amputee feels more comfortable until there is a need for a socket change due to, for example, residual limb volume change. This process is repeated for the next new socket which causes a decrease in the amputee's quality of life.

The consistency of rectification of Patella Tendon Bearing (PTB) for both inter-prosthetist and intra-prosthetist variability were investigated (Convery et al., 2003). Two prosthetists each rectified five identical plaster models of a residual limb. The plaster models were measured before and after rectification for a total of 1800 points using a CNC machine and digital calliper gauge with high accuracy and precision. Results show that there is both inter- and intra-prosthetist inconsistency in plaster cast rectification. The casting consistency of Hands-on (PTB) and Hands-off (Pressure cast) sockets has also been compared using a manikin model (Buis et al., 2003). It was shown that the Hands-off concept has more consistent results than the Hands-on socket for shape capturing. The Hands-off concept showed a constant pattern of maximum radius variation of 1.4 mm whereas the Hands-on concept had a maximum radius variation of approximately 2.4mm and 5mm in the distal part and proximal part of the measured part respectively. Researchers suggested the establishment of a reliable reference grid in relation to skeletal structure of the residual limb is required for comparison purposes.

1.4 Reference Grid

For any volume and shape measurement a reliable reference datum is required. Comparing consistency of Hands-on and Hands-off shape capturing in volume and shape is complicated due to establishing a reliable reference grid for inter- and intra-

socket comparison. Buis et al. showed that it is possible to use the tibia bone in the MRI images as a reference grid for 3-D alignment of multiple image volume using the Analayze® software (Buis et al., 2006). The only rigid entity in the residual limb is the tibia bone which can be used for this purpose. Smith et al. obtained two SXCT scans of seven transtibial residual limbs for each of the two sessions. The tibia was segmented from SXCT scans using the Analayze® software, and then used to register all inter and intra session scans to a common coordinate system. The results of their study showed that this technique of registration has an error of approximately 1% relative to the mean volume of the residual limb (Smith et al., 1996).

Both Computer tomography (CT) and MRI can be used to scan the residual limb and the image information can be used to spatially register the volume images to a common coordinate system using the mutual information in tibia. Therefore, any inter and intra cast shape and volume difference of the residual limb soft tissue can be measured after registering two images of the residual limb. The MRI is superior to CT mainly due to avoiding the ionising radiation in repetitive imaging.

1.5 Geometric Assessment:

External and internal geometric assessment of the residual limb has been done mainly for the assessment of residual limb volume and maturation. Furthermore, it has been designed to be applied to the data in the computer aided design of prosthetic socket and finite element studies. Few studies intended to use the geometrical assessment for socket fitting evaluation.

1.5.1 External Geometric Assessment:

Simple measuring equipments such as measuring tape and callipers are used for circumferential and longitudinal measurement of the residual limb. Water displacement method was used for cross-sectional and overall volume measurement. The Water overflow method was also attempted. The residual limb was immersed in a water tank and overflow water was weighted to measure the volume of the residual limb. The precision of this method was reported up to 1.1% (Smith et al., 1995). Other external measuring modalities include using contacting probe (Torres-Moreno

et al., 1989, Houston et al., 1992, Zuniga et al., 1977). Errors in this method could result from residual limb movement during measurement time and possible distortion of soft tissue due to physical contact of the device. It was shown that optical scanning, which is another method of surface residual limb surface scanning, had 2.2% precision for volume measurement and 2.4mm accuracy for distance measurement (Commean et al., 1996a, Smith et al., 1995, Commean et al., 1996b, Saunders and Vickers, 1984). Laser scanning has also been used for this purpose (Johansson and Oberg, 1998, Houston et al., 1995, Fernie Gr - Halsall et al., 1984, Fernie et al., 1985, Engsberg et al., 1992). The surface scanning methods are mostly used in the CAD system and provide quantifying data about the surface counter of the residual limb. However, the information regarding the internal structure is neglected. The external forces from the socket are transmitted from the residual limb soft tissue to the internal structure such as the tibia bone. The internal geometric assessment of the residual limb and relating the surface counter of the residual limb or internal socket shape to the tibia is important for better understanding of socket shape and design.

1.5.2 External and Internal Geometric Assessment:

X-ray, Computed tomography (CT), MRI and ultrasound were used for quantifying the internal and external residual limb structures. X-rays were used to view 2-D images of residual limb. The condition of skeletal tissue and the rough dimensions of surrounding soft tissue could be somewhat monitored by x-ray. The tibia movement in the socket and contact between socket and residual limb was assessed by X-ray (Grevsten and Erikson, 1975, Lilja M - Johansson et al., 1993, Meier et al., 1973). Apart from poor soft tissue visibility, the traditional x-ray did not permit volumetric and other 3-D measurement.

Ultrasound has been used to scan the residual limb soft tissue (Morimoto et al., 1995, Douglas et al., 2002a, He et al., 1996, He et al., 1997, Huang and Zheng, 2005). Resultant tissue indentation due to direct contact of ultrasound transducer to the residual soft tissue is a concern in using ultrasound for geometric assessment of the residual limb. Also, placing the residual limb in a water bath to avoid contact

deformation of the soft tissue results in a greater distance of the transducer from the limb, hence less image quality. Furthermore, placing the transducer over the socket causes a socket-transducer coupling problem (Douglas et al., 2002b).

Both CT and MRI can provide soft tissue and bone images of the residual limb as well as 3-D images of the limb. From number of 2-D transverse slices, the CT can provide the 3-D model of the residual limb. Data resulting from the CT had been used in the CAD system (Faulkner and Walsh, 1989) as well as in finite element studies (Zachariah et al., 1996 , Commean et al., 1997, Shuxian et al., 2005). Socket, residual soft tissue and bone can be extracted from Spiral X-ray CT with a resolution better than 1mm , accuracy of 2.2 mm (Commean et al., 1996a, Liu et al., 1997). However, the CT technology suffers from the ionising radiation especially in repeated measurements.

MRI is a high resolution imaging technique which can provide a clear distinction between tissues. Since MRI is an expensive device few studies had been done on amputees. It has been used to establish a computational model of the residual limb and to monitor the morphological changes in residual limb soft tissue (Douglas et al., 1998, Lilja et al., 1998, Torres Moreno et al., 1999), in diagnosis of the tibia mechanical stress and post-operative complications (Foisneau-Lottin et al., 2003, Henrot et al., 2000), to generate a CAD model for transtibial residual limbs using reverse engineering techniques (Udai and Sinha, 2008).

Compared to other imaging modalities MRI provides better images of the limb's soft tissue. Torres Moreno et al. (1999) used 8 bit colour look up to enhance regions of similar tissue density to differentiate tissue regions. The image facilitates visualization of differences between residual soft tissue from that of an intact limb (Torres Moreno et al., 1999).

Additionally, changes in the total cross-sectional area and circumference of the residual limb was measured as well as changes in the cross-sectional area of different muscles (Lilja et al., 1998).

The common drawback of MRI is chemical shift artefact resulting from chemical property of the tissues. As a result of differences in overall magnetic field, in the chemical artefact each nuclei experience is mainly displayed as a shift in location of different material in the image, namely water and fat. The chemical shift artefact is explained in the next section. In the extraction of bone and skin from MRI images of trans-femoral residual limb, investigators concluded that the chemical shift resulting from the skin fat lead to the underestimation of the limb by thickness of the skin (Douglas et al., 1998).

2 Magnetic Resonance Imaging (MRI)

2.1 Introduction

Magnetic Resonance Imaging (MRI) is a non-invasive medical visualisation method which uses a strong magnet and radio waves to produce detailed cross-sectional images of the internal body.

In the nineteen forties, Felix Bloch and Edward Purcell independently discovered the magnetic resonance phenomenon and developed an instrument which could measure liquid and solid materials. Between 1950 and 1970, Nuclear Magnetic Resonance (NMR) was developed and used for chemical and physical molecular analysis. In 1971 Raymond Damadian and his colleagues at the State University of New York designed and built a superconducting magnet in their laboratory and took the first human body image, initiating scientists' interest in magnetic resonance for the detection of disease. Numerous scientists developed the MRI to a technique which is used currently to produce 2-D or 3-D images of the internal human body (McRobbie et al., 2007).

2.2 MRI System

The full MRI system consists out of three designated areas; a magnetic radiation shielded room housing the scanner, also indicated as the "magnet" and its receiver coils. Additionally, there is a control room, accommodating the control and imaging computer. Support systems for the electronics and cryogenic cooling for the magnet are situated in the third area.

The MRI system itself consists of the magnet, radiofrequency transmitter and receiver coils, magnetic fields gradients, a computer system for scanner control and patient couch.

2.2.1 The Magnet

The magnet produces a strong magnetic field and is the main part of MRI scanner. Common types of magnets are permanent magnets (up to 0.3T[1]), resistive electromagnets (up to 0.6T) and superconducting electromagnets (0.5 T and higher). MRI systems commonly used clinically have up to 3T field strength. Higher field strength is mostly used for research purposes. The magnets are either open or closed bore. The bore is the opening of the system in which the patient lies during scanning. The closed bore looks like a narrow long tube whereas an open bore magnet is mostly open on the sides and does not surround the patient completely, making it suitable for obese people and those with claustrophobia.

2.2.2 Radiofrequency Coils

An MRI image is produced as a result of the magnetic resonance signal emitted from protons within an imaging volume inside a magnetic field. These signals are created in a response to radio frequency (RF) pulses generated by RF transmitter coils. Then the signals are received by receiver coils which are used to produce an image, (see section 2.5 for more detail). Receiver coils include a body coil inside the scanner and several other coils for regional body scanning such as knee coil, neck coil, spine coil etc.

2.2.3 Gradients

Gradient coils produce small linear magnetic fields which superimpose on the main magnetic field in a way that the overall magnetic field inside the scanner is slightly stronger in some locations than others. The strength and direction of gradient magnetic field change during the scan so that each voxel experience a different magnetic field, hence; resonate at a different frequency. Through these gradients the spatial encoding of the imaging volume is possible. The gradients are applied at three orthogonal directions namely, slice selection gradient (Gs) in x direction, phase

[1] Tesla (T) is the unit for measuring the magnetic field density. For the sake of comparison, the earth magnetic field is approximately 0.05T.

encoding gradient (Gp) in y direction and frequency encoding gradient (Gf) also called readout gradient in z direction.

2.3 MRI Capabilities

Compared to the other imaging techniques, such as Computer Tomography (CT) and ultrasound, MRI provides a better contrast between body tissues. It is a powerful method of choice which can provide accurate information about anatomy and abnormalities. A superior advantage of MRI to CT is avoiding the ionising radiation exposure of patients.

2.4 Contra Indication

There are no known side effects of an MRI scan. Projectile, claustrophobia and magnet noise can be considered as its drawbacks. Any metallic object in the vicinity of the scanner moves as a result of the powerful magnetic field, causing a phenomenon called projectiles. Additionally, metallic objects inside the body, such as surgical clips, or foreign material (artificial joints, metallic bone plates or prosthetic devices, etc.) can not only significantly distort the images obtained by the MRI scanner but can also move and cause serious harm to the patient. Patients with heart pacemakers, metal implants, or metal chips or clips in or around the eyeballs cannot be scanned with an MRI because of the risk that the magnet may move the metal in these areas. Patients should lie inside the scanner bore which is a narrow long tube. Therefore, people with claustrophobia may find it uncomfortable. Also the noise from gradients and radiofrequency transmitter is annoying for some people.

2.5 Basics of MRI

MRI is based on the behaviour of hydrogen nuclei inside the magnetic field. Hydrogen nuclei can be found in water and fat which make up to 75% of the human body, (McRobbie et al., 2007). Each hydrogen nuclei has an electrical charge and spin. As a result of spinning, the hydrogen produces a small magnetic field. These magnetic fields are randomly oriented, see Figure 2-1. The entire MRI is based on the manipulation of this magnetic field which is done by a short application of radiofrequency energy while the nuclei are surrounded by a powerful magnetic field.

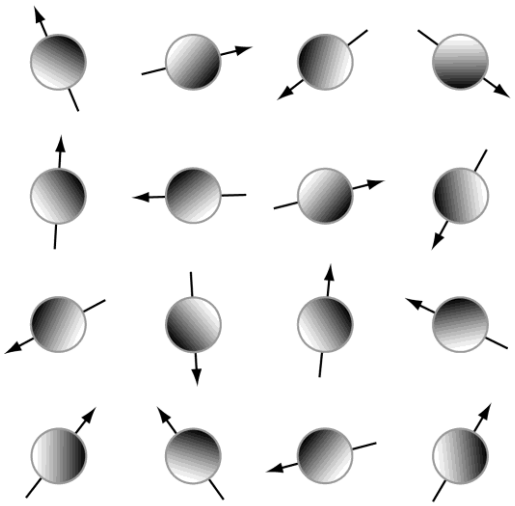

Figure 2-1: Randomly oriented magnetic field of nuclei

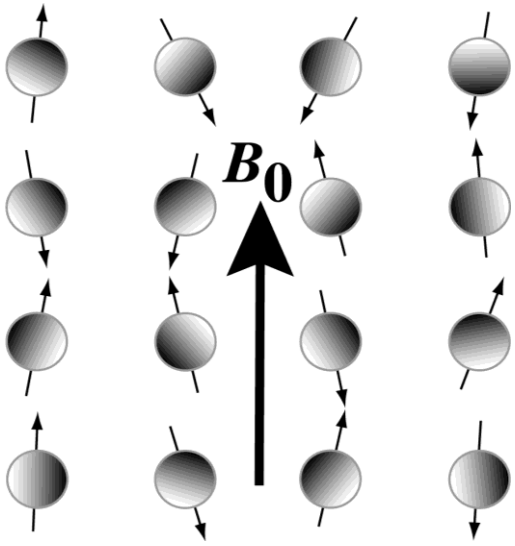

Figure 2-2: Nuclei in a strong magnetic field (B_0)

When nuclei are placed in a strong magnetic field it will be aligned either parallel or anti-parallel to the direction of the magnetic field, which is referred to as high or low energy states respectively, see Figure 2-2. The parallel and anti-parallel magnetisations cancel each other out and only a small amount of magnetisation remains called net magnetisation. The sum of all magnetisation vectors of protons is referred to as the magnetisation vector (M_O), Figure 2-3. At a certain time, a radiofrequency (RF) pulse with a certain frequency is applied to the tissue and protons at low frequency to absorb this energy. As a result, the net magnetisation

vector diverts towards the transverse plane, see Figure 2-4. When the RF pulse is switched off, the net magnetisation vector returns back to its previous state, which induces an electric current in the receiver coil. The electric current in the receiver coil is translated into an image by the MRI machine hardware. The transverse magnetisation decays with a time constant T2 (spin-spin relaxation time) and net magnetisation grows with time constant T1 (spin-lattice relaxation time). Different body tissue has different T1 and T2, therefore producing different electric charge in the receiver coil resulting in the production of a greyscale image.

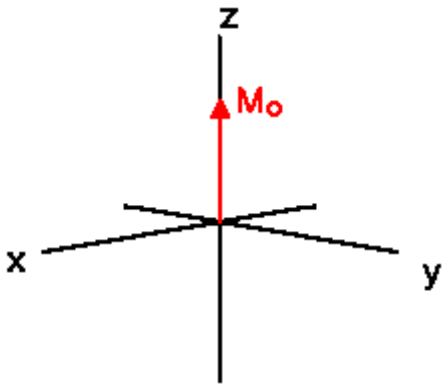

Figure 2-3: Net magnetization vector (M_O)

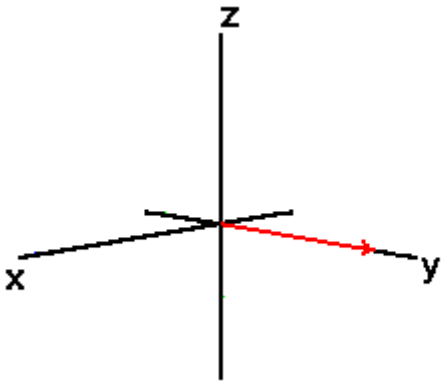

Figure 2-4 : Net magnetization vector diverts towards transverse plane after the RF pulse

2.5.1 Image Contrast

Image contrast is the relative difference of signal intensity between adjacent tissues. As mentioned before different tissue, e.g. muscle, fat, bone marrow, etc, have different T1 and T2 relaxation times in the MRI and each shows different signal intensity in the MRI images. The image contrast not only depends on T1 and T2 times but also is a result of magnetic field strength, proton density of tissue and more importantly on the selection of pulse sequences. Pulse sequences are carefully selected timings of radiofrequency (RF) and gradient pulses which are repeated many times during a scan. The timings include Repetition Time (RT), and Time of Echo (TE) which can be changed by the operator to select the desired image contrast. The time interval between pulses and the amplitude and shape of the gradient waves will control MR signal receiving and influence the characteristics of the MR images.

2.5.2 Pulse Sequence

There are many pulse sequences in use of which spin echo, inversion recovery and gradient echo are the main ones. In the case of gradient echo and inversion recovery pulse sequences, inversion time (TI) and flip angle are mostly used to describe them respectively.

2.5.3 Free Induction Decay (FID)

The net magnetization (M_O) diverts to X-Y plane after application of the RF pulse. When the pulse is stopped the transverse magnetization decays toward zero. As the net magnetization returns toward equilibrium it induces an electrical charge in the receiver coil located around the subject. The transverse magnetization decays with time constant T_2 so that an induction decay curve is produced, see Figure 2-5. This electrical signal is converted to more conventional frequency based signals using Fourier transform analysis.

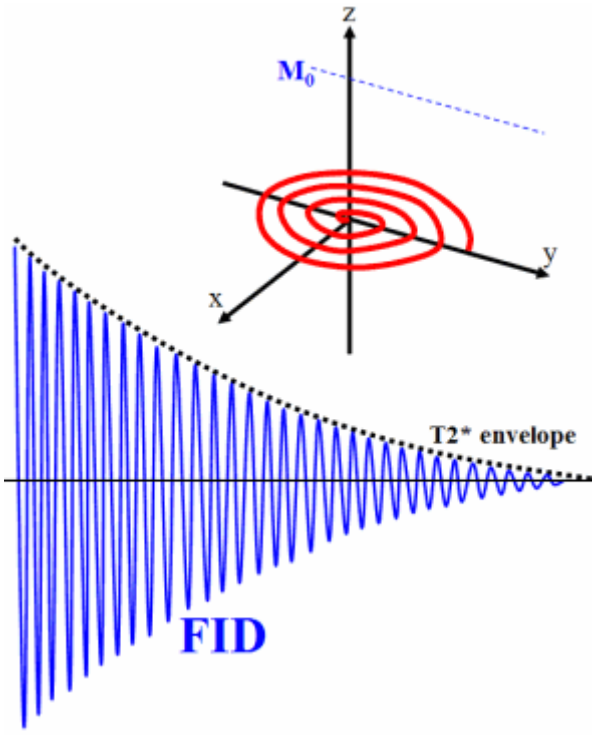

Figure 2-5: Free Induction Decay (Higgins, 2003)

2.5.4 Timing Diagram

The timing diagram is a schematic diagram which illustrates the steps of hardware activity involved in a pulse sequence, Figure 2-6. The timing diagram contains a number of horizontal lines so that each line is assigned to each hardware activity. A usual diagram has a line for the radio frequency transmitter and also one for each gradient of Gs, Gp and Gf (see section 2.2.3). Time during sequence execution is indicated along the horizontal axes. The timing diagram can be used for 2D and 3D pulse sequences.

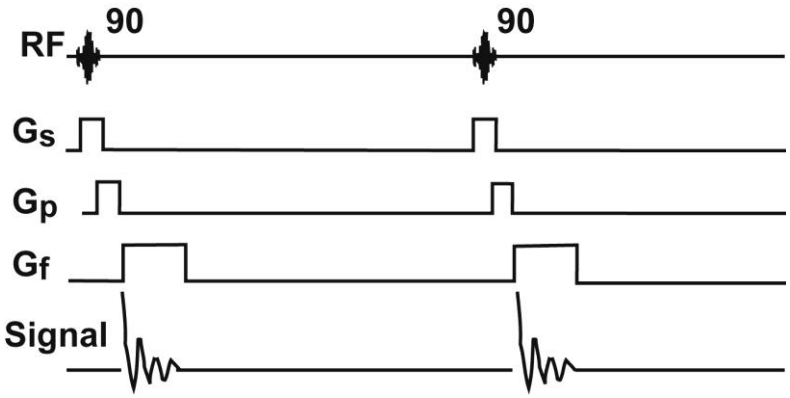

Figure 2-6: Timing diagram

2.5.5 Spin echo

In the spin-echo imaging sequence the 90 degree pulse rotates the magnetization down into the X-Y plane. The transverse magnetization begins to de-phase. At some point in time after the 90^o pulse, an 180^o pulse is applied in conjunction with the slice selection gradient. A phase encoding gradient is applied between the 90^o and 180^o pulses.

The frequency encoding gradient is applied after the 180 degree pulse during the time that the echo is collected. The recorded signal is the echo. The FID, which is found after every 90^o pulse, is not used. One additional gradient is applied between the 90^o and 180^o pulses. This gradient is along the same direction as the frequency encoding gradient. It de-phases the spins so that they will re-phase by the centre of the echo.

A period called the echo time (TE) is the time between the start of the RF pulse and the maximum in the signal. The entire sequence is repeated every TR seconds until all the phase encoding steps have been recorded.

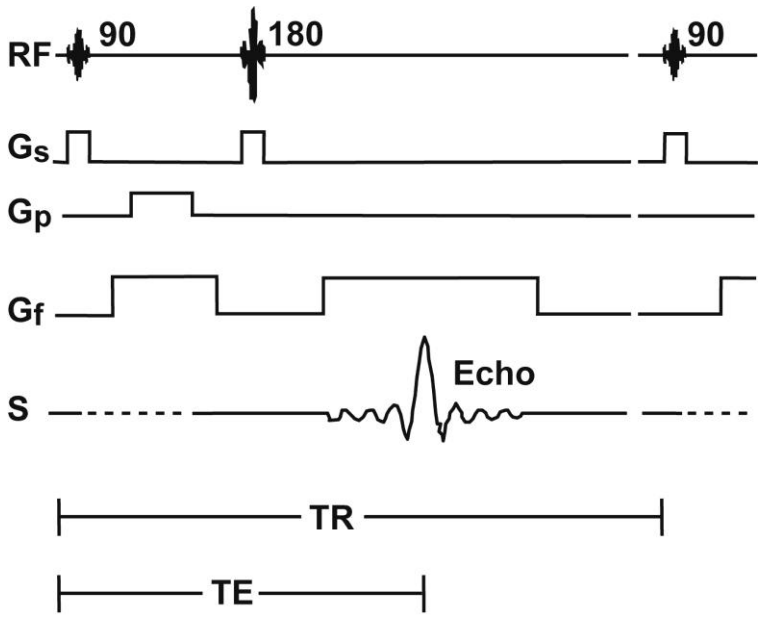

Figure 2-7: Spin echo pulse sequence

2.5.6 Gradient Echo Pulse Sequence

For maximum signal, all pulse sequences require transverse magnetization to recover to its equilibrium position along the Z axis before the sequence is repeated. In this case if the T1 is long, the imaging sequence will be significantly long. If the magnetization does not fully recover to equilibrium the signal is less than if full recovery occurs. If the net magnetization is rotated less than 90 degree its M_o component will recover to equilibrium much more quickly, but there will be less signal.

The gradient echo imaging sequence is the application of these principles. In this sequence a RF pulse is applied to the imaged object. This RF pulse typically produces a rotation angle of between 10 degree and 90 degree, called a flip angle. A slice selection gradient is applied with the RF pulse. Then, a phase encoding gradient is applied. A de-phasing frequency encoding gradient is applied at the same time as the phase encoding gradient so as to cause the spins to be in phase at the centre of the acquisition period. This gradient is negative in sign from that of the frequency encoding gradient turned on during the acquisition of the signal. An echo is produced

when the frequency encoding gradient is turned on because this gradient refocuses the de-phasing which occurred from the de-phasing gradient.

The TR period is shorter than the spin echo sequence. In a gradient echo, a gradient is used instead of a 180 degree RF pulse to re-phase the spins. Imaging with a gradient echo is intrinsically more sensitive to magnetic field inhomogeneities because of the use of the refocusing gradient. The use of a small flip angle and of a gradient for the refocusing of magnetization vectors gives this sequence a time advantage. Therefore it is widely used for fast scan images, including 3D acquisitions.

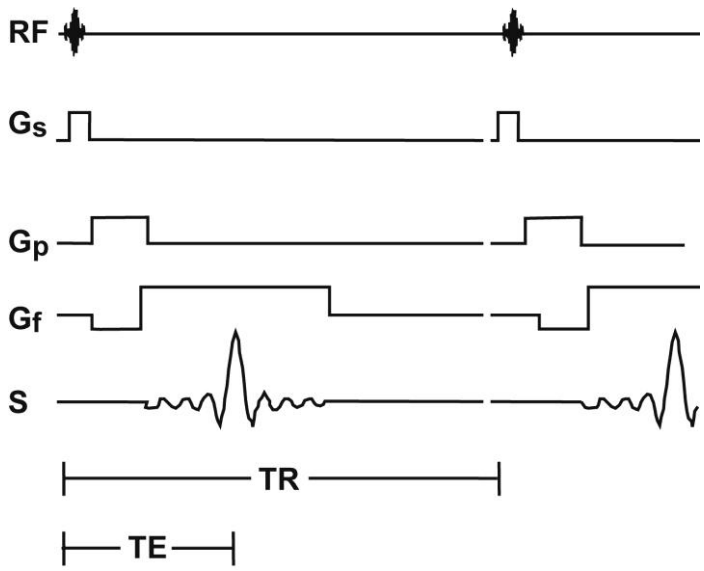

Figure 2-8: Gradient echo pulse sequence

2.5.7 Inversion Recovery

An inversion recovery sequence, which uses a spin-echo sequence to detect the magnetization, will be presented. The RF pulses are 180-90-180. An inversion recovery sequence which uses 90-FID signal detection is similar, with the exception that a 90-FID is substituted for the spin-echo part of the sequence.

The timing diagram for an inversion recovery imaging sequence has entries for the RF pulses, the gradients in the magnetic field, and the signal. A slice selective 180o RF pulse is applied in conjunction with a slice selection gradient. A period of time equal to TI elapses and a spin-echo sequence is applied.

The remainder of the sequence is equivalent to a spin-echo sequence. This spin-echo part recorded the magnetization present at a time TI after the first 180o pulse. (A 90-FID sequence could be used instead of the spin-echo.) All the RF pulses in the spin-echo sequence are slice selective. The RF pulses are applied in conjunction with the slice selection gradients. Between the 90 degree and 180 degree pulses a phase encoding gradient is applied.

The phase encoding gradient could not be applied after the first 180o pulse because there is no transverse magnetization to phase encode at this point. The frequency encoding gradient is applied after the second 180 degree pulse during the time that the echo is collected.

The recorded signal is the echo. The FID after the 90^{o} pulse is not used. The entire sequence is repeated every TR seconds. The inversion recovery sequence has the advantage that it can provide a very strong contrast between tissues having different T1 relaxation times or to suppress tissues like fluid or fat. Conversely, the disadvantage is that the additional inversion radio frequency RF pulse makes this sequence less time efficient than the other pulse sequences.

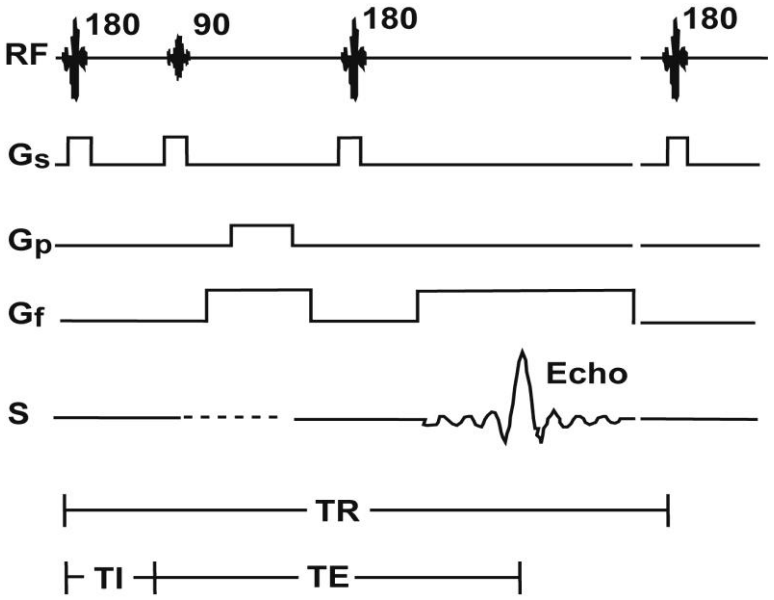

Figure 2-9: Inversion recovery pulse sequence

2.6 MRI Artefacts

The accuracy of MRI is influenced by artefacts and image distortions associated to this technology. The common artefacts which can affect MRI accuracy are mechanical and chemical shift. The mechanical shift is a result of motion of the subject in the scanner during the imaging process which causes a blurred image. The chemical shift is a result of the chemical properties of materials inside the magnetic field. A nucleus spin in a magnetic field depends on the magnetic field which it experiences. The total magnetic fields experienced by a nucleus is a sum of magnetic fields of the scanner and local magnetic fields resulting from electron movement around the nuclei in their orbits. Therefore different numbers of electrons cause different amounts of local magnetic fields at each nucleus which is reflected in the resonance frequency. This variation in resonance frequency causes spatial misregistration of material in frequency encoding direction. In the human body water and fat are the source of hydrogen nuclei. Since each of these materials has different molecules and hence the resultant RF is different, their manifestation in the image is different. Because of the fact that the chemical shift artefact is always in one direction with a same amount, it could be compensated for.

2.7 MRI in Volume and Dimensional Measurement

MRI is a superior method in bone and soft tissue volume and dimension measurement because it is based on superconducting magnets. Furthermore, it is possible to use coronal, sagittal and transverse images in MRI.

MRI accuracy in volume and dimension measurement was reported in several studies (Aisen et al., 1986, Cyteval et al., 2002, Eckstein et al., 1994, Haubner et al., 1997, McGibbon, 2003, Mitsiopoulos et al., 1998, Mortimore et al., 1998, Walton et al., 1997). MRI can be used to estimate accurate morphological information of different tissues, e.g. bone, muscle and articular cartilage.

Mitsiopoulos et al (1998) and his colleagues showed that MRI can provide an accurate area and volume measurement of the skeletal muscle and adipose tissue free skeletal muscle (ATFSM). ATFSM area in 119 images (SD 38.9 ± 22.3) and cadaver (39.5 ±23.0) were not different. It was shown that the MRI volume estimates are in good agreement with those of cadaver sections (Mitsiopoulos et al., 1998) (correlation for regression analysis was 0.98 to 0.99 for all variables, $p<0.001$) In a retrospective study Aisen et al. (1986) included twenty six patients with bone or somatic soft tissue sarcoma with the aim to compare MRI and CT in delineating the tumour and evaluating the extent of disease. They argued that MRI is the superior method in assessing the extent of disease because of the fact that the MRI system used was based on a superconducting magnet. MRI was additionally superior in delineating the tumour because it is possible to use coronal as well as sagital transverse imaging planes in MR images.

Three different types of structure exist in the construction of the bone; cortical bone, trabecular bone and bone marrow. Since the outer layer of the bone (cortical bone) has low water content it has less signal intensity compared to other tissues such as the trabecular bone and the marrow region. The cortical bone is not visible in MRI. However, it is a very thin layer and even thinner in residual limb(Torres Moreno et al., 1999). The trabecular bone and marrow region make the most of the bone. Since the marrow region contains both water and fat (Vande Berg et al., 1998), there is a likelihood of chemical shift artefact in this region in MR images. However, this

artefact does not affect results of volume measurement. Cyteval et al. (2002) measured vertebral body dimensions using MRI in order to compare the MRI measurement of the vertebral area and volume with direct cadaver measurements. In their study water displacement was used for volume measurement of cadaver vertebra. The intraclass correlation coefficient between MRI and immersion methods was 0.95. It was concluded that MRI is a feasible, reproducible and accurate method for area and volume measurement of vertebral bodies (Cyteval et al., 2002).

In addition to the chemical shift, difficulties which can affect the volume measurement are confounded of isointense adjacent structure and erroneous boundary point. However using an effective algorithm can be a solution to these problems. Gomberg et al. developed an algorithm for the detection of the cortical boundary and volume in such a complex anatomical region as the femoral neck. The algorithm was based on transacting the cortical bone along test lines (profiles) to locate cortical boundaries along each line. Because of the high resolution of the method and allowing imaging in arbitrary planes, MRI can be used as a means to access cortical bone architecture providing the appropriate algorithm. (Gomberg et al., 2005). Furthermore, it has been shown that MRI is an effective method in collecting data of bone geometry (Murdoch et al., 2002). Murdoch et al. (2002) used MRI to obtain the anatomy dimensions of the humerus and showed that it is a safe and reproducible method. They calculated total bone and bone canal diameter, cortical bone thickness, basic intermedulary canal shape and length of the bone in twenty volunteers (Murdoch et al., 2002)

Knee cartilage is another structure which is attached to the end of the bone composed of 75% - 80% water (Treppo et al., 2000), therefore it has proper signal intensity. Eckstein et al. assessed the cartilage volume by MRI and compared the results with those obtained from anatomical sections. It was concluded that MRI can provide a valid estimate of cartilage volume. Haubner et al. (1997) assess the accuracy of a three-dimensional measurement of articular cartilage based on MRI in the knee joint, by comparing the results with those of CT topography human cadavers. They segmented the cartilage semi-automatically in MRI and CT by means of a grey value oriented to a shape-based interpolation routine. It was shown that there was a high

agreement between two methods (r=0.995) and that accurate 3-D assessment of articular cartilage can be performed using MRI.

2.8 Factors Influencing Accuracy of MRI Measurement

The main factors which can influence the accuracy of MRI include: voxel size, slices interval, pulse sequence and image segmentation.

2.8.1 Voxel Size

A voxel abbreviation for "volume element" can be thought of as a three dimensional version of the pixel. A pixel is the smallest element of a digital image which is organized in rows and columns of a matrix to make the image. Each pixel in the image can be thought of as a location in the computer memory containing a number which controls the signal intensity of the image. The MR image is not a 2D image of the object as it is seen in the screen; it has depth. It is composed of several numbers of voxels in rows and columns in a matrix. For example a $1\times1\times3$ mm^3 voxel means the smallest part of the image is a square of 1×1 mm^2 and the image (slice) thickness is 3 mm.

It is quite usual that a voxel contains two or more different body structures, especially at the boundary of the tissues. In this case the signal intensity of the voxel is the sum of all signals from the various tissues. Therefore, if the voxel dimensions are too large, it is obvious that tiny structures cannot be resolved. This is known as the "partial volume effect" which can influence the total counts in a volume (Brooks and Di Chiro, 1977). It is not possible to avoid the partial volume effect since the smaller voxels need more scanning time and have low signal-to-noise ratio(McRobbie et al., 2007).

2.8.2 Image Interval

In order to decrease the scanning time, the MRI scan is sometimes taken with intervals between the slices. This leads to loss of information in-between the slices. The effect of a gap between slices in MRI accuracy depends on the size of the tissue and its counter. It is important to choose an interval between sections that accurately represent the contour of the limb, while consuming the least image acquisition and

analysis time. Obviously, the less the interval between image sections, the more accurate the volume measurement will be. The counter of the stump has a direct impact on the selection of intervals between sections. Tracy et al. conducted a study to describe the error associated with different intervals between sections in serial axial images that encompassed the entire quadriceps femoris muscle for volume measurement at one point in time or change in muscle volume longitudinally. The volume measurement was calculated from images with a thickness of 9mm and a 1mm gap was used as a criterion measure. Afterwards investigators included every 2nd section (1.1 cm gap), every 4th section (3.1 cm gap) every 6th section (5.1 cm gap), every 8th section (7.1 cm gap) and every 10th section (9.1 cm gap) along the thigh, starting from the patella. Then these alternatives were compared with criterion volume measure. It was concluded that a 31mm interval between slices can provide MRI measurements accurate to ±1.7% in 95% of occasions in a large and mixed group of subjects (Tracy et al., 2003). The underestimate bias was greater for subjects with larger muscle volume and subjects whose muscle volume change is more. They also showed that the larger the muscle the greater the amount of error in volume measurement will be. Additionally, for muscles with greater volume fluctuation the greater error is in the volume measure in longitudinal studies.

Using MRI in conjunction with stereology and B-mode ultrasound, Walton et al. showed that seven sections through the quadriceps muscle are required to achieve 4-5 % coefficient of error for the muscle cross section and volume measurement (Walton et al., 1997) However Mitsiopoulos showed that if the spacing between images is between 10 and 40 mm the volume can be estimated with an error less than 1%. (Mitsiopoulos et al., 1998) Apparently the amount of muscle volume measurement error is related to the contour of muscle. Also, larger muscle has greater error in volume measurement. Mitsiopoulos measured the adipose tissue free skeletal muscle volume which may cause less error in volume measurement with wider image intervals.

2.8.3 Image Segmentation

Accuracy and reliability of the MRI measurement highly depends on the segmentation process of the image. It could be done manually by tracing the

boundary between different tissues. In order to quantify the accuracy of manual segmentation of the soft tissue metastasis, Zentai et al. (2004) evaluated the 3D models using the expectation-maximization algorithm named the STAPLE (Simultaneous Truth and Performance Level Estimation) algorithm through measuring sensitivity and specificity. Three observers performed five segmentations of the region of interest in a random order. Then the estimated true segmentation (ground truth) was calculated based on multiple images as follows:

Intra-observer combined ground truth (ICG)

Cross-observer combined ground truth (CCG)

All-observer combined ground truth (ACG)

ICG had the highest value of sensitivity and specificity but ACG reduced the sensitivity. CCG were analysed with the specific bias removed in ICG because of systematic biases of each observer and random noise. Investigators concluded that the 3D model can be made accurate to a probability that the model is 90% correct. Although several studies have shown that manual segmentation is a reliable method (Gomberg et al., 2005, Tracy et al., 2003, Walton et al., 1997, Zentai et al., 2004), automated segmentation has less inter/intra-observer variation due to less operator intervention (Douglas et al., 1998)

However, the reproducibility in volume measurement for fatty tissue was low compared to total tissue measurement when automatic segmentation was used by Mortimore. This might result from the chemical shift of fat. Chemical shifting artefact can be corrected by the appropriate number of pixels in the readout gradient direction(Mortimore et al., 1998).

2.8.4 Pulse Sequence

In general the image contrast depends on spin-lattice relaxation time (T1), spin-spin relaxation time (T2) and proton density (PD) characteristics of the tissue. High PD gives high signal intensity which gives brighter voxels. Fluids - e.g. CSF, synovial fluid, oedema- have longer T1 and T2; water based tissue like muscle, cartilage, and

brainhave midrange T1 and T2; and fat based tissues such as fat and bone marrow have short T1 and T2. T1 is always longer for a given tissue than T2 (McRobbie et al., 2007). Tissue with long T2 gives the highest signal intensity, resulting in a bright appearance, whilst long T1 is completely different and gives the weakest signal and hence produces the dark voxels.

Both spin echo (SE) and gradient echo (GE) sequences can produce T1, T2 and PD images. For T1-weighted SE image the TR and TE should be short to improve T1 differences between tissues. These images are known as 'anatomy scans' since they illustrate the boundaries between tissues very well wherein the fluids are very dark - water-based tissues are mid-grey and fat-based tissues are very bright. T2-weighted SE images need long TR and TE so it takes longer to achieve these images. These scans are known as 'pathology scans' because the abnormal fluids appear brighter than other tissues. PD-weighted SE images can be produced by applying short TE and long TR. This makes an image based on proton density of the tissue. It has some useful clinical applications such as discriminating knee articular cartilage from menisci and bone.

In the gradient echo sequence TR has much less effect on the image contrast and usually a short TR is chosen. Therefore, the flip angle is important for the contrast of the image whereby a large flip angle ($<50^{o}$) and short TE produce T1-weighted images and small flip angle with long TE produce T2 images. The GE images are very quick to acquire and have excellent SNR and resolution which are often used to acquire 3D volume scanning.

2.8.5 Contrast Agents

The contrast agents are metallic elements with strong paramagnetic susceptibility which improve image resolution and quality through increasing the signal to noise ratio. These materials affect the T1 and T2 times so that the signal intensity of the tissue increases (Rohrer M - Bauer et al., 2005). A common used contrast agent is based on gadolinium. It can be either injected into the body or orally taken which shortens the T1 time and increases the signal intensity (Caravan et al., 1999). The

copper sulphate has the same effect as the gadolinium compounds and is mostly used as a marker in the MR imaging (Alesch, 1994).

2.9 MR Imaging of Residual Limb and Prosthesis

The physiological property of soft tissue and bone in the residual limb will change after amputation because of a decrease in function of the residual limb. This change should be considered when taking the MR image of the limb. In a study in 1999, Torres Moreno and his colleagues demonstrated that the MRI facilitates visualization of differences between residual soft tissues from that of an intact limb. They highlighted that the amount of adipose tissue was higher in the residual limb compared to the sound limb. Also, a larger cross-sectional area of modular cavity in the residual limb and a thinner femoral cortical layer were found compared to the femoral bone in other limbs (Torres Moreno et al., 1999). The increased fat is a result of a decrease in the muscular activity of the residual limb.

The adipose tissue, especially the subcutaneous fat, causes the chemical shift which increases in volume and shape measurement error. Douglas et al. segmented skin and bone in the MRI images of a trans-femoral stump. Instead of manually tracing the tissue boundaries using a mouse they used an algorithm for defining skin and bone geometry through automatic extraction of skin and bone from transverse MR. The only manual intervention was the selection of a seed point on the bone in the first image (K-mean Clustering). In this study the chemical shift of fat and skin was neglected. Also the algorithm picked up a part of fat and skin which was shifted, therefore underestimated the limb by the thickness of the skin. Because of the chemical shift in the skin, average computer-to-observer agreement was smaller than the average inter-observer agreement for skin compared to bone. Furthermore, there was greater variability in the skin boundaries (Douglas et al., 1998)

Apart from the chemical shift resulting from the residual limb fat, the movement of the limb during scanning results in a blurred image. In imaging the intact limb, the contact of the distal end of the limb to the table of the scanner provides stability and therefore the mechanical movement of the limb would be minimal. However, this is not true for the residual limb. Also the floppy tissue of the residual limb may

exaggerate the movement. The plaster cast around the limb would decrease this movement (Torres Moreno et al., 1999). However, movement of the residual limb inside the plaster cast might occur. Buis et al. showed that this movement is 0.3 mm in the antero-posterior direction, (Buis et al., 2006).

2.10 Summary

Magnetic Resonance Imaging (MRI) is based on the behaviour of hydrogen nuclei inside a magnetic field. This is a safe, nonionising image modality with a reasonable contrast between tissues. It is a powerful method of choice which can provide accurate information about different body tissues.

MRI image contrast depends not only on nuclei responses to radiofrequency pulses within a magnetic field, but also on magnetic field strength, proton density of tissue and careful selection of pulse sequences.

Spin echo, gradient echo and inversion recovery pulse sequences are the most commonly used pulse sequences. The gradient echo pulse sequence has the short scanning time advantage, with excellent signal-to-noise ratio and resolution, which is widely used for fast scanning including 3D acquisition.

Artefacts and image distortions are drawbacks to MRI technology. The so called *chemical shift* and *mechanical shift* are the common MRI artefacts. Mechanical shift is a result of the motion of subject during scanning. A chemical shift results from differences in the chemical property of different materials, exhibiting an image shifting of fat tissue in relation to the adjacent tissues.

Studies have shown that MRI is an accurate method of soft tissue and bone dimension and volume measurement and has been used to estimate accurate morphological information of different tissues e.g. bone, muscle and articular cartilage (Aisen et al., 1986, Cyteval et al., 2002, Eckstein et al., 1994, Haubner et al., 1997, McGibbon, 2003, Mitsiopoulos et al., 1998, Mortimore et al., 1998, Walton et al., 1997). Other than chemical shift, factors influencing the accuracy of MRI in

volume and dimension measurements are voxel size, slice interval, image segmentation and selection of pulse sequence.

Prior to using MRI in volume and shape quantification of residual limb, the question of whether there is any artefact in the image resulting from commonly used materials in the production of the socket should be answered. Additionally, the accuracy of MRI in soft tissue shape and volume measurement, when soft tissue is surrounded with common casting materials, is needed.

2.11 Aim and Objectives

Residual limb shape capturing (casting) is the first stage in socket manufacturing. Casting consistency has a great influence on the quality of socket fit. Investigating the casting consistency is the first stage in understanding socket fit and design. This will put a foundation for research on other stages of socket manufacturing and prosthetic management such as rectification, and socket alignment. To do so, a reliable reference grid is required for cast shape and volume comparisons. This can be done by setting the tibia bone, the only rigid entity in the residual limb, as a reference datum in MRI images of the residual limb. The main aim of this study is to investigate inter and intra socket shape capturing consistency of two different transtibial prosthetic socket concepts namely, Hands-on and Hands-off, using the Magnetic Resonance Imaging reference grid.

Prior to using MRI in volume and shape quantification of the residual limb, the question of whether there is any artefact in the image resulting from commonly used materials in the production of socket should be answered. Quality of MRI measurement is influenced by artefacts associated to this technology such as chemical shift. The subcutaneous fat is the major source of fat in the limb. The accuracy of soft tissue dimensional measurement can be affected by chemical shift resulting from fat tissue. This can be exaggerated more when common casting materials show a shift in MRI images. The shifted image of the skin can be superimposed on adjacent casting materials, affecting the accuracy of the soft tissue boundary detection. To date the soft tissue volume and dimension measurements is not performed considering the aforementioned issue.

The accuracy of boundary detection in MRI images not only depends on possible chemical shift resulting from fat and /or socket material but also depends on the image signal intensity of adjacent materials. Therefore, the accuracy of MRI in soft tissue shape and volume measurement when soft tissue is surrounded with common casting materials is needed.

Also quantity measurement is influenced by variability in both the subjects and measurement process. The accuracy and repeatability of MRI geometric measurements can be affected by factors such as subject positioning and movement inside the scanner, and operator-dependent interactions during acquisition and image processing.

Therefore objectives of the study are summarised as follows:

- Repeatability of the MRI geometric measurement
- Examining the possible image artefact associated to common socket materials
- Accuracy of MRI volume and shape measurement when using casting materials
- Establishment of a reference grid using bone
- Making a best compromise between image resolution and time of scanning
- Use MRI to compare Hands-off and Hands-on casting concepts

To reach the objectives of the study two experiments were conducted. The first experiment planned to check for the repeatability of MRI geometric measurements and examined the possible image artefact resulting from socket materials. Then, the second experiment was carried out to measure the accuracy of MRI volume and shape measurement when using casting materials.

3 Experimental Accuracy and Repeatability Validation of MRI for Prosthetic Research Purposes

3.1 Introduction

In this experiment a standard substance was scanned and the MRI measurements were then compared to that of actual values.

3.2 Methods

Glass tubes, (L=100mm, Ø=5mm), filled with water were used as reference markers, Figure 3-1. The MRI signal is a result of hydrogen nuclei behaviour within the magnetic field which can be found in water. Water makes up more than half of the human body. This is the best substance to use as a reference marker for measurement purposes and to evaluate whether there is a distortion in the image of socket materials. Additionally, to optimise the marker return signal intensity the water was doped with Copper Sulphate (CS), in the ratio of one gram per litre of water. The contrast agent is a chemical substance which can increase the image contrast by altering the T_1 and T_2 relaxation times. For detail of T_1 and T_2 see Section 2.5.

Figure 3-1: NMR glass tube

3.2.1 Placement of the Marker Tubes Inside the Scanner

Marker tubes filled with CS doped water needed to be placed in three orthogonal planes in order to evaluate the accuracy and repeatability of MRI dimension measurement in all directions. Since these tubes were used as reference markers for

the purpose of chemical shift measurement they needed to be a certain distance from the socket material specimen.

In order to place the marker tubes inside the bore of the scanner in a known location, marker tubes were placed in a purpose designed test rig, Figure 3-2. The rig was designed using CAD software (Solidworks) in order to incorporate the required reference markers and a specimen container. A powder based rapid prototype 3D printer (Zprinter 310) was utilised to accurately reproduce the test rig which was strengthened with cyanoacrylate based infiltrate.

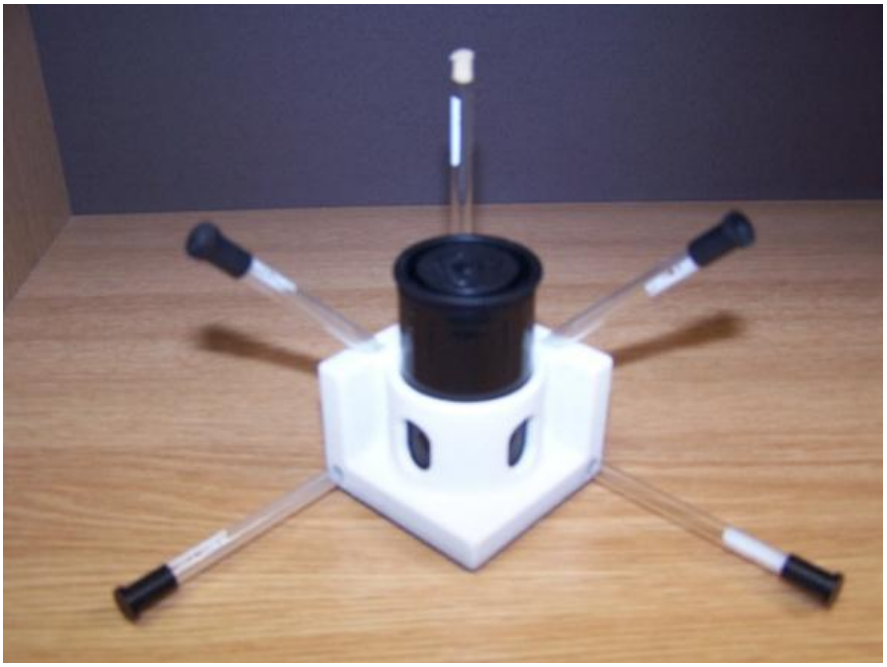

Figure 3-2: Test rig made using Zprinter

To ensure the feasibility of using the test rig as a base for placing tubes and materials inside the scanner an MRI scan of the specimen was taken. The scanner settings are summarised in Table 3-1.

Table 3-1: Pulse sequence parameters

Pulse sequence	FSPGR
Repetition time (S)	6.9
Time of echo (S)	1.5
Inversion time (ms)	500
Bandwidth(KHz)	31.25
Flip angle(Deg)	12
Matrix	256×256
Slice thickness (mm)	1.8
Voxel dimensions (mm)	1.8×1.09×1.09
Number of average	1

The image illustrated that there was an interfering effect of the test rig material in relation to the reference makers, Figure 3-3. This might be a result of magnetic susceptibility of the test rig material (Condon, 2006). Magnetic susceptibility differences between adjacent substances inside a magnetic field might result in microscopic gradients or variation in the magnetic field strength near or across the interface of two materials. This artefact is known as a susceptibility artefact, which could result in bright and dark areas with spatial shifting of surrounding material. Test rigs without cyanoacrylate infiltrate showed similar effects as illustrated in Figure 3-4.

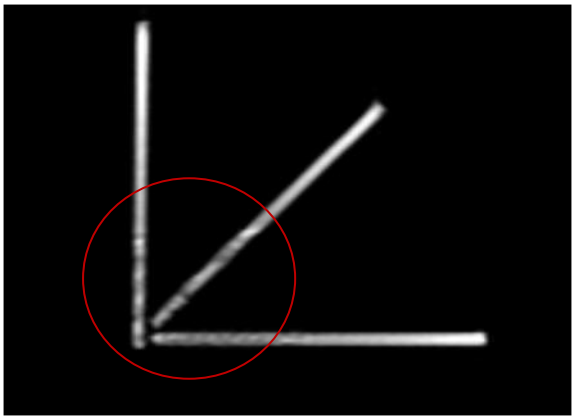

Figure 3-3: Cyanoacrylate infiltrated material interference effect

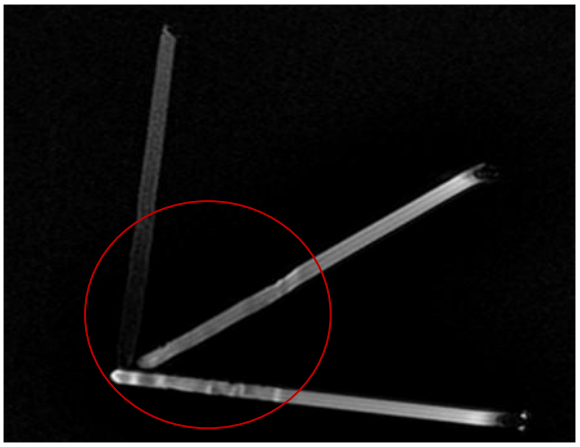

Figure 3-4: Image of interference of rig material without cyanoacrylate infiltrate

The artefact effect as described above could be described as an unexpected anomaly. Because of the artefact effect of the powder based 3D printer material a different type of rapid prototyping process called ‘fusion deposit manufacturing’ (FDM) incorporating an ABS plastic material was used to reproduce the test rig. The preliminary results after a MRI scanning session showed a similar artefact effect as experienced with the powder based materials as illustrated in Figure 3-5.

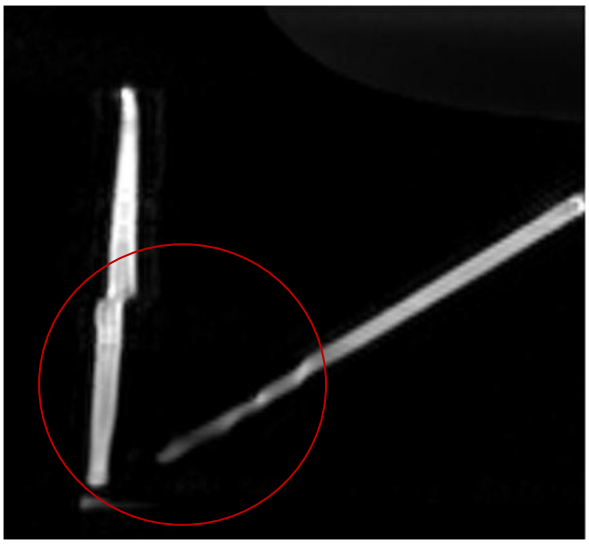

Figure 3-5: image of plastic test rig

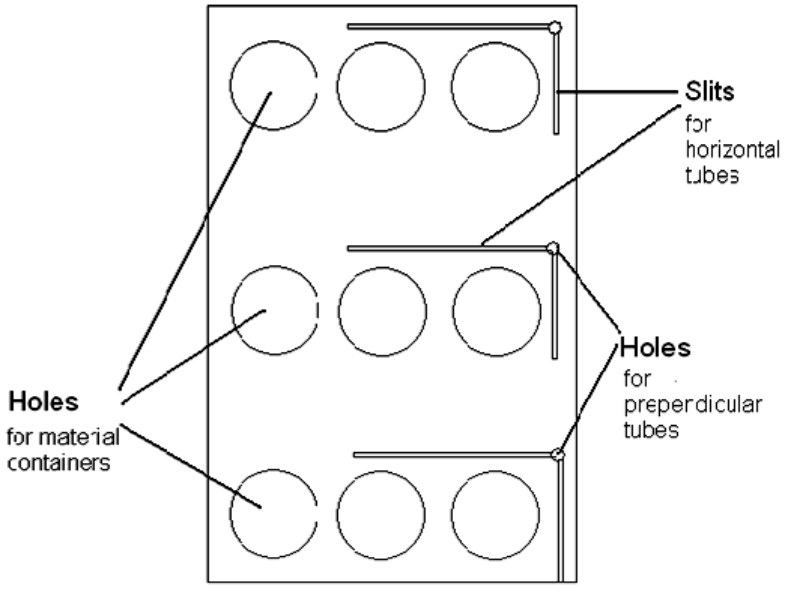

Figure 3-6: Perspex plate with nine holes for containers slits for horizontal marker tubes and three small holes for perpendicular marker tubes

To eliminate the susceptibility artefact it was decided to use a material that has the same magnetic susceptibility as water. Perspex is a material that can be used for this purpose (Moerland et al., 1995). However Perspex material is not compatible with 3D printers. Hence, a Perspex plate with dimensions of 300 mm ×160 mm was used to produce a test rig. Three sets of marker tubes were placed on the plate perpendicular to each other. To place the tubes horizontally on the plate six recesses were made so that the marker tubes could be positioned accurately, Figure 3-6. Additionally, three holes were made to fit marker tubes perpendicular to the plate.

Each set of marker tubes were to be used as reference markers for examining possible image distortion of socket material. For this purpose three holes were made next to each set of marker tubes which were used to place the material containers during scanning.

All the holes and recesses were made using a validated CNC machine (Deckel^{TM}). The accuracy and validity of the machine was tested (Convery et al., 2003) and it was shown to have an accuracy of 0.005 mm. The marker tubes were placed in the holes and recesses and secured with a drop of superglue. In order to keep the plate steady inside the bore of the MRI machine during scanning, a Perspex cylinder of 326 mm long and 172 mm diameter was used.

To fixate the plate inside the Perspex tube three Acrylic plastic round rods (8mm diameter) were used. After placing the plate inside the cylinder one rod at the end of the tube was in contact with the edge of the plate to prevent from slippage, Figure 3-7.

Figure 3-7: Perspex tube with Perspex plate inside including the glass tubes and containers

3.2.2 Scanning Marker Tubes

The Perspex cylinder containing marker tubes and the empty material containers were placed in the MRI scanner and scanned nine times. After each scanning the Perspex tubes were removed and then placed back again and scanned to examine for scan/re-scan variability. The imaging parameters are summarized in Table 3-1.

3.3 Data Processing

The MRI machine takes images in the form of slices (Figure 3-8.a) over a predetermined length or volume, (Figure 3-8.b). A slice looks like a greyscale image

of a cross-section of the imaging volume. This single slice information is filed in Digital Imaging and Communications in Medicine (DICOM) format. Subsequently, DICOM data is exported to the state-of-the-art visualization software (AnalyzeDirect, Inc; Overland Park, Kansas) developed at the Mayo Clinic Biomedical Imaging Resource in Rochester, Minnesota, USA. Analyze® 7.0 is a comprehensive software package for multi-dimensional display, processing, and measurement of multi-modality biomedical images.

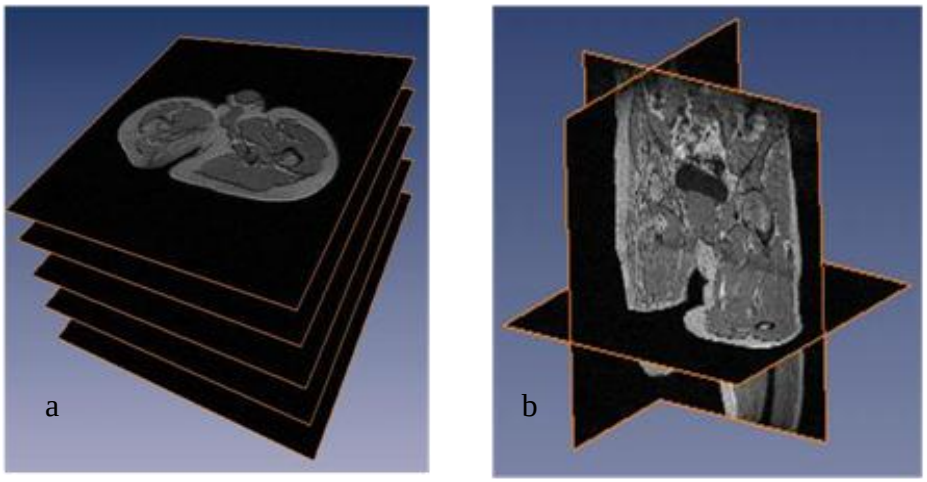

Figure 3-8: MRI consists of number of slices

3.3.1 Loading and Processing Images to the Software

All files were downloaded as a separate volume in the main workspace of the software. The voxel - the smallest part of each slice - had a dimension of 1.8×1.09×1.09 (mm). As the voxel dimensions were not the same in all directions the resulting image appeared elongated in one direction which corresponds to the bigger dimension, in this case 1.8 mm. To deal with this issue the software is capable of resizing the voxel size to isotropic dimension voxels. After resizing, the volume was the same size of the real life specimen. Since the marker tubes were not exactly parallel to the long axis of the bore of the scanner all the slices were realigned

parallel to the reference markers. To carry out this manoeuvre, all cubic volumes were loaded, realigned three times, each time in one direction, and saved at the end.

3.3.2 Measurement

The software is able to measure angles and distances using the 'Calliper' feature. The lengths and distances of the reference tubes were measured in all nine scans in order to evaluate for accuracy and repeatability of reference tube length measurement. Prior to this common reference coordinates were assumed for images.

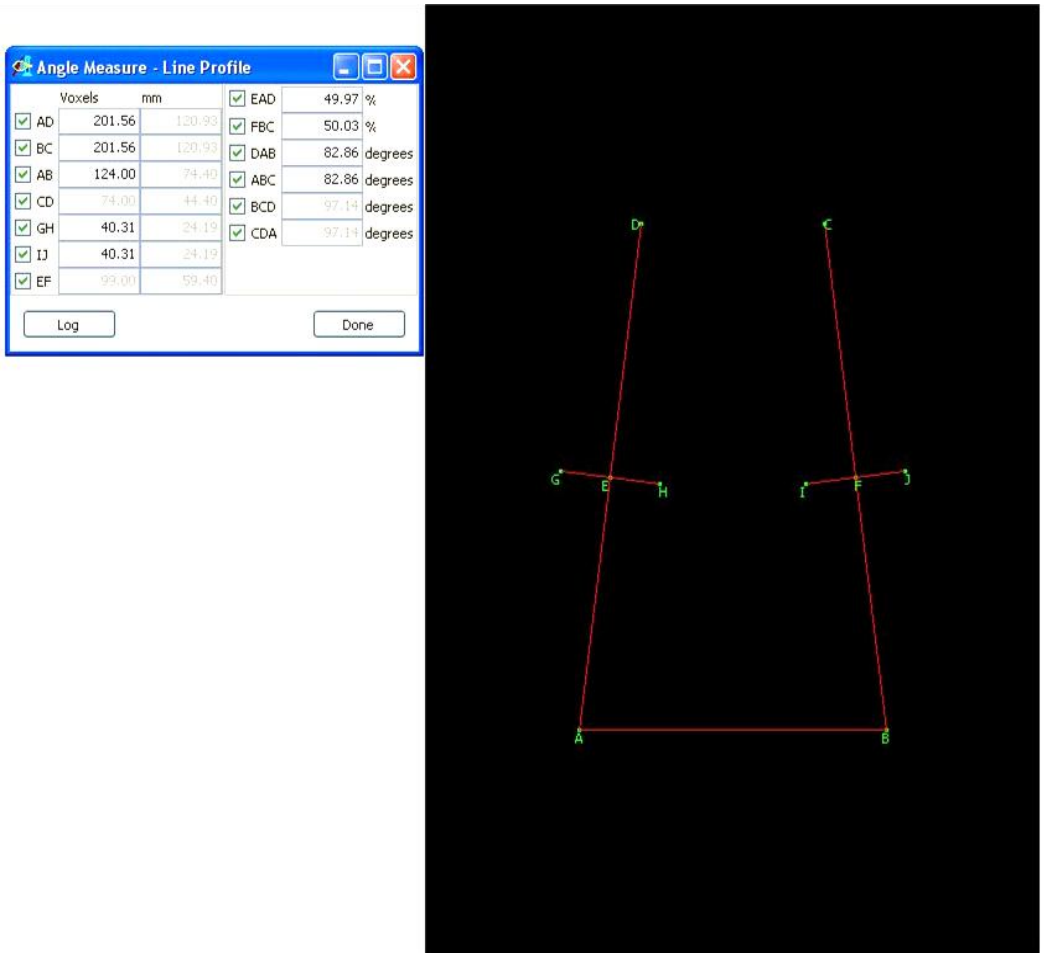

Figure 3-9: Calliper line feature of the software. Distances and angels are given in the left box

3.3.2.1 Coordinate System in Images

The upper right point of the image wherein two projected lines representing the tubes meet each other (labelled A in Figure 3-10) was arbitrarily selected as the origin of the coordinate system. The coordinate system was set in each slice according to the

image direction in the MRI bore, Figure 3-11 , so that the positive Z and positive X direction were to the bottom and to the left of the image respectively, Figure 3-10. The positive Y direction was to the depth of the image. However, for the ease of measurement the signs of the coordinates did not necessarily match that of the MRI system.

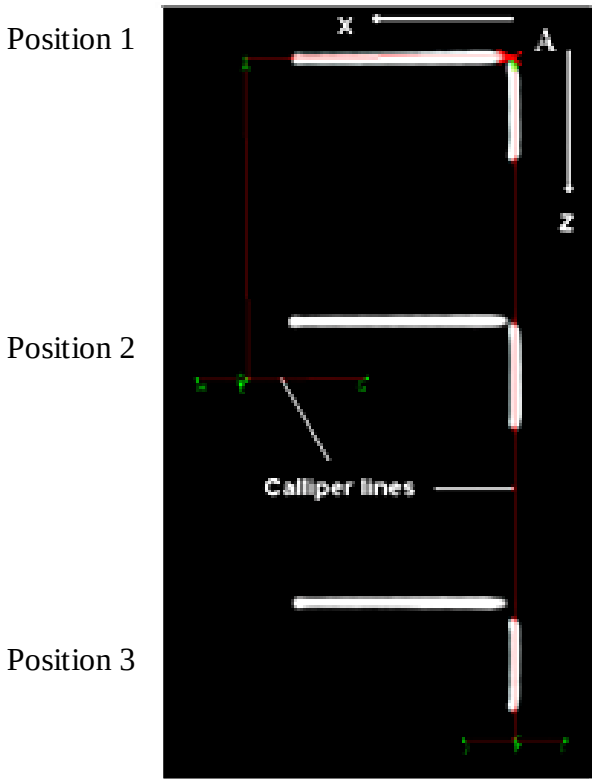

Figure 3-10: Reference point, coordinate system and calliper lines.

Figure 3-11: The scanner's coordinate system

3.3.2.2 Tube Length Measurement

The internal diameter of the marker tubes was 4.20 mm and the MRI slice thickness was 1.9083 mm after voxel dimension resizing. Considering the slice thickness and the diameter of the marker tubes, after slice alignment in relation to the reference marker tubes in all directions, the tube lengths were highlighted in at least three consecutive slices. Therefore, lengths of all tubes in all three orthogonal planes in three consecutive slices were measured in all nine scans.

3.4 Data Analysis

Differences in the marker tube lengths of the actual markers and markers derived from MRI were calculated. Subsequently, the effect of different scan, slice, direction and position factors on the mean of tube length difference was tested in order to examine if there was a difference in the mean of marker tube length difference for various levels of these factors, i.e. to check if the mean length difference is the same for the first scan, second scan, etc. (level 1, 2 etc.) and then to check the mean length difference is similar for slice 1, slice 2 and 3 etc. The scan factor had nine levels, each level representing one repetition of the MRI scanning. In each scan, the lengths of the marker tubes were measured in three consecutive slices in which tubes were highlighted so that three levels were considered for each slice factor. Also three levels of direction factor represented the three orthogonal directions of x, y and z. Finally three positions were assumed for each scan number coding as 1, 2 and 3, Figure 3-10.

The difference of actual value and MRI value for all measurements was compared using the confidence and tolerance limits. The tolerance of measurements is a factor affecting the accuracy of measurements.

3.4.1 Effect of Scan, Slice, Direction and Position of Tubes on the Measurements

The differences in actual tube length and those of the MRI measurements were calculated. The factorial Analysis of Variance (ANOVA) test was used to test the effect of scan, slice, direction and position factors on means of tube length differences. ANOVA is used when there is two or grouping variables, such as scan, slice, direction and position in this thesis, to test whether or not means of several groups are equal, therefore; generalise the t-test to more than two groups. Using t-test for testing means of several groups increase the chance of committing type 1 error, i.e. error of rejecting null hypothesis when it is actually true, (Altman, 1999).

The mean and standard deviation of marker tube length and the difference between actual values and MRI for different levels of each factor is summarised in Table 3-2. Marker tube lengths used in this experiment were different in the x, y and z directions. The mean and standard deviation of tube length in different directions is highlighted in Table 3-2. The overall tube length mean was calculated for other factors (scan, slice and position). The difference in mean length was less than 0.5mm in all tests with a standard deviation of less than 2mm in all tests.

Table 3-2: Mean and standard deviation for tube length and difference between actual values and MRI for different levels of each factor

Factor	Factor level	Tube length mean (mm)	Mean difference (Real value-MRI) (mm)	SD (mm)
Scan	1	55.26	0.45	1.68
	2	55.29	0.48	1.65
	3	54.42	-0.38	1.55
	4	54.80	0.00	1.86
	5	54.67	-0.14	1.54
	6	54.88	0.07	1.46
	7	54.29	-0.51	1.62
	8	54.54	-0.27	1.48
	9	54.98	0.17	1.79
Slice	1	54.48	-0.33	1.63
	2	54.83	0.02	1.68
	3	55.08	0.27	1.63
Direction	1=x	93.21	-0.13	1.23
	2=z	43.36	0.19	1.90
	3=y	38.97	0.03	1.26
Position	1	46.56	0.08	1.76
	2	63.69	-0.19	1.63
	3	54.14	0.06	1.59

The statistical significance of the possible effect of the factors and interaction plots was analysed using SPSS version 17.0 and summarised in Table 3-3. The purpose of an interaction plot is to visualise levels of one variable on the X axis and has a separate line for the means of each level of the other variable (legend variable). The plot shows the amount of variability of mean for each level of one factor in relation to levels of another factor.

Table 3-3: Significance results of tube length difference

Tube length difference	Significance(p<0.05)
Scan (1 to 9)	0.485
Slice (1 to 3)	0.569
Direction (x, y, and z)	0.512
Position (1 to 3)	0.795
Scan * Slice	1
Scan * Direction	0.93
Scan * Position	1
Slice * Direction	0.188
Slice * Position	0.019
Direction * Position	0.344

Results indicate that there is generally no significant effect of the factors on the mean difference of measurements. However, a significant result ($p<0.05$) was found for slice-position interaction. Figure 3-12 shows the interaction plot for the slice-position for differences in tube length.

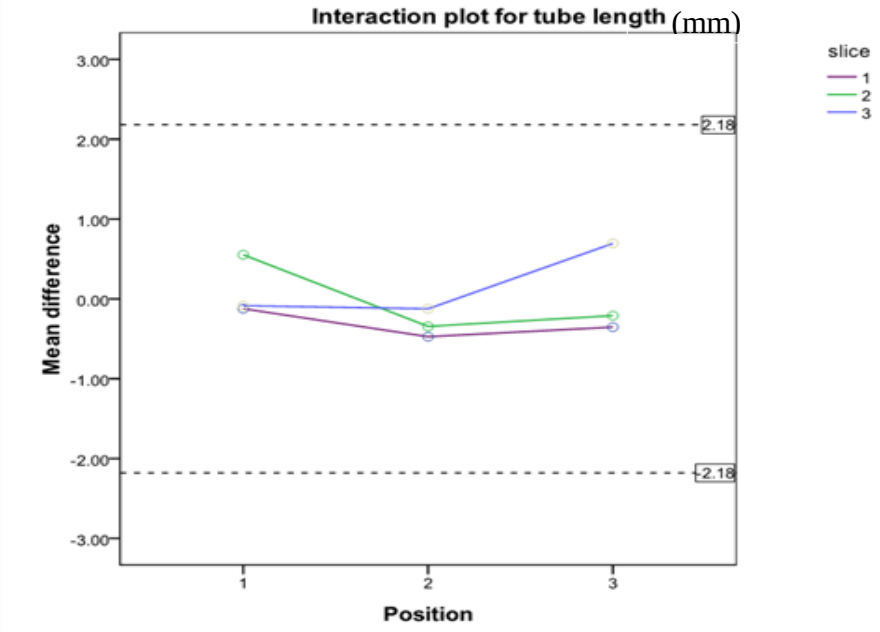

Figure 3-12: Slice -position Ineraction plot for tube length diference

The slice-position interaction plot shows that the mean difference is slightly higher in position 1 and stays fairly constant in position 2 and 3 for slices 1 and 2. The third slice follows the reverse pattern which has a higher mean value in position 3. In the plots the mean and upper and lower tolerance limit lines were plotted to show visually if the means of variables lie within the tolerance limit. For details of tolerance limit see Section3.4.3. It shows that all means lie within the tolerance limit of measurements.

3.4.2 Comparing MRI Values with Actual Values for Tube Lengths in X, Y and Z Directions

Prior to measuring the differences between MRI measurements with actual values it is necessary to calculate the tolerance level of the measurements in MRI.

3.4.3 Tolerance of measurements

The phenomenon "partial volume effect" is affecting the accuracy of measurements. The partial volume effect is the error resulting from measuring the voxels which lie at the border of the subject being imaged. It is important where the borders of the subject end in the image. Figure 3-13 shows a subject in a 7 × 9 matrix of an image. Each square resembles a voxel. In the left image the boundary of the subject and the edge of the voxel row superimpose on each other and in the right image it lies in the middle of the voxel row. The voxels at the boundary of the subjects light up causing the addition of an extra row of voxels to the volume of the subject in the image, which in turn increases the tolerance limit of measurements.

In order to measure the length of tubes in images two points were positioned manually at each end of the tube and the distance of the points was given by the Analyze software. It was not possible to locate these points in the middle of the voxel (where the boundary of the object ends in the right image in Figure 3-13), therefore, the measurements were under- or overestimated by one voxel size depending on the location of these points. Additionally, even when the boundary of the subjects matches the edge of the voxel row (left image in Figure 3-13), the point locating

might be associated with ±1 × voxel dimension random error. Therefore, the overall tolerance of measurements is ±2.18 mm

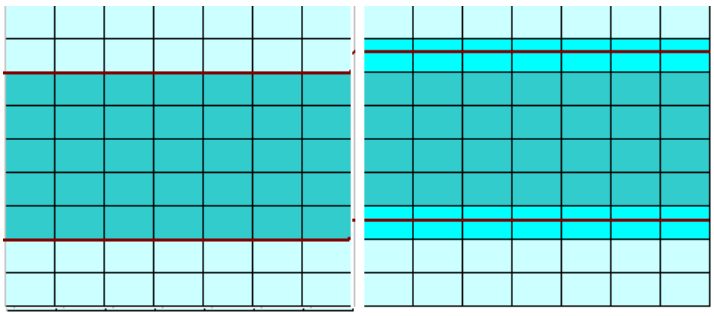

Figure 3-13: Borders of an object in a matrix of voxels

3.4.3.1 Confidence Interval and Tolerance Interval

The tolerance of measurements in each of the x, z and y directions is ±2.18 mm. Having the actual values and the tolerance, the tolerance intervals (TI) can be calculated. TI was calculated as the length of tubes plus and minus the tolerance of measurement. If the confidence interval (CI) of the measurements falls within the tolerance intervals, there is not a clinically significant difference between the measurements and the actual values. In this thesis the 95 percent CI which is mean ± (1.96 × standard error) was calculated. 95% CI is a range which does not include the true population value 5% of the time (Altman, 1999).

3.4.3.2 Examining the Length of Tubes

CI and TI for all tube length measurements are summarized in Table 3-4. The plot of CI and TI shows all CI falls within the tolerance intervals, Figure 3-14. The actual tube lengths were measured using a digital vernier calliper with an accuracy of 0.01 mm which was 43.42 mm, 93.42mm and 39.00 mm in z, x and y directions respectively.

Table 3-4: CI and TI for tube length in X, Y and Z directions

Tube Length	Direction	Mean (mm)	Lower limit (mm)	Upper limit (mm)	sd/tolerance
Confidence interval	Z	43.42	43.10	43.78	1.90
	X	93.28	93.04	93.52	1.23
	Y	39.02	38.77	39.28	1.26
Tolerance interval	Z	43.42	41.24	45.60	2.18
	X	93.42	91.24	95.60	2.18
	Y	39.00	36.82	41.18	2.18

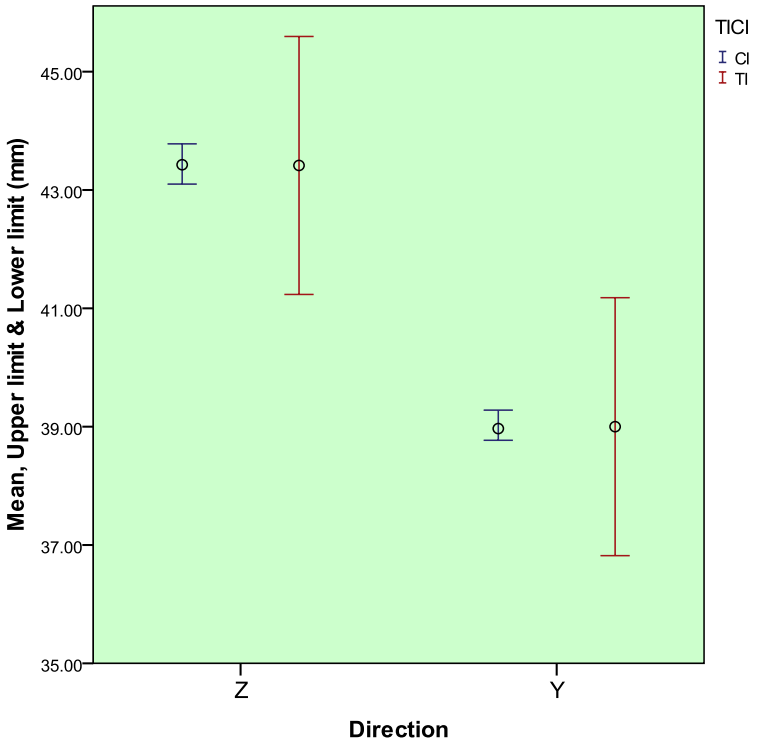

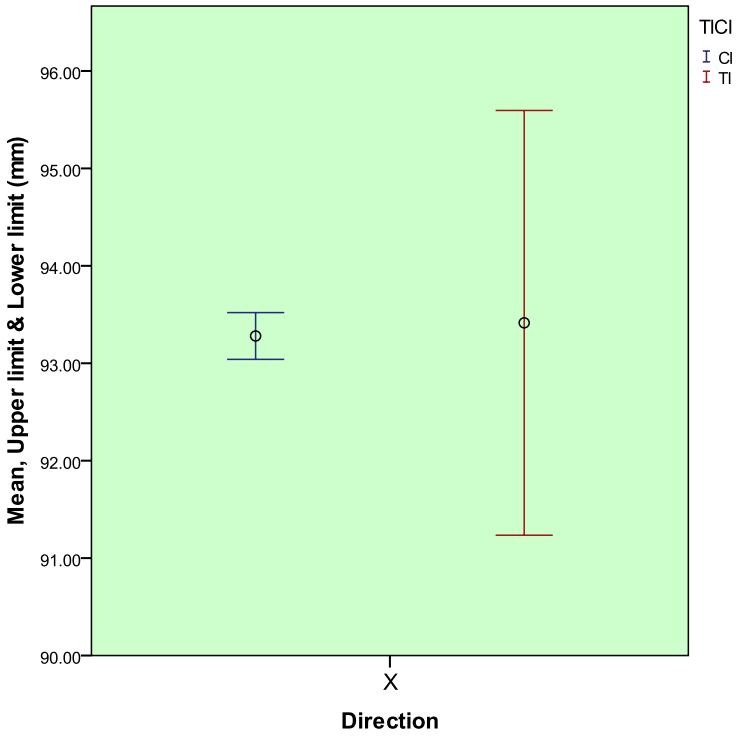

Figure 3-14 : CI and TI for tube length in Z, Y and X directions

3.5 Discussion

The aim of this study was to investigate accuracy and repeatability of MRI in dimensional measurements. This was required in order to be able to examine for possible chemical shift artefact resulting from socket materials. Nine glass marker tubes filled with water doped with 1g/l Copper Sulphate were scanned nine times. Tube lengths were measured in MRI scans and compared to actual values for the accuracy and repeatability of measurements.

The results show accuracy of MRI dimensional measurement. The tube length mean absolute difference was 1.39mm (2.98 %), (min= 0.13mm (0.30 %), max= 5.47mm (14.03%), SD=0.89). Mitsiopoulos et al. (1998) examined the validity of volume estimates by MRI using two phantoms filled with paramagnetic solution. MRI scanning included sixteen images of 10-mm spacing and seven images of 40-mm spacing. MRI and actual value (derived from a volumetric flask) difference was about 3.0% for phantom one and <2.6% for phantom two (Mitsiopoulos et al., 1998). They indicate that when spacing between slices is between 10 and 40 mm, volume can be measured with an error <1%. The mean absolute difference in this thesis is similar to percentage difference in the study by Mitsiopoulos. However, in the phantom study by Mitsiopoulos the slice spacing was bigger than that of this thesis; 10 and 40 mm compared to 1.8mm. In addition they measured the volume of phantoms which had a grade from beginning to end whereas in this study just the length measurement was performed. The volume measurement of phantoms in MRI images with a bigger slice gap could result in more measurement error.

Mean cross-sectional areas of polyvinyl tubes filled with peanut oil were measured in MRI images and then compared with the actual values (Ross et al., 1991). They reported an error of 0.06% ranging from 0.1 to 1.5%. The error in the study by Ross et al. was less than what was found in this thesis.

The accuracy of MRI volumetric measurement was examined using a 17-cm spherical phantom filled with water doped with a gadolinium-based contrast agent as well as a complex anatomically realistic phantom by Byrum et al. (1996). The complex phantom, made of layers of plastic, was filled with fluid to produce contrast

(Byrum et al., 1996). They reported an error of 3% for spherical phantom and 2.5 to 5% error in complex phantom volume measurement. The relatively high difference error in their study compared to this thesis is possibly due to a segmentation process error. In all afore mentioned studies the MRI volume and/or surface area measurements of the phantoms were compared to the actual values whereas in this study the distance measurement was validated. One would expect the MRI error would be higher for surface area and volume measurement because of partial volume effect and the segmentation method.

The measurement error due to different scan repetitions could result from variability in scanner image acquisition or intra-rater inconsistency. The results suggest that the scan-rescan reproducibility is high. The effect of different levels of scan factor (nine scans) on the mean difference of tube length measurement was not significant ($p>0.05$). In examining the inter-scan reproducibility of carotid morphology measurement in eighteen individuals, researchers found no significant difference between repeated scans ($p>0.05$) (Li et al., 2010). Furthermore, the total body adipose tissue measurement of three rats, the researcher found 0.02 ± 0.9(SD) cm^2 difference in two consecutive MRI scans when not removing the animals between trials (Ross et al., 1991). In this thesis scan 4 had the minimum absolute mean difference (Mean=0.004, SD=1.864), and the maximum absolute mean difference relates to scan 7 (Mean= -0.512, SD=1.620).

The tolerance of measurement in this study was ±2.18 mm defined by the voxel dimension. The standard deviation of measurements in x, y and z directions are less than the tolerance limits. The results show that MRI is an accurate and repeatable method for dimensional measurement when using water doped with copper sulphate. In addition, it shows that water tubes can be used as reference land marks for the purpose of examining chemical shift and shape distortion of socket materials in MRI images.

3.6 Summary

Nine glass marker tubes filled with water doped with 1g/l Copper Sulphate were scanned nine times. Tube lengths were measured in MRI scans and compared to

actual values for the accuracy and repeatability of measurements. The results show that MRI is an accurate and repeatable method in dimensional measurement. Distances can be measured using MRI irrespective of the orthogonal directions. Additionally, the position of specimens has no clinical significance on the accuracy of dimensional measurement considering the voxel dimensions.

4 Examination of Suspected Chemical Shift and Shape Distortion of Various Materials Commonly Used in Prosthetic Sockets When Measured Using MRI

4.1 Introduction

The main objective of the overall study is to quantify the socket shape and volume of two different socket designs using MRI. Prior to using MRI in volume and shape quantification of socket designs, the question of whether there is any artefact in the image resulting from commonly used materials in the production of a socket should be answered. The quality of MRI measurements is influenced by artefacts associated to this technology. Artefacts in the form of image distortion and chemical shift are the common types of artefacts in MRI (see section 2.6.)

This experiment was carried out to see whether the common socket materials are visible in the MRI and if so is there any chemical shift and or image distortion in the image

4.2 Methods

To examine for the possible chemical shift of socket material and shape distortion in the image, seven different material specimens commonly used in transtibial socket fabrication were used. These material specimens included; silicone, silicone gel, polyurethane, polypropylene, Pe-lite (closed cell foam), laminate and plaster bandage. Laminate was made from acrylic resin as matrix and layers of perlon stockinet, carbon fibre and glass fibres were used as reinforcement materials. All material specimens were made to fit the plastic container (film container) with a known dimension and placed in the test rig with a known distance from the reference markers prior to insertion into the scanner.

4.2.1 Material Preparation

All containers were symmetrical with a 30mm internal diameter and a height of 48.9 mm, Figure 4-1.Materials were filled in containers in a way that they were in close contact with the wall and bottom of the containers so that the material shape was an

exact replica of the interior shape of the containers. Additionally, the trapped air between the material and container as well as in the material itself was avoided by meticulously stacking material layers together. Air in the material was avoided as it results in regional differences in the magnetic field which cause distortion in adjacent materials or tissues.

Figure 4-1: Cylindrical containers

All "soft" specimens were cut and placed in containers, Figure 4-2. Each container contained only one type of material specimen and was filled to a level higher than the middle of the containers. This provided enough thickness of material in MRI images, in x and z directions, to be able to check for image distortion in at least three slices, see section 4.3.1.1.

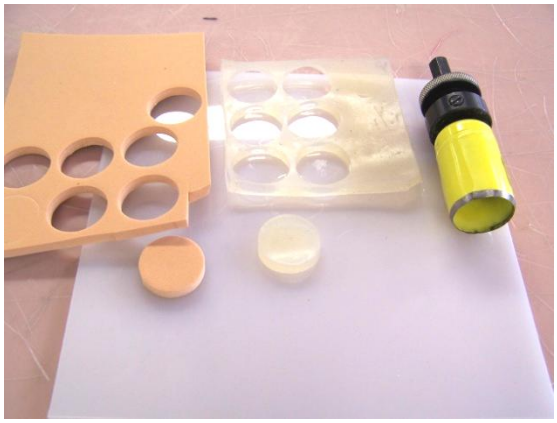

Figure 4-2: Disks of Pe-lite and Polyurethane

In order to make a block of laminate, material commonly used in hard socket fabrication was used. The block was cut and carved to the desired shape and dimension, Figure 4-3. Several pieces of polypropylene sheet were heated and stacked together then carved the same way as laminates, to make a cylindrical shape of this material.

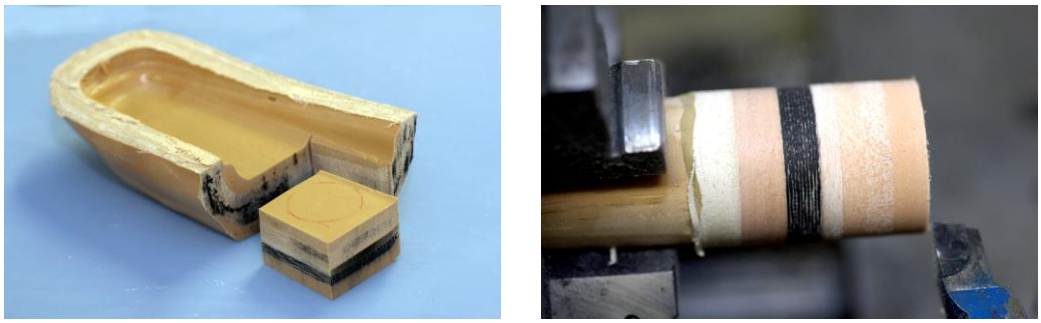

Figure 4-3: Preparing laminate

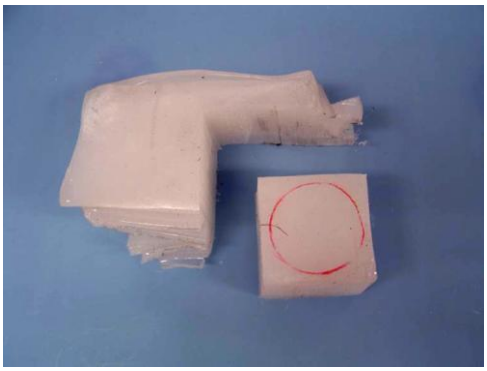

Figure 4-4: Stack of polypropylene

4.2.2 Reference markers

Glass tubes, (L=100mm×Ø=5mm), filled with water were again used as reference markers. One gram per litre Copper Sulphate was used as a contrast agent to increase the intensity of the signal.

4.2.3 Placing Materials Inside the Scanner

In order to place the specimen container and reference tube inside the bore of the scanner in a known distance from each other, a Perspex plate with dimensions of 300

mm ×160 mm was used. Three rows of hole were made on the plate, one in the middle of the plate and one row at each end. The diameters of the holes were in the same size of the exterior diameter of the containers so that the containers would be able to pass through the holes without any wobbling.

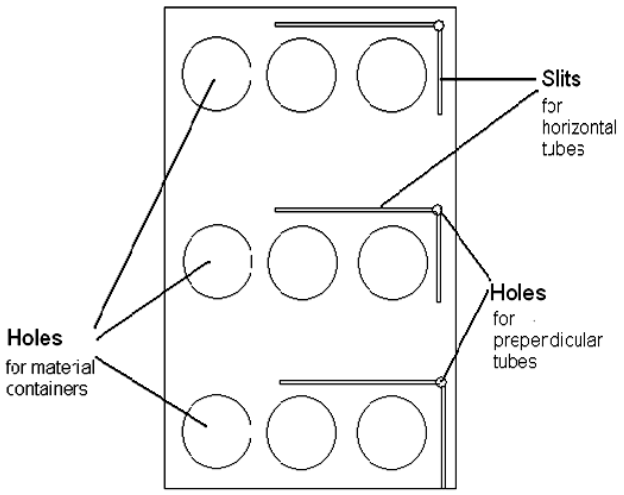

Figure 4-5: Perspex plate with nine holes for containers slits for horizontal marker tubes and three small holes for perpendicular marker tubes

Holes were made using a Deckel CNC machine. The accuracy and validity of the machine was tested and it was shown to have an accuracy of 0.005 mm (Convery et al., 2003). Three perpendicular marker tubes were used for each row of materials. For more information see Section 3.2.1.

In order to keep the plate steady inside the bore of the MRI machine during scanning, a Perspex tube of 326 mm long and 172 mm diameter was used. It would also make it possible to validate a known space inside the scanner defined by the interior volume of the tube, since in the main study when amputees will be recruited the residual limb will be scanned within the same volumetric area. Therefore the behaviour of material within the known volume area of the tube was evaluated. To fit the plate inside the Perspex tube three round acrylic rods (8mm diameter) were used, see Section 3.2.1.

4.2.4 Scanning the Materials

Three containers were filled with plaster bandage before scanning. Since the MRI is based on hydrogen nuclei in water the plaster bandage should be scanned while it is still wet. Plaster bandages used in casting was used for this purpose. In order to increase the signal intensity, water was doped with three different concentrations of copper sulphate of 1g/l, 2 g/l and 3 g/l and then was used to make the plaster bandage wet. The plaster bandage was fitted inside the containers and the excess water was drained and left to cure for 10 minutes before scanning.

Nine places for nine material containers were made in order to scan each material in each location inside the tube. All containers were number labelled from 1 to 9, one for each material. The tube containing all nine containers was scanned nine times. After each running of the scanner the tube was removed from the bore of the machine and all containers were shuffled around to place all materials in all nine locations, Table 4-1. The number code for location and material can be seen in Table 4-1 and Figure 4-6. Therefore, all materials were scanned in all nine locations. The pulse sequence parameters are summarised in Table 4-2.

Table 4-1: Number code table for shuffling the containers

Location / Scans	1	2	3	4	5	6	7	8	9
1	1	2	3	4	5	6	7	8	9
2	9	1	2	3	4	5	6	7	8
3	8	9	1	2	3	4	5	6	7
4	7	8	9	1	2	3	4	5	6
5	6	7	8	9	1	2	3	4	5
6	5	6	7	8	9	1	2	3	4
7	4	5	6	7	8	9	1	2	3
8	3	4	5	6	7	8	9	1	2
9	2	3	4	5	6	7	8	9	1

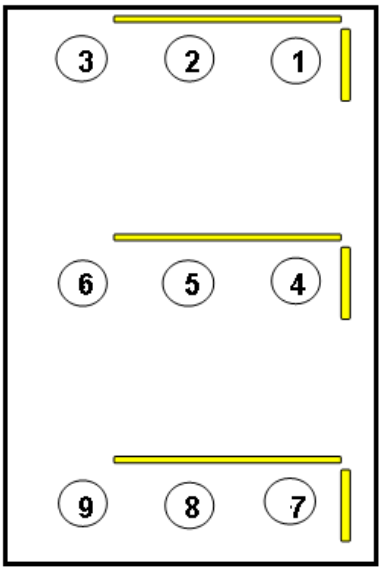

1: Silicone liner
2: Silicone gel liner
3: Polyurethane
4: Polypropylene
5: Pe-Lite
6: Laminate
7: POP+1g/l CU
8: POP+2g/l CU
9: POP+3g/l CU

Figure 4-6: Number code for location of materials

Table 4-2: Pulse sequence parameters

Pulse sequence	FSPGR
Repetition time (S)	6.9
Time of echo (S)	1.5
Inversion time (ms)	500
Bandwidth(KHz)	31.25
Flip angle(Deg)	12
Matrix	256×256
Slice thickness (mm)	1.8
Voxel dimensions (mm)	1.8×1.09×1.09
Number of average	1

4.3 Data Processing

All images was downloaded to Analyze® 7.0 software and then image voxels were resized and finally all slices in all three directions were aligned to reference tubes. For a full description of the process refer to Section 3.3.1.

4.3.1 Measurement

First, distances from the centre of the materials to the reference lines were measured to check for the possible shift in the location of materials. Then, diameters of the materials were calculated from measurements to examine the possible image distortion.

4.3.1.1 Material Measurement in X and Z Directions

For measurement of materials, the calliper feature of the software was set so that its lines were passing through the middle of the reference water tubes. The upper right point of the image wherein two lines meet each other, point A in Figure 3-10, was again chosen as the reference point from which all distances were measured. This point was assumed as the origin of the coordinate system. For a description of the assumed coordinate system refer to Section 3.3.2.1.

The parallel calliper lines were manually set to the counter of the image of each material in x, and z directions, in three slices, the first, middle and the last slices, Figure 4-7. The diameter of the material and the distance from the centre of materials' image to the origin of the assumed coordinate system were calculated. In order to decrease random error the image was viewed in double size.

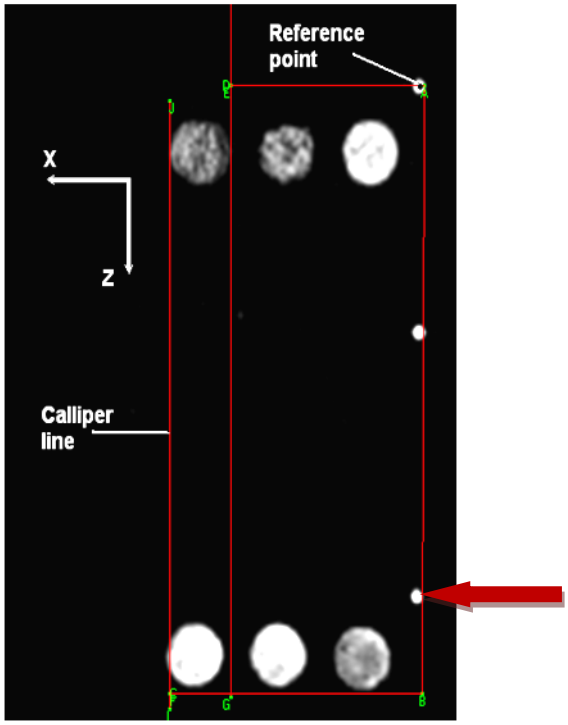

Figure 4-7: Reference point, coordinate system and calliper lines. Red arrow shows a shift in dots due to alignment of tubes parallel to the plate

4.3.1.2 Material Measurement in Y Direction

The same process was done for the y-plane slices. In this plane the bottom border of the material to Z=0 were measured in three slices, Figure 4-8 and Figure 4-9. The materials were highlighted in about 30 contiguous slices. The 10^{th}, 15^{th} and 20^{th} slice of each material was used for this purpose. This gives enough space between slices whilst providing reasonable view of the materials for placing the calliper lines at the bottom border of the image.

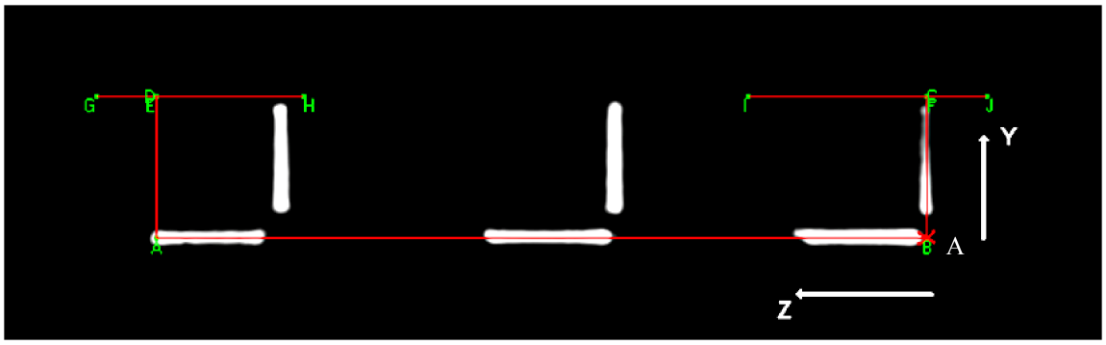

Figure 4-8: Coordinates in zy plane

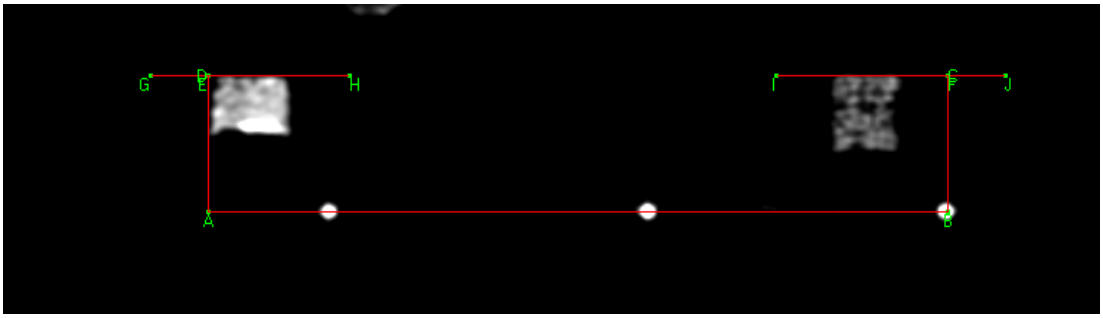

Figure 4-9: placing calliper lines at the bottom border of materials

4.4 Data Analysis

The objective of those experiments was to find whether commonly used prosthetic socket materials are visible in the MRI images and if so is there any spatial mis-registration and/or image distortion of the material in MRI images.

It was found that three material specimens were not visible in the images. Figure 4-10 shows the chromo-depth volume render of the materials in scan 9. For these three materials, Pe-lite, polypropylene and laminates, this occurred because of a lack of unbound atoms in the materials.

4.4.1 Effect of Scan, Slice, Direction and Position on Measurements

Before examining the material location in relation to the reference markers and possible image distortion, the effect of different factors of scan, slice, direction and

position of material inside the scanner on mean of variables was tested using factorial ANOVA and interaction plots. For more details on the test and plot refer to section 3.4.

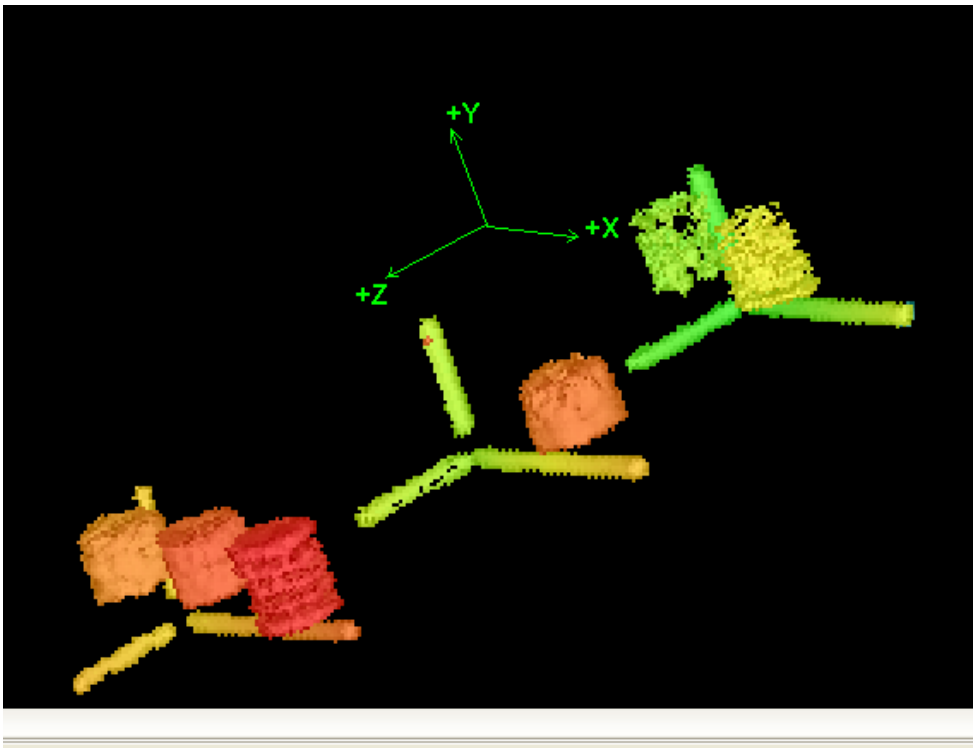

Figure 4-10: 3D chromo-depth volume render of materials

4.4.1.1 Effect of scan, slice, direction and position of material on the mean difference of distance measurements

Difference of MRI value and actual values for the distance of centre of each material to x, y and z reference axis were calculated. Then the effects of factors of scan, slice, direction and position of material in the scanner were tested. The scan factor had nine levels, each level representing one repetition of the MRI scanning. In each scan, material distances were measured in three slices so three levels were considered for each slice factor. Also three levels of direction factors represent the three orthogonal directions of x, y and z. Three positions were allocated for material along each of the x and z directions as shown in the Figure 4-11. Also it shows the position of materials which were visible in each of the nine scans.

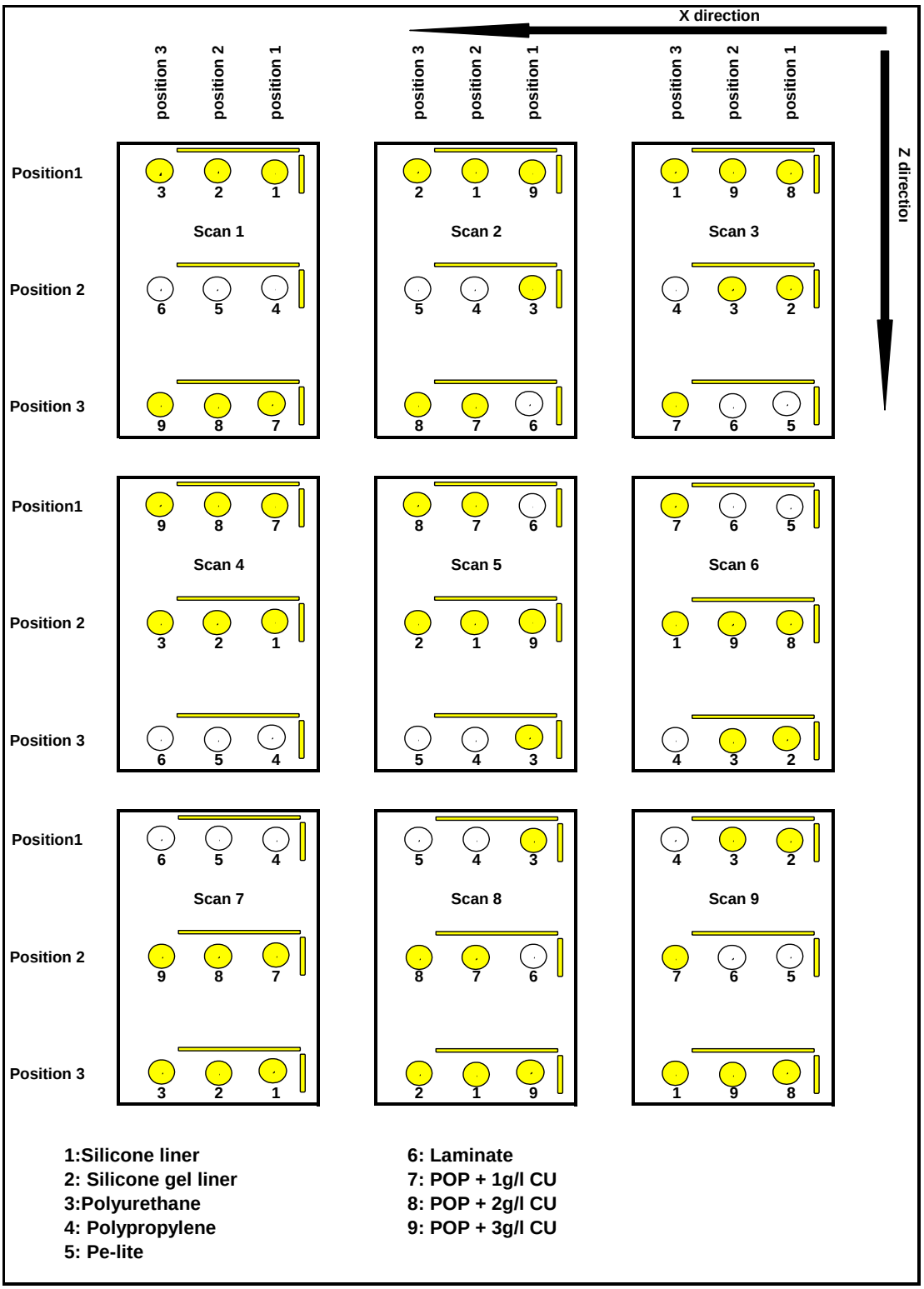

Figure 4-11: Position of materials in x and z directions in all nine scans: materials which were visible in the image are shown in yellow

The mean and standard deviation of distance of materials and the difference between actual values and MRI for different levels of each factor is summarised in Table 4-3.

Table 4-3: Mean and standard deviation for material distance (mm) from reference markers (mm) and difference between actual values and MRI for different levels of each factor

Factor	Factor level	Mean Distance (mm)	Mean difference (mm) (Real value-MRI)	SD
Scan	1	83.363	0.268	1.347
	2	89.791	0.300	1.405
	3	83.163	0.286	1.331
	4	80.055	0.262	1.331
	5	80.623	0.498	1.149
	6	92.599	0.611	0.945
	7	97.278	0.301	1.148
	8	86.532	0.365	1.470
	9	87.549	0.554	1.015
Slice	1	91.062	0.341	1.275
	2	90.857	0.470	1.213
	3	78.398	0.337	1.251
Direction	1=x	63.783	-0.167	1.541
	2=z	145.349	-0.014	0.476
	3=y	51.185	1.331	0.839
Position	1	75.771	0.451	1.195
	2	92.086	0.345	1.302
	3	92.461	0.353	1.243
Material	1	81.465	-0.064	1.330
	2	79.752	0.352	1.204
	3	82.374	-0.042	1.387
	7	84.394	0.725	0.882
	8	97.169	0.558	1.318
	9	95.478	0.769	1.031

The statistical significance of the possible effect of the factors and interaction causational error was analysed using SPSS version 17.0 and summarised in Table 4-4. The results show a significant effect of direction factor on the mean of difference ($p<0.05$).

Table 4-4: Significance results of distance difference

Material distance difference	Significance (p<0.05)
Scan (1 to 9)	0.724
Slice (1 to 3)	0.556
Direction (x, y, and z)	0.000
Position (1 to 3)	0.651
Scan * Slice	0.998
Scan * Direction	0.796
Scan * Position	1.000
Slice * Direction	0.514
Slice * Position	0.789
Direction * Position	0.514

Bonferroni's the post hoc test was conducted on the direction factor. This test breaks down the main effect of this factor by comparing levels in pairs. Table 4-5 summarises the results of the post hoc test. It shows that there is not a significant difference between mean difference in the x and z directions, whereas mean difference in the y direction is significantly different from that of both x and z directions.

Table 4-5: Mean difference and significance of pair level for direction factor

Direction	Mean difference (mm)	Significance (p<0.05)
x * z	-0.153	0.458
x * y	-1.499	0.000
z * y	-1.345	0.000
y * z	1.345	0.000

In the next step the direction-material interaction plot was drawn to see the effect of levels of direction factor on mean difference of materials, Figure 4-12, Table 4-7. The plot shows that material distance was on average overestimated. In other words material was shifted 1.34 mm in the positive y direction. Furthermore, it shows that all POP materials have similar variability in mean difference and differ from elastomeric materials. Polyurethane has a constant mean difference for direction x

and z and increases in direction 3. However, mean differences for all materials lie within the tolerance limits of measurements.

Table 4-6: Mean difference (mm) and standard deviation of each material location measurement in x, y and z directions

Material	X direction		Z direction		Y direction	
	Mean (mm)	SD	Mean (mm)	SD	Mean (mm)	SD
Silicone	-1.010	1.584	-0.197	0.541	1.015	0.693
Silicone gel	-0.214	1.600	0.210	0.542	1.060	1.012
polyurethan	-0.850	1.197	-0.809	0.293	1.531	0.733
POP+1g/l CU	0.630	1.147	0.211	0.658	1.337	0.635
POP+2g/l CU	-0.224	1.639	0.210	0.254	1.690	0.755
POP+3g/l CU	0.666	1.264	0.290	0.291	1.351	0.996

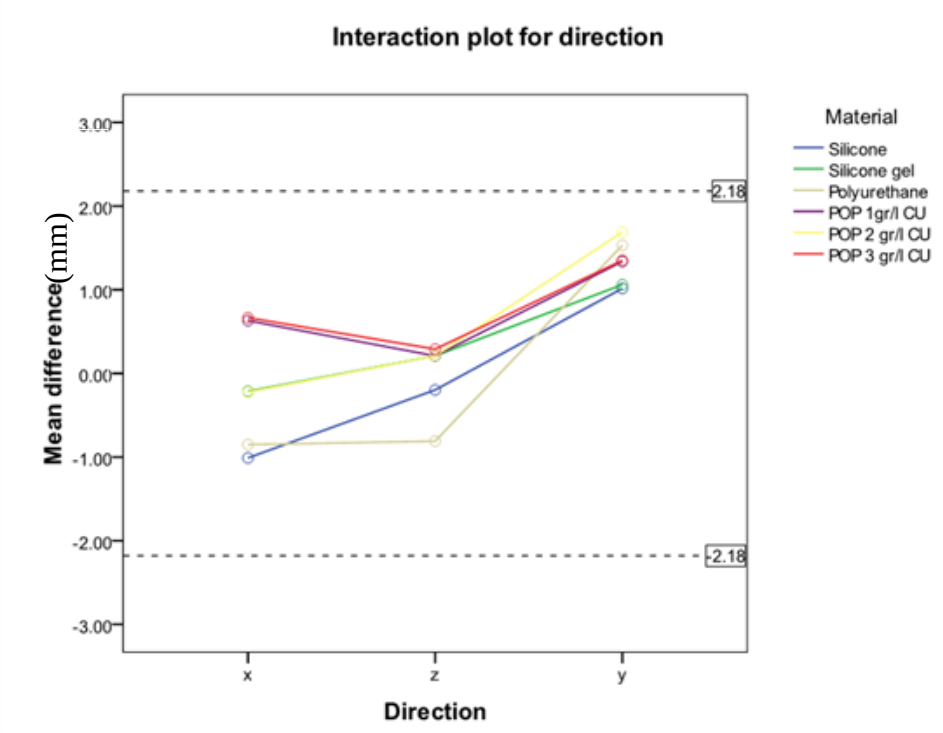

Figure 4-12: Direction-material interaction plot

4.4.1.2 Effect of Scan, Slice and Position of Material on the Mean of Diameter Measurements

It is possible that the centre of the material in the image remains in the same position as the real position whilst the image is distorted in one or two dimension images. Therefore, to examine for the possible image distortion, the diameter of material images in two directions of x and z were calculated and compared to actual values. In the first stage, same as for the centre of materials, the effect of factors of scan, slice, direction and position were evaluated. Factor levels were the same as for the material distance measurement except that the direction has two x and z levels.

The mean and standard deviation of distance of materials and the difference between actual values and MRI for different levels of each factor is summarised in Table 4-7.

Table 4-7: Mean and standard deviation for material diameter (mm) from reference markers (mm) and difference between actual values and MRI for different levels of each

Factor	Factor level	Mean diameter (mm)	Mean difference (mm) (Real value-MRI)	SD
Scan	1	29.049	0.950	1.701
	2	30.475	-0.475	1.593
	3	29.800	0.199	1.952
	4	29.653	0.346	2.036
	5	30.559	-0.559	1.580
	6	30.018	-0.018	2.097
	7	30.574	0.574	1.787
	8	29.888	0.111	1.499
	9	29.745	0.255	1.900
Slice	1	29.721	0.278	1.730
	2	29.988	0.011	2.095
	3	30.211	-0.211	1.663
Direction	1=x	29.935	0.064	1.950
	2=z	30.012	-0.012	1.737
Position	1	29.831	0.168	1.817
	2	30.112	-0.112	1.861
	3	29.978	0.022	1.861
Material	1	29.446	0.553	1.204
	2	28.112	1.887	2.002
	3	30.240	-0.240	1.925
	7	30.302	0.302	1.318
	8	30.888	-0.888	1.455
	9	30.852	-0.852	1.443

The statistical significance of the possible effect of different levels of factors on mean diameter, using factorial ANOVA, is summarised in Table 4-8. The results show that there is not any significant effect of scan, slice, direction and position factors on the mean of diameter measurements.

Table 4-8: Significance results of diameter difference

Material diameter difference	Significance (p<0.05)
Scan (1 to 9)	0.104
Slice (1 to 3)	0.373
Direction (x and z)	0.223
Position (1 to 3)	0.707
Scan * Slice	0.662
Scan * Direction	0.283
Scan * Position	0.107
Slice * Direction	0.160
Slice * Position	0.672
Direction * Position	0.941

4.4.2 Comparing MRI Measurements to Actual Values

In order to check for possible chemical shift of materials in MRI, the distance from the centre of the materials to the reference tubes measured using MRI was compared to actual values. Then to examine for image distortion the diameter of materials was compared to the real diameter.

4.4.2.1 Comparing the Distance of Material Measured by MRI to Actual Value in X, Z and Y Axis

The Bland & Altman plot was plotted for each material-direction. As a result for each material two Bland & Altman plots were drawn; one for each of the x and z directions. The Bland & Altman method is used to compare two measurement techniques (Bland and Altman, 1986). In this method the difference of two methods is plotted against the average of two methods. Horizontal lines are drawn at the mean difference and at the mean difference plus and minus 1.96 times the standard deviation of the differences (mean+/-1.96sd). 95% of the data should lie between the agreement limit (mean+/-1.96sd) if the distribution of the differences is normal and scatter randomly around the mean line. The Bland and Altman plot graphically shows the agreement between a new measurement technique and the old established

method. The used of correlation coefficient may be inappropriate as it measures the correlation between methods rather the agreement.

The Bland & Altman plots of distance of the centre of the materials from the reference markers were created (Appendix, Figure 13-1 to Figure 13-12). In Bland and Altman plots relating to the location of materials in x direction, the difference values were scattered randomly around the mean difference line and no noticeable trend was observed. In the z direction, the difference values spread in three vertical columns because there were only three actual values, each relating to one position of materials, hence; this trend could not be related to the measurement technique.

4.4.2.2 Comparing Diameter of Materials Measured by MRI to Actual Value in XY-Plane

To compare the MRI mean diameter of materials to the real mean values the confidence intervals of all materials in both x and z directions were calculated, Table 4-9, and were compared to the tolerance of measurements, Figure 4-13 and Figure 4-14. The real diameter for all materials was 30 mm and the upper and lower tolerance limits were 32.18 and 27.82 mm respectively.

Results show that the diameters of silicone and POP+1 g/l CU do not have a difference from the actual value in the Z direction, and in the x direction CI of silicone and all three different copper sulphate concentrated Plaster of Paris remain within the tolerance limit.

Table 4-9: Mean and confidence & tolerance limits for diameter of material in x and z direction

CI	Material	Mean (mm)	Upper Limit	Lower limit	SD
Z direction	Silicone	30.06	29.64	30.48	1.06
	Silicone gel	28.15	27.57	28.72	2.46
	Polyurethane	29.32	28.69	29.96	1.6
	POP+1g/lCU	30.42	29.88	30.97	1.35
	POP+2g/lCU	31.11	30.58	31.64	1.33
	POP+3g/lCU	30.99	30.34	31.65	1.65
X direction	Silicone	28.83	28.42	29.23	1.01
	Silicone gel	28.07	27.09	29.04	2.46
	Polyurethane	31.15	30.44	31.86	1.8
	POP+1g/lCU	30.18	29.67	30.69	1.28
	POP+2g/lCU	30.66	30.05	31.28	1.56
	POP+3g/lCU	30.7	30.22	31.18	1.21

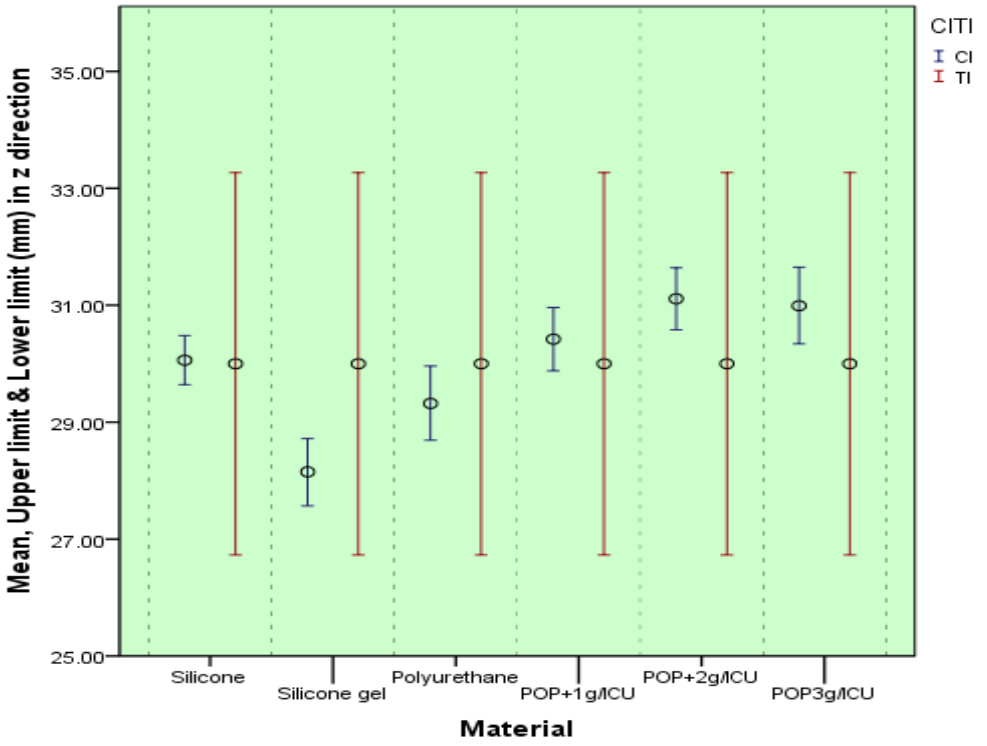

Figure 4-13: Mean and confidence & tolerance limits for the diameter of the material in z direction

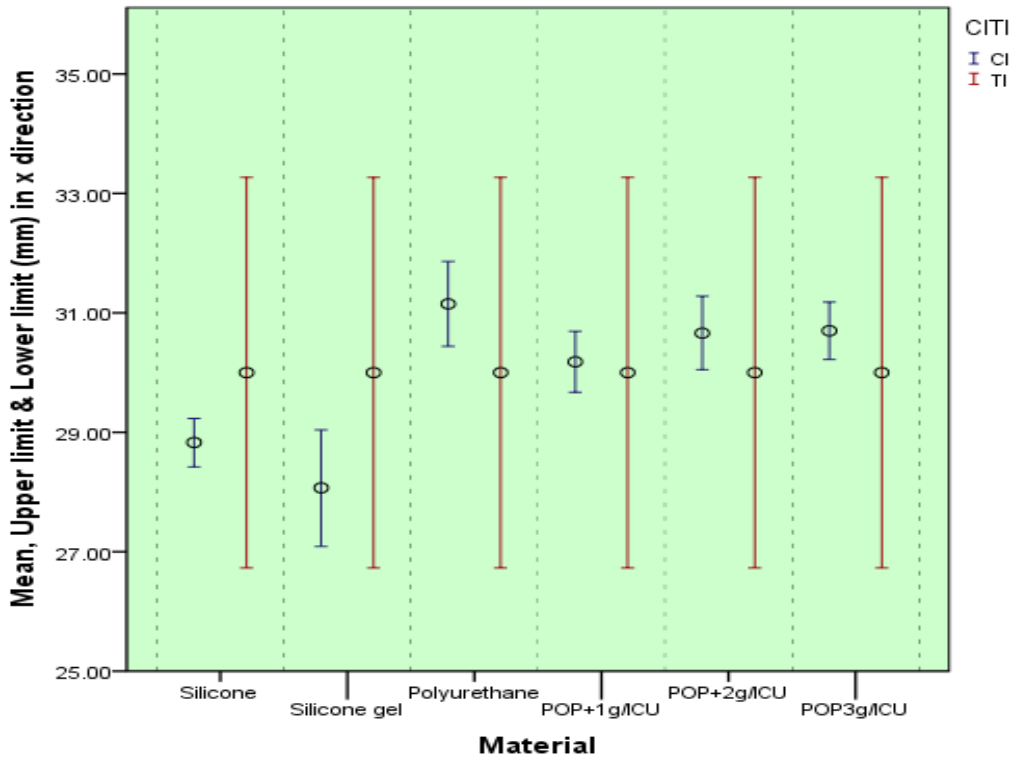

Figure 4-14: Mean and confidence & tolerance limits for diameter of material in x direction

4.5 Discussion

This experiment was conducted because of the main concern of MRI artefacts, mainly chemical shift, resulting from common socket material on MRI images. This occurs as a result of differences in resonance frequency of the same nuclei in different molecular environments due to them experiencing different amounts of the magnetic field. In a previous study, the processing frequencies of silicone (breast implant), water and fat were measured using proton MRI spectroscopy as 2175, 2550 and 2250 Hz respectively (Steinbach et al., 1992). Almost the same results were found for spectroscopic analysis of frequency difference between water, lard and silicone vitreous ocular implant (Bash et al., 1995). They showed 220 Hz frequency difference between water and lard and 80 Hz frequency difference between lard and silicone.

Previous research has reported a chemical shift artefact on T1-weighted, T2-weighted and proton density MRI images of breast silicone implant phantoms (Steinbach et al., 1992). They showed the chemical shift artefact on T1-weighted MRI images was minimal relative to the T2-weighted images. In a phantom study of silicone fluid polymer and silicone lubrication oil, Bash et al. found chemical shift on both T1-weighted and T2-weighted images with more prominence on the T2-weighted image (Bash et al., 1995). The amount of chemical shift depends on the magnetic field strength and the selection of pulse sequence bandwidth (Bash et al., 1995, Smith et al., 1990). Chemical shift may increase by increasing the magnetic field strength and decreasing the sequence bandwidth.

In this study the measured chemical shift of silicone was -1.010, -0.197 and 1.015 mm in x, z, and y directions respectively. The silicone gel showed x=-0.214, z=0.210 and y=1.060 mm chemical shift and for polyurethane this was -0.850, -0.809 and 1.531 mm in x, z and y directions respectively. The absolute shifting of material for all material including different CS concentrate POP was <1.7mm. This was not significant considering the measurement tolerance of ±2.18 mm and Bland & Altman plots. This is in agreement with a pilot study by Buis et al. in which no detectable chemical shift of silicone (used for prosthetic liners) was reported (Buis et al., 2006).

For all materials the x and z diameters were measured accurately within the tolerance limits POP with all three different concentrations of CU diameter was slightly overestimated by MRI in both x and z directions. The overestimation was worse for POP with higher amounts of CS (2mg/l and 3mg/l) because the signal intensity increases more if more contrast agent is used. This results in over-projection of the section thickness i.e. more voxels light up at the boundary of the object (Gadeberg et al., 1999). Silicone gel diameter was underestimated in MRI and polyurethane diameter was underestimated in the y direction but overestimated in the x direction. However, the silicone diameter measurement was within the tolerance limit with a relatively small standard deviation, Table 4-9, Figure 4-13 and Figure 4-14. This shows there is no significant over- or under-projection of the silicone.

4.6 Summary

This experiment was carried out to ascertain the common socket materials are visible in the MRI and if so is there any chemical shift and or image distortion in the image. In comparing the socket concept the boundary between the residual limb and casting material needs to be detected. All MRI measurements in this experiment were based on the boundary of materials, and it was suggested, based on the results of this study, that materials which were measured more accurately in diameter within the remit of tolerance of measurement, e.g. Silicone and POP+1 g/l CU, would be used for subsequent experiments.

5 Accuracy of Animal Soft Tissue Volume and Surface Area Measurement Using MRI

5.1 Introduction

The accuracy of soft tissue shape and volume measurement using MRI needs to be defined. Main factors which can influence the accuracy of MRI include image voxel size, pulse sequence and the image segmentation process, see Chapter 2. In this experiment animal specimens were used to check for the accuracy of MRI dimension, surface area and volume measurement when using POP and silicone.

5.2 Methods

To examine the accuracy of dimensional measurements using MRI, dimensional measurements in MRI were compared to the actual values in specimens. Since the chemical shift resulting from subcutaneous fat influences the accuracy of dimensional measurements, the specimen needed to contain skin. Therefore, for the purpose of this study a leg of pork with skin was used.

MRI takes images in the form of slices in which dimensions and surface area of the cross sections of the specimen can be measured. Furthermore, because of the 3D format of MRI images the volume of the specimen can also be measured. The volume and surface area values need to be compared with the corresponding actual values of the specimen. Therefore, it is necessary to accurately relate the MRI slices to the real life cross sections and volumes of specimens. To do so, a number of sections of a leg of pork, with different diameter and size, were sandwiched between Perspex sheets. After wrapping silicone and/or plaster of Paris around the circumference of the specimens, two cross sections of the specimens were photographed and then scanned using MRI. Consequently, the photographs of cross sections were related to the corresponding MRI slices for measurement comparisons. In addition, volumes of specimens were measured using the water suspension method and then compared to MRI volume measurement.

5.2.1 Preparing Animal Specimen

The boundary detection of the subject is important for dimensional measurements. The accuracy of boundary detection of skin in MRI depends on the signal intensity difference of the skin to the surrounding materials. In the Patella Tendon Bearing casting concept just the POP will be used, whereas, in Pressure Cast the limb is surrounded by silicone and then POP covers the silicone liner. The signal intensity of silicone and POP+1gr/lit Copper Sulphate was measured in MRI images in the first experiment. The silicone has 1.5 times stronger signal intensity in MRI than fresh POP doped with 1gr/lit copper sulphate. Therefore, there is a possibility that the materials around the limb influence the skin boundary detection, hence affect the dimensional measurements.

In order to examine the accuracy of MRI measurements, the skin should be segmented once surrounded with silicone and then with POP. Also, in order to test the possible effect of diameter and size of specimen on accuracy of measurements, three different diameters of animal leg sections were used; small, medium and large. As a result, six pieces with different diameters were prepared. Since sections of animal specimens needed to be sandwiched between two Perspex sheets, sections were cut with enough thickness for wrapping the silicone and POP easily after placing between two Perspex sheets. For this purpose six pieces of frozen leg of pork were cut in slices with 46mm thickness. Two cross sections of each slice of each specimen were parallel to each other to make close contact with the Perspex sheets.

5.2.2 Preparing Perspex Sheets

Animal specimens were sandwiched between two transparent sheets so that photographs of the cross section could be taken, Figure 5-1. Perspex is a transparent material; however, there is a possibility of it influencing MR images of meat. Magnetic susceptibility difference between adjacent substances inside the magnetic field results in microscopic gradients or variation in the magnetic field strength near or across the interface of two materials. This artefact, known as ‘susceptibility artefact,’ results in bright and dark areas with spatial shifting of surrounding material. To eliminate the susceptibility artefact it was suggested to use a material

which has the same magnetic susceptibility as water. Perspex is a substance which can be used for this purpose (Moerland et al., 1995).

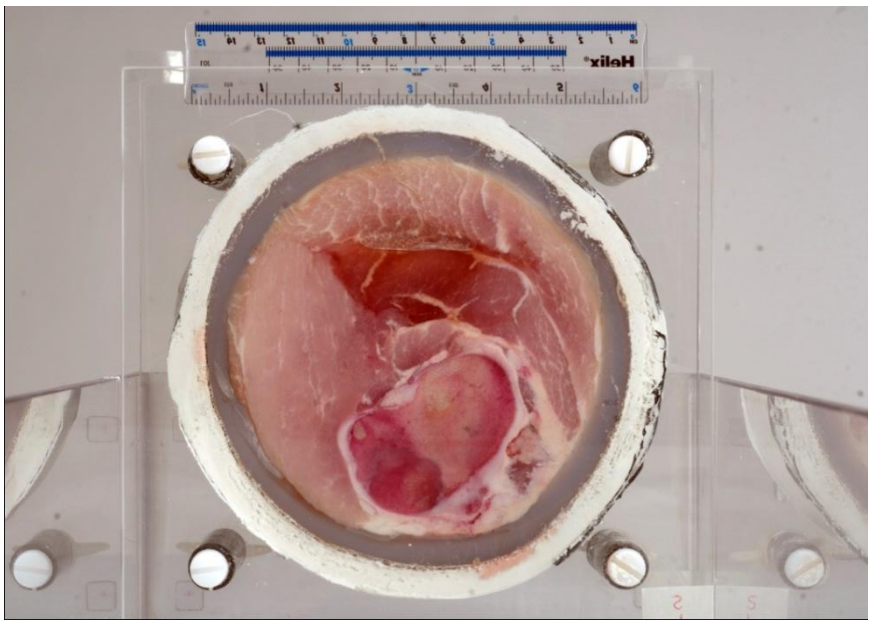

Figure 5-1: Animal specimen within a Perspex rig

Twelve Perspex sheets were prepared. Two Perspex sheets were used for each specimen. In each specimen one of the Perspex sheets again contained two marker tubes (100mmL × 5mmØ) perpendicular to each other as reference markers in MR images, Figure 5-2. The marker tubes were filled with water doped with 1 gr/lit copper sulphate. A ruler was also attached to the surface of the Perspex sheet for magnification correction of photographs. In order to avoid the focusing artefact in photographs, the ruler was attached to the same surface of the Perspex sheet which was in close contact to the cross section of the soft tissue

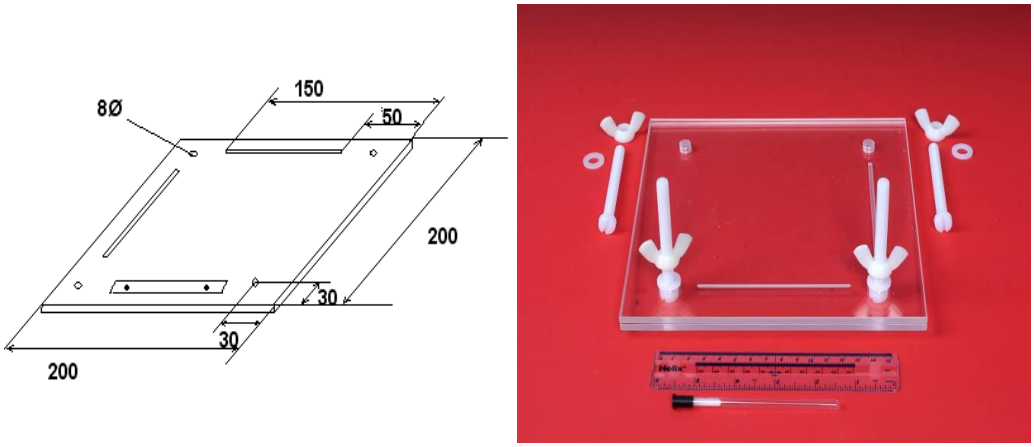

Figure 5-2: Perspex sheets; left: dimensions of the Perspex sheets, right: Perspex sheets, plastic screws & nuts and glass tube

5.2.3 Placing Animal Soft Tissue Specimen Between Perspex Sheets

Two sets of three different diameters - small, medium and large - animal leg sections were prepared, each set for each casting concept, PTB and P-Cast. Therefore, three sections of animal specimen were wrapped with POP which had been wet by water doped with 1gr/lit Copper Sulphate and next, three other sections were covered with a ring of silicone liner and then wet POP.

Two Perspex sheets were placed on the table of a drill while four carbon fibre poles, 46 mm in length, were placed between the Perspex sheets. The chuck of the drill was lowered down until it was in close contact with the upper Perspex sheet and then the drill's chuck screw was adjusted in this position. Then, the poles were removed and a piece of meat was placed between the Perspex sheets and the chuck was fixed at the previous position. This made it possible to wrap plaster without interruption from the poles. Then the POP was wrapped tightly so that the soft tissue was in close contact with the Perspex sheet, Figure 5-3**.** Before the POP was hardened the poles were returned to their place and then two Perspex sheets were fixed together using four plastic screws and bolts in each corner of the Perspex sheets. Three pieces of meat

were wrapped with POP and the other three with silicon liner rings and then POP using this method.

All specimens were prepared a day before scanning to prevent the POP from drying, and all wet POP were covered with plastic sheets and adhesive tape to isolate them from air exposure. Therefore, the POP kept wet until the scanning time.

Figure 5-3: Wrapping POP using a drill

5.2.4 Photography

The cross sections of all specimens were photographed so that the surface area of meats could be measured and compared with that of MRI measurements. To avoid any distortion in photographs the camera lens was placed in line with the centre of the specimen with no angle. Also the camera was at the same distance for all specimens. To do so a rig and a grid were made.

The rig was a box 200 mm wide so that the Perspex sheets could fit inside. It was 600mm long. For positioning the camera lens, a grid was made and placed at one end of the rig for adjusting the location of the camera, Figure 5-4. Then the specimen was placed at the other end. In this way the camera was always at the same distance and in the same position for all images. Also using the grid the angle of the camera lens was adjusted so that its centre was in the same line as the centre of the specimen. After adjusting the position of the camera, the angle of the camera was double checked using the grid inside the field of view of the camera so that it was parallel to the surface of the phantom.

Each surface of meats was given a three-letter code, Table 5-1. The first letter stands for POP or silicone in which P refers to POP and S to silicone. The second letter refers to the diameter of the slice of meat; L, M and S refer to large, medium and small respectively. Since there were two surfaces available for photography, one was coded as A and other one was B. The cross section of meat which was facing the water marker tubes was coded as A in all cases for the purpose of consistency.

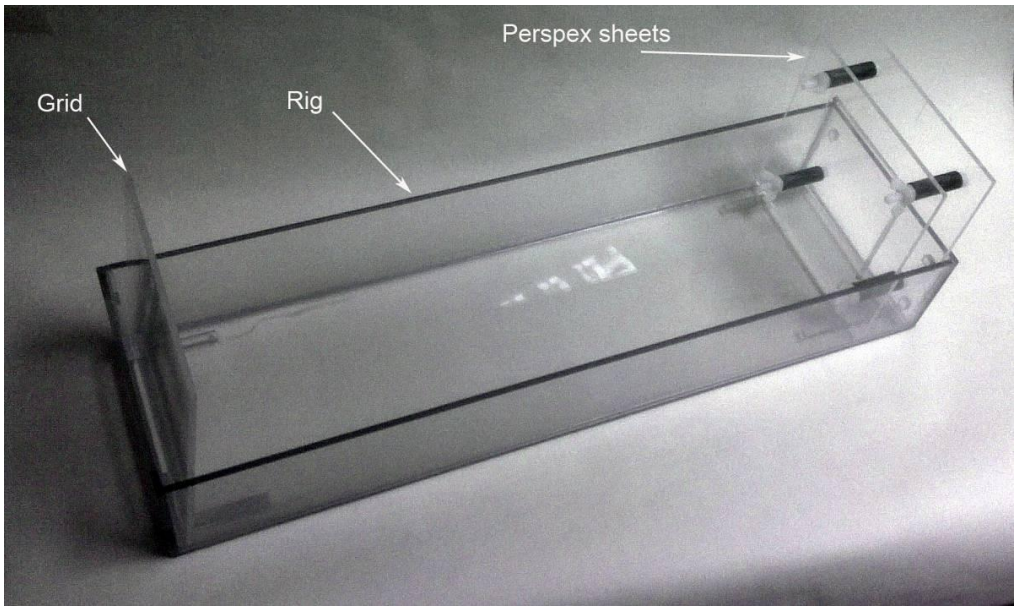

Figure 5-4: Grid used for adjusting of angle and distance of camera from specimens and consistent photography of all specimens

Table 5-1: Letter codes for each cross section of the specimens

Size	POP		Silicone	
	Surface facing to marker tubes	Surface facing opposite to marker tubes	Surface facing to marker tubes	Surface facing opposite to marker tubes
Large	PLA	PLB	SLA	SLB
Medium	PMA	PMB	SMA	SMB
Small	PSA	PSB	SSA	SSB

5.2.5 MRI Scan

The same MRI pulse sequence as the first experiment was used for this experiment. However to get the best resolution the leg of a normal person, (the author), was scanned for a reasonable resolution within eight minutes time. The leg was covered with silicone liner and then wrapped with POP doped with 1gr/lit copper sulphate. It was shown that within eight minutes and twenty eight seconds the smallest achievable voxel size is 1.17×1.17×0.6 mm with slice thickness of 1.2mm by scanning 300mm length of the limb. The imaging protocol is summarized in Table 5-2.

Table 5-2: Pulse sequence

Pulse sequence	Sagital FSPGR
Repetition time(S)	6.9
Time of echo(S)	1.5
Inversion time(ms)	500
Bandwidth(KHz)	31.25
Flip angle(Deg)	12
Matrix	256×256
Voxel	1.17×1.17×0.6
FOV(cm)	30
Slice thickness(mm)	1.2
Number of average	1

5.2.6 Real Measurements

The surface area of phantoms was required to be measured in photographs and then compared to surface area measurements using MRI. To examine the accuracy of measurements in photographs, diameters of each specimen were measured in x and y directions in both surfaces at the midpoint of the Perspex sheets, black cross hairs in Figure 5-5, using a digital vernier calliper. Then, these measurements were compared to the measurements from the photographs.

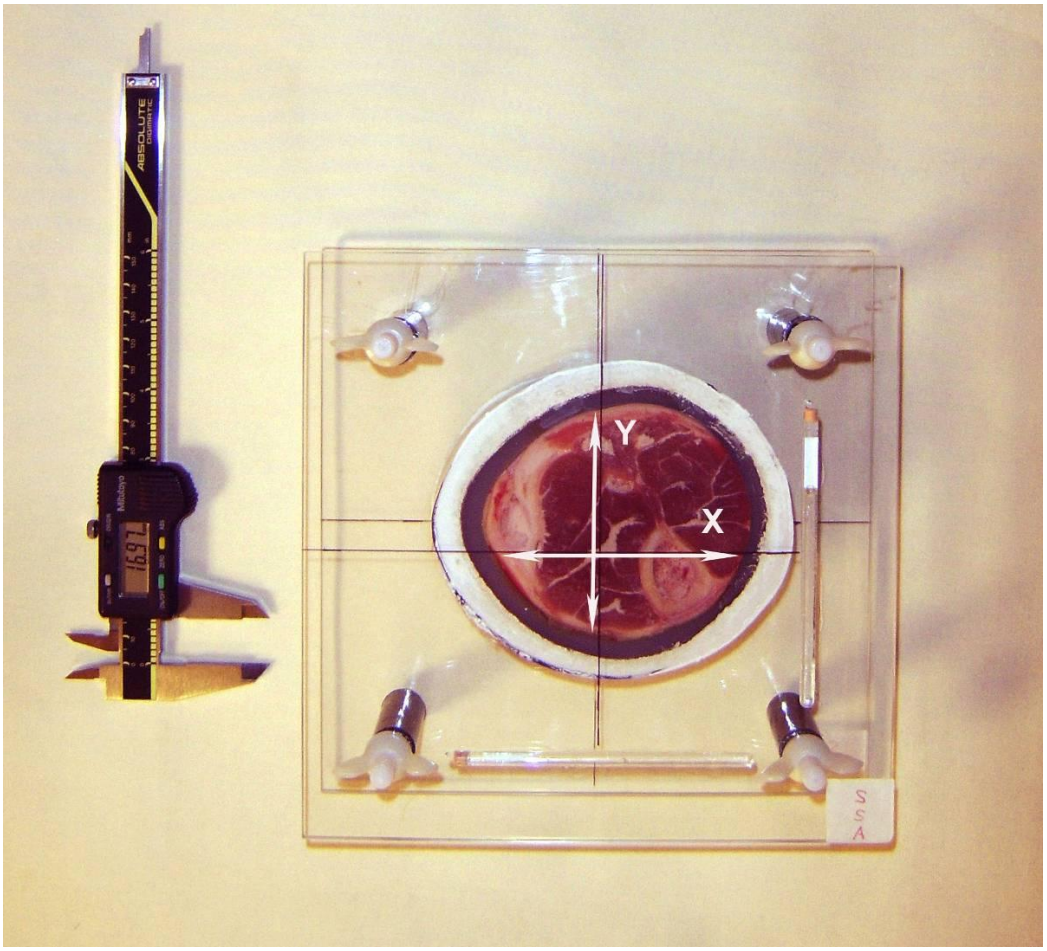

Figure 5-5: X & Y diameter measurements of cross sections of meats

5.2.7 Volume measurement

Since the volume of different socket concept is of interest, volume measurement accuracy needs to be examined. After MR imaging, the volume of all specimens were measured using the water suspension technique. Animal specimens were not frozen during this procedure.

The suspension technique used here involves the suspension of an object below the surface of the water, using a string, in a container placed on an electronic scale. The scale had an accuracy of 1gram, Figure 5-6.

To a first approximation, the volume of the immersed object is simply the increase in weight divided by the density of the fluid.

$$V = \frac{\Delta \omega}{\rho}$$

Where ρ is the measured density of water and Δw is the difference of water before and after suspension of the object. Since the density of water is one unit, the volume of the object is equal to the increase in the water weight after suspending the specimen.

Figure 5-6: Volume measurement using water suspension method

5.3 Data Processing

5.3.1 Processing and Measuring Photographs

All photographs were downloaded to Adobe Photoshop CS3 Extended software. Using the Photoshop Extended Measurement feature it is possible to measure any area defined with the ruler tool or with a selection tool, including irregular areas selected with the lasso, quick select or magic wand tools. Additionally, it has a measurement scale feature which sets a specified number of pixels in the image equal to a number of scale units, such as inches, millimetres, or microns. Once a scale is created, it is possible to measure areas and receive calculations and log results in the selected scale units.

After downloading images to the software, each image's contrast and colour was automatically adjusted. Then, using the measurement scale feature, the scale was

adjusted using the image of a ruler in each photo and then diameters and surface area of meats were measured in all photographs, Figure 5-7

Meat diameters were measured in both x and y directions at the mid point of the Perspex sheets, red cross hairs in Figure 5-7. Afterwards, the boundary of meat was traced using the Magnetic Lasso tool. The Magnetic Lasso tool is especially useful for quickly selecting objects with complex edges set against objects with different contrasts. Edges were refined further to adjust for errors in boundary selection. At the end, the surface area of the meat was given by the software.

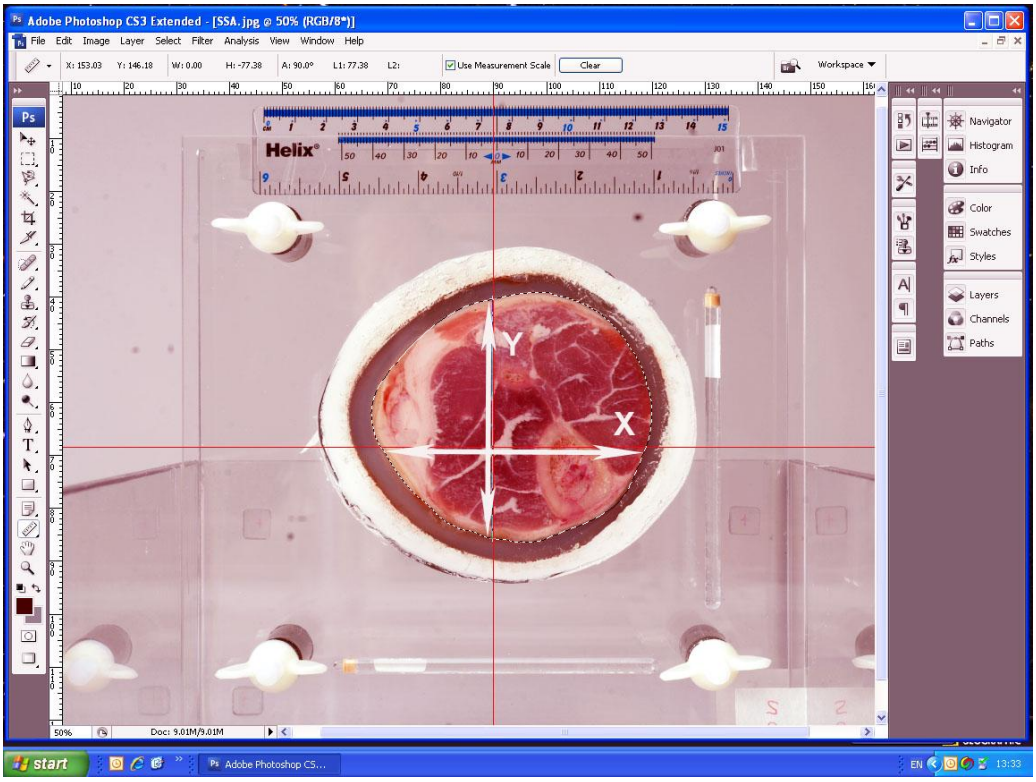

Figure 5-7: Diameter and surface area measurement of phantoms cross sections using Adobe Photoshop Extended.

5.3.2 Measurements Using MRI

All MRI data was in the DICOM format and transferred to the Analyze software. The MRI machine takes images of the body in the form of slices. This single slice

information is filed in Digital Imaging and Communications in Medicine (DICOM) format. The scanning consists of a sequence of 2D slices which together make a volume of the section.

All files were downloaded as a separate volume in the main work space of the software. Since the voxel - the smallest part of each slice- dimensions are not the same in all directions, the generated volume was extended in one direction and compressed in other. To deal with this issue the software is capable of resizing the voxel size to a cubic shape. Therefore, the downloaded volume was the same size as the real life specimen. In the next step, since the phantoms were not exactly parallel to the long axis of the bore of the scanner, all slices were aligned parallel to the reference water tubes. This makes slices parallel to the surface of the cross section of the meats so that the slice which corresponds to that of the photographs could be chosen. Before doing any measurement the region of interest in all slices were segmented.

5.3.2.1 Segmentation

The Analyze software does the segmentation of the object manually, automatically and semi-automatically. The automatic segmentation applies thresholding, morphology erosion and dilation with a region growing steps in an attempt to automatically segment an object within a volume. Since the signal intensity of the subcutaneous fat and the silicone liner are close to each other, automatic segmentation was not applicable because software cannot differentiate between these two parts to hit the boundary. Therefore, a semi-automatic segmentation was chosen.

To do the segmentation, a seed point was placed within the area of interest in the first slice of the volume and then the threshold was set so that the boundary was detected automatically. If there was an error in borders it was corrected using the edit tool. This procedure was repeated for each slice of the whole volume, Figure 5-8. Then, segmented slices were saved as an object map, Figure 5-9.

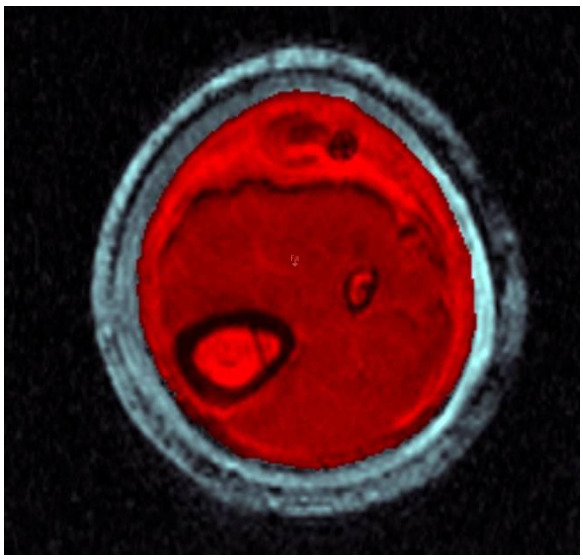

Figure 5-8: Semi-automatic segmentation of meat in each slice

.

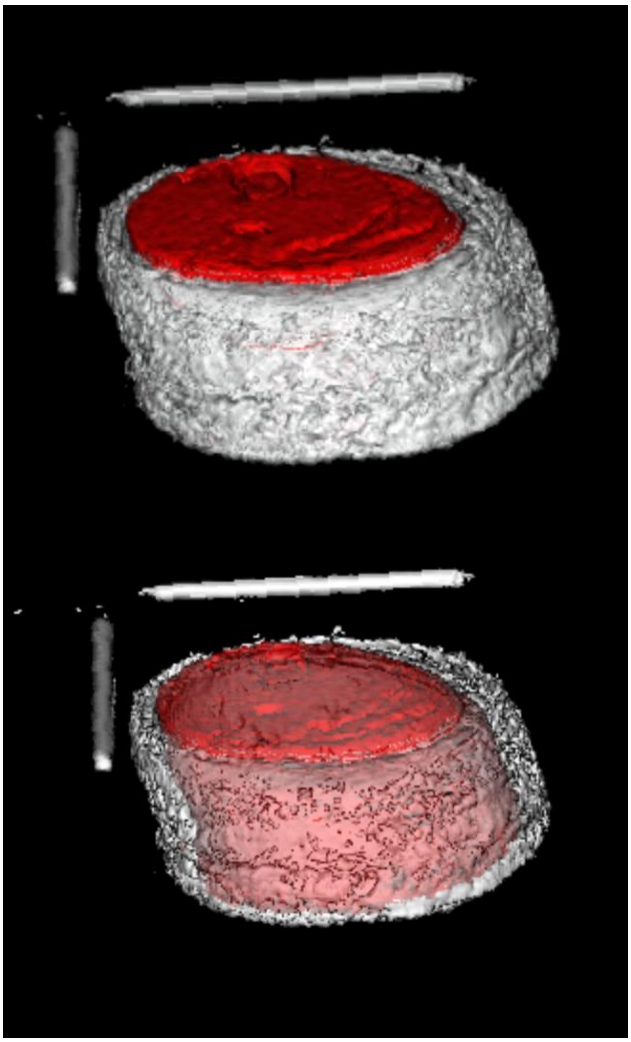

Figure 5-9: Volume render object map of meat

5.3.2.2 Volume and Area Measurement

In order to measure volume of specimens and the surface area of the meat in the first and last slice both the original volume and object map was downloaded at the same time in the software. Using the Measure Tool, the volume of the region of interest was measured. This provided value for the whole volume as well as individual slices.

5.3.2.3 Diameter Measurement

Diameters of each cross section of meat were measured in MR images. In order to measure the diameters at the same location as the photos, i.e. at the centre point of the Perspex sheets, the calliper lines of the Analyze measurement tool were placed at the centre of the marker tubes, perpendicular to the corresponding tube, Figure 5-10. Then the diameter in x and y directions were measured in the first and last slice of each volume, Figure 5-11.

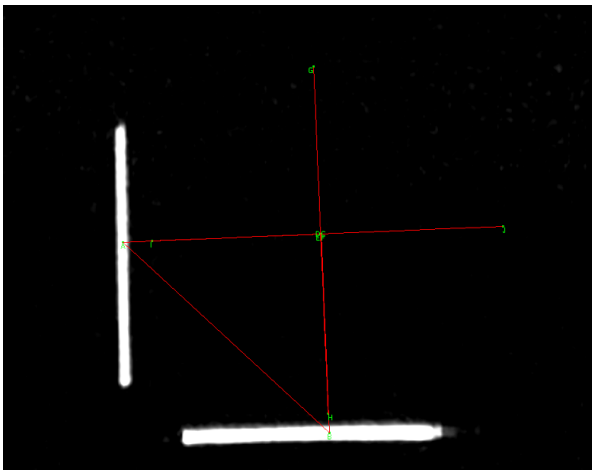

Figure 5-10: Setting calliper lines to the centre and parallel to the reference water tubes

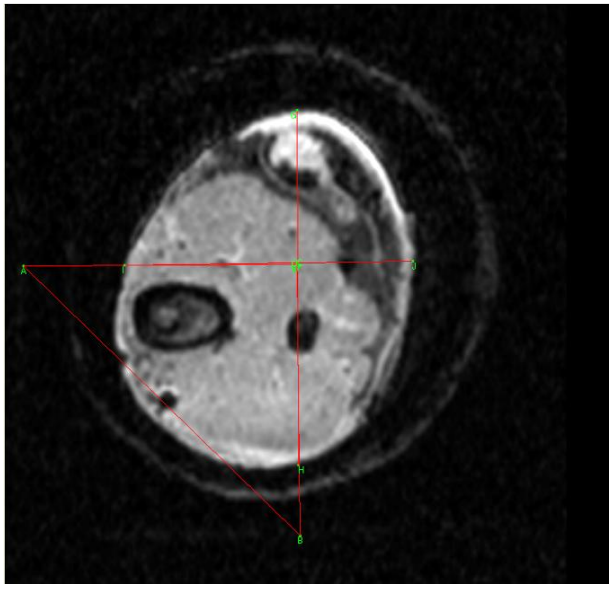

Figure 5-11: Diameter measurements using the calliper lines

5.4 Data Analysis

In order to measure the accuracy of MRI soft tissue measurements, MRI data was compared to the data from photos. Although there was a ruler in the photos for scaling purposes, diameter measurements were taken from each specimen in vivo to examine for accuracy of measurements using the Adobe Photoshop software. The Bland & Altman plot was used for the comparison of two different measurements.

5.4.1 Comparing Real and Photo Diameter Measurements

The mean difference of real diameter measurements and those of the photo diameter was 0.18mm (0.17%) with standard deviation of 0.90 mm and in which the measurements from the photos were overestimated. The minimum and maximum measurement differences were -1.67 (-1.65%) and 1.31 (1.29%) respectively. The difference of measurements was plotted against the average of two measurements. No noticeable trend can be observed in the Bland & Altman plot, Figure 5-12.

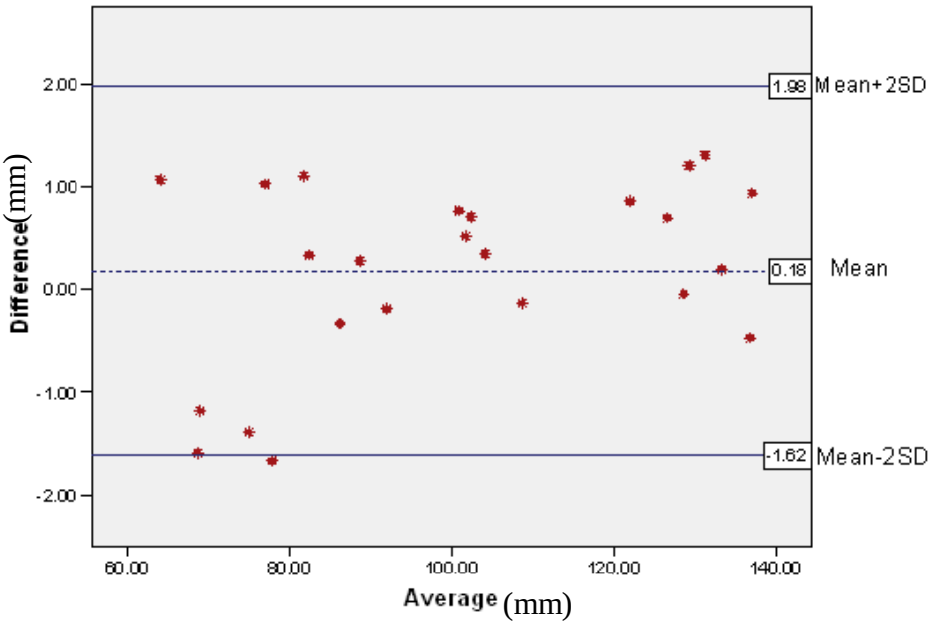

Figure 5-12: Bland & Altman plot for vernier calliper diameter measurement to that of photos

5.4.2 Comparing Real and MRI Diameter Measurements

The mean difference of the real diameter measurements and the MRI diameter was -0.36 mm (-0.35%) with standard deviation of 0.68 mm and with measurements using MRI underestimated. The minimum and maximum measurement differences were -1.25 (-1.24%) and 0.74 (0.73%) respectively. Differences of measurements were plotted against the average of two measurements. In the Bland & Altman plot, the data spread randomly within the agreement limits with a slightly more density below the mean difference line, Figure 5-13.

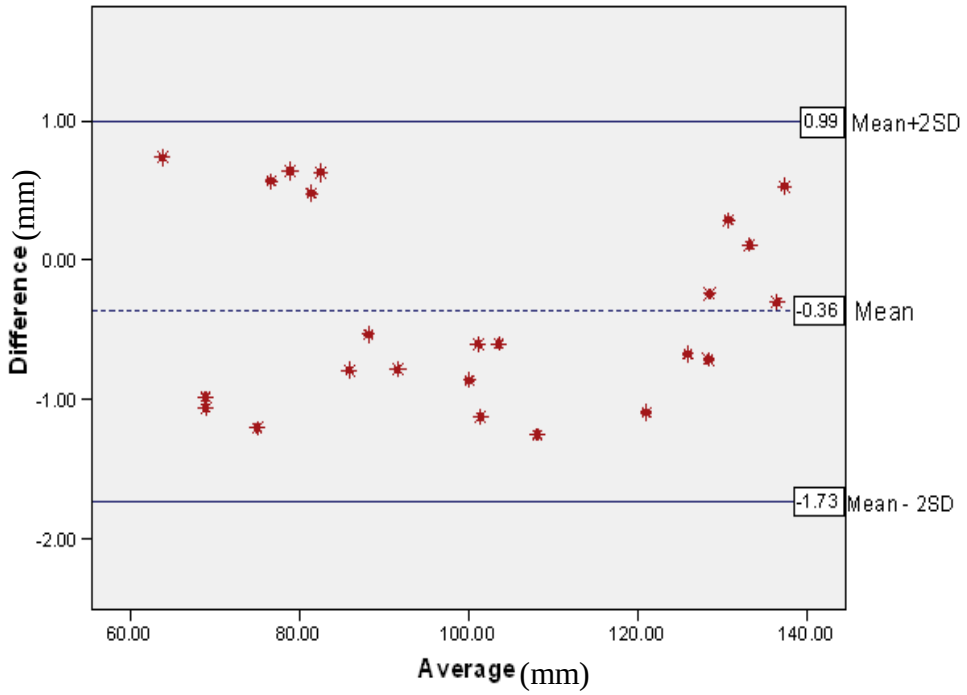

Figure 5-13: Bland & Altman plot for vernier calliper diameter measurement to that of MRI

5.4.3 MRI Accuracy in Surface Area Measurement

The mean difference of MRI surface area measurement to that of the photo was -25.87 mm^2 (0.30%) with standard deviation of 27.01 mm^2 and with measurements from MRI underestimated. The minimum and maximum measurement differences were -68.87 mm^2 (-0.8%) and 15.83 mm^2 (0.18%) respectively. Differences of measurements were plotted against the average of two measurements. In the Bland & Altman plot there is a week positive correlation i.e when the average surface area increases the absolute difference increases, Figure 5-14.

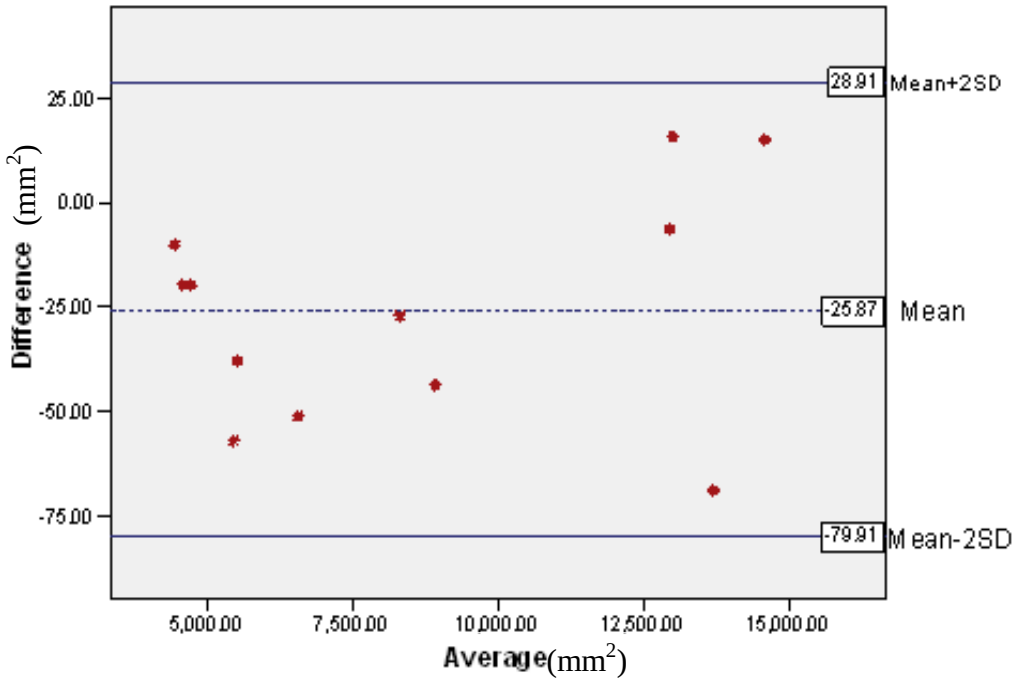

Figure 5-14: Bland & Altman plot for surface area measurement using MRI and photos

5.4.4 MRI Accuracy in Volume Measurement

The mean difference of MRI volume measurement to that of water suspension method was –1157mm^3 (-0.27 %) with standard deviation of 8682 mm^3 and the measurements from the MRI were underestimated. The minimum and maximum measurement differences were -10243 mm^3 (-2.40 %) and 9443 mm^3 (2.27 %) respectively. Differences of measurements were plotted against the average of two measurements. In the Bland & Altman plot no noticeable trend can be observed, Figure 5-15.

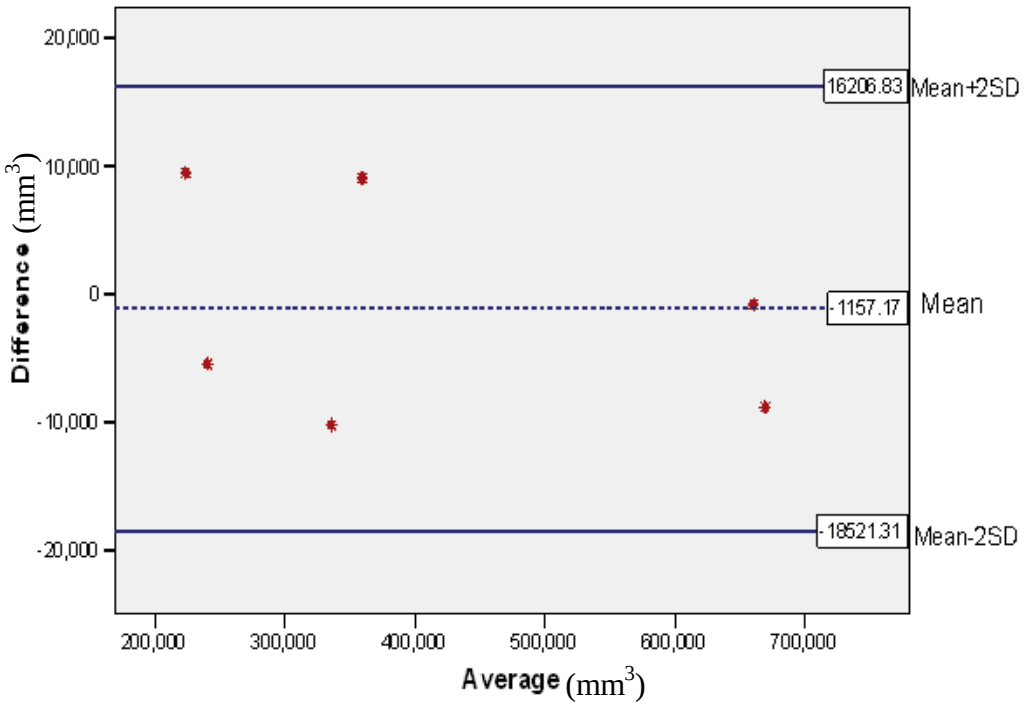

Figure 5-15: Bland & Altman plot for MRI and water suspension volume measurement.

5.5 Discussion

Accuracy of soft tissue surface area and volume measurement in MRI depends on voxel size, image resolution and segmentation procedure. Higher resolution and smaller voxel size requires more scanning time. In an experiment the best achievable voxel size and image resolution within eight minutes and twenty eight seconds time was defined.

In this experiment semi automatic image segmentation was chosen for segmenting the region of interest, i.e. bone and soft tissue, from the surrounding material, e.g. silicone and POP. Semiautomatic segmentation provides the possibility of fine adjustment for errors occurring by image processing software in boundary detection in parts of image with close signal intensity.

Surface area and volume of meat specimens were measured in MRI images and then compared with actual values. Results, Table 5-3, show that MRI is a highly accurate method in soft tissue surface area and volume measurement.

Table 5-3: MRI soft tissue surface area and volume measurement

Absolute difference	Minimum difference		Mean difference		Max difference		SD
		%		%		%	
MRI Diameter Measurement mm	0.11	0.8	0.69	0.79	1.25	1.59	0.31
MRI Surface area measurement mm2	6.33	0.5	31.01	0.43	68.87	1.04	20.26
MRI volume measurement mm3	831	0.13	7315.83	2.25	10243	4.31	3572.04

Cross sections of cadaver thigh muscle were measured at two points - lower and upper thigh - by Beneke et al. (Beneke et al., 1991). Differences between MRI and photographs were 1.2 % which shows a slightly bigger error than this study. This can be attributed to a limited number of images as well as a slight variation of the MRI scanning plane and the plane of photography in Beneke's study. Additionally, changes in the cross-section of soft tissue may have occurred after freezing the cadaver before photography in their study. In another study, Engstrom et al. measured serial cross-sections of cadaveric thigh muscles and reported that MRI measurement provided accurate and precise estimation of surface area of most thigh muscles (Engstrom et al., 1991). MRI to actual value ratio was between 0.93 and 1.07. Similar as Beneke's study, this higher error is likely to be due to freezing the cadaver for photography, the limited number of images and also difficulty in boundary detection of closely opposed muscles in the images. They segmented each muscle separately, whereas, in the present study the whole soft tissue boundary was traced which resulted in a smaller error.

Validation of MRI volume measurement has previously been undertaken mostly using phantoms comprised of materials other than soft tissue and bone to be able to compare the actual volume of phantoms with that of MRI. In a study the volume of phantoms were measured by MRI accurately with an error less than 1% (Mitsiopoulos et al., 1998). However, the material used in phantoms cannot represent the soft tissue. Cyteval et al. (2002) measured vertebral body dimensions using MRI in order to compare the MRI measurement of vertebral area and volume with direct

cadaver measurements. In their study water displacement was used for volume measurement of cadaver vertebra. The intraclass correlation coefficient between MRI and immersion methods was 0.95. It was concluded that MRI is a feasible, reproducible and accurate method for area and volume measurement of vertebral bodies (Cyteval et al., 2002). Mitsiopoulos and his colleague showed that MRI can provide an accurate area and volume measurement of the skeletal muscle and adipose tissue free skeletal muscle (ATFSM). The ATFSM area in 119 images (38.9 ± 22.3) and cadaver (39.5 ±23.0) were not different. It was shown that the MRI volume estimates are in good agreement with those of cadaver sections (Mitsiopoulos et al., 1998) (correlation for regression analysis was 0.98 to 0.99 for all variables, $p<0.001$). Hence the literature is in agreement with the data presented in this chapter using real meat and bone.

5.6 Summary

The voxel size, image resolution and segmentation process has an influence on accuracy of MRI measurements. Cross sectional diameter and surface area and volume of animal specimen were accurately measured using MRI. The results show that the chosen imagining parameters and the semi-automatic segmentation method can be used in residual limb volume and the cross-sectional surface area measurement while wrapped with silicon liner or POP.

6 The Clinical Inter- and Intra Socket Shape and Volume Consistency Utilising a Validated MRI Approach.

6.1 Introduction

Capturing the shape of the residual limb is the first stage in the prosthetic socket manufacturing process influencing the quality of the socket fit. The aim of this study was to examine inter- and intra shape capturing consistency of Hands-off and Hands-on casting concepts using MRI.

Residual limbs were cast of twelve persons with a unilateral below the knee amputation and scanned twice for each casting concept. Subsequently, all four volume images of an amputee were registered to a common coordinate system using the tibia. Afterwards, the circularity and surface area of transverse cross sections of the residual limbs as well as residual limb volume were calculated for each volume image.

The next progressive step involved the calculation of the absolute inter- and intra shape difference and then superimpose the colour coded volume images to visually displaying the results in the form of cylindrical unwrapped maps and movies of the sequence of the transverse, sagittal and coronal slices.

6.2 Sample Size

As no similar study could be found on inter- and intra cast concept consistency on real subjects, there was not enough data to be used in sample size calculation. Walter, Eliasziw, & Donner (Walter et al., 1998) developed a method for calculating required sample size (n) and the number of repetitions (k) for each subject, when intra class correlation (ICC) is used to measure the reliability. Their method is based on the functional approximation with a small conservative bias. They set a table for the required values of sample size for a given k and a desired minimal & maximal acceptable level of reliability ($\rho_{0,}$ ρ_1 respectively) if α= 0.05 and β=0. 2 (power of 0.8).

This approximation calculates the sample size when the number of repetition k is defined (fixed). In other words for each number k, the required sample size can be calculated. Therefore; first, the number of repetitions have to be decided. In this project, because of practical and logistical constraints, the number of repetitions could not be more than two. In order to complete two casting procedures and two MRI scans in, ideally, a single session takes four hours for two replicates as illustrated in Figure 6-1 and Table 6-1 respectively.

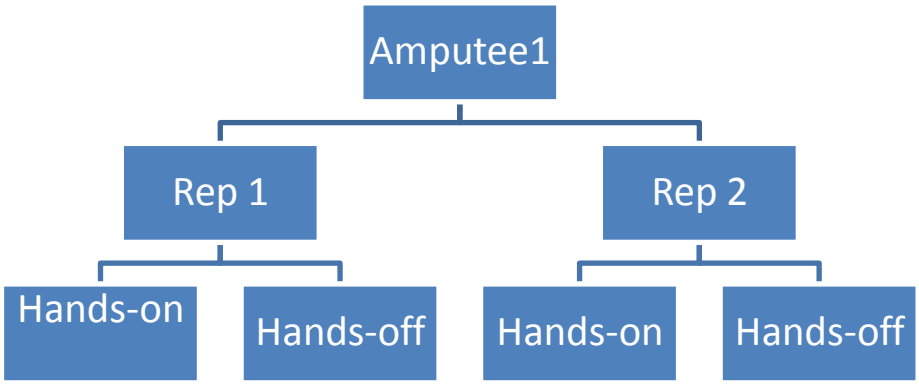

Figure 6-1: Casting flow chart.

Table 6-1: Data capturing time table

Task/Minutes	5	10	15	20	25	30	35	40	45	50	55	60	65	70	75	80	85	90	95	100	105	110	115	120	125	130	135	140	145	150	155
Screening Procedure and consent taking																															
Prosthesis removing																															
H-on casting																															
POP curing																															
MRI scanning									*	*						*	*														
Removing the H-on cast																															
waiting for new cast																															
H-off casting																															
POP curing																															
MRI scanning																			*	*						*	*				
Removing the H-off cast																															
Break																															

All repetitions needed to be done in one session due to the possibility of diurnal volume change (Zachariah et al., 2004). As a result of the relative high cost of MRI scanning and therefore to make each session more financially efficient, two parallel sessions, involving two volunteer subjects were conducted.

For the sample size calculation we chose $\rho_0 = 0.6$ and $\rho_1 = 0.9$ which translates into moderate to high consistency in casting concepts. Having $\rho_0 = 0.6$, $\rho_1 = 0.9$ and k=2 and using the approximation method, twelve amputee's were required to participate in this study. The Ethical approval was granted by NHS Glasgow Ethics Committee (Refrence no. SN08NE446), Appendix 13.4. The R&D management approval and the University sponsorship are also attached to the Appendix 13.5. Potential volunteers with an established residual limb (at least six months of using prosthesis) without blisters and other skin problems were considered. Prior to inclusion of the study candidates were screened by the resident clinical physicist, according a standard safety protocol as outlined by the Southern General Hospital in Glasgow. (Appendix 13.9).

6.3 Subjects Recruitment

An invitation letter including the MRI safety checklist and participants information sheet (Appendix 13.8, 13.90 and 13.4) were sent to registered people with a below the knee amputation at the Prosthetics and Orthotics department, Westmarc, located at the Southern General Hospital, in Glasgow.

6.4 Casting and Scanning Procedure

The residual limb was cast 4 times in a session, twice using the Hands-on and twice using the Hands-off method, with the aim to investigate the inter and intra cast variability. All casts had to be taken in a single session sequence i.e. after the application and removal of a cast using one method, another cast using the other method was applied. The outcome measures were volume and shape of the residual limb after applying each cast. However, there was a possibility that each cast influences the original volume of the residual limb and hence affecting volume of

residual limb for the following cast. In order to minimise this effect, a random selection sequence was adopted as illustrated in Table 6-2.

Table 6-2: Randomly allocating casting sequence for each participant.

	Time1	Time 2	Time 3	Time 4
Order 1	H-ON	H-OFF	H-ON	H-OFF
Order 2	H-OFF	H-ON	H-OFF	H-ON
Order 3	H-ON	H-ON	H-OFF	H-OFF
Order 4	H-OFF	H-OFF	H-ON	H-ON
Order 5	H-ON	H-OFF	H-OFF	H-ON
Order 6	H-OFF	H-ON	H-ON	H-OFF

The socket shape capturing method taught and practiced at the National Centre for Prosthetics and Orthotics (NCPO) University of Strathclyde, with the aim of producing a PTB type of prosthetic socket, was used for the hand-on concept, Figure 6-2. This method is described in detail in "trans-tibial prosthetics" manual distributed by NCPO (2002). For the Hands-off concept the ICECAST Compact® pressure casting device developed by the Össur Company was utilised (Carlsson and Hirons, 1997) This method involves the placement of the residual limb in an external device consisting of a double layer flexible bladder. First, a silicon liner is rolled over the residual limb. Then, the POP is wrapped over the liner and, while the POP is still wet, the bladder is attached to the liner's distal pin and rolled over the residual limb and inflated. The pressure, 80 mmHg, is maintained until the cast is set. Figure 6-3 . No direct influence of the prosthetist is required other than to determine the pressure level. In both concepts, Plaster of Paris (POP) is used for casting the residual limb. Water used to wet the POP was doped with 1 gr/lit Copper Sulphate for better segmentation of the MRI scan. All casts were made by a certified prosthetist. To

prevent the slippage of the cast, it was locked over the condyles in both Hands-off and Hands-on techniques.

The only difference in the casting method was using eight layers of perlon stockinet between residual limb and the overlaying POP or silicone liner in both casting methods. Eight layers of stockinet is not normally used in clinical practice. This was to create a gap (≈ 3mm) between the residual limb skin and the casting material to avoid the overlapping of the subcutaneous fat and the material due to the fat chemical shift. If the fat image had superimposed to the surrounding casting material, then the segmentation of the residual limb from material would have been impossible, hence; resulting in inaccuracy in residual limb skin boundary detection. Considering the incompressible property of the layers of stockinet, the slight effect of stockinet on the results is negligible compared to segmentation inaccuracy.

Figure 6-2: Hands-on casting

Figure 6-3:Hands-off casting using IceCast flexible loading medium

After curing of the POP the participant was positioned in the MRI scanner bore and scanned. In order to prevent image distortion resulting from movement of limb inside the scanner, the subject was asked to lie down on the MRI machine table in the prone position. In this position the patella rested on a knee cap receptacle made from polyethylene foam. Since the patella is in close contact with the weight bearing skeleton with little soft tissue coverage it prevented deformation of the POP cast. Additionally, in order to prevented undesirable movement from the hip joint, the thigh region was fixed using pads and straps. After each MRI imaging session, the cast was removed and another plaster cast was applied by the same prosthetist and then scanned using the MRI. The MRI data acquisition sequence is summarised in Table 6-3.

Table 6-3: MRI pulse sequence

Pulse sequence	Sagittal FSPGR
Repetition time(S)	6.9
Time of echo(S)	1.5
Inversion time(ms)	500
Bandwidth(KHz)	31.25
Flip angle(Deg)	12
Matrix	256×256
Voxel dimension(mm3)	1.17×1.17×0.6
FOV(cm)	30
Slice thickness(mm)	1.2
Number of average	1

6.5 Determination of the Volume of a Towelling Sock over the Residual Limb

In order to interpret the shape and volume results in a clinical meaningful way the volume of one layer of a towel sock over a residual limb model was measured using water displacement.

A transparent water tank with an overflow spout was used, Figure 6-4. The tank was filled with de-ionised water until the excess water was discharged from the spout. A rig was used to hold the model over the water tank. This rig had a clamp arrangement on the vertical post which could be adjusted and tightened so that the model could be stopped to the same height each time it was lowered.

The model was immersed into the water to the mid patellar level and the displaced water was collected and weighted using a precision balance (accuracy of 0.1 gram) and the reading was recorded (reading 1), Figure 6-4. Subsequently, the model was raised and a single towelling sock (Otto Bock) was donned. A condom was used to isolate the sock from the water. Considering the thin film thickness of the condom, relative to the thickness of the sock, the effect on volume measurement is negligible. The model was lowered into the water tank to the same height as before and the displaced water was added to the previous water and weighted again (reading 2), Figure 6-5. The accuracy of water displacement using the method mentioned above has been established by McGarry (2009) to be within 2.46% with no statistical significance between gold standard and water displacement. Measurements using Dekel^{TM} CNC milling machine and a displacement tool, both with an accuracy of 0.005mm, were used as gold standard. The technique was also repeatable (CoV <2.5%) (McGarry, 2009).

Figure 6-4: water weighting of residual model

The percentage sock volume was measured using the following formula;

Sock volume (%) = ((reading2 – reading1)/reading1) ×100

This was ((1765.1 ×1635.2) / 1635.2) × 100 = 7.943 %. In addition thickness of the sock was also measured using a dial thickness gauge (accuracy of 0.001 inch) as to be 2.28 mm, Figure 6-6.

Figure 6-5: Water weighting of residual limb covered with one layer of towel sock

Figure 6-6: Measuring thickness of a layer of towel sock

7 Results of casting

MRI data was exported to a dedicated workstation for analysis and subject identifiers were omitted. Therefore, data files were anonymous and all computers where data was stored were password protected.

DICOM files within a single scan, with non-descriptive or anatomically sequential file names, were grouped into a volume image and sorted into a sequential order. The smallest part of each slice, the three dimensional voxel, was not same in all directions of the generated volume. It was z = y =1.17 mm and x = 0.6 mm so that the scan of residual limb was extended in one direction (z and y) and compressed in another direction (x), Figure 7-1a. To make a volume with real dimensions, the voxel size was modified to an isotopic cubic shape (x=z=y=0.6mm) Figure 7-1b.

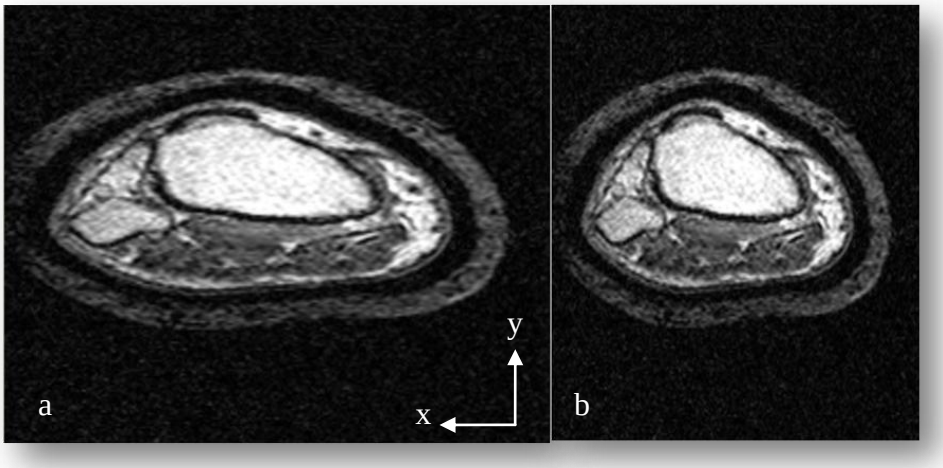

Figure 7-1: Volume image a) before and b) after voxel resizing

7.1 Segmentation

The Analyze software does the segmentation of the object manually, automatically and semi-automatically. The automatic segmentation applies thresholding, morphology erosion and dilation with a region growing steps in an attempt to automatically segment an object within a volume. Soft tissue and bone, defined by the residual limb skin surface, were segmented semi-automatically from surrounding materials, e.g. silicone and Plaster of Paris. In semi-automatic segmentation process a seed point was located within the Region of the Interest (ROI) and then by adjusting the threshold range boundary of the ROI was detected and traced automatically. In about fifty percent of slices, some part of the trace was not adjusted correctly and laid either outside or inside of the ROI (showed with an arrow in Figure 7-2.a). In this case, the boundary of the skin was adjusted manually for a minimal error, Figure 7-2.b. Using this approach, all slices within a volume were segmented and saved. All volume and transverse cross section measurements of residual limb are based on the boundary of the skin.

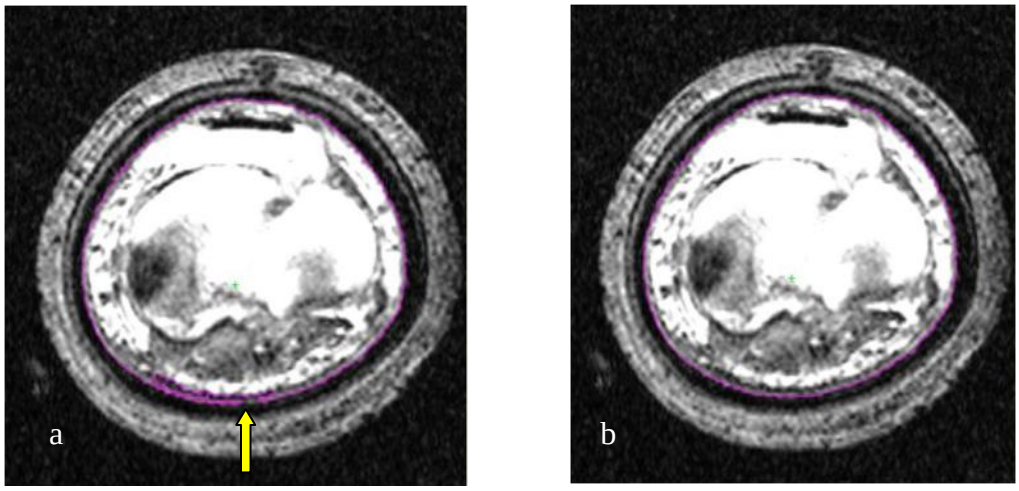

Figure 7-2: Semi-automatic segmentation

7.2 Registration

Prior to soft tissue volume and shape comparison, a common coordinate system for all volume images is required. To do this, all volume images were registered using a Normalised Mutual Information algorithm which allows the precise alignment of 3-D data to be achieved. This mutual information can be found using the tibia, the only rigid entity in residual limb.

To allow spatially registration of several volume images of the same residual limb one of the volume images was selected randomly and then the tibia bone was semi-automatically segmented as described above. After segmenting, the tibia was aligned so that the transverse image slices were parallel to the proximal surface of the bone, Figure 7-3. Finally, all other volume images were spatially registered to the aligned segmented tibia bone, Figure 7-4 and Figure 7-5.

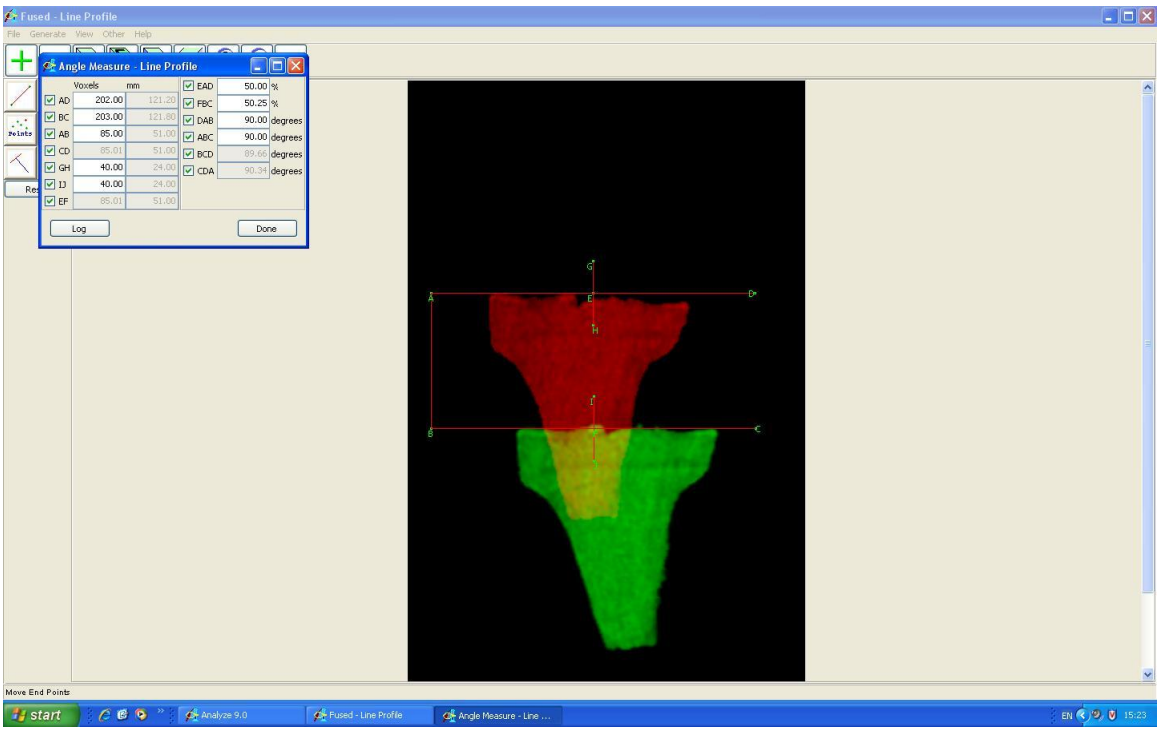

Figure 7-3: Alignment of the tibia bone to the central axis of the volume image.

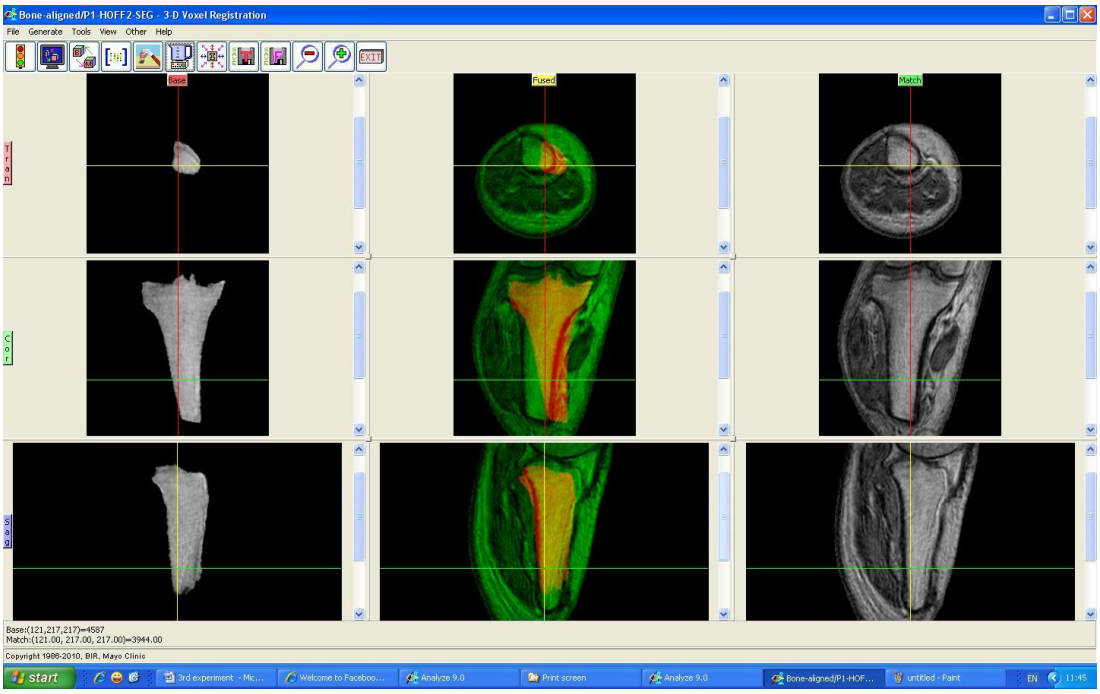

Figure 7-4: Volume registration in relation to the aligned tibia bone (pre-registration)

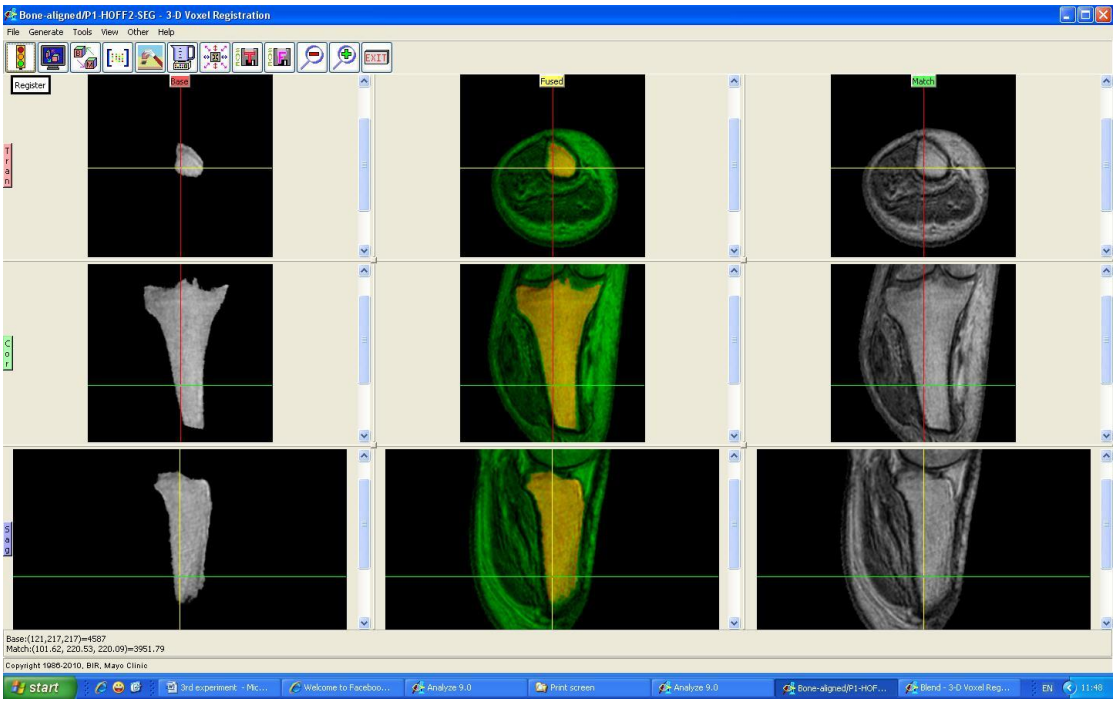

Figure 7-5: Volume registration relative to the aligned tibia bone (post-registration)

7.3 Data Result Processing

After registering all the volume data of the same amputee, slice number 30 as measured from the tibial plateau (proximal surface of the tibia) was selected and all slices above this slice was removed from all volume data, Figure 7-6. The 30th slice was selected because some residual limbs were long relative to the field of view so that the region above this slice was not visible in the image. This procedure enabled a consistency in anatomical residual limb length for the shape and volume comparison for all subjects. Furthermore, the remaining area is the area of the residual limb mostly contributing in weight bearing during prosthesis use. Afterwards, in order to be able to measure the shape differences between two volume images, all data were reformatted into the binary (black and white) format.

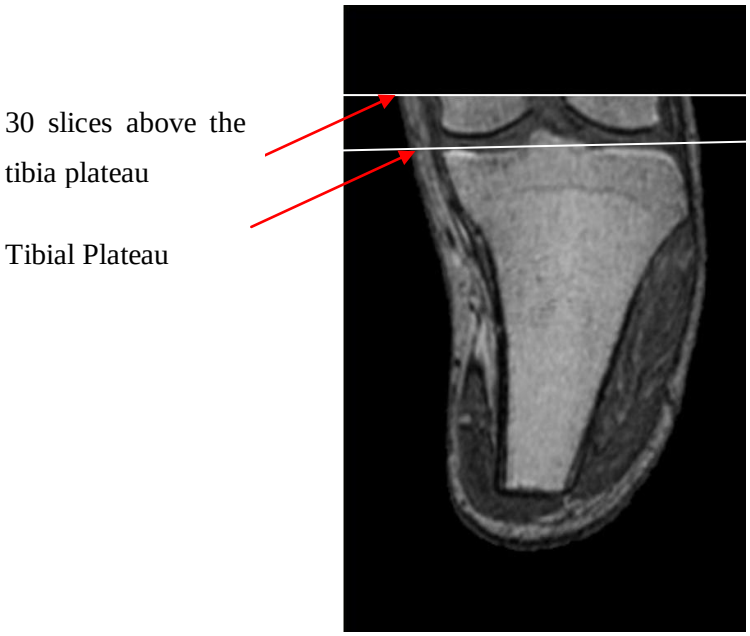

Figure 7-6: Transverse cutting plane

To create the absolute shape difference image of two diffeent volume images a three-stage process was adopted. In the first stage, all binary data points of the first volume image not in common with the second one were removed, green areas in the Figure 7-7a. The resultant volume image was labelled as Scan x. In the second stage, all binary data points of the second volume image not in common with the first volume image were removed and labelled as Scan y, red areas in Figure 7-7a. In the last stage, two scans of x and y were superimposed on each other to create the absolute shape difference image of two volume images, Figure 7-7b.

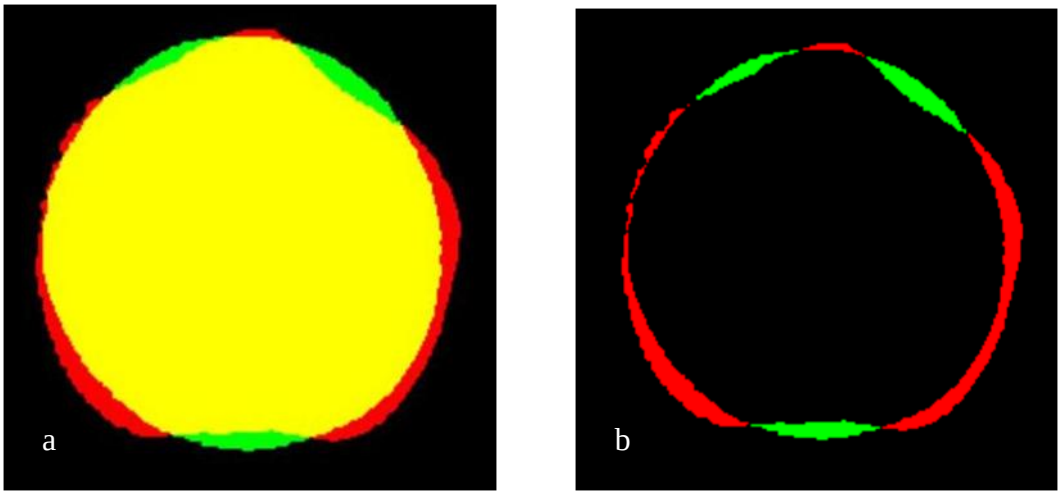

Figure 7-7: Shape difference between Hands-off and Hands-on a: superimposed slices of two scans. Yellow region is the common points between Hands-on and Hands-off. b: absolute shape difference. The red areas relate only to H-on and green areas to H-off cast.

7.4 Displaying the Results Visually for Inspection

The shape differences of a pair of volume images was measured as described in previous section then the shape differences were colour coded. Afterwards, the sequential slide showing video of sagittal, coronal and transverse slices were produced. Eighteen videos were made for each pair of Hands-off and Hands-on casting repetitions for each amputee, total of two hundred and sixteen video sequences. Each video title involves patient number code, first volume image and second volume image. In all videos the first volume image was green colour coded and the second volume image was red colour coded. For example "P2-Hoff1-H-on22" video showing shape differences of first repetition of the Hands-off casting and second repetition of the Hands-on cast of the second patient in green and red respectively. All videos can be found in the attached cd.

Cylindrical unwrapped image of the cast superimposed volume images were also made to show the 3D images in a 2 dimensional map. The Analyze software uses the

surface data points of the volume to create a 2D map. Seventy two maps were made for each pair of volume images. The number and colour coding were similar to that of videos. In addition to the green and red colours, yellow colour regions can be seen which represents no or minimal shape difference. The map of the Hands-off1 against Hands-off2 for the first amputee is presented below, Figure 7-8, and the rest can be found in the enclosed cd. The blue star in each map represents the approximate location of the patellar tendon area.

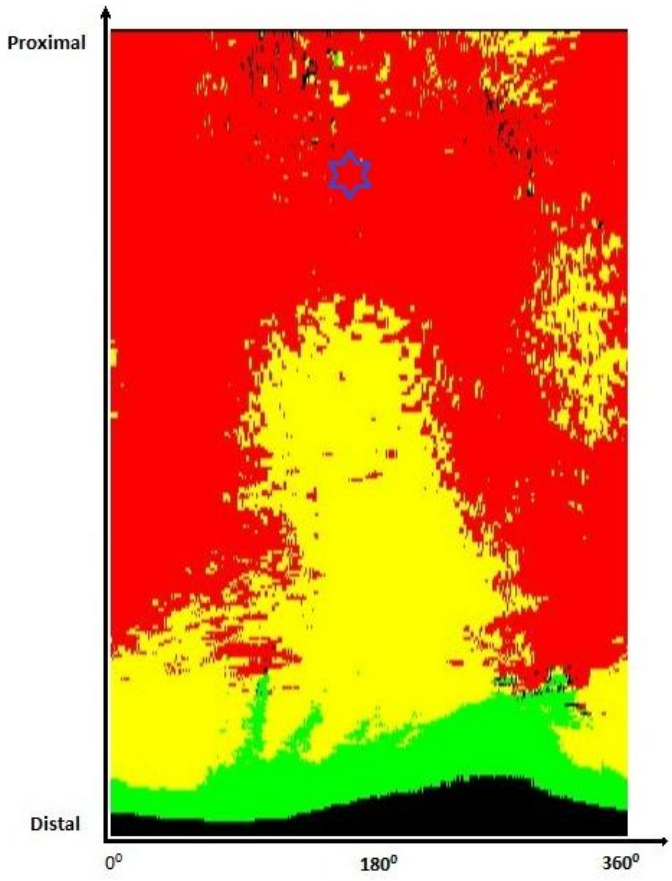

Figure 7-8: Cylindrical unwrapped 2D image of the Hands-off1 and Hands-off2, Patient 1. Red regions: Skin surface in H-off1 is displaced outward relative to the H-off2, Green regions: Skin surface in H-off2 is displaced outward relative to H-off1, Yellow area: no skin surface displacement in neither H-off1 nor H-off2.

7.5 Data Analysis

Intraclass Correlation Coefficient (ICC), Coefficeint of variation (COV), Paired t-test were used to measure the consistency of each casting concept(i.e. Hands-on and Hands-off) and Bland & Altman graph was used for agreement between two casting concepts.

ICC is the measure of reliability of the ratings. The ICC value greater than 0.7 is regarded as acceptable. (Evers, 2001). The COV is the standard deviation divided by the mean and is used to show the amount of deviation as percentage of the mean. The limitation is the sensitivity of COV when the mean value is near zero. The COV of less than 5% judged to be as acceptable repeatability (Campbell et al., 2007).

7.5.1 Intra Cast Surface Area and Circularity of the Transverse Cross Sections

The transverse cross-sectional surface area (CSSA) and cross-sectional circularity (CSC) of residual limb in all slices of each volume image (both repetition of Hands-off and Hands-on casts) were calculated. In order to calculate the CSC the ratio of two perpendicular diameters of the transverse cross section of the residual limb was calculated in several points around the circumference of that cross section and then averaged. A circle will give a circularity of 1. One would expect that the hands-off method would result in more circular shape of transverse cross sections of the residual limb due to the uniform pressure around the soft tissue during casting.

The mean and standard deviation of surface area and circularity are presented in Table 13-1 and Table 13-2 respectively. In addition, the CSSA and CSC values were plotted against the slice number, Figure 13-13 to Figure 13-36. Slices were numbered from proximal to distal region i.e the first proximal slice was numbered slice 1. Because of the size of the tables and the number of the graphs, these are enclosed in the appendix.

The tables and the figures show that on average the Hands-on cast results in a slightly larger CSSA. The average mean CSSA for Hands-off repetition 1 (H-off1) , Hands-off repetition 2 (H-off2), Hands-on repetition 1 (H-on1) and Hands-on

repetition 2 (H-on2) are 6185.98mm2, 6211.44 mm2, 6711.81 mm2 and 6620.16 mm2 respectively. In addition, the overall standard deviation of surface area is greater for Hands-on concept compared to that of Hands-on concept which was 2448.98, 2459.64, 2541.05 and 2500.54 for H-off1, H-off2, H-on1 and H-on2 respectively.

In overall, compared to Hands-off concept, the CSSA is larger in the first one sixth of the proximal region for both repetitions of the Hands-on concept, then, in the second one sixth proximal regions it is almost the same amount as the Hands-off casting, except in patient 5, Figure 13-22. This region is the area on which prosthetist apply pressure to indent the cast, i.e. the patellar tendon area and the popliteal region. In the middle 1/3 of the residual limb the Hands-on casting concept results in a larger CSSA in nearly 33% of scanned residual limbs, Figure 13-16, Figure 13-18, Figure 13-28 and Figure 13-32 . In patient 1 and 7 (16% of cases) resulted CSSA of both Hands-on repetitions are larger than just one repetition of the Hands-off method, Figure 13-14 and Figure 13-28. For patient 4, 6, 11 and 12 (33%), in the middle region, the CSSA is the same for both Hands-off and Hands-on (both repetitions) casting concepts, Figure 13-20, Figure 13-24, Figure 13-34 and Figure 13-36. The CSSA of the H-on1 is larger than all three other repetitions in this region for patient 9, Figure 13-30. In addition results show that the Hands-off method produce a longer residual limb in all participants.

Inter and intra cast CSC of the transverse sections is in general consistent trough out the length of the residual limb except for the distal region. The exceptions are Hands-off1 in patient 2, H-on1 and H-on2 for patient3, H-on2 in patient 8 (Figure 13-15, Figure 13-17 and Figure 13-27) in which the standard deviation is large (highlighted in green in Table 13-2). Additionally, this table shows that the Hands-off method produces a slightly more circular transverse cross section of the residual limb. The average CSC mean was 1.196, 1.188, 1.203 and 1.216 for H-off1, H-off2, H-on1 and H-on2 respectively.

Due to the large number of slices in the volume images performing statistical analysis for all slices was not practical. Therefore, three slices were chosen randomly

in each of proximal, middle and distal regions of each cast using the Random command in Microsoft Excel, Figure 7-9. For the details on how these regions were defined see section 7.5.5.

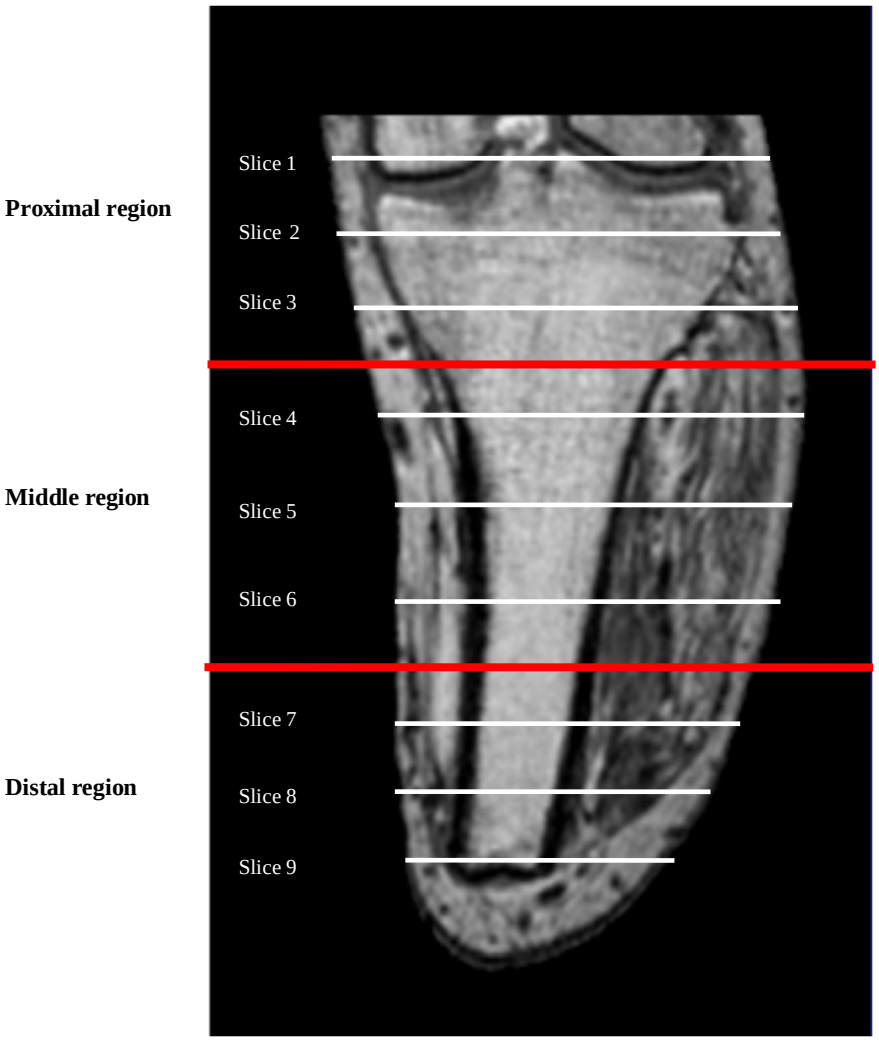

Figure 7-9: Location of nine randomly selected slices

The CSSA and CSC data of these nine slices are presented in Table 13-3 to Table 13-20. Each table contains values for each repetition of both casting methods of twelve amputees, average of two repetitions, difference, absolute difference and percentage absolute difference of two repetitions of each casting method. Mean and standard deviation (SD) of each value are also included in the tables. Besides, result of paired t-test statistical significance of difference of two repetitions of each casting method is included in the tables. In addition, percentage CSSA and CSC difference resulting from thickness of one layer of towelling sock is summarised in each table for both Hands-off and Hands-on method.

In order to interpret the intra-cast CSSA difference to one towelling sock criteria, first the average of two repetitions of each casting method was used as CSSA to calculate the radius (r) of transverse cross sections. The CSSA$= \pi r^2$ then the radius is:

$r = \sqrt{(CSSA/\pi)}$

Then, having the thickness of one layer of towelling sock as 2.18 mm, section 6.5, the percentage sock CSSA was calculated.

Percentage sock CSSA $= 100 (\pi (r + 2.28)^2 - \pi r^2) = 100\pi (4.56 r + 5.20)$

In order to interpret the intra-cast CSSA difference to one towelling sock criteria, the following formula was used:

Percentage sock CSC = 100 ((Diameter +4.56) / Diameter) -1)

In the tables, the percentage absolute intra-cast CSSA and CSC difference more than percentage sock CSSA is highlighted in green.

In the first slice which was located in the far proximal region of the residual limb the mean CSSA in both repetitions of the Hands-on method is larger than that of the Hands-off method. Two out of twelve residual limbs had the intra-cast CSSA

absolute difference more than one sock criteria in the Hands-on method, Table 13-3. The intra-cast CSSA mean difference in Hands-on method is greater than that of Hands-off method. This was 246.8 mm2 and -30 mm2 for Hands-on and Hands-off respectively, hence; the hands-on method has less CSSA repeatability than Hands-off method in the far proximal region (slice 1). In addition, compared to Hands-off method, the Hands-on casting resulted in a greater intra-cast CSSA error as the intra-cast SD is larger in Hands-on than the Hands-off method (564.9 mm2 versus 247.7 mm2).

The second slice, located in the middle part of the proximal region, showed the same CSSA intra-cast error and repeatability as in the first slice for both Hands-on and hands-off methods. However, the CSSA difference between Hands-on and Hands-off in slice 2 was less than that of slice 1. In slice 2 the intra-cast CSSA mean difference was 160.7 mm2 and -51.4 mm2 for Hands-on and Hands-off respectively. Besides the intra-cast CSSA standard deviation was 491.2 mm2 and 245.5 mm2 for Hands-on and Hands-off respectively. Same as slice 1, the mean CSSA of the residual limb in each repetition of the Hands-off method was larger than that of Hands-off casting in slice 2. Similar to slice 1, in slice 2 hands-on intra-cast CSSA absolute difference in two subjects was greater than one sock criteria.

In slice 3 the intra-cast CSSA mean difference of two casting methods are almost similar to each other but the Hands-on intra-cast SD is almost twice as much as the Hands-off SD (379.24 mm2 and 211.11 mm2 for Hands-on and Hands-off respectively). The Hands-on resulted in a larger CSSA than the Hands-off method, Table 13-5.

Intra-cast CSSA mean difference and SD of Hands-on and Hands-off in the middle region of the residual limb, slice 4, 5 and 6, remain almost similar to each other. Hence, the intra-cast repeatability and error are almost the same in both casting methods. However, the hands-on method results in a slightly larger CSSA in this region compared to the Hands-off method, Table 13-6, Table 13-7 and Table 13-8.

In slice 7 and 8 the intra-cast CSSA mean difference of two casting concepts is close to each other but the Hands-off intra-cast SD is smaller than that of Hands-on method, Table 13-9 and Table 13-10. However the Hands-on and Hands-off intra-cast SD difference in these two slices is less than that of slice 1 and 2. The Hands-on CSSA is larger than that of Hands-off method in slice 7 but smaller than Hands-off casting in slice 8.

The CSSA of Hands-off method is larger than the CSSA of hands-on casting in the last slice. In addition the Hands-on intra-cast CSSA difference is less than that of Hands-off method but the SD has a little difference. Five subjects show the intra-cast CSSA difference larger than one sock criteria in Hands-on method compared to three subjects in Hands-off casting, Table 13-11. The CSC tables show that there is not much difference between Hands-on and Hands-off in inter-cast CSC mean difference and SD in slice 1 to 8, Table 13-12 to Table 13-19. The tables also show that the Hands-off method results in a smaller CSC values, hence; more circular cross sections.

In the last slice, slice 9, the Hands-off intra-cast CSC difference is larger than that of Hands-on method (0.10 and 0.01 for Hands-off and Hands-on respectively), Table 13-20. Additionally the inter-cast circularity SD is greater in Hands-off casting than the Hands-on method (0.30 and 0.19 for Hands-off and Hands-on respectively).

The CSSA mean of both repetitions of two casting method and average of two repetitions, CSSA mean difference and absolute mean difference of two repetition of each casting method for all nine randomly selected slices are summarised in Table 7-1 and the standard deviation of above variables is included in Table 7-2.

The Hands-off intra-cast CSSA mean difference is smaller than that of hands-on method in all nine slices, hence more repeatable, Figure 7-10. It can also be noticed that the Hands-on casting resulted in a greatest intra-cast mean difference in slice 1 and 2. Additionally the Hands-n intra-cast SD is greater in slice 1 and 2 compared to other slices, Figure 7-11. The Hands-on intra-cast SD in these two slices is greater than that of hands-off method.

The CSC mean of both repetitions of two casting methods and average of two repetitions, CSC mean difference and absolute mean difference of two repetition of each casting method for all nine randomly selected slices are summarised in Table 7-3 and the standard deviation of above variables is included in Table 7-4.

It can be noticed that there is not much difference in Hands-off and Hands-on method in intra-cast CSC mean difference and SD, Figure 7-12and Figure 7-13. Both casting methods resulted in a greater intra-cast mean difference and SD at the far distal region (slice 9) compared to more proximal regions (slice 1 to 8).

Table 7-1: Residual limb cross sectional surface area means (mm2), randomly selected slices

		Hands-off (mm2)					Hands-on (mm2)				
Region	Slice	Rep 1	Rep 2	Ave 1+2	Diff 1-2	Abs Diff 1-2	Rep 1	Rep 2	Ave 1+2	Diff 1-2	Abs Diff 1-2
Proximal	1	8799.0	8829.3	8814.2	-30.3	207.4	9484.5	9219.6	9352.0	264.9	487.0
	2	8605.0	8656.3	8630.7	-51.4	194.9	9006.1	8845.4	8925.8	160.7	376.7
	3	8319.5	8342.6	8331.0	-23.1	151.6	8619.7	8607.4	8613.5	12.3	280.7
Middle	4	7530.9	7567.0	7548.9	-36.0	150.3	7879.9	7860.9	7870.4	19.1	206.4
	5	6940.7	6963.8	6952.2	-23.1	195.9	7242.2	7209.0	7225.6	33.2	233.7
	6	6497.2	6508.9	6503.1	-11.7	206.2	6772.8	6756.8	6764.8	16.0	251.9
Distal	7	5042.8	5058.3	5050.5	-15.5	195.3	5126.4	5133.5	5129.9	-7.1	302.9
	8	3504.8	3528.9	3516.8	-24.1	207.5	3229.5	3276.2	3252.9	-46.8	315.2
	9	2082.8	2213.5	2148.1	-130.7	263.0	1380.9	1465.1	1423.0	-84.3	276.3

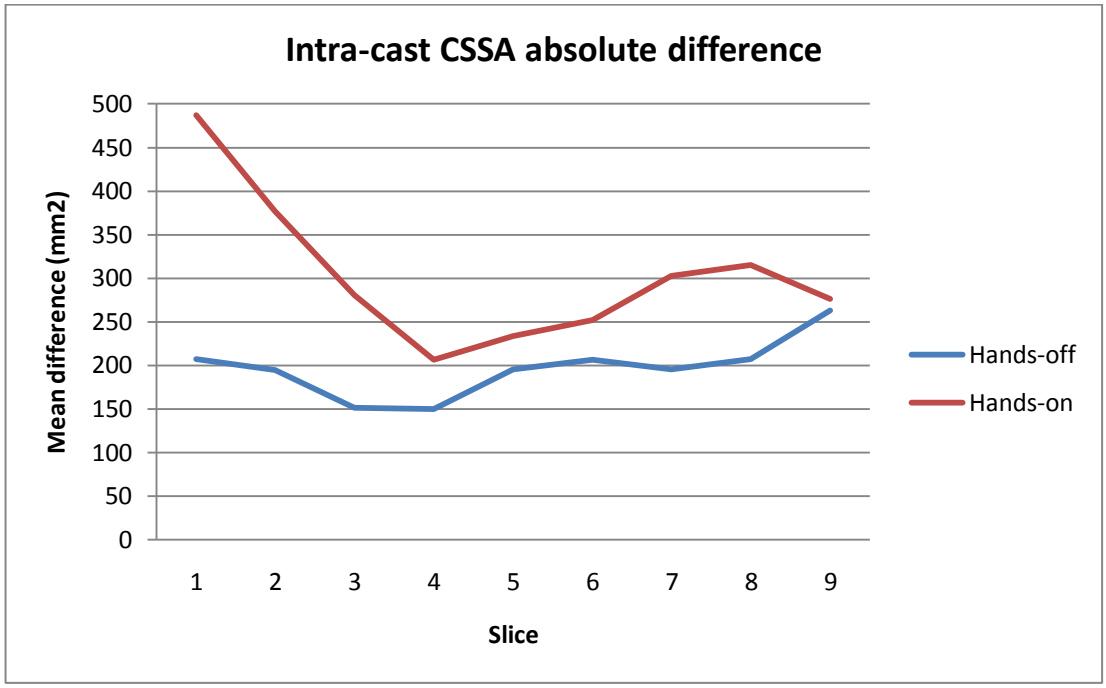

Figure 7-10: Intra cast cross sectional absolute mean difference, Hands-off and Hands-on

Table 7-2: Residual limb cross sectional surface area SD (mm2), randomly selected slices

		Hands-off (mm2)					Hands-on (mm2)				
Region	Slice	Rep 1	Rep 2	Ave 1+2	Diff 1-2	Abs Diff 1-2	Rep 1	Rep 2	Ave 1+2	Diff 1-2	Abs Diff 1-2
Proximal	1	1150.1	1170.8	1153.9	247.7	124.1	1489.1	1186.5	1316.4	564.9	370.1
	2	1134.3	1168.0	1144.7	245.5	147.3	1420.6	1174.7	1280.1	491.2	338.6
	3	1075.4	1087.5	1076.3	211.1	141.7	1360.1	1169.3	1254.1	379.2	240.9
Middle	4	1241.3	1243.0	1237.6	213.4	149.4	1276.3	1217.9	1239.9	274.1	170.5
	5	1428.1	1369.4	1391.1	298.1	218.2	1448.0	1412.9	1423.2	289.6	159.7
	6	1254.3	1161.8	1198.0	324.8	243.5	1294.5	1215.2	1245.5	317.0	177.5
Distal	7	1306.1	1201.7	1245.9	301.0	222.0	1743.3	1533.8	1629.6	401.2	246.8
	8	1328.0	1180.5	1248.6	279.5	178.1	1860.1	1610.9	1726.9	426.0	274.8
	9	1428.9	1277.3	1341.7	382.0	298.5	1898.8	1604.4	1747.0	388.3	274.3

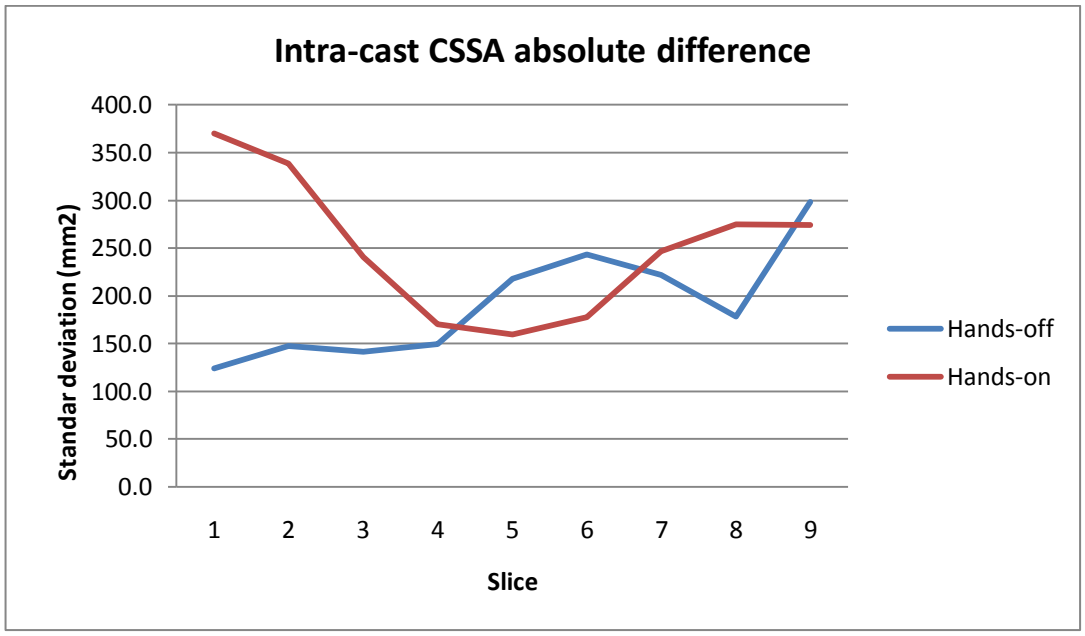

Figure 7-11: Intra-cast cross sectional absolute difference SD, Hands-off and Hands-on casts

Table 7-3: Residual limb cross sectional circularity mean, randomly selected slices

		Hands-off					Hands-on				
Region	Slice	Rep 1	Rep 2	Ave 1+2	Diff 1-2	Abs Diff 1-2	Rep 1	Rep 2	Ave 1+2	Diff 1-2	Abs Diff 1-2
Proximal	1	1.16	1.16	1.16	0.00	0.03	1.18	1.20	1.20	-0.02	0.02
	2	1.16	1.16	1.16	0.00	0.02	1.19	1.20	1.20	-0.01	0.02
	3	1.18	1.16	1.17	0.02	0.04	1.19	1.20	1.19	-0.01	0.03
Middle	4	1.17	1.16	1.17	0.01	0.03	1.18	1.19	1.18	0.00	0.03
	5	1.18	1.16	1.17	0.01	0.03	1.18	1.18	1.18	0.00	0.01
	6	1.17	1.17	1.17	0.00	0.03	1.18	1.19	1.19	-0.01	0.03
Distal	7	1.19	1.19	1.19	0.00	0.04	1.20	1.20	1.20	-0.01	0.03
	8	1.20	1.21	1.21	0.00	0.04	1.20	1.22	1.21	-0.02	0.04
	9	1.32	1.22	1.27	0.99	0.10	1.34	1.33	1.33	0.01	0.11

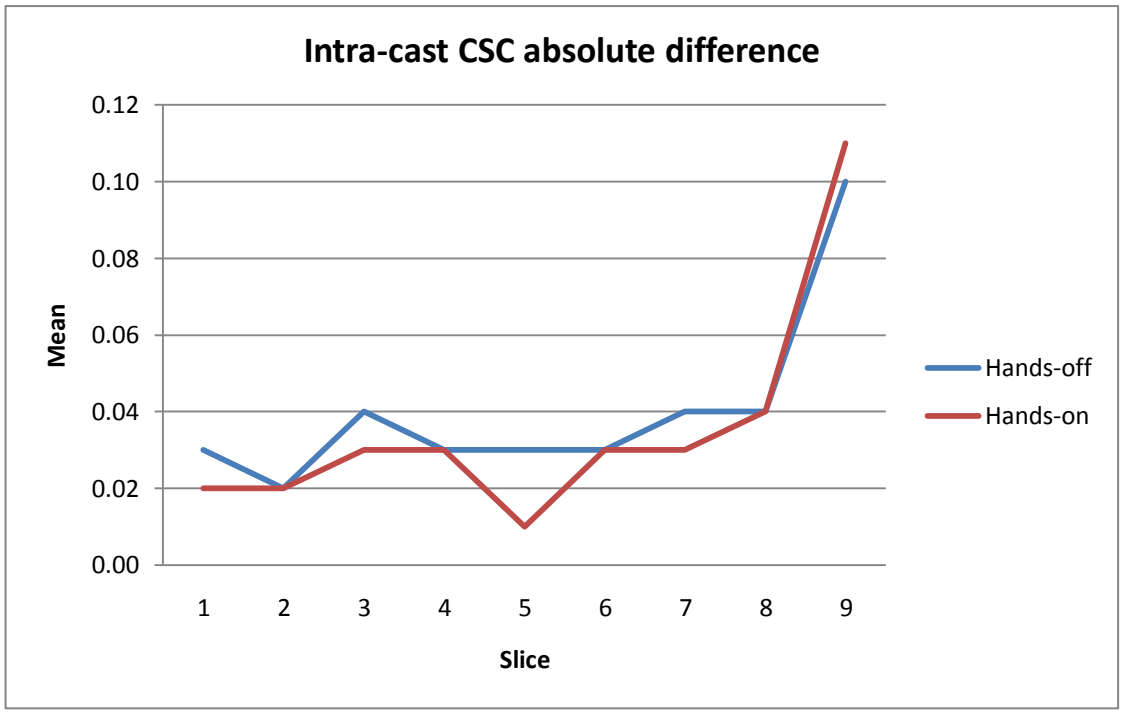

Figure 7-12: Intra cast circularity absolute mean difference, Hands-off and Hands-on

Table 7-4: Residual limb cross sectional circularity SD, randomly selected slices

		Hands-off					Hands-on				
Region	Slice	Rep 1	Rep 2	Ave 1+2	Diff 1-2	Abs Diff 1-2	Rep 1	Rep 2	Ave 1+2	Diff 1-2	Abs Diff 1-2
Proximal	1	0.03	0.02	0.01	0.04	0.03	0.02	0.04	0.03	0.02	0.02
	2	0.03	0.02	0.02	0.03	0.02	0.03	0.02	0.03	0.03	0.02
	3	0.05	0.02	0.03	0.05	0.03	0.05	0.04	0.04	0.03	0.02
Middle	4	0.04	0.02	0.03	0.04	0.02	0.03	0.04	0.03	0.04	0.03
	5	0.04	0.02	0.03	0.04	0.02	0.03	0.04	0.03	0.02	0.01
	6	0.03	0.02	0.02	0.03	0.02	0.02	0.04	0.03	0.04	0.03
Distal	7	0.04	0.04	0.03	0.04	0.02	0.03	0.04	0.03	0.03	0.02
	8	0.04	0.03	0.03	0.05	0.03	0.04	0.06	0.04	0.06	0.04
	9	0.33	0.04	0.18	0.30	0.30	0.17	0.15	0.13	0.19	0.15

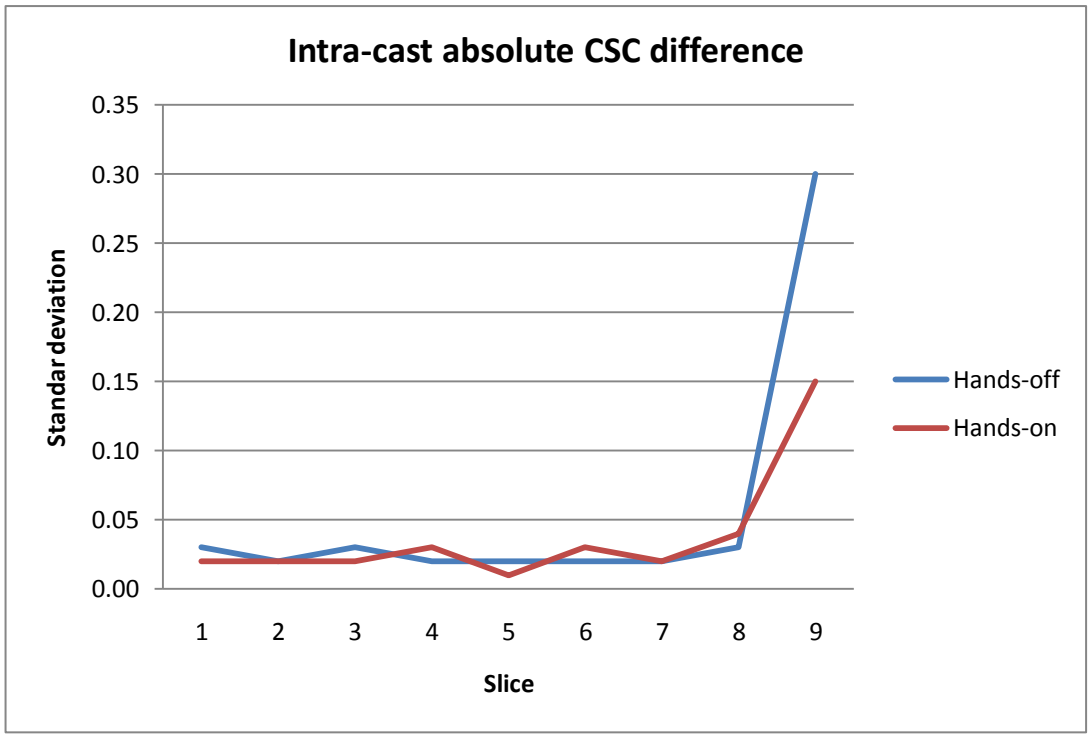

Figure 7-13: Intra-cast circularity absolute difference SD, Hands-off and Hands-on casts

The results show that there is no significance difference ($p>0.05$) between two repetitions of Hands-off and Hands-on casting concepts except for the circularity of Hands-on method in the first slice. In addition, Bland & Altman limits of agreement were plotted for each selected slice for each pair of reading, Figure 1 to Figure 36 in the "Bland and Altman plots" document in the cd.

7.5.2 Comparing Inter Casting Transverse Cross Sectional Surface Area and Circularity Variability

To examine if there is any surface area and circularity difference between two Hands-on and Hands-off methods, average of two repetitions of each method for surface area and circularity was calculated then mean differences were tested using t-test, Table 7-5. When the normal distribution of the values was not assumed the Mann-Whitney test was used. The Shapiro-Wilk test was used to see if the distribution of the values significantly differs from a normal distribution.

Table 7-5: Statistical significance, mean and standard deviation of the average readings for surface area (mm2) and circularity

Slice	Surface area			Circularity		
	Mean (SD) mm2		Significance (p<0.05)	Mean (SD)		Significance (p<0.05)
	H-off	H-on		H-off	H-on	
Slice 1	8814.17 (1153.86)	9352.04 (1316.86)	0.299	NA	NA	NA
Slice 2	8630.65 (1144.70)	8925.77 (1280.10)	0.558	1.165 (0.021)	1.197 (0.027)	0.004
Slice 3	8331.04 (1076.31)	8613.50 (1254.04)	0.560	1.174 (0.030)	1.194 (0.038)	0.204*
Slice 4	7548.94 (1237.56)	7870.39 (1239.85)	0.532	1.169 (0.030)	1.186 (0.032)	0.083*
Slice 5	6952.24 (1391.10)	7225.61 (1423.22)	0.639	1.171 (1.181)	0.267 (0.035)	0.431
Slice 6	6503.08 (1197.98)	6764.81 (1245.45)	0.605	1.170 (0.022)	1.191 (0.030)	0.072
Slice 7	5050.52 (1245.90	5129.90 (1629.57)	0.895	1.194 (0.315)	1.203 (0.033)	0.497
Slice 8	3576.83 (1248.63)	3252.85 (1726.88)	0.273*	1.210 (0.027)	1.214 (0.039)	0.794*
Slice 9	2148.13 (1341.69)	1423.00 (1747.04)	0.021*	1.278 (0.180)	1.337 (0.129)	0.650

*Normality was not assumed

The results show that there is a significant difference between the Hands-on and Hands-off in surface area at the far distal region (slice 9) and in circularity in the proximal region (slice 2). Average of two repetitions of circularity could not be calculated for slice one because the two repetitions of the Hands-on method in this slice were significantly different, Table 13-12, hence; neither of hands-on repetitions nor the average of circularity could be assumed as a true value. The Bland and Altman plots are presented in "Bland and Altman plots" document in the cd, Figure 37 to Figure 54.

7.5.3 Length difference

The lengths of all residual limbs were calculated as the number of transverse slices in which the residual limb appears multiply by the slice thickness (0.6 mm). This method of length measurement is accurate because it doesn't have the error resulting from manually locating the proximal and distal end of the residual limb. Additionally the length measurement is consistent in all amputees in that the transverse slices were aligned parallel to the tibial plateau (the reference datum). In addition, in all residual limb images the 30^{th} slice above the tibial plateau was chosen as a cutting plane.

Figure 7-14 shows the length of residual limb for two repetitions of each casting method. The mean and standard deviation of length measurement are summarized in Table 7-6. This table shows that the length difference within each casting concept is minimal but the difference is noticeable between casting concepts.

Table 7-6: Mean (mm) and standard deviation of residual limb length

Cast	Mean (mm)	Sd
H-off1	156.70	33.63
H-off2	157.05	34.36
H-on1	148.90	35.42
H-on2	149.65	34.37

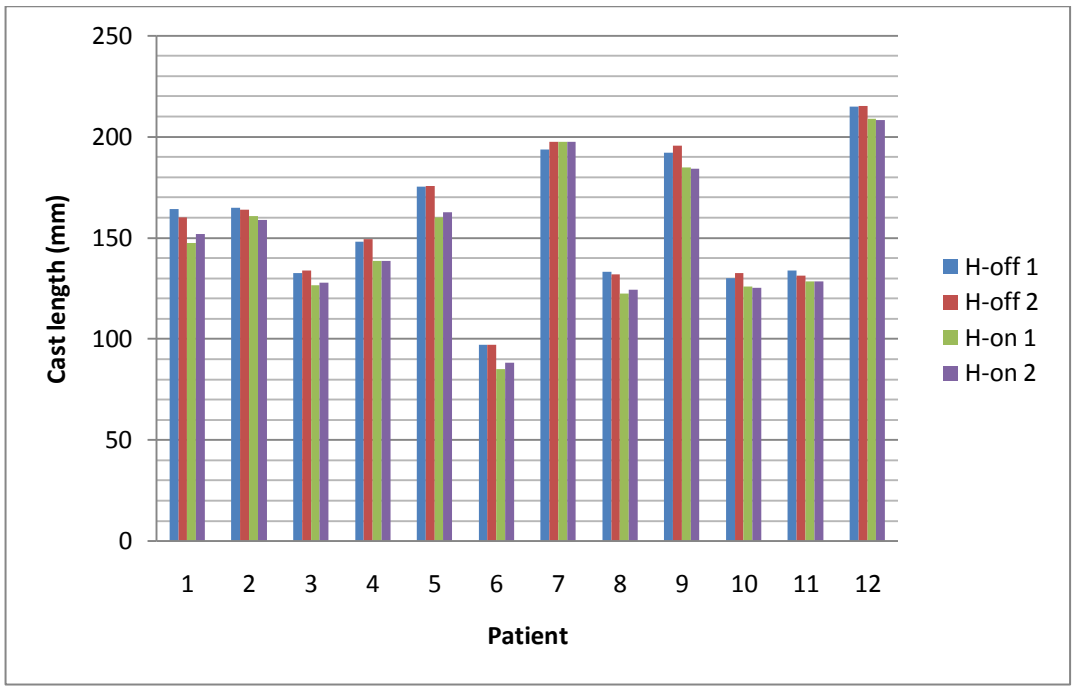

Figure 7-14: length of two repetitions of each casting concept

The ICC results show that both Hands-off and Hands-on concepts are repeatable for residual limb length Table 7-7. In the next step the average of two repetitions of each casting concept were calculated and then compared using T-test. Lengths mean difference between Hands-off and Hands-on was not significant (Mean difference = 7.6 mm, SD = 4.315, p=0.595). The Bland and Altman plots for inter and intra cast lengths are presented in Figure 7-15, Figure 7-16 and Figure 7-17.

Table 7-7: ICC for residual limb length

Lenght	H-off	H-on
ICC	0.998	0.999

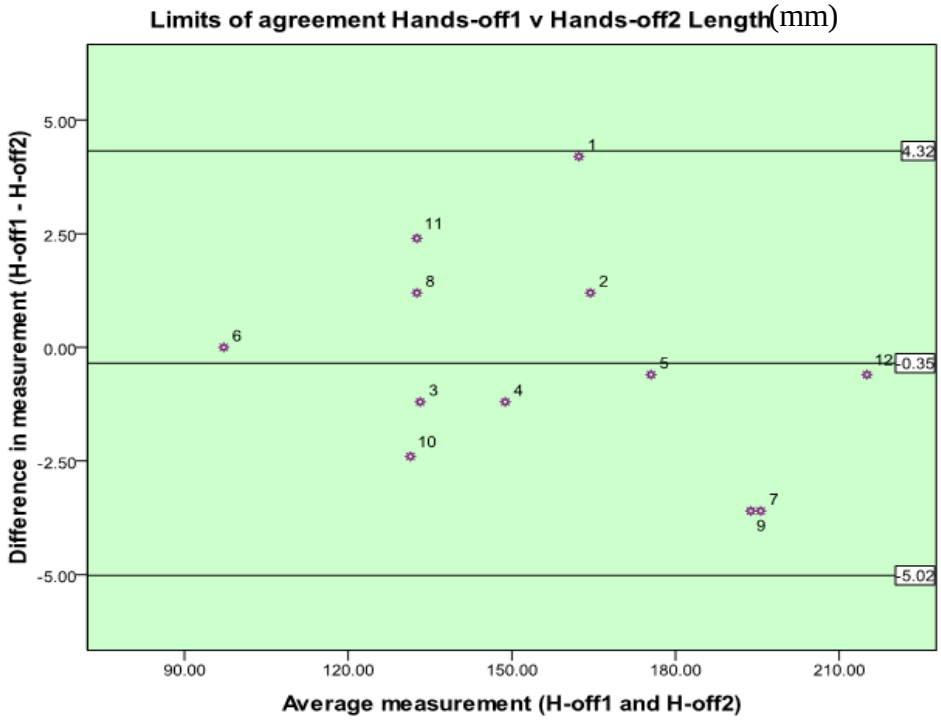

Figure 7-15: Bland and Altman plot for Hands-off1 and Hands-off2 length

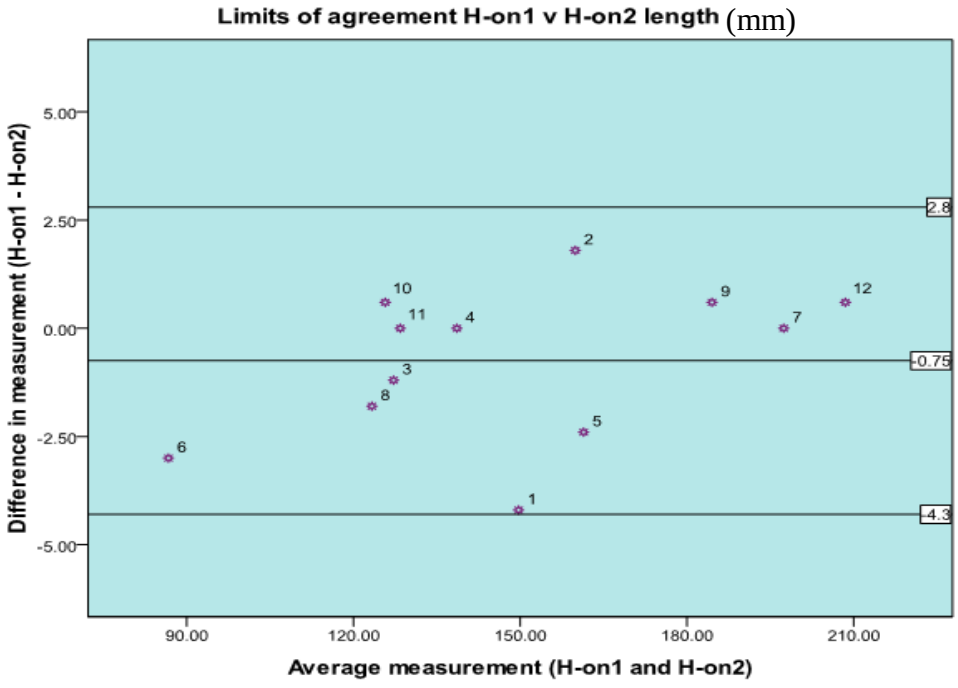

Figure 7-16: Bland and Altman plot for Hands-on1 and Hands-on2 length

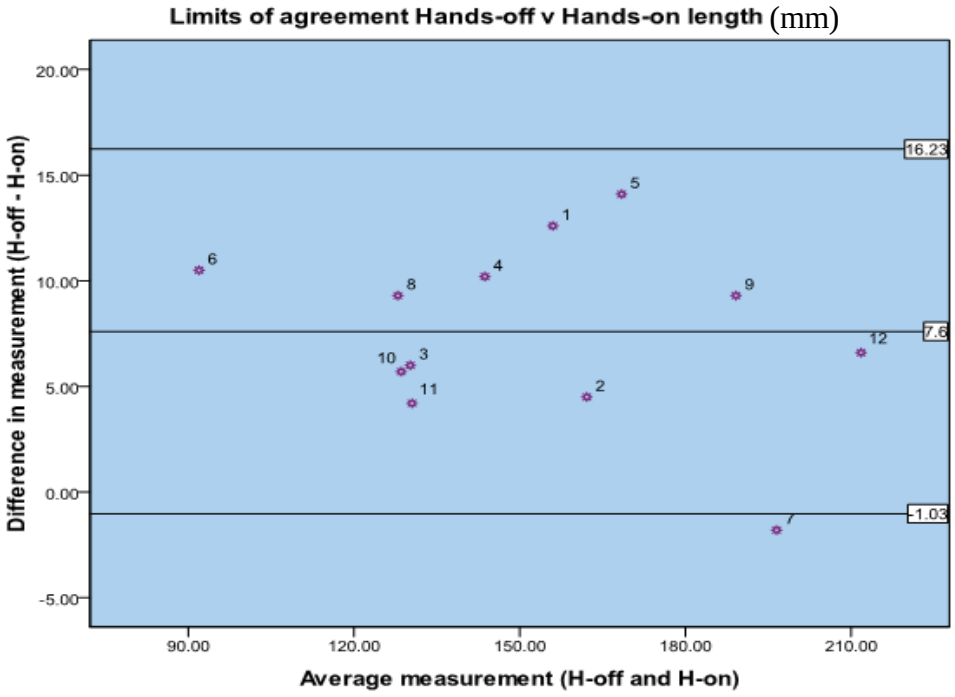

Figure 7-17: Bland and Altman plot for Hands-off and Hands-on length

7.5.4 Volume Measurement

Volume of all volume images were measured using the Analyze software. The means and standard deviations of two repetitions of each casting concept is summarised Table 7-8. The Figure 7-18 shows the volume of each cast for twelve amputees.

Table 7-8: Mean (mm^3) and standard deviation of volume measurement

Cast	Mean (mm3)	SD
Hands-off 1	993910.27	350350.74
Hands-off 2	997189.23	343389.39
Hands-on 1	1025034.61	372591.91
Hands-on 2	1012988.99	350130.56

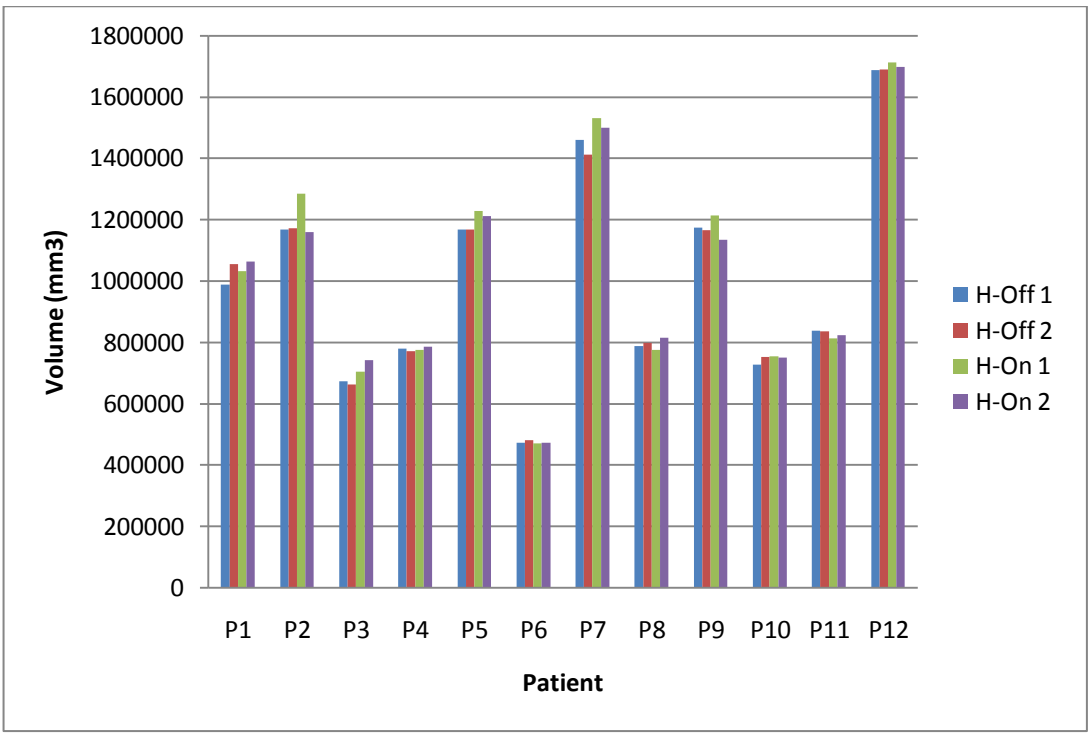

Figure 7-18: Volume of four casts for each amputee

The ICC test reveals that the two readings of both Hands-off and Hands-on concepts are repeatable, Table 7-9. Having no significance difference between volume reading of two repetitions of each concept, average of readings were calculated for comparing volume of two casting concepts Table 7-10. The results of t-test shows that there is no significant difference between Hands-off and Hands-on volume (mean difference = 23462.04 mm^3, SD = 29734.80, p=0872). The Bland and Altman plots for inter and intra cast lengths are presented in Figure 7-19, Figure 7-20 and Figure 7-21.

Table 7-9: ICC test for repeatability of each casting concept

Test	H-off	H-on
ICC	1.00	0.99

Table 7-10: Mean and standard deviation of average volume measurement of Hands-off and Hands-on casting

Cast	Mean (mm3)	SD
Hands-off	995549.75	3466.29.16
Hands-on	1019011.8	360720.99

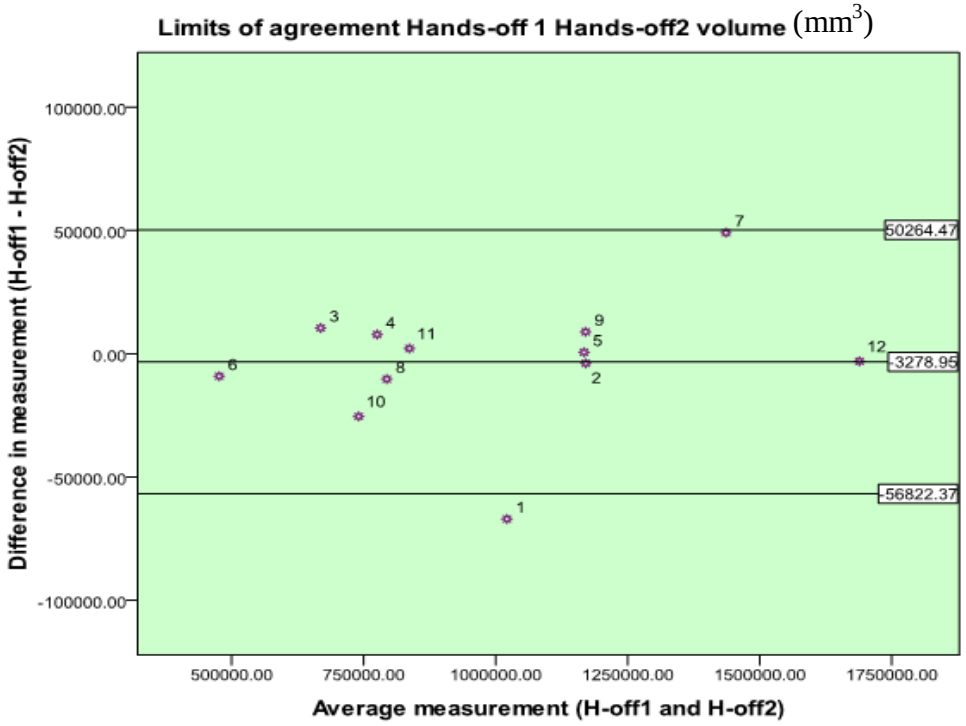

Figure 7-19: Bland and Altman plot for Hands-off1 and Hands-off2 volume

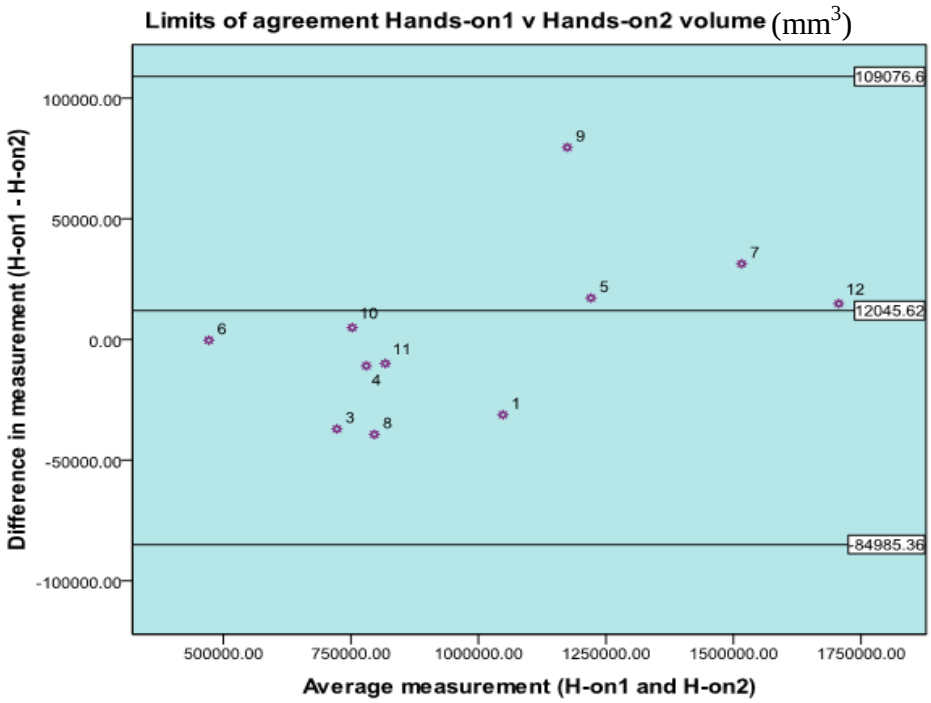

Figure 7-20: Bland and Altman plot for Hands-on1 and Hands-on2 volume

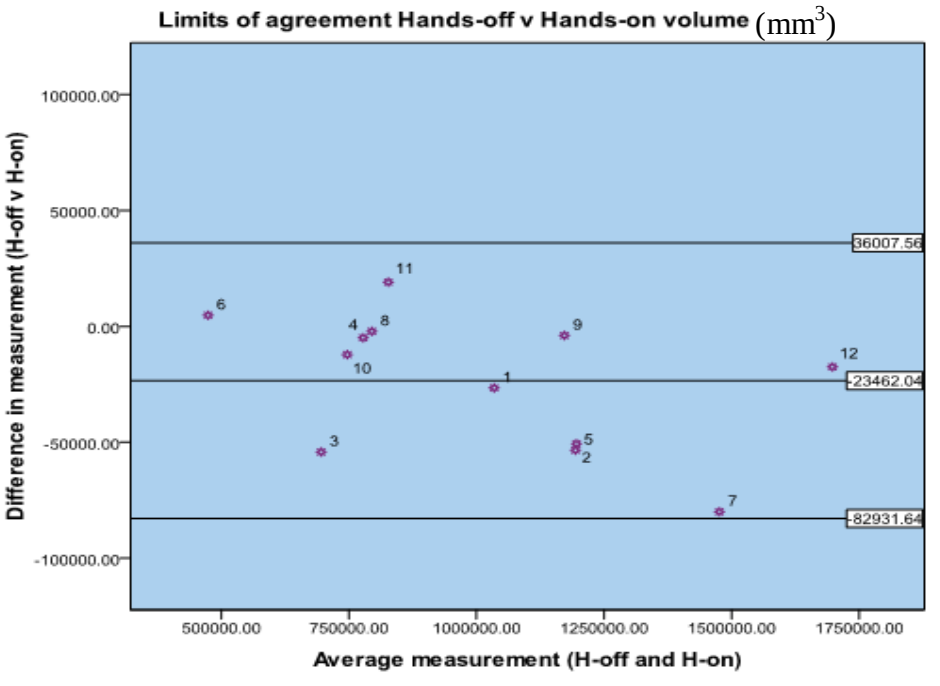

Figure 7-21: Bland and Altman plot for Hands-off and Hands-on volume

7.5.5 Regional volume difference

Although there is not an overall volume difference within and between casting concepts, regional volume differences were examined to check for the possibility of that the regional volume difference cancelling out other. To do so, each volume image was sectioned in four regions of antro-lateral (A-L), antro-medial (A-M), postro-lateral (P-L) and postro-medial (P-M) by defining two sagittal and coronal cutting planes. The sagittal cutting plane was defined as passing through the intercondylar tubercles of the tibia (Havet et al., 2007) and the coronal cutting plane passing through the midpoint of the tibia plateau (Han et al., 2008). Additionally volume images were sectioned into three distal, middle and proximal regions using two transverse cutting planes. In order to define these cutting planes average length of all four cast of each amputee were calculated and then divided by three.

The PTB socket focuses on the application of forces on the pressure tolerant areas of the residual limb based on biomechanical principles of gait cycle (Radcliffe and Foort, 1961). Considering these principles, several studies investigated the residual limb-socket overall interface pressure as well as regional pressure mapping, i.e. proximal, middle, distal, medial, lateral, anterior and posterior (Dumbleton et al., 2009, Seelen et al., 2003, Goh et al., 2003). In this thesis the same approach was taken to compare the regional volume and shape differences to comply with the PTB biomechanical principle.

The mean and standard deviation of the volume (mm3) for each region of two repetitions of each casting concept and volume difference between two repetitions are summarized in Table 7-11. Looking at mean difference columns, it can be noticed that volume variation between two repetitions of Hands-on casting method is larger than that of Hands-off concept in all regions except for distal and middle regions of the residual limb, Figure 7-22.

Table 7-11: The mean and standard deviation of volume (mm3) for each region of two repetitions of each casting concept and volume difference between two repetitions

Region	Mean (SD) mm3		Mean difference (SD) mm3	Mean (SD) mm3		Mean difference (SD) mm3
	H-off 1	H-off 2	H-off1 - H-off2	H-on 1	H-on 2	H-on1 - H-on2
A-L	285567.53 (144163.88)	284904.17 (143181.02)	663.35 (4466.00)	287513.47 (140635.44)	275816.08 (135721.14)	11697.39 (18394.33)
A-M	184602.26 (61934.75)	184430.92 (62131.10)	171.34 (5135.96)	191006.50 (64020.38)	1803092.77 (58299.46)	7913.73 (10871.89)
P-L	312730.60 (115808.00)	314824.59 (113839.87)	- 2093.99 (11326.17)	319797.14 (127496.42)	327316.82 (125287.45)	- 7519.68 (13678.61)
P-M	221712.65 (60022.84)	221641.40 (59877.60)	71.25 (15103.64)	236744.99 (66843.42)	235752.47 (59361.07)	992.52 (24387.24)
Distal	190600.10 (64744.37)	191701.39 (63435.98)	- 1101.28 (11641.72)	176594.38 (73801.56)	176779.01 (65441.12)	- 184.63 (16398.34)
Middle	365797.29 (126577.84)	364928.64 (122581.30)	2804.93 (14301.54)	382273.05 (127010.40)	379468.12 (121486.35)	868.64 (13325.32)
Proximal	449826.34 (150318.7)	450846.36 (151331.43)	- 1020.02 (11601.41)	477764.39 (164951.10)	468144.53 (156290.14)	9619.86 (21634.93)

Figure 7-22: difference between two repetitions of Hands-off and Hands-on casting concepts

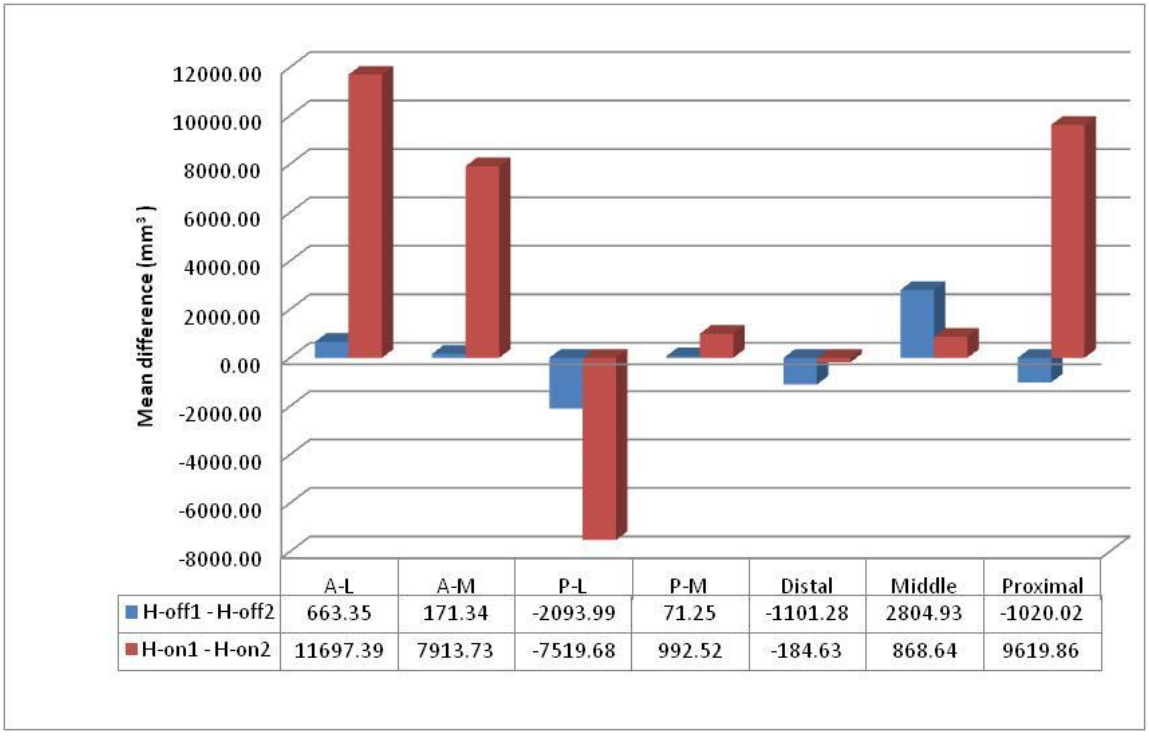

The result of ICC test shows that resulted volume of residual limb by both Hands-on and Hands-off concepts is repeatable in all regions, Table 7-12.

Table 7-12: ICC test for regional volume repeatability of Hands-off and Hands-on concepts

ICC	H-off	H-on
A-L	1.000	0.988
A-M	0.997	0.977
P-L	0.995	0.993
P-M	0.971	0.931
Distal	0.948	0.975
Middle	0.995	0.994
Proximal	0.997	0.990

The average of two repetitions of Hands-off and Hands-on volume measurements in each region were calculated then compared using t-test, Table 7-13. Results show that there is no significance difference between volume measurements for Hands-on and Hands-off methods ($p>0.05$). The Bland and Altman plots for inter and intra cast regional volumes are presented in Figure 55 to Figure 75 in the "Bland and Altman plots" document in the cd.

Table 7-13: Significance of Hands-on and Hands-off volume difference, t-test

Region	Mean (SD) mm3		Significance (0.05)
	H-off	H-on	
A-L	285235.85 (143655.94)	281664.77 (137893.76)	0.951
A-M	61979.83 (17892.036)	60984.99 (17604.85)	0.921
P-L	313777.59 (114589.20)	323556.98 (126211.59)	0.844
P-M	59472.72 (17168.29)	62025.84 (17905.32)	0.563
Distal	191150.74 (63828.64)	176686.69 (69263.14)	0.600
Middle	365362.97 (124417.33)	380870.60 (124073.179)	0.763
Proximal	450336.35 (150714.33)	472954.46 (160314.44)	0.725

7.5.6 Shape difference

The shape difference between two repetitions of each casting method was measured (section 7.3). The mean and standard deviation was calculated for the shape difference of each casting method. Coefficient of Variation (CoV %) was also calculated to examine for the shape consistency of each method, Table 7-14. The results show that both methods have high CoV, hence; little shape consistency exists between two repetitions of each method. However, shape consistency is slightly higher for Hands-on method than Hands-off method (CoV Hands-on = 49.68% and CoV Hands-off = 61.97%) but the mean shape difference is higher in Hands-on concept. In other words, although the Hands-off method has less mean shape difference, the standard deviation is higher relative to the mean value.

Table 7-14: Mean, standard deviation and CoV (%) for shape difference of Hands-off and Hands-on methods repetitions

Mean (SD) mm3		CoV	
H-off	H-on	H-off	H-on
53523.24 (33169.73)	90464.92 (44964.24)	61.970	49.680

7.5.7 Regional shape difference

Same as regional volume difference the regional shape difference was measured for seven regions Table 7-15. It can be seen that the CoV is higher for Hands-off casting, hence less repeatable than the Hands-on method in all regions. However, the mean difference is higher for Hands-on method, Figure 7-23.

Table 7-15: Mean, standard deviation and CoV (%) for regional intra cast shape difference of Hands-off and Hands-on methods

Region	Mean (SD) mm3		CoV	
	H-off	H-on	H-off	H-on
A-L	13262.40 (8748.46)	23305.66 (13229.65)	65.960	56.770
A-M	8906.41 (6400.15)	16092.95 (8621.07)	71.860	53.570
P-L	16355.30 (10419.91)	25402.99 (14007.36)	63.710	55.140
P-M	14341.32 (10869.77)	25661.52 (17497.69)	75.790	68.190
Distal	19870.41 (13333.14)	25574.58 (14187.62)	67.100	55.480
Middle	15290.86 (10851.94)	30938.05 (19594.40)	70.970	63.330
Proximal	17604.79 (10146.99)	33950.67 (14858.50)	57.640	43.770

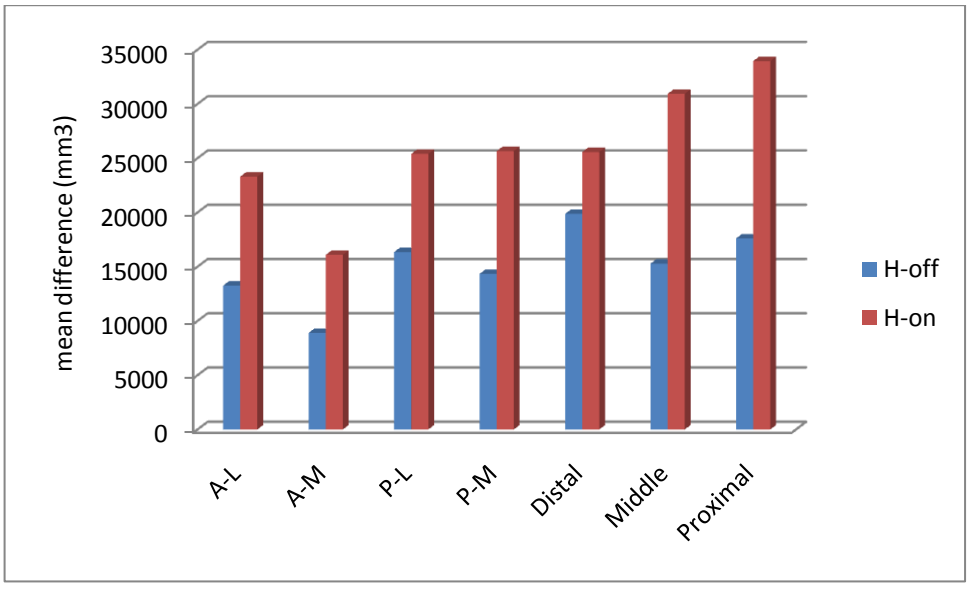

Figure 7-23: regional intra cast shape difference of Hands-off and Hands-on methods

7.5.8 Clinical Significance of the Results

In order to put the results of the study into a clinical context, one layer of a towel sock, with thickness of 2.28 mm, would increase the volume of the cast by 7.94% (section 6.5.). This was calculated based on volume of one residual limb model. However, this was in agreement with volume increase in 48 residual limb images, after 2.28 mm increase in radius of transverse cross section of the residual limb, when calculated using Analyze software.

To examine if the volume difference of two repetitions of each casting method is different from the volume of one layer of towel sock over the residual limb, first, 92.06% of one of the randomly selected repetitions was calculated then subtracted from the other repetition. For example, if the H-off1 was selected the calculation would be as:

$$V\text{-}H\text{-}off_{sock} = (0.9206 \times V_{H\text{-}off1}) - V_{H\text{-}off2}$$

Where $V\text{-}H\text{-}off_{sock}$ is the volume difference between residual limb with one layer of sock and without the sock, $V_{H\text{-}off1}$ is the volume of first repetition of Hands-off casting concept and $V_{H\text{-}off2}$ is the volume of the second repetition of the Hands-off concept. The one-sample t-test was used to test the following hypotheses:

H_0= $V\text{-}H\text{-}off_{sock}$ is zero

and

H_1= $V\text{-}H\text{-}off_{sock}$ is smaller than zero

If H_0 is rejected ($p<0.05$) then the volume difference between two repetitions of Hands-off casting concept is less than the volume of one sock over the residual limb.

The same process was repeated for $V\text{-}H\text{-}on_{sock}$ to examine if the volume difference between two repetitions of Hands-on casting concept is less than the volume of sock over the residual limb.

In the next step, the volume of one layer of sock was examined against the volume difference between two casting methods. Since no significance difference was found for inter-cast volume variability, the average volume of two repetitions of each casting method was calculated and then afore mentioned process was repeated as

$$V_{sock} = (0.9206 \times V_{H\text{-}off}) - V_{H\text{-}on}$$

The mean, standard deviation and results of one-sample t-test is summarized in Table 7-16. The results show that the 92.06% of one repetition of casting concept is significantly different from the second repetition ($p<0.05$). In addition, 92.06% of average of Hands-off casting repetitions is significantly different from average of Hands-on casting repetitions ($p<0.05$).

Table 7-16: Mean, standard deviation and significance of one layer of sock

	Mean	SD	Significance(p<0.05)
$V\text{-}H\text{-}off_{sock}$	-82195.43	32406.75	0.000
$V\text{-}H\text{-}on_{sock}$	-69342.12	41870.52	0.000
V_{sock}	-102508.69	48609.5	0.000

In order to compare the amount of shape difference of casting concepts to the volume of one layer of sock over the residual limb, the 7.94% of average volume of four repetitions were calculated and then compared to the shape difference of each casting concept using Independent-sample t-test. The results are summarized in Table 7-17. The difference between volume of one layer of sock and the Hands-off shape difference is significant ($p<0.05$) but Hands-on shape difference is not significantly different from the volume of a towel sock ($p>0.05$)

The result of statistical test and the line graph (Figure 7-24) shows that the Hands-off casting shape difference is less than 7.94% of total residual limb volume, whereas; there is no significant difference between the Hands-on shape difference and 7.94% of total residual limb volume.

Table 7-17: t-test significance, mean difference (mm3) and standard deviation of volume of one layer of sock and the intra-cast shape difference

	Mean difference (mm3)	SD	Significance
Hands-off	-26454.85	17865.87	0.000
Hands--on	10486.82	41532.30	0.400

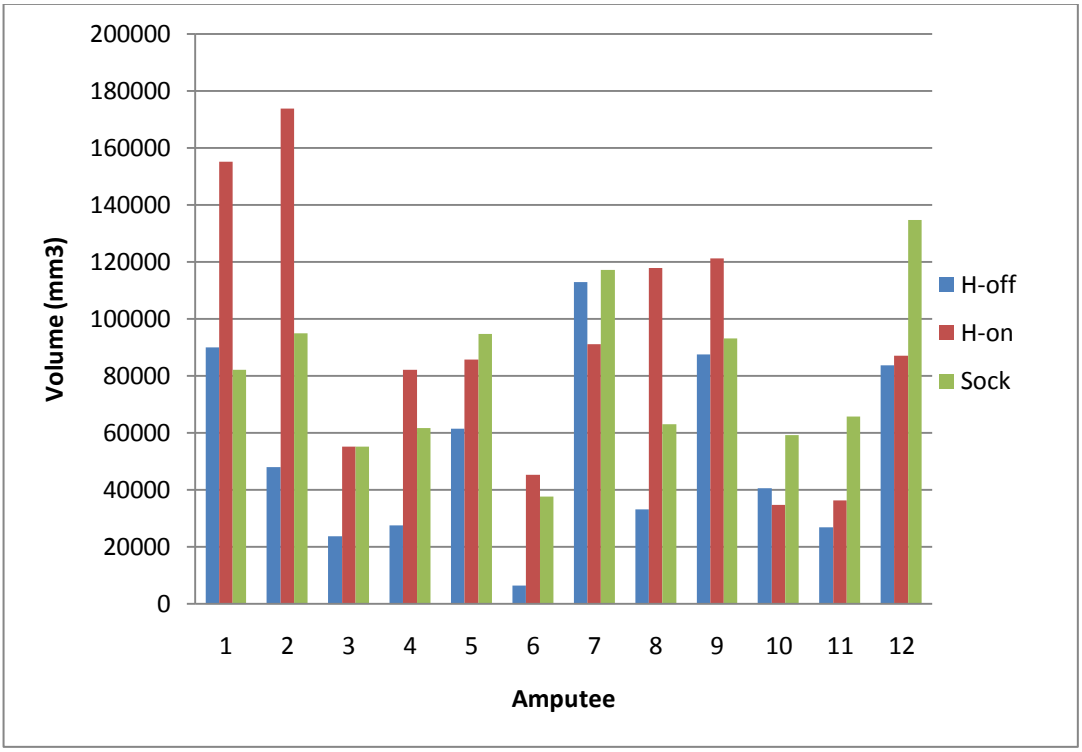

Figure 7-24: Sock volume, Hands-off and Hands-on shape difference

8 Discussion

Direct comparison of the shape and volume of prosthetic sockets is complicated due to the experienced complexity to establish a reliable reference grid, (Buis et al., 2006). Lemaire and Johnson (Lemaire and Johnson, 1996) have been utilising an alignment procedure that involved the calculation of the centroid of each transverse slices and determined the line of best fit through the centroids with the aim to establish a common axis for two shapes. The alignment technique described showed a between-radial-point average error of 2.5 mm after an automatic alignment procedure and a 1.4 mm error after further manual alignment. This method is depending on the centroids, hence; the shape of the each cast. Additionally relating the surface counter of the residual limb to the tibia is eliminated.

For this study the tibia, because of its rigidity, was used to align the two different volume images to a common reference grid system. The tibia was semi-automatically segmented from one of four scans of each amputee's residual limb and used to register all scans using the Analyze software. The Analyze software uses the Normalised Mutual Information algorithm to spatially register the two volumes.

A study to investigate the accuracy of registration was published by Buis (Buis et al., 2006). They reported that the maximum variation of the registration of two consecutive scans of same POP was 1.2 mm (2 pixels). Ninety five percent of the scan showed less than 0.62 (1 pixel) variations. Also registration showed to have an error of approximately 1% relative to mean volume of the residual limb (Smith et al., 1996).

In this manuscript nine transverse slices, three in each regions of distal, middle and proximal, were randomly chosen for the purpose of statistical analysis of the transverse cross section surface area and circularity values. The results of the paired t-test show that both Hands-off and Hands-on have the intra-cast cross sectional surface area consistency in all three regions. Moreover, both have the intra-cast cross sectional circularity consistency in all regions except the first slice of the proximal region in the Hands-on concept ($p<0.05$). This slice was located on average at 2mm

above the tibia plateau (min: 14 mm above the tibia plateau and max: 28mm below the tibia plateau). The lack of consistency in the circularity of the transverse cross section of the residual limb in the proximal region might be explained by the manual dexterity of the clinician while indenting the POP over the residual limb during casting. Similar findings in relation to manual dexterity have been reported by Buis Et al (Buis et al., 2003). Additionally, the POP cast was indented over the femoral condyles to create a suspension method for the cast during the scanning procedure. Additionally the circularity inconsistency, in this region, may have resulted from the hand shaping of the POP at the patellar tendon region and the popliteal area.

The transverse cross sectional surface area difference between two casting method were not statistically significant at any level except the distal part (last slice). However, there was a relatively large difference in the cross sectional surface area between two methods at the distal part, Table 7-5. This could be explained by the uniform force application around the residual limb and the distal traction of the soft tissue in the Hands-off casting resulting in a longer residual limb and, if the volume is unchanged, the smaller cross sectional surface area. Although not statistically significant, the Hands-off method resulted in a smaller overall cross sectional surface area in all amputees Table 13-1.

There is no statistical significant difference in the transverse cross sectional circularity of two casting methods except at the proximal level (slice two). The average location of the selected slice two was 15 mm (min 8 and max: 38 mm) below the tibia plateau, which is approximately at the mid patellar tendon level. This was expected as the residual limb is indented at mid patellar tendon and the popliteal area in the Hands-on casting method.

The circularity value is slightly smaller for the Hands-off method than the Hands-on method hence showing more circularity for Hands-off method, however; this was not statistically significant. This could be due to the uniform pressure around the residual limb using the air bladder.

In the Bland and Altman plots, in an ideal case scenario, the mean difference between two measurement systems should be zero. These plots also show the agreement limits defined by the standard deviation of the difference, hence, showing the variability of two measurement methods. The Bland and Altman plots of cross sectional surface area difference of two repetitions of casting concepts (intra cast surface area consistency) reveals that the Hands-on casting concepts have a greater mean difference and variability at the proximal regions (slice one and two) compared to the lower regions of the residual limb. The surface area mean difference and variability of two repetitions of the Hands-off concepts (intra cast surface area consistency) remain almost similar throughout the length of the residual limb. The intra cast surface area variability of Hands-on casting is larger in the proximal regions compared to that of Hands-off casting (slice one, two and three). The intra cast circularity variability at the proximal region and far distal region (slice one and two and eight) is larger in Hands-on method than the Hands-off method. As it was mentioned earlier the greater surface area and circularity variability in these regions could be explained by manual dexterity of the clinician.

The bland and Altman plots illustrating the differences of the Hands-off and Hands-on surface area and circularity are showing that the mean difference and variability of the inter cast surface area and circularity is larger than that of either Hands-off or Hands-on intra cast results. This was expected as the Hands-on casting has a different approach in shaping the residual limb than the Hands-off method. In addition, the inter cast surface area variability is greater at the distal and proximal regions than that of middle part of the residual limb (slice 1, 2, 3, 7, 8 and 9). Furthermore, the inter cast circularity variability is bigger at the distal region compared to the middle and proximal regions (slice seven, eight and nine).

Buis et al. investigated the shape capturing consistency of Hands-on and Hands-off concepts using a manikin model (Buis et al., 2003). It was shown that the Hands-off concept has more consistent results than the Hands-on socket for shape capturing. The Hands-off concept showed a constant pattern of maximum radius variation of 1.4 mm whereas the Hands-on concept had a maximum radius variation of approximately 2.4mm and 5mm in the middle and proximal part of the model

respectively. The results of their study is in agreement with the result of this study as the cross sectional surface area variability in Hands-off casting shows a constant pattern throughout the length of the residual limb, whereas; the Hands-on concept results in bigger surface area variation at the proximal region. Additionally the overall surface area standard deviation value is bigger for Hands-on concept than that of Hands-off concept, Table 13-1.

Kahle calculated the percentage diameter relative to the residual limb of the Hydrostatic socket (HS) and PTB sockets while was worn by amputees on full load which was +19.4% and +4.4% for A-P diameter at the tibial tuberosity level for HS and PTB sockets respectively (Kahle, 1999). Medilateral percentage differences were as HS= +6.3 % and PTB = +3.7%. This was not confirmed in this study as no sagittal or coronal diameter measurements were carried out. The mean cross sectional surface area of the residual limb showed no significant difference between Hands-on and Hands-off method, although; the resulted surface area was slightly smaller in the Hands-off method. Both investigated casting concepts are showing intra cast length consistency with a high ICC value, Table 7-7. The Bland and Altman plots are showing that the mean difference between two repetitions of the Hands-on casting is greater than that of the Hands-off casting but has a lower standard deviation.

Since both casting methods result in a highly consistent length the average of two repetitions were calculated for the inter cast length comparison using t-test. Although the Hands-off method resulted in 7.6 mm longer residual limb, this difference was not statistically significant ($p=0.595$). Kristinsson reasoned that the combination of the radial pressure around the residual limb and the effect of the silicon liner on downward displacement of the skin results in elongation of the residual limb soft tissue (Kristinsson, 1993). In Hands-off method the residual limb soft tissue is elongated due to the traction applied by the casting device to the distal pin attached to the liner. Kahle reported a length percentage differences, relative to the length of the residual limb, were as 20.1 % and -3.8 % for HS and PTB respectively (Kahle, 1999). No statistical significant differences were found within the intra cast volumes for both the Hands-off and Hands-on casting concepts, Table 7-9. Additionally, it

was found that the average volume of two repetitions of the Hands-on casting concept was not significantly different than that of Hands-off method ($p<0.05$).

Yiğiter et al. measured the volume of the PTB and PTS sockets using water filling method up to the patellar tendon region (Yiğiter et al., 2002). The two socket volumes, PTB = 772.2 ±238.2 PTS = 600.0 ± 182.8, were different. In this study the mean volume difference was 23462.04 mm^3 in which the Hands-on method, same as the results of the study by Yiğiter, resulted in a bigger volume size. However, the percentage volume difference in this study was 2.35% compared to 22.29% in Yiğiter study. Yiğiter measured the volume of sockets whereas in this study the volume of POP cast was measured. Following the shape capturing, the socket is made after the process of cast rectification which includes adding or removing plaster on the positive plaster cast of residual limb in the PTB concept. This may add to the further volume difference of the Hands-on and Hands-off sockets.

Although the result of the ICC test show that there is an intra cast volume consistency for both casting concepts, the Bland and Altman limits of agreement plots show that the mean volume difference of two repetitions of Hands-off casting method is less than that of Hands-on method with less variability (standard deviation), Figure 7-19 and Figure 7-20.

Based on hydrostatic weight bearing, if the volume of the residual limb can be contained in a socket of the same volume a hydrostatic weight bearing system is established as long as no tissue escape from the volume (Klasson and Buis, 2006, Kristinsson, 1993). This principle relies on assumption that the residual limb tissue is not leaking from a tight socket. Although the resulted volume of the residual limb is slightly less than that of the Hands-on method the difference is not statistically significant.

It is important to consider that the above result is only valid for the casting procedure. The situation may be different in a weight bearing condition where there is a fluctuating loading and unloading condition as typically experienced during the gait cycle. Considering the incompressibility and the viscoelastic behaviour of the

soft tissue it can be assumed that the residual limb volume would not significantly change.

The inter and intra regional volume difference was examined in two ways. First, it was tested in four regions of antro-lateral (A-L), antro-medial (A-M), postro-lateral (P-L) and postro-medial (P-M). Then the volume difference was checked in three regions of distal, middle and proximal. The result of the ICC test shows that resulted volume of residual limb by both Hands-on and Hands-off concepts is repeatable in all regions also there is no significance difference between volume measurements of Hands-on and Hands-off method.

The Bland and Altman limits of agreement plots show that the Hands-off casting has less volume variability in A-L and A-M regions than P-L and P-M regions and slightly more variability in the middle region than the proximal and distal regions. This suggests that the amount of Hands-off intra cast volume variability is more in regions that has larger soft tissue volume. The Hands-on method has the more variability in P-M region than the other three regions of A-L, A-M and P-L. This also suggests that the intra cast volume variability is more in regions with larger soft tissue volume. However, Hands-on method has less variability in the distal and middle regions than the proximal region. In contrast to the Hands-off method, this area is not the region of larger soft tissue volume rather the region in which a prosthetist uses hand to pre-shape the cast.

The volume variation between two repetitions (intra-cast) of the Hands-on casting method was larger than for the Hands-off concept. This was in all regions except for distal and middle regions of the residual limb. The Hands-off concept has a smaller intra-cast mean difference but a greater SD relative to the mean value in those regions.

The P-M and P-L inter cast volume difference and variability is larger than that of A-L and A-M regions. Additionally, the distal and proximal inter cast volume variability is larger in the distal and proximal regions than that of middle region.

The CoV was calculated to examine the residual limb shape consistency of each casting method. The CoV was 49.68% and 61.97% for Hands-on and Hands-off concept respectively. The CoV less than 5% is assumed as acceptable repeatability (Campbell et al., 2007). Hence, neither the Hands-on nor the Hands-off method has the acceptable shape consistency. The reason for a high CoV in both casting concept is that the standard deviation of shape difference is large relative to the mean difference value. The shape consistency is slightly higher for Hands-on method than Hands-off method. However, the Hands-off method has less mean shape difference but the standard deviation is higher relative to the mean value. In the Hand-on casting, the shape inconsistency was expected due to the manual dexterity. In the Hands-off method, the shape inconsistency is probably due to inconsistent bladder air pressure within casting repetitions as the final shape of the cast is defined by air pressure which is adjusted manually during casting. Additionally, the alignment of proximally force applied to the casting device may also add to a further shape inconsistency. This could be resolved by reducing prosthetists' manual interfering in setting the air pressure and force application.

The regional intra cast shape difference was calculated for both casting concept and then CoV was caculated. The CoV was higher for Hands-off casting, hence; less repeatable. However, the mean difference between two repetitions of Hands-off is less than that of Hands-on method in all seven regions. This shows that intra cast shape standard deviation of Hands-on method is smaller relative to the mean value.

In both Hands-off and Hands-on casting concepts, the posterior region of the residual limb has bigger mean shape difference than the anterior region. Additionally the P-M region has the highest shape CoV in both Hands-on and Hands-off methods, hence; less shape consistency. The P-M region of the residual limb has relatively larger soft tissue mass. The A-M region shows the least mean shape difference in both casting concept and has the smallest shape CoV in Hands-on method (highest shape consistency). However, the P-L region has the lowest CoV in Hands-off method. The A-M region of the residual limb has the least soft tissue mass.

The middle region of the residual shows the maximum shape inconsistency in both casting concept. However the proximal region shows the bigger mean shape difference than the distal and middle regions in the Hands-on concept. In Hands-off concept the distal region has the highest mean shape difference.

In the study described by Buis et al. where a manikin model was used it was reported that the greatest variation of the used Hands-on method was found to be at the posterior region. And the greater variation for Hands-off concept was mostly located in the lateral region (Buis et al., 2003).

The results show that the intra cast volume and shape mean difference is lower in Hands-off method but the SD is high relative to the mean. The shape consistency of the Hands-off casting method depends on three factors. First, maintaining the consistent bladder pressure during casting and re-casting. Second, direction of proximally applied force to the bladder by the prosthetist and lastly, time delayed after POP application and use of bladder over the residual limb.

In some cases the resulted residual limb was longer and slimmer in one repetition of the Hands-off concept than the other, If the amount of the equal pressure over the residual limb applied by the bladder increases, having the overall volume of the residual limb constant, the transverse cross sectional surface area will decrease and the length will increase. For example, Figure 13-14, shows that the first repetition of the Hands-off cast had smaller cross sectional surface area but resulted in a longer residual limb.

During the Hands-off casting the prosthetist applies a proximally direction force to the bladder. The direction of this force in relation to the long axis of the residual limb has to be consistent in a repeated casting. One would expect that the direction of the applied force to the bladder would not change the resulted residual limb shape as based on hydrostatic principle the force applied to an enclosed fluid medium would distribute equally to the entire volume. However, in the Hands-off casting the bladder is attached to the distal pin of the silicone liner and the liner is in close

contact with the skin. Any change in the direction of the proximally applied force to the bladder would result in a slight change in the force applied over the residual limb.

In the first repetition of Hand-off casting for the second amputee, the bladder was used a little while after the POP application. In this case the POP was partially cured. Despite the equal pressure by the bladder and the pressure equalising property of the liner, the resulted residual limb shape was not the same as the other repetition in circularity, Figure 13-15. The shape formation of a semi-rigid wall cylinder under a uniform pressure would not necessarily be equal throughout the entire medium. This could be, thought of as the different behaviour of a flexible inflated balloon and an empty can of drink both under a uniform external load.

In order to identify the proper time for the permanent prosthetic fitting, Lilja and Oberg measured post amputation volume fluctuation of the residual limb using laser scanning. Based on amputees experience, they assumed the bad fit criteria as to be one or two layers of socks over the residual limb, i e using one or two socks by the amputee, then the new socket must be made. They measured the percentage volume of the one and two socks over the residual limb as to be 5.2% and 9.4% (Lilja and Oberg, 1997). Their results of sock volume percentage is in agreement with that of Fernnie and Holliday (Fernie and Holliday, 1982). Also Saunder calculated the uniform volume change of 5% in a limb with 90mm diameter would be 1mm change in diameter (Sanders et al., 2003).

The percentage volume difference of one layer of the towel sock was measured using water displacement technique. This was 7.94% for a sock thickness of 2.28 mm. The difference between this study and those of Lilja and Saunder is possibly due to the thickness of the sock used.

The results show that the either intra cast or the inter cast volume differences are not clinically significant i.e. the amount of inter and intra volume difference is less than the volume of one towel sock over the residual limb.

The result of statistical test and the line graph (Figure 7-24) shows that the Hands-off casting shape difference is less than 7.94% of total residual limb volume, whereas; there is no significant difference between the Hands-on shape difference and 7.94% of total residual limb volume. This results show the intra-cast shape difference of shape capturing process. The results of this study are only true for the casting stage of the prosthetic socket fabrication. This shows that the Hands-off method results in smaller inter cast shape mean difference, hence more repeatable.

In the Hands-off casting method an air bladder based casting device (icecast copact) is used to apply an equal pressure around the residual limb during casting. When a uniform force is applied to the soft tissue it responds with the same amount of force. If the tissue is assumed incompressible and it does not escape under the load the soft tissue shape would be a result of the compliance of the soft tissue. The residual limb soft tissue consists of several layers of different properties, each responding differently under load. The force flow chooses the stiffest path as the stiffer tissue takes charge and deforms first (Klasson and Buis, 2006). Additionally, the shape of underlying rigid structures, i.e. bone, in combination with the overlying soft tissue thickness is playing roll in defining the final shape of the residual limb under a uniform pressure. As it was confirmed in this study the volume of the residual limb is consistent in both casting concepts i.e. soft tissue is incompressible and is not escaping under a load. Having the properties of the soft tissue unchanged during repeated casting and under the same amount of a uniform pressure, applied by the bladder, the residual limb shape is expected be consistent in a repeated casting. This could be a reason for the less intra cast shape and volume differences in the Hands-off casting method and showing no clinical significant shape inconsistency.

A “good socket fit” depends on the stiffness of the coupling with no pain and or tissue damage. This study relates to the inter and intra cast shape and volume consistency of two common casting methods, hence; one cannot really conclude that one or another casting method is superior from the “good fit” point of view. A casting method may result in either consistent “good fit” or consistent “bad fit” socket.

In summary, the Hands-off method resulted in less overall intra cast volume and shape mean difference and standard deviation compared to that of Hand-on casting. This suggests that the Hands-off is more consistent technique. Hands-off regional intra cast volume mean differences and standard deviations were less than that of the Hands-on method in all regions except in the middle and distal regions, hence; it is more consistent than the Hans-on method in those regions. However, it is worthy of note that the difference was not statistically significant in any cases. Additionally, the inter cast volume difference was not statistically significant either.

The Hands-off intra cast shape mean difference and standard deviation was less than that of Hands-on method for both overall and regional shape. Therefore, the Hands-off resulted in more consistent shape of the residual limb. However the CoV was high for both casting method. This indicates that, although the Hands-off method has lower mean difference and standard deviation, it has a large standard deviation relative to the mean value, hence; statistically neither of two casting techniques is repeatable. The shape inconsistency of the residual limb in Hands-on method is due to the nature of the technique, i.e. manual dexterity and in the Hands-off method is because of manually setting the air pressure and alignment of proximally direction force to the casting device during POP setting. It is recommended to adopt an automatic approach in setting air pressure and alignment of the casting device in order to decrease the prosthetist influence in casting.

9 Limitations of the Study

It was not feasible to calculate the percentage volume and/or shape difference relative to the residual limb in this study. This was not possible because of the limitation of scanning the residual limb without a POP cast with the aim to establish a baseline volume image. Scanning the residual limb while the amputee is lying down in the scanner will result in the soft tissue deformation due to gravity. Therefore this could not be use as a baseline volume image of the residual limb for the shape comparison purposes.

Eight layers of perlon sock was used in both casting methods to create a gap between skin and the casting materials to eliminate the image segmentation error resulting from subcutaneous fat chemical shift. The sock is an incompressible material. Care was given as to avoid any sock folding or applying over tension over the residual limb. However, eight layers of sock over the residual limb during casting are not normally used in clinical practice. The semi-automatic segmentation used in this study was based on adjusting the threshold range. If no gap was made, the image of subcutaneous fat would have superimposed on the surrounding casting materials resulting in errors in segmentation process or even impossible to detect the skin-socket material boundary. Therefore, any possible effect of socks over residual limb assumed to be negligible compared to the segmentation error resulting from fat chemical shift artefact.

The overall shape and volume difference of casting concepts were tested against the volume of one layer of a towel sock over the residual limb to put the results in a clinical context. The clinical significance of the regional volume and shape was not tested. However, it would have been possible to calculate the surface area of the different regions of the residual limb in MRI images and then, having the thickness of the sock, the clinical significant could be tested for each region. This was not performed in this study due to the time constraint as surface measurement and following data processing are time consuming.

Following the casting amputees were moved from the casting room to the MRI scanner room using a hospital trolley and carefully transferred to the scanner table. In addition in both casting concepts the POP was applied above the knee to create a grip over the femoral condyles. However, possibility existed that the cast had a slight movement over the residual limb.

10 Conclusion

The results show that both casting method has intra cast volume consistency and there is no significant volume difference between two methods. Additionally, inter and intra cast mean volume difference was not clinically significant based on the volume of one sock criteria. This supports the hydrostatic weight bearing principle as it is based on assumption that the residual limb soft tissue is incompressible with no tissue escape while it is constrained within a socket.

Based on the results of this study, neither Hands-off method nor Hands-on method results in a consistent residual limb shape as the coefficient of variation of differences of two repetitions of each casting concept was high. Although the resulted shape of the residual limb in Hands-off method was not repeatable, the intra cast shape difference was smaller than the volume of a socket i.e. the Hands-off shape difference is not clinically significant. However, there is no significant difference between Hands-on shape difference and a volume of a sock over the residual limb i.e. the Hands-on shape difference is not clinically significant but equal to the maximum acceptable limit for a poor socket fit.

Both casting concepts show a consistent cross sectional surface area along the length of the residual limb. The Intra cast cross sectional circularity was repeatable in both casting method except at the far proximal part of the residual limb in the Hands-on method. Additionally, the Hands-on method shows more surface area and volume variability in this region than the middle and distal part. Besides, the intra cast surface area and circularity variability of the Hans-on method was larger in this region than that of Hands-off method. Furthermore, the mean Hands-on shape difference is higher in this region than the distal and middle regions. In addition the inter-cast surface area variability was larger at the proximal region than that of middle region. This was expected as a prosthetist uses hand dexterity to indent the patellar tendon region and the popliteal area in the Hands-on casting.

The Hands-off method showed greater circularity variability than the Hands-on casting in the middle region of the residual limb. Furthermore, the Hands-off intra

cast volume variability was larger in this region compared to the distal and proximal regions. Additionally, both casting methods showed larger intra cast shape variability in this region than the proximal and distal region of the residual limb. This region is a region with relatively large soft tissue mass. Large intra cast shape variability of Hands-on method in the middle region is probably due to the POP wrapping as each time prosthetist wraps the POP with a different circular tension which results in a different soft tissue shape in this region. The Hands-off method resulted in large volume and shape variability in the middle region is probably because of the inconsistent intra cast bladder pressure and the alignment of the proximally direction force applied to the bladder. It is recommended some form of automatically setting the air pressure and force alignment is employed to resolve these issues.

The Hands-off intra cast shape difference was larger at the distal region than the proximal and distal regions. In addition, there was a greater inter cast surface area, circularity and volume variability in this region. Besides, the Hands-off intra cast circularity variability was larger in this region compared to that of Hands-on method. At the distal region the Hands-off cast resulted in a longer shape residual limb. The length of the residual limb depends on the meticulously setting and maintaining the bladder pressure and the proximally applied force to the bladder by prosthetist.

Both casting method showed a large inter and intra cast volume and shape difference and variability at the P-M region. Apart from the P-M region, inter cast volume variability was high at the P-L region. At the P-L region both casting concepts showed a large intra cast shape difference but the Hands-off method shows the least intra cast shape CoV in this region compared to other three regions of A-L, A-M and P-M. However, Hands-on method showed the least intra-cast shape CoV at the A-M region followed by the P-L region.

As opposed to the volume comparison, the inter cast shape comparison was not possible due to the lack of the intra cast shape consistency. Therefore, calculating the average shape of the two repetitions was not logical as none of repetitions could be assumed as true value. However, the inter cast transverse surface area and circularity showed that the surface area is different at the distal region of the residual limb and

the circularity is different at the proximal region. Also the Bland and Altman plots of the surface area and circularity show that the distal region shows greater inter cast variability in surface area and circularity and the proximal region shows a large inter cast surface area variability.

In overall the Hands-off method resulted in a less intra cast length, volume and shape mean difference but the larger standard deviation relative to the mean value. This suggests that the Hands-off resulted in a smaller volume, shape and length difference compared to the Hands-on method. However, because of the large intra cast shape standard deviation relative to the mean difference, Hands-off resulted in a shape inconsistency. One should take into consideration that although the Hands-off resulted in a shape inconsistency, the intra cast shape difference is less than the clinical significant level of poor socket fit, based on volume of one layer of towelling sock, whereas; the Hands-on intra cast shape difference is equal to volume of one layer of sock over the residual limb.

11 Further Studies

As no similar study could not be found on inter- and intra cast concept consistency on real subjects, there was not enough data to be used in sample size calculation. Sample size of twelve was decides based on the functional approximation described for reliability studies by Walter et al. (Walter et al., 1998). It is suggested to use larger sample size based on the results of this study to explore the possible statistical significance of minor regional and or overall inter and intra cast volume differences.

In this study one prosthetist cast the participants' residual limb. Bias in casting is probably existed as there might be an interpretation of the casting procedure. Due to time and money constrains having two or more clinician in this study was not practical. Therefore it is suggested for later studies inter and intra rater consistency of the casting could be examined. The same approach can be attained to evaluate inter and intra shape and volume of cast rectification in different socket concepts.

An air bladder used for the pressure casting. As it was discussed earlier in the discussion section, some inconsistency in results might have occurred due to the nature of the device. Other pressure casting devices, such as the hydro-cast method can be utilised to evaluate the shape and volume consistency of the pressure casting method.

This study attempted to compare the intra and inter cast shape and volume of two Hands-off and Hands-on casting concepts, the first stage of socket manufacturing. In order to get better understanding of the different socket geometry, it is suggested to evaluate the Hands-off and Hands-on final socket geometry and relate this to the internal structures as tibia bone in future studies. In addition the same evaluation studies can be conducted for sockets in a weight bearing conditions as well as effect of change in the alignment of the prosthetic components on this issue. In addition, it is suggested to evaluate the behaviour of the residual limb soft tissue under two casting condition and to consider factors such as muscle contraction, tissue composition etc.

The quality of socket fit relies on the socket-residual limb coupling stiffness providing comfort with no pain or tissue damage to the amputee. Therefore, it is recommended to consider "amputee's comfort" in any socket/prosthesis investigation. When objective assessment of socket geometry, soft tissue characteristics, prosthetic components, etc is combined with amputees' subjective feedback, then the better understanding of the socket designs would be possible.

12 References

AISEN, A. M., MARTEL, W., BRAUNSTEIN, E. M., MCMILLIN, K. I., PHILLIPS, W. A. & KLING, T. F. (1986) MRI and CT evaluation of primary bone and soft-tissue tumors. *American Journal of Roentgenology,* 146**,** 749-756.

ALESCH, F. (1994) A simple technique for making a stereotactic localiser both CT and MRI compatible. Technical note. *Acta Neurochir (Wien),* 127**,** 118-20.

ALTMAN, D. G. (Ed.) (1999) *Practical Statistics for Medical Research*, Chapman & Hall/CRC

BASH, C., ROTHMAN, M., HAMET, M., SORCE, D., ZOARSKI, G., MIHARA, F. & NUMAGUCHI, Y. (1995) MRI of silicone vitreous ocular implants with phantom correlation. *Neuroradiology,* 37**,** 313-316.

BENEKE, R., NEUERBURG, J. & BOHNDORF, K. (1991) Muscle cross-section measurement by magnetic resonance imaging *Eur J Appl Physiol,* 63**,** 424-429.

BLAND, J. M. & ALTMAN, D. G. (1986) Statistical methods for assessing agreement between two methods of clinical measurement. *Lancet,* i**,** 307-310.

BROOKS, R. A. & DI CHIRO, G. (1977) Slice geometry in computer assisted tomography. *J Comput Assist Tomogr,* 1**,** 191-199.

BUIS, A., BLAIR, A., CONVERY, P., SOCKALINGAM, S. & MCHUGH, B. (2003) Pilot study: data-capturing consistency of two trans-tibial casting concepts, using a manikin stump model: a comparison between the hands-on PTB and hands-off ICECAST compact concepts. *Prosthet. Orthot. Int.,* 27**,** 100-106.

BUIS, A., CONDON, B., BRENNAN, D., MCHUGH, B. & HADLEY, D. (2006) Magnetic resonance imaging technology in transtibial socket research: A pilot study. *J Rehabil Res Dev.,* 43**,** 883-90.

BYRUM, C. E., MACFALL, J. R., CHARLES, H. C., CHITILLA, V. R., BOYKO, O. B., UPCHURCH, L., SMITH, J. S., RAJAGOPALAN, P., PASSE, T., KIM, D., XANTHAKOS, S., RANGA, K. & KRISHNAN, R. (1996) Accuracy and reproducibility of brain and tissue volumes using a magnetic resonance segmentation method. *Psychiatry Research-Neuroimaging,* 67**,** 215-234.

CAMPBELL, M. J., MACHIN, D. & WALTERS, S. J. (Eds.) (2007) *Medical statistics: a textbook for the health sciences*, Willy.

CARAVAN, P., ELLISON, J. J., MCMURRY, T. J. & LAUFFER, R. B. (1999) Gadolinium(III) Chelates as MRI Contrast Agents: Structure, Dynamics, and Applications. *Chem Rev,* 99**,** 2293-352.

CARLSSON, B. R. & HIRONS, R. R. (1997) Design and test of a new ICECAST pressurized casting instrument. *BAPO Newsletter.*

CLUITMANS, J., GEBOERS, M., DECKERS J - RINGS, F. & RINGS, F. (1994) Experiences with respect to the ICEROSS system for trans-tibial prostheses. *Prosthet Orthot Int.,* 18**,** 78-83.

COLEMAN, K. L., BOONE, D. A., LAING, L. S., MATHEWS, D. E. & SMITH, D. G. (2004) Quantification of prosthetic outcomes: elastomeric gel liner with locking pin suspension versus polyethylene foam liner with neoprene sleeve suspension. *JRRD,* 41**,** 591-602.

COMMEAN, P. K., SMITH, K. E., CHEVERUD, J. M. & VANNIER, M. W. (1996a) Precision of surface measurements for below-knee residua. *Arch Phys Med Rehabil,* 77**,** 477-86.

COMMEAN, P. K., SMITH, K. E. & VANNIER, M. W. (1996b) Design of a 3-D surface scanner for lower limb prosthetics: a technical note. *J Rehabil Res Dev,* 33**,** 267-278.

COMMEAN, P. K., SMITH, K. E., VANNIER, M. W., SZABO, B. A. & ACTIS, R. L. (1997) Finite element modeling and experimental verification of lower extremity shape change under load *Journal of Biomechanics,* 30**,** 531-536.

CONDON, B. (2006) Magnetic suseptibility artefact. IN SAFARI, M. R. (Ed.). Glasgow.

CONVERY, P., BUIS, A., WILKIE, R., SOCKALINGAM, S., BLAIR, A. & MCHUGH, B. (2003) Measurement of the consistency of patellar-tendon-bearing cast rectification. *Prosthet Orthot Int.,* 27**,** 207-213.

COVEY, S. J., MUONIO, J. & STREET, G. M. (2000) Flow Constraint and Loading Rate Effects on Prosthetic Liner Material and Human Tissue Mechanical Response. *JPO,* 12**,** 15-32.

CYTEVAL, C., THOMAS, E., PICOT, M. C., DERIEFFY, P., BLOTMAN, F. & TAOUREL, P. (2002) Normal vertebral body dimensions: a new measurement method using MRI. *Osteoporos Int. ,* 13**,** 468-473.

DASGUPTA, A. K., MCCLUSKIE, P. J. A., PATEL, V. S. & ROBINS, L. (1997) The performance of the ICEROSS prostheses amongst transtibial amputees with a special reference to the workplace--a preliminary study. *Occup Med (Lond),* 47**,** 228-236.

DATTA, D., HARRIS, I., HELLER, B., HOWITT, J. & MARTIN, R. (2004) Gait, cost and time implications for changing from PTB to ICEX sockets. *Prosthet Orthot Int.,* 28**,** 115-120.

DATTA, D., VAIDYA, S. K., HOWITT J - GOPALAN, L. & GOPALAN, L. (1996) Outcome of fitting an ICEROSS prosthesis: views of trans-tibial amputees. *Prosthet Orthot Int.,* 20**,** 111-115.

DOUGLAS, T., SOLOMONIDIS, S., LEE, V. S. P., SPENCE, W., SANDHAM, W. & HADLEY, D. (1998) Automatic segmentation of magnetic resonance images of the trans-femoral residual limb. *Medical Engineering & Physics,* 20**,** 756-763.

DOUGLAS, T., SOLOMONIDIS, S., SANDHAM, W. & SPENCE, W. (2002a) Ultrasound image matching using genetic algorithms. *Medical and Biological Engineering and Computing,* 40**,** 168-172.

DOUGLAS, T., SOLOMONIDIS, S., SANDHAM, W. & SPENCE, W. (2002b) Ultrasound imaging in lower limb prosthetics. *IEEE Trans Neural Syst Rehabil Eng.,* 10**,** 11-21.

DUDEK, N. L., B., M. M., C., M. S. & CHARDON, J. P. (2005) Dermatologic conditions associated with use of a lower-extremity prosthesis. *Archives of physical medicine and rehabilitation,* 86**,** 659-663.

DUMBLETON, T., BUIS, A., MCFADYEN, A., MCHUGH, B. F., MCKAY, G., MURRAY, K. D. & SEXTON, S. (2009) Dynamic interface pressure distributions of two transtibial prosthetic socket concepts *JRRD,* 46**,** 405-416.

ECKSTEIN, F., SITTEK, H., MILZ, S., PUTZ, R. & REISER, M. (1994) The morphology of articular cartilage assessed by magnetic resonance imaging (MRI). Reproducibility and anatomical correlation. *Surg Radiol Anat,* 16**,** 429-438.

EDWARDS, M. L. (2000) Below knee prosthetic socket designs and suspension systems. *Phys Med Rehabil Clin N Am,* 11**,** 585-93.

ENGSBERG, J. R., CLYNCH, G. S., LEE, A. G., ALLAN, J. S. & HARDER, J. A. (1992) A CAD CAM method for custom below-knee sockets. *Prosthet Orthot Int.,* 16**,** 183-8.

ENGSTROM, C. M., LOEB, G. E., REID, J. G., FORREST, W. J. & AVRUCH, L. (1991) Morphometry of the human thigh muscles. A comparison between anatomical sections and computer tomographic and magnetic resonance images. *J Anat,* 176**,** 139-156.

EVERS, A. (2001) The Revised Dutch Rating System for Test Quality. *International Journal of Testing,* 1**,** 155-182.

FAULKNER, V. W. & WALSH, N. E. (1989) Computer Designed Prosthetic Socket from Analysis of Computed Tomography Data. *JPO,* 1**,** 154-164.

FERGASON, J. & SMITH, M. D. (1999) Socket considerations for the patient with a transtibial amputation. *Clin Orthop Relat Res***,** 76-84.

FERNIE GR - HALSALL, A. P., HALSALL AP - RUDER, K. & RUDER, K. (1984) Shape sensing as an educational aid for student prosthetists. *Prosthet Orthot Int.,* 8**,** 87-90.

FERNIE, G. R., GRIGGS, G., BARTLETT, S. & LUNAU, K. (1985) Shape sensing for computer aided below-knee prosthetic socket design. *Prosthet Orthot Int.,* 9**,** 12-6.

FERNIE, G. R. & HOLLIDAY, P. J. (1982) Volume fluctuations in the residual limbs of lower limb amputees. *Archives of physical medicine and rehabilitation,* 63**,** 162-165.

FOISNEAU-LOTTIN, A., MARTINET, N., HENROT, P., PAYSANT, J., BLUM, A. & ANDRE, J. M. (2003) Bursitis, adventitious bursa, localized soft-tissue inflammation, and bone marrow edema in tibial stumps: the contribution of magnetic resonance imaging to the diagnosis and management of mechanical stress complications. *Arch Phys Med Rehabil,* 84**,** 770-777.

GADEBERG, P., GUNDERSEN, H. J. G. & TAGEHOJ, F. (1999) How accurate are measurements on MRI? A study on multiple sclerosis using reliable 3D stereological methods. *Journal of Magnetic Resonance Imaging,* 10**,** 72-79.

GOH, J., LEE, P. & CHONG, S. (2003) Static and dynamic pressure profiles of a patellar-tendon-bearing (PTB) socket. *Proceedings of the Institution of Mechanical Engineers, Part H: Journal of Engineering in Medicine,* 217**,** 121-126.

GOH, J. C., LEE, P. V. & CHONG, S. Y. (2004) Comparative study between patellar-tendon-bearing and pressure cast prosthetic sockets. *J Rehabil Res Dev.,* 41**,** 491-501.

GOMBERG, B. R., SAHA, P. K. & WEHRLI, F. W. (2005) Method for cortical bone structural analysis from magnetic resonance images. *Acad Radiol,* 12**,** 1320-1332.

GREVSTEN, S. & ERIKSON, U. (1975) A roentgenological study of the stump-socket contact and skeletal displacement in the PTB-Suciton Prosthesis. *Ups J Med Sci,* 80**,** 49-57.

HACHISUKA, K., DOZONO, K., HAJIME, O., SABURO, O., HIDEO, S. & KOICHI, S. (1998) Total surface bearing below-knee prosthesis: Advantages, disadvantages, and clinical implications. *Archives of physical medicine and rehabilitation,* 79**,** 783-789.

HAGBERG, K., BRÅNEMARK, R. & HÄGG, O. (2004) Questionnaire for Persons with a Transfemoral Amputation (Q-TFA): initial validity and reliability of a new outcome measure. *JRRD,* 41**.,** 695-706.

HAN, H. S., CHANG, C. B., SEONG, S. C., LEE, S. & LEE, M. C. (2008) Evaluation of anatomic references for tibial sagittal alignment in total knee arthroplasty. *Knee Surgery Sports Traumatology Arthroscopy,* 16**,** 373-377.

HAUBNER, M., ECKSTEIN, F., SCHNIER, M., LOSCH, A., SITTEK, H., BECKER, C., KOLEM, H., REISER, M. & ENGLMEIER, K. (1997) A non-invasive technique for 3-dimensional assessment of articular cartilage thickness based on MRI. Part 2: Validation using CT arthrography. *Magnetic Resonance Imaging,* 15**,** 805-813.

HAVET, E., GABRION, A., LEIBER-WACKENHEIM, F., VERNOIS, J., OLORY, B. & MERTL, P. (2007) Radiological study of the knee joint line position measured from the fibular head and proximal tibial landmarks. *Surgical and Radiologic Anatomy,* 29**,** 285-289.

HE, P., XUE, K., CHEN, Q., MURKA, P. & SCHALL, S. (1996) A PC-based ultrasonic data acquisition system for computer-aided prosthetic socket design. *ieee Trans Rehabil Eng,* 4**,** 114-9.

HE, P., XUE, K. & MURKA, P. (1997) 3-D imaging of residual limbs using ultrasound. *JRRD,* 34**,** 269-278.

HENROT, P., STINES, J., WALTER, F., MARTINET, N., PAYSANT, J. & BLUM, A. (2000) Imaging of painful lower limb stump. *RadioGraphics,* 20**,** S219-S235.

HIGGINS, D. M. (2003) http://www.revisemri.com.

HOAGLUND, F. T., JERGESEN, H. E. & WILSON, L. E. A. (1983) Evaluation of problems and needs of veteran lower-limb amputees in the San Francisco Bay Area during the period 1977-1980. . *JRRD,* 20**,** 57-71.

HOUSTON, V. L., BURGESS, E. M., CHILDRESS, D. S., LEHNEIS, H. R., MASON, C. P., GARBARINI, M. A., LABLANC, K. P., BOONE, D. A., CHAN, R. B., HARLAN, J. H. & BRNCICK, M. D. (1992) Automatic fabrication of mobility aids (AFMA): below-knee CASD?CAM testing and evaluation program results. *J Rehabil Res Dev,* 29**,** 78-124.

HOUSTON, V. L., MASON, C. P., BEATTIE, A. C., LABLANC, K. P., GARBARINI, M., LORENZE, E. J. & THONGPOP, C. M. (1995) The VA-Cyberware lower limb prosthetics-orthotics optical laser digitizer. *JRRD,* 32**,** 55-73.

HUANG, Q. H. & ZHENG, Y. P. (2005) A new scanning approach for limb extremities using a water bag in freehand 3-D ultrasound. *Ultrasound in medicine & biology,* 31**,** 575-583.

JOHANSSON, S. & OBERG, T. (1998) Accuracy and precision of volumetric determinations using two commercial CAD systems for prosthetics: a technical note. *JRRD,* 35**,** 27-33.

KAHLE, J. T. (1999) Conventional and Hydrostatic Transtibial Interface Comparison. *JPO,* 11**,** 85-91.

KAPP, S. & FERGASON, J. R. (2004) Transtibial Amputation: Prosthetic Management. IN SMITH, D. G., MICHAEL, J. W. & BOWKER, J. H. (Eds.) *Atlas of Limb Prosthetics: Surgical, Prosthetic, and Rehabilitation Principles.* NY, American Academy of Orthopaedic Surgeons.

KLASSON, B. (1985) Computer aided design, computer aided manufacture and other computer aids in prosthetics and orthotics. *Prosthetics and Orthotics International,* 9**,** 3-11.

KLASSON, B. (1994) Appreciation of prosthetic socket fitting from basic engineering principle. *NCTEPO, University of Strathclyde*.

KLASSON, B. & BUIS, A. (2006) Prosthethic socket fit; Implication of basic engineering principles. IN SIMPSON, D. (Ed.). NCPO, University of Strathclyde.

KRISTINSSON, O. (1993) The ICEROSS concept: a discussion of a philosophy. *Prosthet Orthot Int.,* 17**,** 49-55.

LEGRO, M. W., REIBER, G., DEL AGUILA, M., AJAX, M. J., BOONE, D. A., LARSEN, J. A., SMITH, D. G. & SANGEORZAN, B. (1999) Issues of importance reported by persons with lower limb amputations and prostheses. *J Rehabil Res Dev.,* 36**,** 155-63.

LEGRO, M. W., REIBER, G. D., SMITH, D. G., DEL AGUILA, M., LARSEN, J. & BOONE, D. (1998) Prosthesis evaluation questionnaire for persons with lower limb amputations: assessing prosthesis-related quality of life. *Arch Phys Med Rehabil,* 79**,** 931-938.

LEMAIRE, E. D. & JOHNSON, F. (1996) A quantitative method for comparing and evaluating manual prosthetic socket modifications. *IEEE Trans Rehabil Eng,* 4**,** 303-9.

LI, F. Y., YARNYKH, V. L., HATSUKAMI, T. S., CHU, B. C., BALU, N., WANG, J. N., UNDERHILL, H. R., ZHAO, X. H., SMITH, R. & YUAN, C. (2010) Scan-Rescan Reproducibility of Carotid Atherosclerotic Plaque Morphology and Tissue Composition Measurements Using Multicontrast MRI at 3T. *Journal of Magnetic Resonance Imaging,* 31**,** 168-176.

LILJA M - JOHANSSON, T., JOHANSSON T - OBERG, T. & OBERG, T. (1993) Movement of the tibial end in a PTB prosthesis socket: a sagittal X-ray study of the PTB prosthesis. *Prosthet Orthot Int.,* 17**,** 21-6.

LILJA, M., HOFFMANN, P. & OBERG, T. (1998) Morphological changes during early trans-tibial prosthetic fitting. *Prosthet Orthot Int.,* 22**,** 115-122.

LILJA, M. & OBERG, T. (1997) International Forum: Proper Time for Permanent Prosthetic Fitting. *JPO,* 9**,** 90-95.

LIU, J., ZHANG, R. & RUAN, S. W. G. (1997) Calibration and analysis of measurement system for surface of the stump. *Chinese J Biomed Eng,* 16**,** 147-53.

LYON, C. C., KULKARNI, J., ZIMERSONC, E., ROSS, E. V. & BECK, M. H. (2000) Skin disorders in amputees. *Journal of the American Academy of Dermatology,* 42**,** 501-507.

MCCURDIE, I., HANSPAL, R. & NIEVEEN, R. (1997) ICEROSS - a consensus view: A questionnaire survey of the use of ICEROSS in the United Kingdom. *Prosthetics and Orthotics International,* 21**,** 124-128.

MCGARRY, A. (2009) Evaluation of the Tracer Cad and T ring prosthetic shape capture systems. *NCPO.* Glasgow University of Strathclyde.

MCGIBBON, C. A. (2003) Inter-rater and intra-rater reliability of subchondral bone and cartilage thickness measurement from MRI. *Magnetic Resonance Imaging,* 21**,** 707-714.

MCROBBIE, D. W., MOORE, E. A., GRAVES, M. J. & PRINCE, M. R. (2007) *MRI From Picture to Proton,* Cambridge University Press.

MEIER, R. H., MEEKS, E. D. & HERMAN, R. M. (1973) Stump-socket fit of below-knee prostheses: comparison of three methods of measurement. *Arch Phys Med Rehabil,* 54**,** 553-8.

MITSIOPOULOS, N., BAUMGARTNER, R. N., HEYMSFIELD, S. B., LYONS, W., GALLAGHER, D. & ROSS, R. (1998) Cadaver validation of skeletal muscle measurement by magnetic resonance imaging and computerized tomography. *J Appl Physiol,* 85**,** 115-122.

MOERLAND, M. A., BEERSMA, R., BHAGWANDIEN, R., WIJRDEMAN, H. K. & BAKKER, C. J. G. (1995) Analysis and correction of geometric distortions in 1.5 T magnetic resonance images for use in radiotherapy treatment planning. *Physics in Medicine and Biology,* 40**,** 1651-1664.

MORIMOTO, A. K., BOW, W. J. & STRONG, D. S. (1995) 3D ultrasound imaging for prosthesis fabrication and diagnostic imaging. *Other Information: PBD: Jun 1995.*

MORTIMORE, I. L., MARSHALL, I., WRAITH, P. K., SELLAR, R. J. & DOUGLAS, N. J. (1998) Neck and total body fat deposition in nonobese and obese patients with sleep apnea compared with that in control subjects. *Am J Respir Crit Care Med,* 157**,** 280-283.

MURDOCH, A. H., MATHIAS, K. J. & SMITH, F. W. (2002) Measurement of the bony anatomy of the humerus using magnetic resonance imaging. *Proc Inst Mech Eng [H],* 216**,** 31-35.

MURDOCH, G. (1968) The Dundee socket for below-knee stump amputation. *Prosthet Int,* 3**,** 15-21.

NARITA, H., YOKOGUSHI, K., SHI, S., KAKIZAWA, M. & NOSAKA, T. (1997) Suspension effect and dynamic evaluation of the total surface bearing (TSB) trans-tibial prosthesis: A comparison with the patellar tendon bearing (PTB) trans-tibial prosthesis. *Prosthetics and Orthotics International,* 21**,** 175-178.

NASDAB (2009) The Amputee Statistical Database for the United Kingdom 2009/07. Edinburgh, National Amputee Statistical Database (NASDAB).

PEARSON, J. R., HOLMGREN, G., MARCH, L. & OBERG, K. (1973) Pressures in critical regions of the below-knee patellar-tendon-bearing prosthesis. *Bull Prosthet Res,* 10**,** 53-76.

RADCLIFFE, C. W. & FOORT, J. (1961) The patellar-tendon-bearing below-knee prosthesis. Berkeley University of California,Biomechanics Laboratory

ROHRER M - BAUER, H., BAUER H - MINTOROVITCH, J., MINTOROVITCH J - REQUARDT, M., REQUARDT M - WEINMANN, H.-J. & WEINMANN, H. J. (2005) Comparison of magnetic properties of MRI contrast media solutions at different magnetic field strengths. *Invest Radiol,* 40**,** 715-24.

ROSS, R., LEGER, L., GUARDO, R., DE GUISE, J. & PIKE, B. G. (1991) Adipose tissue volume measured by magnetic resonance imaging and computerized tomography in rats. *J Appl Physiol,* 70**,** 2164-2172.

SANDERS, J. E., GOLDSTEIN, B. S. & LEOTTA, D. F. (1995) Skin response to mechanical stress : Adaptation rather than breakdown—A review of the literature. *J Rehabil Res Dev,* 32**,** 214-226.

SANDERS, J. E., MITCHELL, S. B., ZACHARIAH, S. C. & WU, K. (2003) A digitizer with exceptional accuracy for use in prosthetics research: A technical note. *Journal of Rehabilitation Research and Development,* 40**,** 191-195.

SANDERS, J. E., ROGERS, E. L., SORENSON, E. A., LEE, G. S. & ABRAHAMSON, D. C. (2007) CAD/CAM transtibial prosthetic sockets from central fabrication facilities: how accurate are they? *JRRD,* 44**,** 395-406.

SAUNDERS, C. G. & VICKERS, G. W. (1984) A generalized approach to the replication of cylindrical bodies with compound curvature. *J Mech Trans Automat Des,* 106**,** 70-76.

SEELEN, H. A. M., ANEMAAT, S., JANSSEN, H. M. H. & DECKERS, J. H. M. (2003) Effects of prosthesis alignment on pressure distribution at the stump/socket interface in transtibial amputees during unsupported stance and gait. *Clin Rehabil,* 17**,** 787-796.

SELLES, R. W., JANSSENS, P. J., JONGENENGEL, C. D. & BUSSMANN, J. B. (2005) A randomized controlled trial comparing functional outcome and cost efficiency of a total surface-bearing socket versus a conventional patellar tendon-bearing socket in transtibial amputees. *Archives of physical medicine and rehabilitation,* 86**,** 154-161.

SHUXIAN, Z., WANHUA, Z. & BINGHENG, L. (2005) 3D reconstruction of the structure of a residual limb for customising the design of a prosthetic socket. *Medical engineering & physics,* 27**,** 67-74.

SMITH, A. S., WEINSTEIN, M. A., HURST, G. C., DEREMER, D. R., COLE, R. A. & DUCHESNEAU, P. M. (1990) Intracranial chemical-shift artifacts on MR images of the brain: observations and relation to sampling bandwidth. *American Journal of Roentgenology,* 154**,** 1275-1283.

SMITH, K. E., COMMEAN, P. K., BHATIA, G. & VANNIER, M. W. (1995) Validation of spiral CT and optical surface scanning for lower limb stump volumetry. *Prosthet Orthot Int.,* 19**,** 97-107.

SMITH, K. E., COMMEAN, P. K. & VANNIER, M. W. (1996) Residual-limb shape change: three-dimensional CT scan measurement and depiction in vivo. *Radiology,* 200**,** 843-850.

STEINBACH, B. G., HISKES, S. K., FITZSIMMONS, J. R. & LANIER, L. (1992) Phantom evaluation of imaging modalities for silicone breast implants. *Investigative Radiology,* 27**,** 841-846.

TORRES-MORENO, R., FOORT, J., MORRISON, J. B. & SAUNDERS, C. G. (1989) A reference shape library for computer aided socket design in above-knee prostheses. *Prosthet Orthot Int.,* 13**,** 130-9.

TORRES MORENO, R., JONES, D., SOLOMONIDIS, S. & MACKIE, H. (1999) Magnetic Resonance Imaging of Residual Soft Tissues for Computer-Aided Technology Applications in Prosthetics-A Case Study. *JPO,* 11**,** 6-11.

TRACY, B. L., IVEY, F. M., JEFFREY, M. E., FLEG, J. L., SIEGEL, E. L. & HURLEY, B. (2003) A more efficient magnetic resonance imaging-based strategy for measuring quadriceps muscle volume. *Med Sci Sports Exerc,* 35**,** 425-433.

TREPPO, S., KOEPP, H., QUAN, E. C., COLE, A. A., KUETTNER, K. E. & GRODZINSKY, A. J. (2000) Comparison of biomechanical and biochemical properties of cartilage from human knee and ankle pairs. *J Orthop Res,* 18**,** 739-48.

TROWER, T. A. (2006) Changes in lower extremity prosthetic practice. *Phys Med Rehabil Clin N Am,* 17**,** 23-30.

UDAI, A. D. & SINHA, A. N. (2008) Processing Magnetic Resonance Images for CAD Model development of Prosthetic Limbs Socket. *Industrial and Information Systems, 2008. ICIIS 2008. IEEE Region 10 and the Third international Conference on.*

VANDE BERG, B. C., MALGHEM, J., LECOUVET, F. E. & MALDAGUE, B. (1998) Magnetic resonance imaging of normal bone marrow. *Eur Radiol,* 8**,** 1327-34.

WALTER, S. D., ELIASZIW, M. & DONNER, A. (1998) Sample size and optimal designs for reliability studies. *Statistics in Medicine,* 17**,** 101-110.

WALTON, J. M., ROBERTS, N. & WHITEHOUSE, G. H. (1997) Measurement of the quadriceps femoris muscle using magnetic resonance and ultrasound imaging.

WIRTA, R. W., GOLBRANSON, F. L., MASON, R. & CALVO, K. (1990) ANALYSIS OF BELOW-KNEE SUSPENSION SYSTEMS EFFECT ON GAIT. *Journal of Rehabilitation Research and Development,* 27**,** 385-396.

YIĞITER, K., SENER, A. G. & BAYAR, K. (2002) Comparison of the effects of patellar tendon bearing and total surface bearing sockets on prosthetic fitting and rehabilitation *Prosthetics and Orthotics International,* 23**,** 206-212.

ZACHARIAH, S. G., SANDERS, J. E. & TURKIYYAH, G. M. (1996) Automated hexahedral mesh generation from biomedical image data: applications in limb prosthetics. *IEEE Trans Rehabil Eng,* 4**,** 91-102.

ZACHARIAH, S. G., SAXENA, R., FERGASON, J. R. & SANDERS, J. E. (2004) Shape and volume change in the transtibial residuum over the short term: preliminary investigation of six subjects. *J Rehabil Res Dev,* 41**,** 683-94.

ZENTAI, C. P., WORKU, D., TUNCALI, K., ZOU, K. H., MORRISON, P. P., WARFIELD, S. K., SEIBEL, R. M. M. & SILVERMAN, S. G. (2004) Validation of 3D assessment of MR imaging-guided precutaneous crytherapy of a soft-tissue metastasis. *International Congress Series* 1268**,** 313-317.

ZHENG, Y. P., MAK, A. F. T. & LEUNG, A. K. (2001) State-of-the-art methods for geometric and biomechanical assessment of residual limbs: a review. *JRRD,* 38.

ZUNIGA, E. N., LEAVITT, L. A., CUZZI, J. R., MUILENBURG, A. L., E., H. R. & KROUSKOP, T. A. (1977) Shape and Volume Measurements of Stump and Prosthetic Socket of Lower Extremity Amputees Using a Stereometric Form Sensor. *4 th Annual Conference on systems and Devices for the Disabled.*

13 Appendices

13.1 BLAND & ALTMAN PLOTS

13.2 TABLES

13.3 CROSS SECTIONAL SURFACE AREA AND CIRCULARITY GRAPHS

13.4 RESEARCH ACCESS LETTER

13.5 R &D MANAGEMENT APPROVAL AND THE UNIVERSITY SPONSORSHIP

13.6 PATIENT INFORMATION SHEET 217

13.7 CONSENT FORM

13.8 PATIENT INVITATION LETTER

13.9 MRI SAFETY CHECKLIST

13.1 Bland & Altman plots

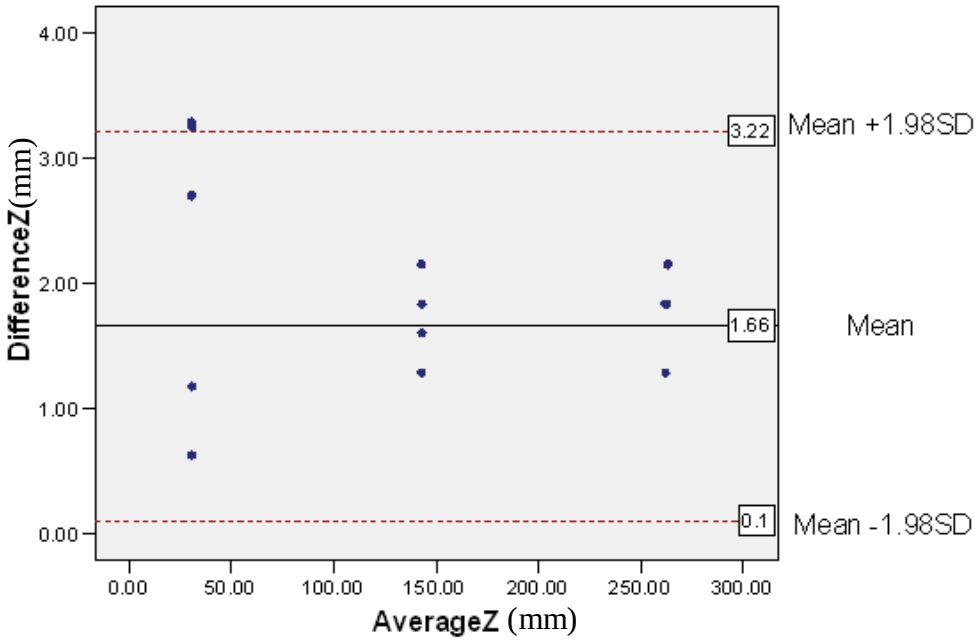

Figure 13-1: Bland & Altman plot for Polyurethane location measurement in Z direction

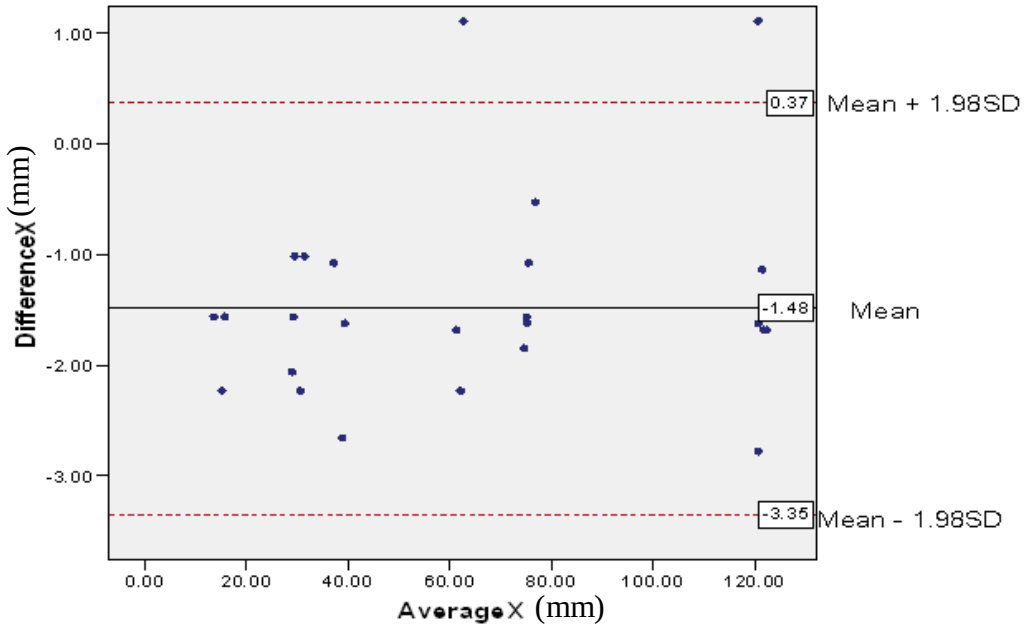

Figure 13-2: Bland & Altman plot for Polyurethane location measurement in X direction

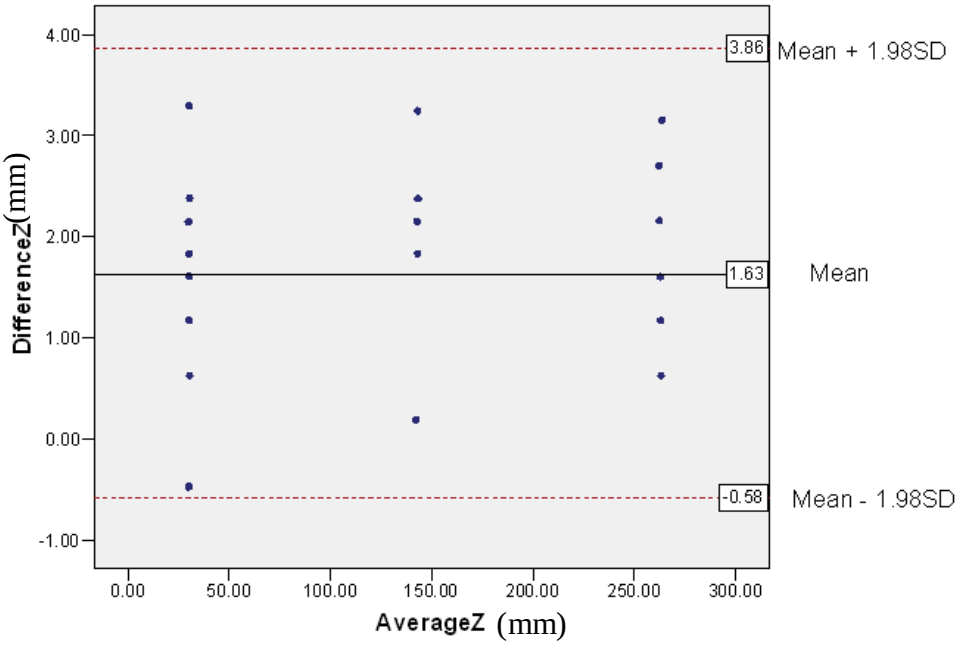

Figure 13-4: Bland & Altman plot for Silicone location measurement in Z direction

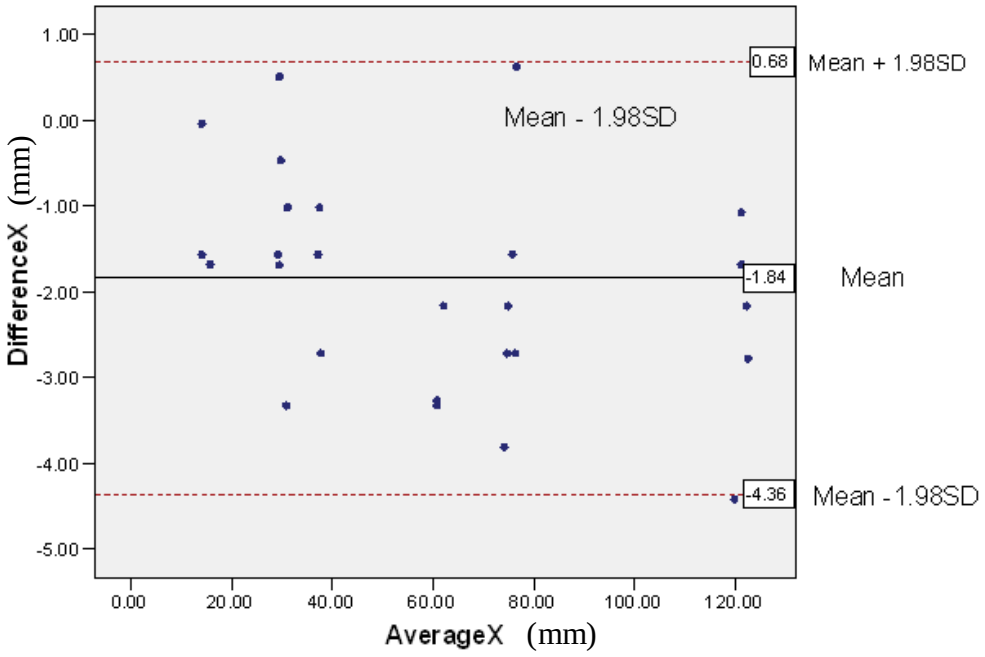

Figure 13-3: Bland & Altman plot for Silicone location measurement in X direction

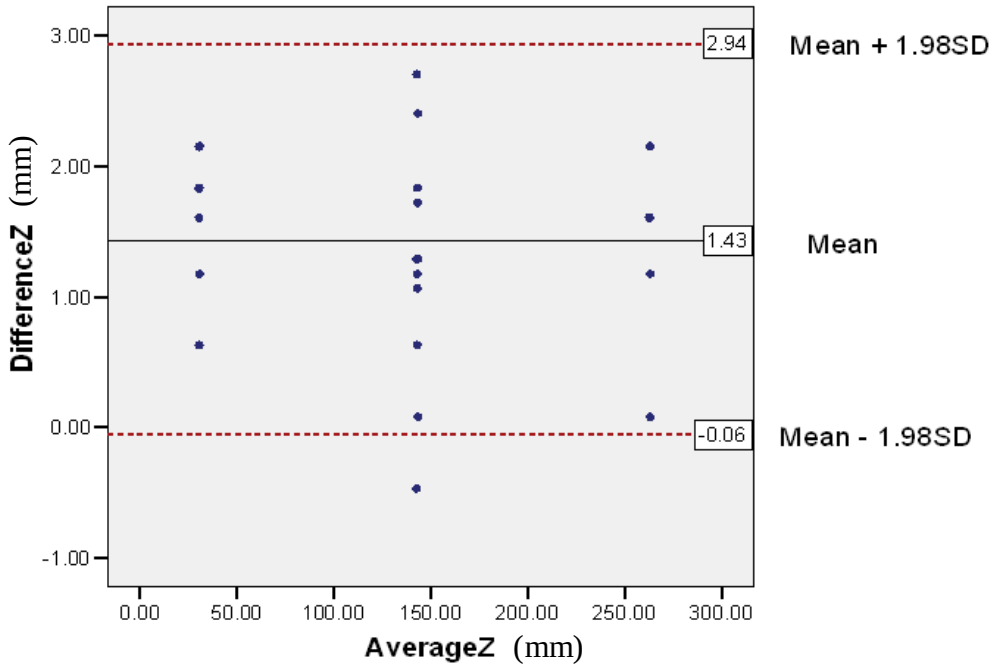

Figure 13-5: Bland & Altman plot for silicone gel location measurement in Z direction

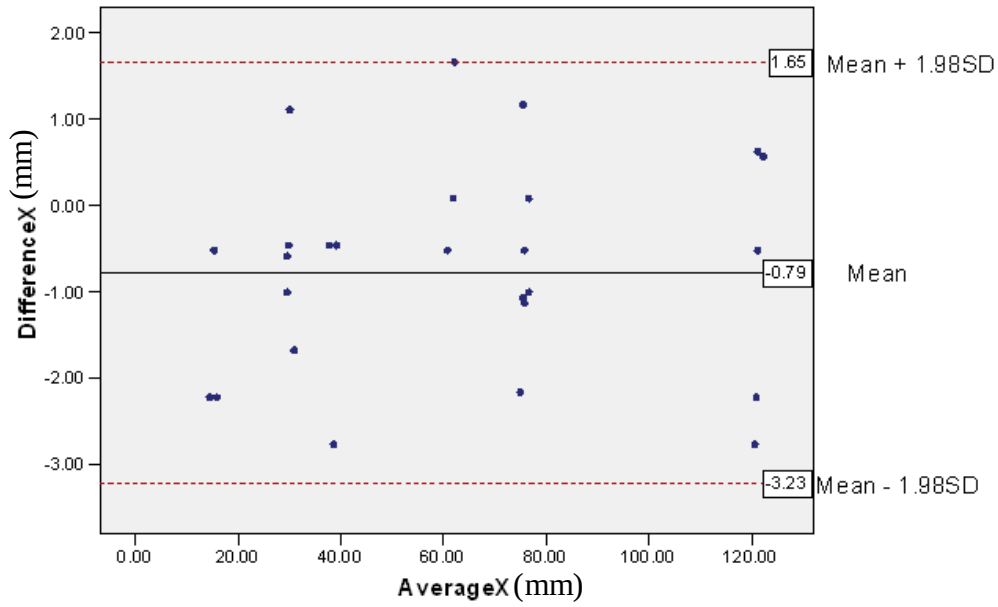

Figure 13-6: Bland & Altman plot for silicone gel location measurement in X direction

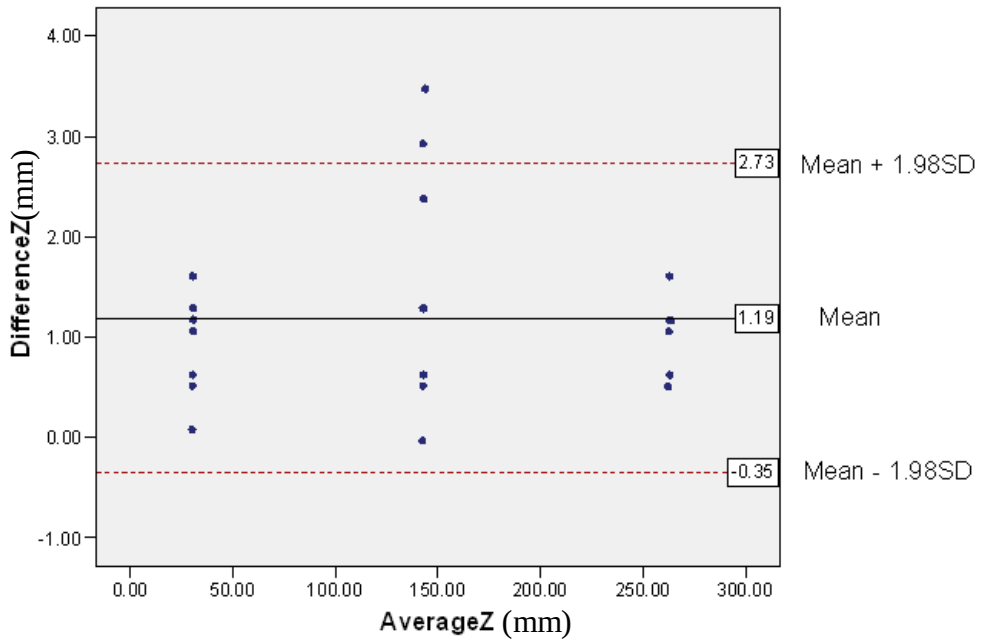

Figure 13-7: Bland & Altman plot for POP+1g/l CU location measurement in Z direction

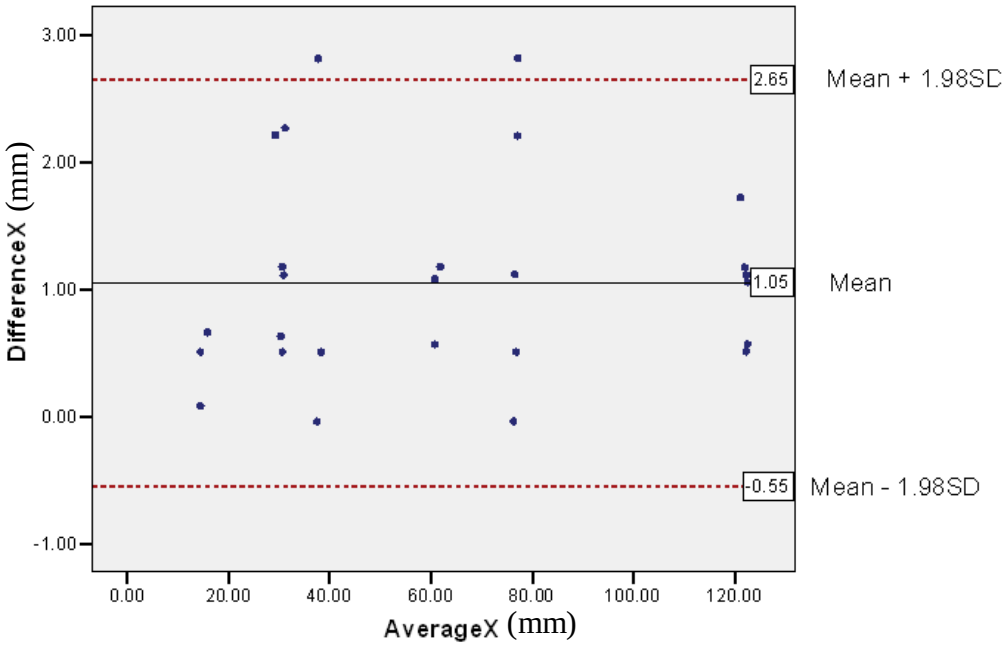

Figure 13-8: Bland & Altman plot for POP+1g/l CU location measurement in X direction

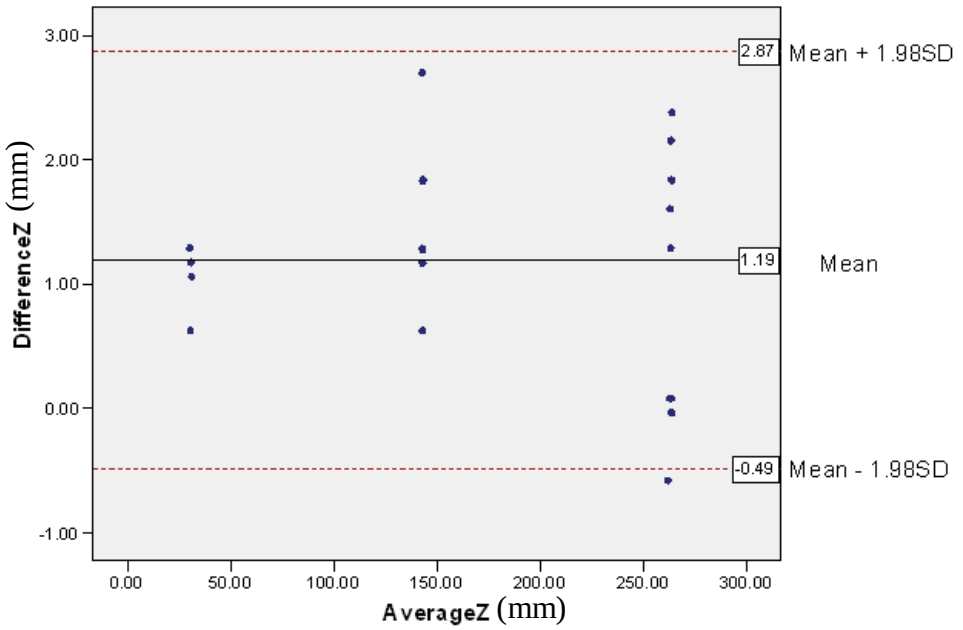

Figure 13-9: Bland & Altman plot for POP+2g/l CU location measurement in Z direction

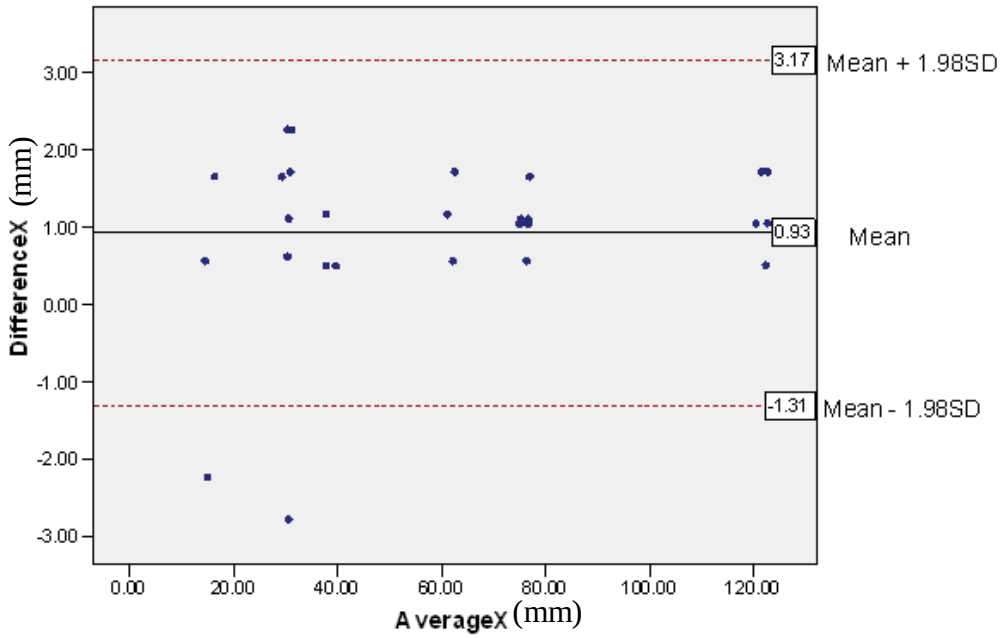

Figure 13-10: Bland & Altman plot for POP+2g/l CU location measurement in X direction

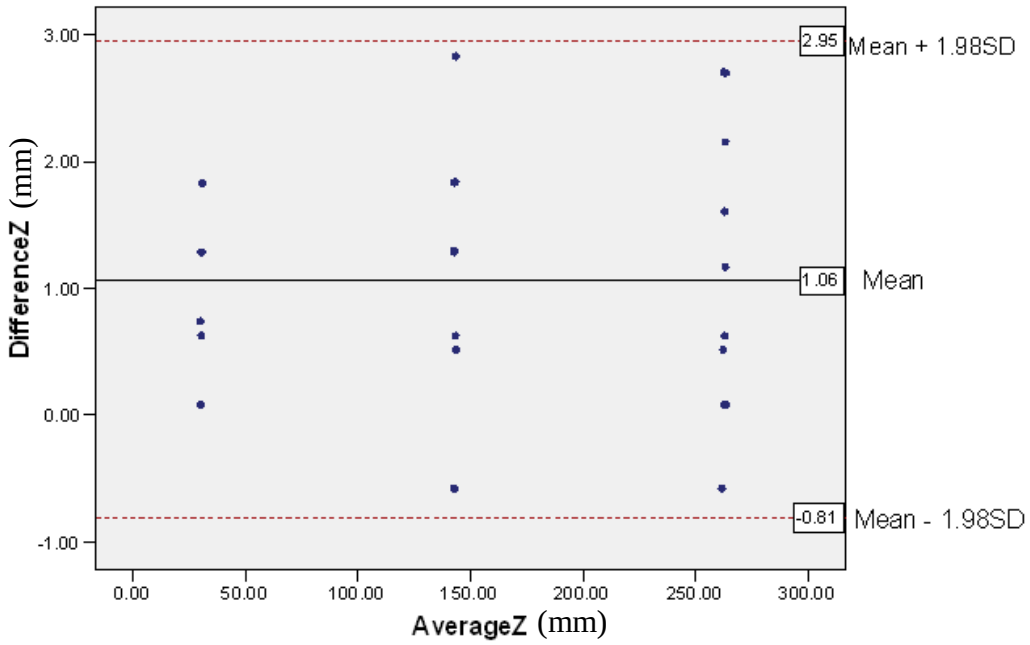

Figure 13-11: Bland & Altman plot for POP+3g/l CU location measurement in Z direction

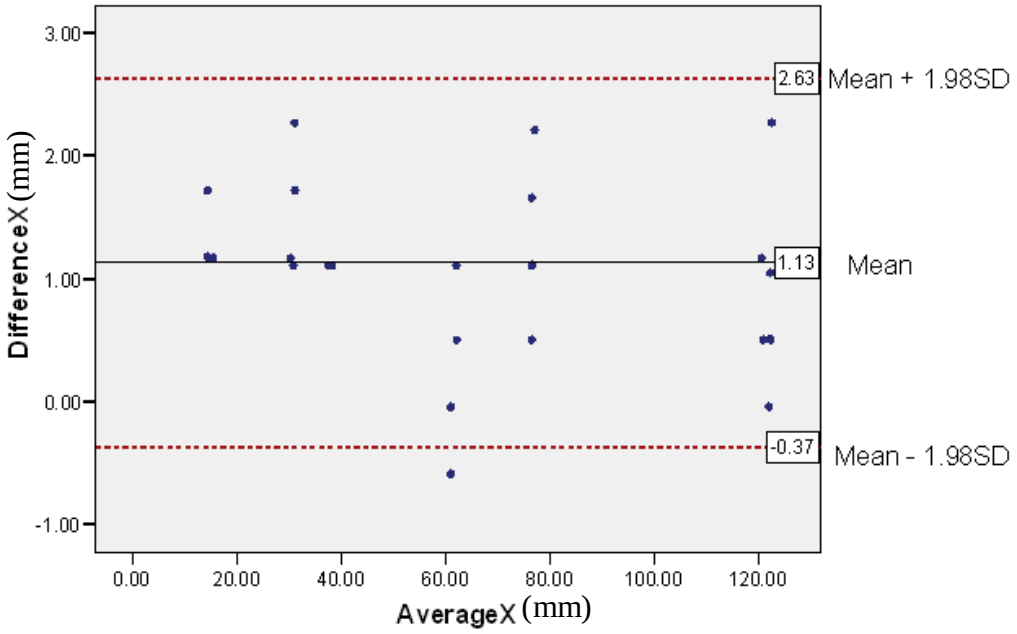

Figure 13-12: Bland & Altman plot for POP+3g/l CU location measurement in X direction

13.2 Tables

Table 13-1: Mean (mm) and standard deviation of cross-sectional surface area two repetitions of Hands-off and Hands-on concepts

	Hands-off						Hands-on					
	Rep 1			Rep 2			Rep 1			Rep 2		
	N	Mean (mm2)	SD	N	Mean (mm2)	SD	N	Mean (mm2)	SD	N	Mean (mm2)	SD
Patient 1	274	6008.74	2396.48	267	6584.46	2419.99	246	6993.93	2483.91	253	7005.85	2379.74
Patient2	275	7081.92	2307.43	273	7158.47	2378.73	268	7984.40	2514.40	265	7287.52	2232.12
Patient 3	221	5081.42	2223.33	223	4957.55	2151.16	211	5562.37	2083.28	213	5799.87	2330.68
Patient4	247	5259.01	2195.78	249	5164.08	2123.68	231	5591.19	2388.76	231	5669.74	2252.07
Patient 5	292	6664.82	2941.17	293	6638.42	3092.38	267	7673.83	3695.80	271	7454.67	3461.37
Patient 6	162	4855.17	2668.26	162	4948.55	2713.62	142	5534.45	2672.02	147	5349.37	2691.61
Patient7	232	7536.55	2651.65	329	7150.26	2737.71	329	7759.54	2808.49	329	7600.66	2804.81
Patient 8	222	5921.45	2355.84	220	6052.84	2449.27	204	6342.83	2210.03	207	6567.51	2297.98
Patient9	320	6118.27	2349.57	324	5996.78	2163.95	308	6569.40	2256.73	307	6158.34	2159.60
Patient 10	217	5590.18	1920.53	221	5680.33	1918.22	210	5993.92	1956.60	209	5983.07	1957.36
Patient 11	223	6259.12	2291.50	219	6358.32	2262.87	214	6328.31	2278.46	214	6405.66	2293.87
Patient 12	358	7855.11	3086.26	359	7847.21	3104.14	348	8207.56	3144.15	347	8159.63	3145.26

Table 13-2: Mean and standard deviation of cross-sectional circularity of two repetitions of Hands-off and Hands-on concepts

	Hands-off						Hands-on					
	Rep 1			Rep 2			Rep 1			Rep 2		
	N	Mean	SD	N	Mean	SD	N	Mean	SD	N	Mean	SD
Patient 1	274	1.160	0.049	267	1.196	0.071	246	1.205	0.061	253	1.184	0.064
Patient2	275	1.271	0.091	273	1.195	0.031	268	1.227	0.033	265	1.218	0.039
Patient 3	221	1.173	0.019	223	1.181	0.031	211	1.241	0.096	213	1.332	0.164
Patient4	247	1.153	0.038	249	1.161	0.044	231	1.163	0.038	231	1.180	0.070
Patient 5	292	1.179	0.050	293	1.164	0.036	267	1.157	0.035	271	1.164	0.028
Patient 6	162	1.236	0.045	162	1.217	0.065	142	1.233	0.136	147	1.248	0.061
Patient7	232	1.181	0.148	329	1.199	0.089	329	1.212	0.097	329	1.219	0.077
Patient 8	222	1.187	0.072	220	1.190	0.092	204	1.192	0.045	207	1.252	0.106
Patient9	320	1.164	0.053	324	1.193	0.143	308	1.181	0.117	307	1.168	0.054
Patient 10	217	1.253	0.177	221	1.207	0.209	210	1.222	0.130	209	1.226	0.110
Patient 11	223	1.204	0.129	219	1.199	0.109	214	1.198	0.065	214	1.204	0.072
Patient 12	358	1.190	0.044	359	1.159	0.048	348	1.209	0.045	347	1.192	0.076

Table 13-3: Cross sectional surface area (mm2) of both repetitions of Hands-on and Hand-off casting, Slice 1

Cast	Hands-off (mm2)							Hands-on (mm2)						
Patient	Rep 1	Rep 2	Ave 1+2	Diff 1-2	Abs Diff 1-2	% Abs Diff 1-2	% Sock Diff	Rep 1	Rep 2	Ave 1+2	Diff 1-2	Abs Diff 1-2	% Abs Diff 1-2	% Sock Diff
1	7990.9	8308.1	8149.5	-317.2	317.2	3.9	9.2	9705.2	8952.5	9328.9	752.8	752.8	8.1	9.8
2	9545.0	9809.6	9677.3	-264.6	264.6	2.7	8.4	10999.0	9835.1	10417.1	1163.9	1163.9	11.2	8.7
3	7957.4	7782.8	7870.1	174.6	174.6	2.2	9.3	8138.2	8951.0	8544.6	-812.9	812.9	9.5	9.7
4	7382.9	7254.0	7318.4	128.9	128.9	1.8	9.7	7631.6	7457.0	7544.3	174.6	174.6	2.3	9.8
5	10543.3	10814.0	10678.7	-270.7	270.7	2.5	8.0	12267.7	11394.4	11831.0	873.4	873.4	7.4	8.4
6	8309.9	8448.5	8379.2	-138.6	138.6	1.7	9.0	8802.7	8545.3	8674.0	257.4	257.4	3.0	9.2
7	9780.1	9596.9	9688.5	183.2	183.2	1.9	8.4	10821.2	10594.1	10707.7	227.2	227.2	2.1	8.8
8	8544.6	8705.9	8625.2	-161.3	161.3	1.9	8.9	8479.1	8711.3	8595.2	-232.2	232.2	2.7	8.9
9	8960.4	8443.8	8702.1	516.6	516.6	5.9	8.9	9564.1	8728.6	9146.3	835.6	835.6	9.1	9.1
10	7256.5	7457.0	7356.8	-200.5	200.5	2.7	9.6	7860.2	7918.2	7889.2	-58.0	58.0	0.7	10.0
11	8555.4	8628.8	8592.1	-73.4	73.4	0.9	8.9	8550.7	8780.0	8665.4	-229.3	229.3	2.7	8.9
12	10761.8	10702.4	10732.1	59.4	59.4	0.6	8.0	10994.0	10767.6	10880.8	226.4	226.4	2.1	8.0
Mean	8799.0	8829.3	8814.2	-30.3	207.4	2.4	8.8	9484.5	9219.6	9352.0	264.9	487.0	5.1	9.1
SD	1150.1	1170.8	1153.9	247.7	124.1	1.4	0.6	1489.1	1186.5	1316.4	564.9	370.1	3.7	0.6
Paired t-test				0.7							0.1			
Sig Y/N				N							N			

Table 13-4: Cross sectional surface area (mm2) of both repetitions of Hands-on and Hand-off casting, Slice 2

Cast	Hands-off (mm2)							Hands-on (mm2)						
Patient	Rep 1	Rep 2	Ave 1+2	Diff 1-2	Abs Diff 1-2	% Abs Diff 1-2	% Sock Diff	Rep 1	Rep 2	Ave 1+2	Diff 1-2	Abs Diff 1-2	% Abs Diff 1-2	% Sock Diff
1	8025.5	8461.1	8243.3	-435.6	435.6	5.3	9.1	8605.4	8593.9	8599.7	11.5	11.5	0.1	8.9
2	8638.5	8749.7	8694.1	-111.2	111.2	1.3	8.9	9103.6	8385.8	8744.7	717.8	717.8	8.2	8.8
3	7746.1	7607.2	7676.6	139.0	139.0	1.8	9.4	8004.2	8692.9	8348.6	-688.7	688.7	8.3	9.0
4	7354.4	7210.4	7282.4	144.0	144.0	2.0	9.7	7568.3	7407.7	7488.0	160.6	160.6	2.1	9.6
5	10478.2	10741.0	10609.6	-262.8	262.8	2.5	8.0	12177.0	11254.0	11715.5	923.0	923.0	7.9	7.6
6	8255.5	8416.4	8336.0	-160.9	160.9	1.9	9.1	8732.5	8517.2	8624.9	215.3	215.3	2.5	8.9
7	9661.7	9607.3	9634.5	54.4	54.4	0.6	8.4	9790.2	9702.0	9746.1	88.2	88.2	0.9	8.4
8	7867.1	8099.3	7983.2	-232.2	232.2	2.9	9.3	7828.2	8095.0	7961.6	-266.8	266.8	3.4	9.3
9	8919.7	8395.9	8657.8	523.8	523.8	6.1	8.9	9477.0	8541.0	9009.0	936.0	936.0	10.4	8.7
10	7155.0	7271.6	7213.3	-116.6	116.6	1.6	9.7	7355.9	7465.0	7410.4	-109.1	109.1	1.5	9.6
11	8548.2	8619.5	8583.8	-71.3	71.3	0.8	8.9	8516.5	8748.0	8632.3	-231.5	231.5	2.7	8.9
12	10609.6	10696.7	10653.1	-87.1	87.1	0.8	8.0	10914.5	10742.8	10828.6	171.7	171.7	1.6	7.9
Mean	8605.0	8656.3	8630.7	-51.4	194.9	2.3	8.9	9006.1	8845.4	8925.8	160.7	376.7	4.1	8.8
SD	1134.3	1168.0	1144.7	245.5	147.3	1.7	0.6	1420.6	1174.7	1280.1	491.2	338.6	3.5	0.6
Paired t-test				0.5							0.3			
Sig Y/N				N							N			

Table 13-5: Cross sectional surface area (mm2) of both repetitions of Hands-on and Hand-off casting, Slice 3

Cast		Hands-off (mm2)							Hands-on (mm2)						
	Patient	Rep 1	Rep 2	Ave 1+2	Diff 1-2	Abs Diff 1-2	% Abs Diff 1-2	% Sock Diff	Rep 1	Rep 2	Ave 1+2	Diff 1-2	Abs Diff 1-2	% Abs Diff 1-2	% Sock Diff
	1	7976.2	8446.7	8211.4	-470.5	470.5	5.7	9.1	8583.5	8718.5	8651.0	-135.0	135.0	1.6	8.9
	2	8533.4	8630.9	8582.2	-97.6	97.6	1.1	8.9	8960.3	8389.4	8674.9	571.0	571.0	6.6	8.9
	3	7736.4	7585.9	7661.2	150.5	150.5	2.0	9.4	7976.5	8677.8	8327.2	-701.3	701.3	8.4	9.1
	4	6940.1	6756.1	6848.1	184.0	184.0	2.7	10.0	7035.5	7254.7	7145.1	-219.2	219.2	3.1	9.8
	5	9539.6	9474.8	9507.2	64.8	64.8	0.7	8.5	11323.4	10651.3	10987.4	672.1	672.1	6.1	7.9
	6	7735.7	7874.6	7805.2	-139.0	139.0	1.8	9.4	7855.6	7919.3	7887.4	-63.7	63.7	0.8	9.3
	7	9561.2	9546.1	9553.7	15.1	15.1	0.2	8.4	9829.4	9732.6	9781.0	96.8	96.8	1.0	8.3
	8	7668.0	7900.2	7784.1	-232.2	232.2	3.0	9.4	7720.9	8021.5	7871.2	-300.6	300.6	3.8	9.3
	9	8293.7	7936.9	8115.3	356.8	356.8	4.4	9.2	8303.0	7990.9	8147.0	312.1	312.1	3.8	9.2
	10	6949.8	6998.0	6973.9	-48.2	48.2	0.7	9.9	6963.5	6965.6	6964.6	-2.2	2.2	0.0	9.9
	11	8428.7	8450.6	8439.7	-22.0	22.0	0.3	9.0	8228.2	8416.8	8322.5	-188.6	188.6	2.3	9.1
	12	10471.3	10509.8	10490.6	-38.5	38.5	0.4	8.0	10656.0	10549.8	10602.9	106.2	106.2	1.0	8.0
Mean		8319.5	8342.6	8331.0	-23.1	151.6	1.9	9.1	8619.7	8607.4	8613.5	12.3	280.7	3.2	8.9
SD		1075.4	1087.5	1076.3	211.1	141.7	1.8	0.6	1360.1	1169.3	1254.1	379.2	240.9	2.7	0.6
Paired t-test					0.7							0.9			
Sig Y/N					N							N			

Table 13-6: Cross sectional surface area (mm2) of both repetitions of Hands-on and Hand-off casting, Slice 4

Cast	Hands-off (mm2)							Hands-on (mm2)						
Patient	Rep 1	Rep 2	Ave 1+2	Diff 1-2	Abs Diff 1-2	% Abs Diff 1-2	% Sock Diff	Rep 1	Rep 2	Ave 1+2	Diff 1-2	Abs Diff 1-2	% Abs Diff 1-2	% Sock Diff
1	7680.6	8251.2	7965.9	-570.6	570.6	7.2	9.3	8335.4	8513.6	8424.5	-178.2	178.2	2.1	9.0
2	8083.0	8141.4	8112.2	-58.3	58.3	0.7	9.2	8786.8	8199.0	8492.9	587.9	587.9	6.9	9.0
3	6403.7	6259.7	6331.7	144.0	144.0	2.3	10.4	6656.8	6961.0	6808.9	-304.2	304.2	4.5	10.0
4	6270.8	6104.2	6187.5	166.7	166.7	2.7	10.5	6281.6	6449.8	6365.7	-168.1	168.1	2.6	10.4
5	7891.9	7866.4	7879.1	25.6	25.6	0.3	9.3	8704.4	8743.7	8724.1	-39.2	39.2	0.5	8.8
6	6162.8	6285.6	6224.2	-122.8	122.8	2.0	10.5	6442.6	6489.4	6466.0	-46.8	46.8	0.7	10.3
7	9302.0	9078.1	9190.1	223.9	223.9	2.4	8.6	9556.2	9401.8	9479.0	154.4	154.4	1.6	8.5
8	7315.2	7545.2	7430.2	-230.0	230.0	3.1	9.6	7575.8	7928.3	7752.1	-352.4	352.4	4.6	9.4
9	6909.5	6811.2	6860.3	98.3	98.3	1.4	10.0	7148.2	6763.3	6955.7	384.8	384.8	5.5	9.9
10	6452.3	6538.7	6495.5	-86.4	86.4	1.3	10.3	7041.6	6872.8	6957.2	168.8	168.8	2.4	9.9
11	7724.2	7773.8	7749.0	-49.7	49.7	0.6	9.4	7715.9	7750.8	7733.3	-34.9	34.9	0.5	9.4
12	10175.0	10148.0	10161.5	27.0	27.0	0.3	8.2	10313.6	10257.1	10285.4	56.5	56.5	0.6	8.1
Mean	7530.9	7567.0	7548.9	-36.0	150.3	2.0	9.6	7879.9	7860.9	7870.4	19.1	206.4	2.7	9.4
SD	1241.3	1243.0	1237.6	213.4	149.4	1.9	0.8	1276.3	1217.9	1239.9	274.1	170.5	2.2	0.7
Paired t-test				0.6							0.8			
Sig Y/N				N							N			

Table 13-7: Cross sectional surface area (mm2) of both repetitions of Hands-on and Hand-off casting, Slice 5

Cast	Hands-off (mm2)							Hands-on (mm2)						
Patient	Rep 1	Rep 2	Ave 1+2	Diff 1-2	Abs Diff 1-2	% Abs Diff 1-2	% Sock Diff	Rep 1	Rep 2	Ave 1+2	Diff 1-2	Abs Diff 1-2	% Abs Diff 1-2	% Sock Diff
1	6943.0	7688.9	7315.9	-745.9	745.9	10.2	9.7	7684.9	7983.0	7834.0	-298.1	298.1	3.8	9.3
2	8074.0	8102.5	8088.3	-28.4	28.4	0.4	9.2	8785.0	8184.6	8484.8	600.5	600.5	7.1	9.0
3	6098.8	5963.8	6031.3	135.0	135.0	2.2	10.7	6487.9	6781.7	6634.8	-293.8	293.8	4.4	10.2
4	5427.4	5422.3	5424.8	5.0	5.0	0.1	11.3	5360.8	5627.2	5494.0	-266.4	266.4	4.9	11.2
5	6688.1	6551.6	6619.9	136.4	136.4	2.1	10.2	6821.6	6870.2	6845.9	-48.6	48.6	0.7	10.0
6	4460.8	4618.1	4539.4	-157.3	157.3	3.5	12.4	4724.6	4483.1	4603.9	241.6	241.6	5.3	12.3
7	8090.6	7577.3	7834.0	513.4	513.4	6.6	9.3	8184.6	8034.5	8109.5	150.1	150.1	1.9	9.2
8	7257.6	7466.0	7361.8	-208.4	208.4	2.8	9.6	7521.8	7817.8	7669.8	-295.9	295.9	3.9	9.4
9	6748.6	6691.0	6719.8	57.6	57.6	0.9	10.1	7029.4	6657.8	6843.6	371.5	371.5	5.4	10.0
10	6179.4	6310.4	6244.9	-131.0	131.0	2.1	10.5	6747.8	6652.4	6700.1	95.4	95.4	1.4	10.1
11	7248.2	7291.1	7269.7	-42.8	42.8	0.6	9.7	7385.8	7290.0	7337.9	95.8	95.8	1.3	9.7
12	10071.7	9882.7	9977.2	189.0	189.0	1.9	8.3	10172.5	10125.7	10149.1	46.8	46.8	0.5	8.2
Mean	6940.7	6963.8	6952.2	-23.1	195.9	2.8	10.1	7242.2	7209.0	7225.6	33.2	233.7	3.4	9.9
SD	1428.1	1369.4	1391.1	298.1	218.2	2.9	1.1	1448.0	1412.9	1423.2	289.6	159.7	2.2	1.1
Paired t-test				0.8							0.7			
Sig Y/N				N							N			

Table 13-8: Cross sectional surface area (mm2) of both repetitions of Hands-on and Hand-off casting, Slice 6

Cast	Hands-off (mm2)							Hands-on (mm2)						
Patient	Rep 1	Rep 2	Ave 1+2	Diff 1-2	Abs Diff 1-2	% Abs Diff 1-2	% Sock Diff	Rep 1	Rep 2	Ave 1+2	Diff 1-2	Abs Diff 1-2	% Abs Diff 1-2	% Sock Diff
1	6358.7	7119.4	6739.0	-760.7	760.7	11.3	10.1	7016.8	7425.7	7221.2	-409.0	409.0	5.7	9.7
2	8016.1	7997.7	8006.9	18.4	18.4	0.2	9.2	8726.7	8126.2	8426.5	600.5	600.5	7.1	9.0
3	5987.2	5834.5	5910.8	152.6	152.6	2.6	10.8	6430.0	6722.6	6576.3	-292.7	292.7	4.5	10.2
4	5150.5	5173.9	5162.2	-23.4	23.4	0.5	11.6	5080.0	5337.0	5208.5	-257.0	257.0	4.9	11.5
5	6500.5	6347.5	6424.0	153.0	153.0	2.4	10.3	6526.1	6584.0	6555.1	-58.0	58.0	0.9	10.2
6	4293.7	4455.7	4374.7	-162.0	162.0	3.7	12.6	4494.6	4277.5	4386.1	217.1	217.1	5.0	12.6
7	7627.7	6985.1	7306.4	642.6	642.6	8.8	9.7	7753.7	7600.0	7676.8	153.7	153.7	2.0	9.4
8	6115.7	6224.8	6170.2	-109.1	109.1	1.8	10.6	6451.6	6849.7	6650.6	-398.2	398.2	6.0	10.2
9	6661.8	6627.6	6644.7	34.2	34.2	0.5	10.2	6975.0	6561.4	6768.2	413.6	413.6	6.1	10.1
10	5703.8	5940.4	5822.1	-236.5	236.5	4.1	10.9	6266.9	6143.0	6205.0	123.8	123.8	2.0	10.5
11	6613.2	6628.7	6620.9	-15.5	15.5	0.2	10.2	6562.4	6563.5	6563.0	-1.1	1.1	0.0	10.2
12	8938.1	8771.8	8854.9	166.3	166.3	1.9	8.8	8989.9	8891.3	8940.6	98.6	98.6	1.1	8.7
Mean	6497.2	6508.9	6503.1	-11.7	206.2	3.2	10.4	6772.8	6756.8	6764.8	16.0	251.9	3.8	10.2
SD	1254.3	1161.8	1198.0	324.8	243.5	3.5	1.0	1294.5	1215.2	1245.5	317.0	177.5	2.4	1.0
Paired t-test				0.9							0.9			
Sig Y/N				N							N			

Table 13-9: Cross sectional surface area (mm2) of both repetitions of Hands-on and Hand-off casting, Slice 7

Cast	Hands-off (mm2)							Hands-on (mm2)						
Patient	Rep 1	Rep 2	Ave 1+2	Diff 1-2	Abs Diff 1-2	% Abs Diff 1-2	% Sock Diff	Rep 1	Rep 2	Ave 1+2	Diff 1-2	Abs Diff 1-2	% Abs Diff 1-2	% Sock Diff
1	4963.7	5555.2	5259.4	-591.5	591.5	11.3	11.5	5055.5	5739.1	5397.3	-683.6	683.6	12.7	11.3
2	6629.0	6545.1	6587.1	83.9	83.9	1.3	10.2	7857.7	7037.2	7447.5	820.4	820.4	11.0	9.6
3	4604.4	4504.0	4554.2	100.4	100.4	2.2	12.3	5320.4	5398.9	5359.7	-78.5	78.5	1.5	11.3
4	4826.2	4869.0	4847.6	-42.8	42.8	0.9	11.9	4703.4	4973.8	4838.6	-270.4	270.4	5.6	12.0
5	3506.8	3308.8	3407.8	198.0	198.0	5.8	14.3	2211.8	2519.6	2365.7	-307.8	307.8	13.0	17.3
6	3379.3	3481.6	3430.4	-102.2	102.2	3.0	14.3	3252.2	3309.8	3281.0	-57.6	57.6	1.8	14.6
7	7096.3	6451.9	6774.1	644.4	644.4	9.5	10.1	7373.5	7203.2	7288.4	170.3	170.3	2.3	9.7
8	4793.8	4756.0	4774.9	37.8	37.8	0.8	12.0	4805.3	5172.5	4988.9	-367.2	367.2	7.4	11.8
9	5688.7	5823.4	5756.0	-134.6	134.6	2.3	10.9	6203.9	5730.1	5967.0	473.8	473.8	7.9	10.7
10	3277.1	3659.4	3468.2	-382.3	382.3	11.0	14.2	3134.2	3042.7	3088.4	91.4	91.4	3.0	15.1
11	4957.2	4968.7	4963.0	-11.5	11.5	0.2	11.8	4669.6	4764.6	4717.1	-95.0	95.0	2.0	12.1
12	6790.7	6776.6	6783.7	14.0	14.0	0.2	10.1	6928.9	6709.7	6819.3	219.2	219.2	3.2	10.0
Mean	5042.8	5058.3	5050.5	-15.5	195.3	4.0	12.0	5126.4	5133.5	5129.9	-7.1	302.9	4.9	12.1
SD	1306.1	1201.7	1245.9	301.0	222.0	4.3	1.6	1743.3	1533.8	1629.6	401.2	246.8	4.4	2.4
Paired t-test				0.9							1.0			
Sig Y/N				N							N			

Table 13-10: Cross sectional surface area (mm2) of both repetitions of Hands-on and Hand-off casting, Slice 8

Cast	Hands-off (mm2)							Hands-on (mm2)						
Patient	Rep 1	Rep 2	Ave 1+2	Diff 1-2	Abs Diff 1-2	% Abs Diff 1-2	% Sock Diff	Rep 1	Rep 2	Ave 1+2	Diff 1-2	Abs Diff 1-2	% Abs Diff 1-2	% Sock Diff
1	3204.0	3454.9	3329.5	-250.9	250.9	7.5	18.7	2299.0	3083.0	2691.0	-784.1	784.1	29.1	35.7
2	6028.5	6005.1	6016.8	23.4	23.4	0.4	10.8	7298.6	6399.3	6849.0	899.3	899.3	13.1	10.1
3	2565.4	2671.9	2618.6	-106.6	106.6	4.1	24.0	2733.8	2838.6	2786.2	-104.8	104.8	3.8	29.5
4	3078.7	3098.5	3088.6	-19.8	19.8	0.6	20.4	2553.1	2802.6	2677.9	-249.5	249.5	9.3	35.1
5	3163.0	2952.0	3057.5	211.0	211.0	6.9	16.0	1632.2	1928.5	1780.4	-296.3	296.3	16.6	23.7
6	2002.0	2063.5	2032.7	-61.6	61.6	3.0	23.9	1257.5	1540.8	1399.1	-283.3	283.3	20.3	55.2
7	5979.6	5377.0	5678.3	602.6	602.6	10.6	36.9	6235.9	5995.4	6115.7	240.5	240.5	3.9	27.0
8	4647.2	4537.4	4592.3	109.8	109.8	2.4	17.9	4586.0	4927.7	4756.9	-341.6	341.6	7.2	24.2
9	2685.6	3019.3	2852.5	-333.7	333.7	11.7	19.6	2688.1	2278.1	2483.1	410.0	410.0	16.5	29.9
10	2615.8	3068.6	2842.2	-452.9	452.9	15.9	20.3	2206.4	2157.1	2181.8	49.3	49.3	2.3	35.8
11	2740.3	2586.2	2663.3	154.1	154.1	5.8	21.0	2103.5	2215.4	2159.5	-112.0	112.0	5.2	33.4
12	3347.6	3511.8	3429.7	-164.2	164.2	4.8	16.0	3159.4	3148.2	3153.8	11.2	11.2	0.4	17.4
Mean	3504.8	3528.9	3516.8	-24.1	207.5	6.2	20.4	3229.5	3276.2	3252.9	-46.8	315.2	10.6	29.7
SD	1328.0	1180.5	1248.6	279.5	178.1	4.7	6.3	1860.1	1610.9	1726.9	426.0	274.8	8.7	11.2
Paired t-test				0.8							0.7			
Sig Y/N				N							N			

Table 13-11: Cross sectional surface area (mm2) of both repetitions of Hands-on and Hand-off casting, Slice 9

Cast	Hands-off (mm2)							Hands-on (mm2)						
Patient	Rep 1	Rep 2	Ave 1+2	Diff 1-2	Abs Diff 1-2	% Abs Diff 1-2	% Sock Diff	Rep 1	Rep 2	Ave 1+2	Diff 1-2	Abs Diff 1-2	% Abs Diff 1-2	% Sock Diff
1	2010.2	2056.7	2033.5	-46.4	46.4	2.3	18.7	224.3	978.8	601.6	-754.6	754.6	125.4	35.7
2	5948.6	5911.2	5929.9	37.4	37.4	0.6	10.8	7124.4	6297.4	6710.9	826.9	826.9	12.3	10.1
3	1192.0	1348.2	1270.1	-156.2	156.2	12.3	24.0	796.3	923.4	859.9	-127.1	127.1	14.8	29.5
4	1650.6	1797.1	1723.9	-146.5	146.5	8.5	20.4	582.1	655.9	619.0	-73.8	73.8	11.9	35.1
5	2855.2	2659.3	2757.2	195.8	195.8	7.1	16.0	1137.6	1449.7	1293.7	-312.1	312.1	24.1	23.7
6	1293.8	1265.0	1279.4	28.8	28.8	2.3	23.9	70.9	470.2	270.5	-399.2	399.2	147.6	55.2
7	31.0	1101.2	566.1	-1070.3	1070.3	189.1	36.8	1066.7	963.0	1014.8	103.7	103.7	10.2	27.0
8	2328.1	2113.6	2220.8	214.6	214.6	9.7	17.9	1041.1	1455.1	1248.1	-414.0	414.0	33.2	24.2
9	1729.4	2004.1	1866.8	-274.7	274.7	14.7	19.6	904.7	767.2	835.9	137.5	137.5	16.5	29.9
10	1441.8	2031.5	1736.6	-589.7	589.7	34.0	20.3	609.5	586.1	597.8	23.4	23.4	3.9	35.8
11	1785.6	1468.4	1627.0	317.2	317.2	19.5	21.0	636.8	719.6	678.2	-82.8	82.8	12.2	33.4
12	2727.0	2805.5	2766.2	-78.5	78.5	2.8	16.0	2376.0	2315.2	2345.6	60.8	60.8	2.6	17.4
Mean	2082.8	2213.5	2148.1	-130.7	263.0	25.2	20.4	1380.9	1465.1	1423.0	-84.3	276.3	34.6	29.7
SD	1428.9	1277.3	1341.7	382.0	298.5	52.4	6.3	1898.8	1604.4	1747.0	388.3	274.3	48.5	11.2
Paired t-test				0.3							0.5			
Sig Y/N				N							N			

Table 13-12: Cross sectional circularity of both repetitions of Hands-on and Hand-off casting, Slice 1

Cast	Hands-off (mm2)							Hands-on (mm2)						
Patient	Rep 1	Rep 2	Ave 1+2	Diff 1-2	Abs Diff 1-2	% Abs Diff 1-2	% Sock Diff	Rep 1	Rep 2	Ave 1+2	Diff 1-2	Abs Diff 1-2	% Abs Diff 1-2	% Sock Diff
1	1.15	1.19	1.17	-0.04	0.04	3.30	4.40	1.17	1.16	1.16	0.01	0.01	1.11	4.18
2	1.15	1.17	1.16	-0.02	0.02	1.36	4.03	1.19	1.22	1.21	-0.02	0.02	1.99	3.96
3	1.17	1.18	1.18	-0.02	0.02	1.55	4.47	1.22	1.23	1.23	-0.01	0.01	1.21	4.37
4	1.14	1.14	1.14	0.00	0.00	0.33	4.64	1.20	1.19	1.20	0.01	0.01	0.63	4.65
5	1.18	1.16	1.17	0.03	0.03	2.42	3.84	1.14	1.16	1.15	-0.01	0.01	1.23	3.71
6	1.19	1.17	1.18	0.02	0.02	1.73	4.34	1.21	1.28	1.25	-0.06	0.06	5.03	4.34
7	1.14	1.20	1.17	-0.06	0.06	5.07	4.03	1.15	1.18	1.17	-0.03	0.03	2.72	3.90
8	1.18	1.18	1.18	0.00	0.00	0.06	4.27	1.20	1.24	1.22	-0.05	0.05	3.80	4.36
9	1.16	1.16	1.16	0.00	0.00	0.02	4.26	1.16	1.17	1.16	-0.02	0.02	1.61	4.22
10	1.24	1.13	1.19	0.11	0.11	9.19	4.63	1.16	1.19	1.18	-0.03	0.03	2.78	4.55
11	1.15	1.17	1.16	-0.02	0.02	1.83	4.28	1.17	1.18	1.17	-0.02	0.02	1.38	4.34
12	1.16	1.14	1.15	0.01	0.01	1.23	3.83	1.18	1.20	1.19	-0.02	0.02	1.60	3.87
Mean	1.16	1.16	1.16	0.00	0.03	2.34	4.25	1.18	1.20	1.20	-0.02	0.02	2.09	4.25
SD	0.03	0.02	0.01	0.04	0.03	2.58	0.27	0.02	0.04	0.03	0.02	0.02	1.28	0.28
Paired t-test				0.88							0.00			
Sig Y/N				N							Y			

Table 13-13: Cross sectional circularity of both repetitions of Hands-on and Hand-off casting, Slice 2

Cast	Hands-off (mm2)							Hands-on (mm2)						
Patient	Rep 1	Rep 2	Ave 1+2	Diff 1-2	Abs Diff 1-2	% Abs Diff 1-2	% Sock Diff	Rep 1	Rep 2	Ave 1+2	Diff 1-2	Abs Diff 1-2	% Abs Diff 1-2	% Sock Diff
1	1.13	1.17	1.15	-0.03	0.03	2.77	4.37	1.21	1.18	1.19	0.04	0.04	3.02	4.28
2	1.23	1.19	1.21	0.04	0.04	3.54	4.26	1.27	1.24	1.26	0.03	0.03	2.16	4.24
3	1.17	1.18	1.17	-0.01	0.01	0.80	4.53	1.19	1.24	1.22	-0.05	0.05	4.09	4.34
4	1.14	1.15	1.14	-0.01	0.01	0.62	4.65	1.19	1.19	1.19	0.00	0.00	0.08	4.59
5	1.17	1.15	1.16	0.02	0.02	1.54	3.85	1.15	1.18	1.17	-0.04	0.04	3.23	3.67
6	1.20	1.17	1.18	0.03	0.03	2.62	4.35	1.23	1.24	1.23	-0.01	0.01	1.03	4.27
7	1.12	1.18	1.15	-0.06	0.06	5.33	4.04	1.20	1.20	1.20	0.00	0.00	0.05	4.02
8	1.15	1.15	1.15	-0.01	0.01	0.59	4.44	1.17	1.22	1.20	-0.06	0.06	4.64	4.45
9	1.15	1.15	1.15	0.00	0.00	0.15	4.27	1.16	1.18	1.17	-0.03	0.03	2.22	4.18
10	1.22	1.18	1.20	0.04	0.04	3.59	4.67	1.20	1.22	1.21	-0.02	0.02	1.53	4.61
11	1.17	1.16	1.16	0.01	0.01	1.15	4.28	1.15	1.19	1.17	-0.04	0.04	2.99	4.27
12	1.17	1.14	1.16	0.03	0.03	2.47	3.85	1.18	1.18	1.18	0.00	0.00	0.07	3.81
Mean	1.16	1.16	1.16	0.00	0.02	2.09	4.67	1.19	1.20	1.20	-0.01	0.02	2.09	4.61
SD	0.03	0.02	0.02	0.03	0.02	1.56	0.27	0.03	0.02	0.03	0.03	0.02	1.57	2.28
Paired t-test				0.60							0.10			
Sig Y/N				N							N			

Table 13-14: Cross sectional circularity of both repetitions of Hands-on and Hand-off casting, Slice 3

Cast	Hands-off (mm2)							Hands-on (mm2)						
Patient	Rep 1	Rep 2	Ave 1+2	Diff 1-2	Abs Diff 1-2	% Abs Diff 1-2	% Sock Diff	Rep 1	Rep 2	Ave 1+2	Diff 1-2	Abs Diff 1-2	% Abs Diff 1-2	% Sock Diff
1	1.12	1.16	1.14	-0.03	0.03	2.87	4.38	1.16	1.15	1.15	0.01	0.01	1.13	4.27
2	1.26	1.22	1.24	0.04	0.04	3.02	4.28	1.30	1.24	1.27	0.06	0.06	4.87	4.26
3	1.16	1.19	1.17	-0.03	0.03	2.67	4.53	1.18	1.25	1.21	-0.07	0.07	6.02	4.35
4	1.13	1.16	1.14	-0.02	0.02	2.15	4.80	1.16	1.18	1.17	-0.02	0.02	1.42	4.70
5	1.18	1.15	1.17	0.04	0.04	3.14	4.07	1.14	1.17	1.16	-0.04	0.04	3.25	3.79
6	1.21	1.16	1.19	0.05	0.05	3.88	4.49	1.26	1.26	1.26	0.00	0.00	0.36	4.47
7	1.15	1.17	1.16	-0.02	0.02	1.85	4.06	1.19	1.22	1.20	-0.04	0.04	3.11	4.01
8	1.15	1.15	1.15	0.00	0.00	0.04	4.50	1.17	1.19	1.18	-0.02	0.02	1.81	4.47
9	1.15	1.18	1.16	-0.03	0.03	2.26	4.41	1.16	1.17	1.16	-0.01	0.01	0.83	4.40
10	1.21	1.14	1.17	0.06	0.06	5.40	4.75	1.20	1.24	1.22	-0.03	0.03	2.78	4.76
11	1.29	1.18	1.23	0.11	0.11	8.78	4.32	1.20	1.17	1.19	0.02	0.02	1.84	4.35
12	1.19	1.14	1.16	0.05	0.05	4.29	3.88	1.17	1.16	1.16	0.01	0.01	0.60	3.85
Mean	1.18	1.16	1.17	0.02	0.04	3.36	4.80	1.19	1.20	1.19	-0.01	0.03	2.33	4.76
SD	0.05	0.02	0.03	0.05	0.03	2.16	0.27	0.05	0.04	0.04	0.03	0.02	1.75	0.29
Paired t-test				0.23							0.34			
Sig Y/N				N							N			

Table 13-15: Cross sectional circularity of both repetitions of Hands-on and Hand-off casting, Slice 4

Cast	Hands-off (mm2)							Hands-on (mm2)						
Patient	Rep 1	Rep 2	Ave 1+2	Diff 1-2	Abs Diff 1-2	% Abs Diff 1-2	% Sock Diff	Rep 1	Rep 2	Ave 1+2	Diff 1-2	Abs Diff 1-2	% Abs Diff 1-2	% Sock Diff
1	1.12	1.16	1.14	-0.04	0.04	3.37	4.53	1.23	1.14	1.19	0.09	0.09	7.61	4.40
2	1.29	1.21	1.25	0.08	0.08	6.36	4.49	1.21	1.19	1.20	0.03	0.03	2.13	4.38
3	1.16	1.16	1.16	0.00	0.00	0.19	5.08	1.21	1.29	1.25	-0.08	0.08	6.21	4.90
4	1.14	1.14	1.14	0.00	0.00	0.17	5.14	1.14	1.16	1.15	-0.03	0.03	2.28	5.06
5	1.17	1.14	1.16	0.03	0.03	2.60	4.55	1.17	1.18	1.17	-0.01	0.01	0.89	4.33
6	1.20	1.19	1.20	0.01	0.01	0.73	5.12	1.25	1.24	1.24	0.01	0.01	0.82	5.02
7	1.15	1.16	1.16	0.00	0.00	0.42	4.21	1.17	1.16	1.17	0.00	0.00	0.38	4.15
8	1.18	1.14	1.16	0.04	0.04	3.09	4.69	1.16	1.21	1.18	-0.05	0.05	4.64	4.59
9	1.15	1.18	1.16	-0.03	0.03	2.64	4.88	1.16	1.13	1.14	0.03	0.03	2.47	4.84
10	1.21	1.16	1.18	0.05	0.05	4.63	5.01	1.17	1.19	1.18	-0.02	0.02	1.70	4.84
11	1.15	1.18	1.17	-0.02	0.02	2.08	4.59	1.17	1.18	1.17	-0.01	0.01	1.22	4.59
12	1.19	1.15	1.17	0.04	0.04	3.24	4.01	1.20	1.19	1.19	0.01	0.01	1.00	3.98
Mean	1.17	1.16	1.17	0.01	0.03	2.46	4.69	1.18	1.19	1.18	0.00	0.03	2.61	4.59
SD	0.04	0.02	0.03	0.04	0.02	1.89	0.36	0.03	0.04	0.03	0.04	0.03	2.31	0.35
Paired t-test				0.26							0.83			
Sig Y/N				N							N			

Table 13-16: Cross sectional circularity of both repetitions of Hands-on and Hand-off casting, Slice 5

Cast	Hands-off (mm2)							Hands-on (mm2)						
Patient	Rep 1	Rep 2	Ave 1+2	Diff 1-2	Abs Diff 1-2	% Abs Diff 1-2	% Sock Diff	Rep 1	Rep 2	Ave 1+2	Diff 1-2	Abs Diff 1-2	% Abs Diff 1-2	% Sock Diff
1	1.13	1.16	1.14	-0.02	0.02	1.85	4.72	1.18	1.15	1.16	0.03	0.03	2.51	4.56
2	1.27	1.18	1.22	0.08	0.08	6.62	4.49	1.22	1.20	1.21	0.02	0.02	1.96	4.39
3	1.17	1.16	1.17	0.01	0.01	1.18	5.20	1.22	1.27	1.24	-0.05	0.05	4.16	4.96
4	1.11	1.15	1.13	-0.04	0.04	3.19	5.49	1.14	1.15	1.15	-0.01	0.01	0.72	5.45
5	1.19	1.16	1.17	0.03	0.03	2.46	4.97	1.16	1.16	1.16	0.00	0.00	0.06	4.88
6	1.22	1.20	1.21	0.02	0.02	1.75	6.00	1.24	1.26	1.25	-0.02	0.02	1.61	5.95
7	1.16	1.17	1.16	0.00	0.00	0.42	4.56	1.15	1.16	1.16	-0.01	0.01	0.76	4.49
8	1.15	1.17	1.16	-0.02	0.02	2.00	4.71	1.16	1.17	1.17	0.00	0.00	0.39	4.61
9	1.15	1.16	1.16	-0.01	0.01	1.12	4.93	1.15	1.14	1.14	0.01	0.01	1.15	4.88
10	1.24	1.16	1.20	0.08	0.08	7.07	5.11	1.15	1.16	1.16	-0.01	0.01	0.88	4.94
11	1.16	1.18	1.17	-0.02	0.02	1.70	4.74	1.18	1.18	1.18	0.00	0.00	0.28	4.72
12	1.18	1.13	1.15	0.05	0.05	4.74	4.04	1.20	1.20	1.20	0.00	0.00	0.29	4.01
Mean	1.18	1.16	1.17	0.01	0.03	2.82	4.91	1.18	1.18	1.18	0.00	0.01	1.23	4.82
SD	0.04	0.02	0.03	0.04	0.02	2.17	0.50	0.03	0.04	0.03	0.02	0.01	1.18	0.50
Paired t-test				0.27							0.62			
Sig Y/N				N							N			

Table 13-17: Cross sectional circularity of both repetitions of Hands-on and Hand-off casting, Slice 6

Cast	Hands-off (mm2)							Hands-on (mm2)						
Patient	Rep 1	Rep 2	Ave 1+2	Diff 1-2	Abs Diff 1-2	% Abs Diff 1-2	% Sock Diff	Rep 1	Rep 2	Ave 1+2	Diff 1-2	Abs Diff 1-2	% Abs Diff 1-2	% Sock Diff
1	1.14	1.17	1.16	-0.03	0.03	2.55	4.92	1.18	1.15	1.17	0.04	0.04	3.15	4.75
2	1.24	1.17	1.21	0.07	0.07	5.88	4.52	1.20	1.18	1.19	0.02	0.02	1.73	4.40
3	1.18	1.21	1.19	-0.03	0.03	2.91	5.26	1.20	1.28	1.24	-0.08	0.08	6.22	4.98
4	1.14	1.15	1.14	-0.01	0.01	1.05	5.62	1.17	1.17	1.17	0.00	0.00	0.27	5.60
5	1.17	1.15	1.16	0.02	0.02	1.95	5.04	1.14	1.15	1.15	-0.01	0.01	0.58	4.99
6	1.20	1.19	1.20	0.01	0.01	1.13	6.11	1.20	1.28	1.24	-0.08	0.08	6.17	6.10
7	1.13	1.15	1.14	-0.02	0.02	1.59	4.73	1.18	1.18	1.18	0.00	0.00	0.05	4.61
8	1.16	1.19	1.18	-0.03	0.03	2.25	5.14	1.19	1.24	1.22	-0.05	0.05	4.24	4.95
9	1.13	1.17	1.15	-0.04	0.04	3.57	4.96	1.14	1.16	1.15	-0.02	0.02	1.59	4.91
10	1.20	1.15	1.18	0.05	0.05	4.48	5.29	1.21	1.21	1.21	-0.01	0.01	0.67	5.13
11	1.19	1.18	1.18	0.01	0.01	0.64	4.97	1.20	1.19	1.19	0.01	0.01	0.66	4.99
12	1.17	1.14	1.16	0.02	0.02	2.01	4.29	1.22	1.18	1.20	0.04	0.04	3.09	4.27
Mean	1.17	1.17	1.17	0.00	0.03	2.50	5.07	1.18	1.19	1.19	-0.01	0.03	2.37	4.97
SD	0.03	0.02	0.02	0.03	0.02	1.52	0.48	0.02	0.04	0.03	0.04	0.03	2.21	0.49
Paired t-test				0.82							0.33			
Sig Y/N				N							N			

Table 13-18: Cross sectional circularity of both repetitions of Hands-on and Hand-off casting, Slice 7

Cast	Hands-off (mm2)							Hands-on (mm2)						
Patient	Rep 1	Rep 2	Ave 1+2	Diff 1-2	Abs Diff 1-2	% Abs Diff 1-2	% Sock Diff	Rep 1	Rep 2	Ave 1+2	Diff 1-2	Abs Diff 1-2	% Abs Diff 1-2	% Sock Diff
1	1.14	1.18	1.16	-0.04	0.04	3.62	5.57	1.19	1.19	1.16	0.00	0.00	0.07	5.50
2	1.23	1.17	1.20	0.06	0.06	5.11	4.98	1.26	1.21	1.20	0.05	0.05	4.13	4.68
3	1.18	1.20	1.19	-0.02	0.02	1.60	5.99	1.24	1.30	1.19	-0.06	0.06	4.52	5.52
4	1.20	1.16	1.18	0.05	0.05	3.83	5.80	1.17	1.18	1.18	-0.01	0.01	0.67	5.81
5	1.18	1.20	1.19	-0.02	0.02	1.38	6.92	1.16	1.15	1.19	0.01	0.01	0.52	8.31
6	1.24	1.28	1.26	-0.04	0.04	3.38	6.90	1.20	1.21	1.26	-0.02	0.02	1.45	7.05
7	1.16	1.18	1.17	-0.02	0.02	1.32	4.91	1.18	1.20	1.17	-0.02	0.02	1.81	4.73
8	1.20	1.26	1.23	-0.06	0.06	4.64	5.85	1.18	1.23	1.23	-0.06	0.06	4.76	5.72
9	1.16	1.17	1.16	-0.01	0.01	0.63	5.33	1.16	1.16	1.16	0.00	0.00	0.42	5.23
10	1.27	1.20	1.24	0.07	0.07	5.66	6.86	1.21	1.23	1.24	-0.02	0.02	1.51	7.27
11	1.18	1.19	1.18	-0.01	0.01	0.91	5.73	1.23	1.22	1.18	0.01	0.01	1.19	5.88
12	1.20	1.14	1.17	0.06	0.06	4.84	4.91	1.24	1.18	1.17	0.06	0.06	4.98	4.89
Mean	1.19	1.19	1.19	0.00	0.04	3.08	5.81	1.20	1.20	1.20	-0.01	0.03	2.17	5.88
SD	0.04	0.04	0.03	0.04	0.02	1.81	0.75	0.03	0.04	0.03	0.03	0.02	1.87	1.11
Paired t-test				0.89							0.74			
Sig Y/N				N							N			

Table 13-19: Cross sectional circularity of both repetitions of Hands-on and Hand-off casting, Slice 8

Cast		Hands-off (mm2)							Hands-on (mm2)						
	Patient	Rep 1	Rep 2	Ave 1+2	Diff 1-2	Abs Diff 1-2	% Abs Diff 1-2	% Sock Diff	Rep 1	Rep 2	Ave 1+2	Diff 1-2	Abs Diff 1-2	% Abs Diff 1-2	% Sock Diff
	1	1.20	1.20	1.20	0.00	0.00	0.07	7.00	1.27	1.20	1.24	0.07	0.07	5.93	7.79
	2	1.26	1.19	1.22	0.08	0.08	6.44	5.21	1.22	1.19	1.21	0.03	0.03	2.55	4.88
	3	1.19	1.25	1.22	-0.06	0.06	4.81	7.90	1.23	1.39	1.31	-0.17	0.17	12.60	7.65
	4	1.17	1.17	1.17	0.00	0.00	0.06	7.27	1.16	1.22	1.19	-0.06	0.06	5.02	7.81
	5	1.16	1.21	1.19	-0.05	0.05	3.86	7.31	1.15	1.17	1.16	-0.02	0.02	1.78	9.58
	6	1.26	1.28	1.27	-0.02	0.02	1.84	8.96	1.21	1.22	1.21	-0.01	0.01	0.41	10.80
	7	1.17	1.23	1.20	-0.06	0.06	4.71	5.36	1.19	1.22	1.20	-0.03	0.03	2.16	5.17
	8	1.18	1.22	1.20	-0.04	0.04	3.44	5.96	1.18	1.22	1.20	-0.04	0.04	3.68	5.86
	9	1.20	1.23	1.21	-0.03	0.03	2.38	7.56	1.15	1.19	1.17	-0.03	0.03	2.68	8.11
	10	1.26	1.19	1.22	0.08	0.08	6.27	7.58	1.25	1.25	1.25	-0.01	0.01	0.43	8.65
	11	1.22	1.25	1.23	-0.03	0.03	2.18	7.83	1.24	1.22	1.23	0.02	0.02	1.25	8.69
	12	1.20	1.16	1.18	0.03	0.03	2.79	6.90	1.23	1.18	1.21	0.05	0.05	3.82	7.19
	Mean	1.20	1.21	1.21	0.00	0.04	3.24	7.07	1.20	1.22	1.21	-0.02	0.04	3.52	7.68
	SD	0.04	0.03	0.03	0.05	0.03	2.10	1.09	0.04	0.06	0.04	0.06	0.04	3.32	1.73
	Paired t-test				0.58							0.38			
	Sig Y/N				N							N			

Table 13-20: Cross sectional circularity of both repetitions of Hands-on and Hand-off casting, Slice 9

	Cast	Hands-off (mm2)							Hands-on (mm2)						
	Patient	Rep 1	Rep 2	Ave 1+2	Diff 1-2	Abs Diff 1-2	% Abs Diff 1-2	% Sock Diff	Rep 1	Rep 2	Ave 1+2	Diff 1-2	Abs Diff 1-2	% Abs Diff 1-2	% Sock Diff
	1	1.21	1.22	1.21	0.00	0.00	0.35	8.96	1.82	1.26	1.54	0.56	0.56	36.44	16.47
	2	1.24	1.20	1.22	0.04	0.04	2.97	5.25	1.25	1.23	1.24	0.01	0.01	1.15	4.93
	3	1.20	1.19	1.20	0.01	0.01	0.97	11.34	1.43	1.65	1.54	-0.22	0.22	14.27	13.78
	4	1.19	1.20	1.19	-0.01	0.01	1.06	9.73	1.21	1.29	1.25	-0.08	0.08	6.53	16.24
	5	1.18	1.18	1.18	-0.01	0.01	0.53	7.69	1.16	1.19	1.17	-0.03	0.03	2.67	11.23
	6	1.26	1.28	1.27	-0.02	0.02	1.52	11.30	1.29	1.45	1.37	-0.16	0.16	11.69	24.56
	7	2.37	1.31	1.84	1.06	1.06	57.55	16.98	1.34	1.34	1.34	0.01	0.01	0.40	12.68
	8	1.21	1.23	1.22	-0.02	0.02	1.38	8.57	1.27	1.31	1.29	-0.04	0.04	3.24	11.44
	9	1.22	1.23	1.22	-0.01	0.01	0.43	9.35	1.32	1.22	1.27	0.11	0.11	8.38	13.97
	10	1.41	1.27	1.34	0.14	0.14	10.39	9.69	1.46	1.55	1.51	-0.09	0.09	6.17	16.52
	11	1.22	1.24	1.23	-0.02	0.02	1.63	10.02	1.34	1.30	1.32	0.04	0.04	2.73	15.51
	12	1.21	1.20	1.21	0.02	0.02	1.32	7.68	1.21	1.19	1.20	0.02	0.02	1.77	8.34
	Mean	1.32	1.22	1.27	0.10	0.11	6.67	9.71	1.34	1.33	1.33	0.01	0.11	7.95	13.80
	SD	0.33	0.04	0.18	0.30	0.30	16.25	2.83	0.17	0.15	0.13	0.19	0.15	9.95	4.87
	Paired t-test				0.29							0.87			
	Sig Y/N				N							N			

13.3 Cross sectional Surface Area and Circularity Graphs

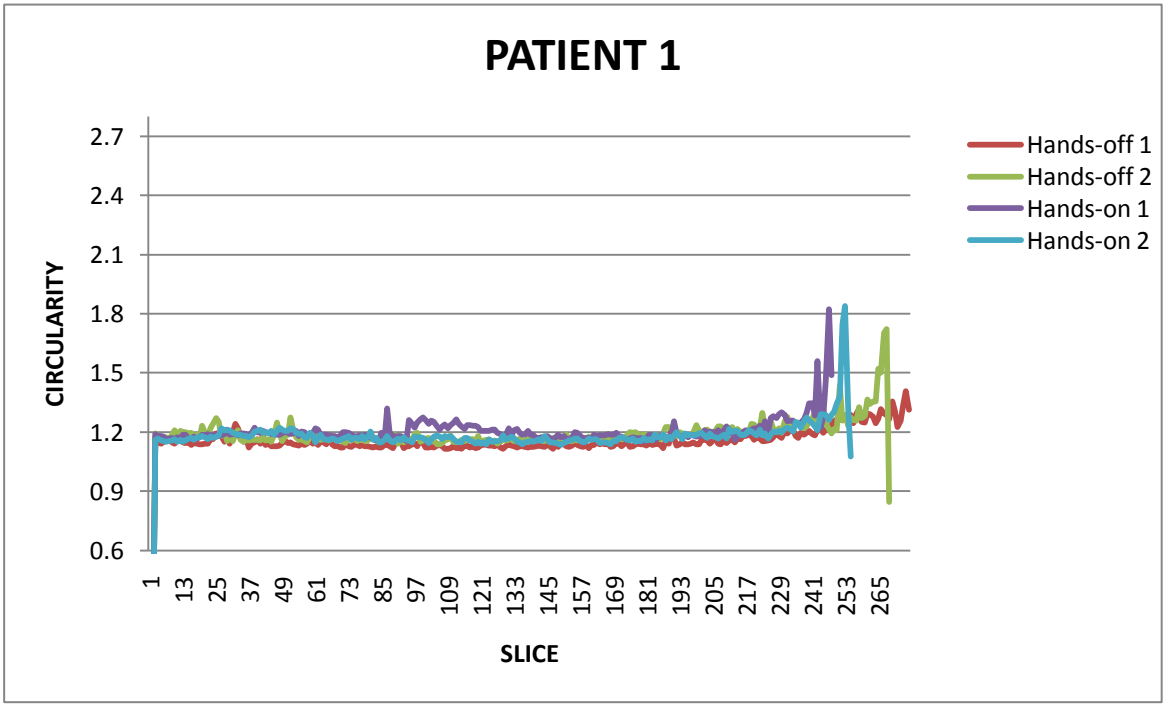

Figure 13-13: Circularity of transverse cross-section of the residual limb, amputee 1

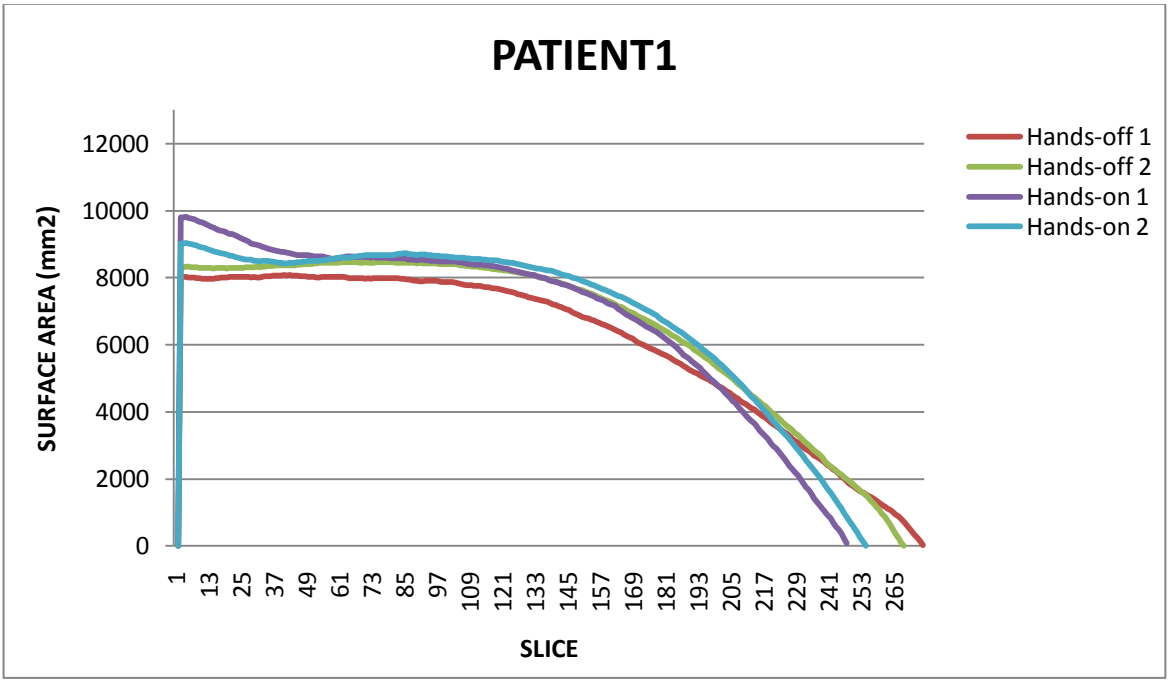

Figure 13-14: Cross sectional surface area of the residual limb, amputee 1

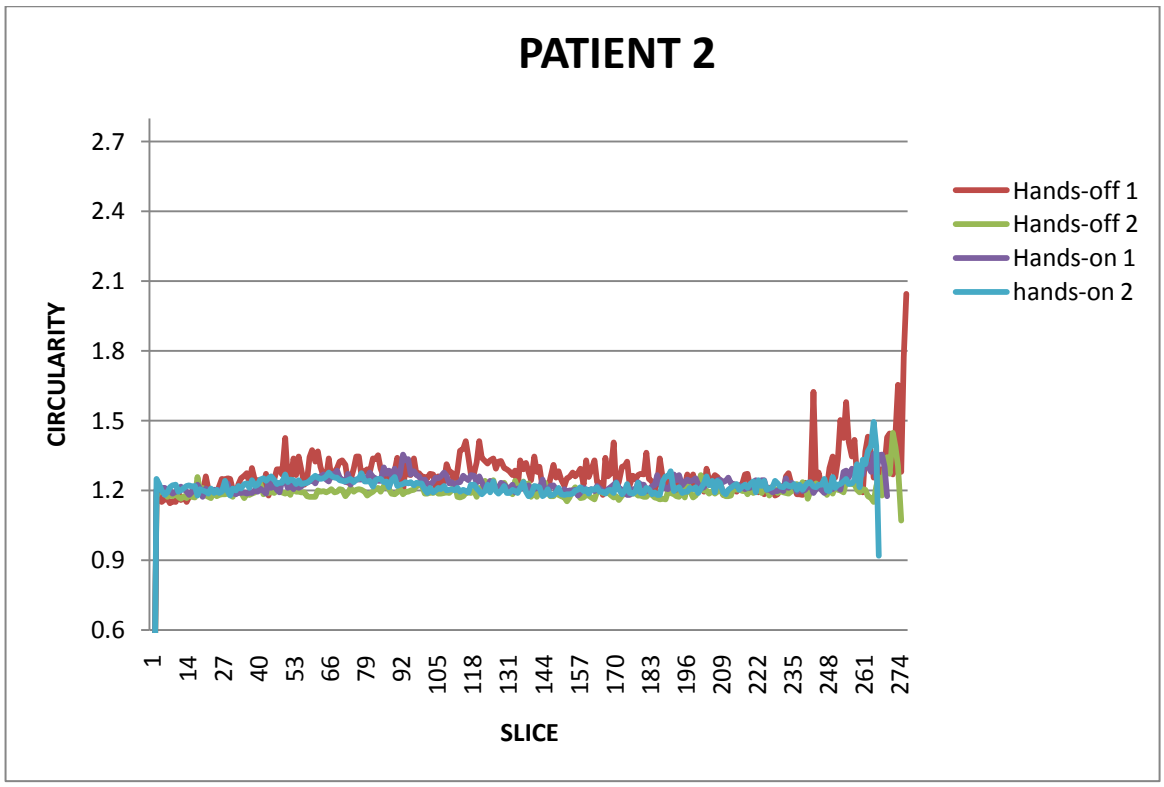

Figure 13-15: Circularity of transverse cross-section of the residual limb, amputee 2

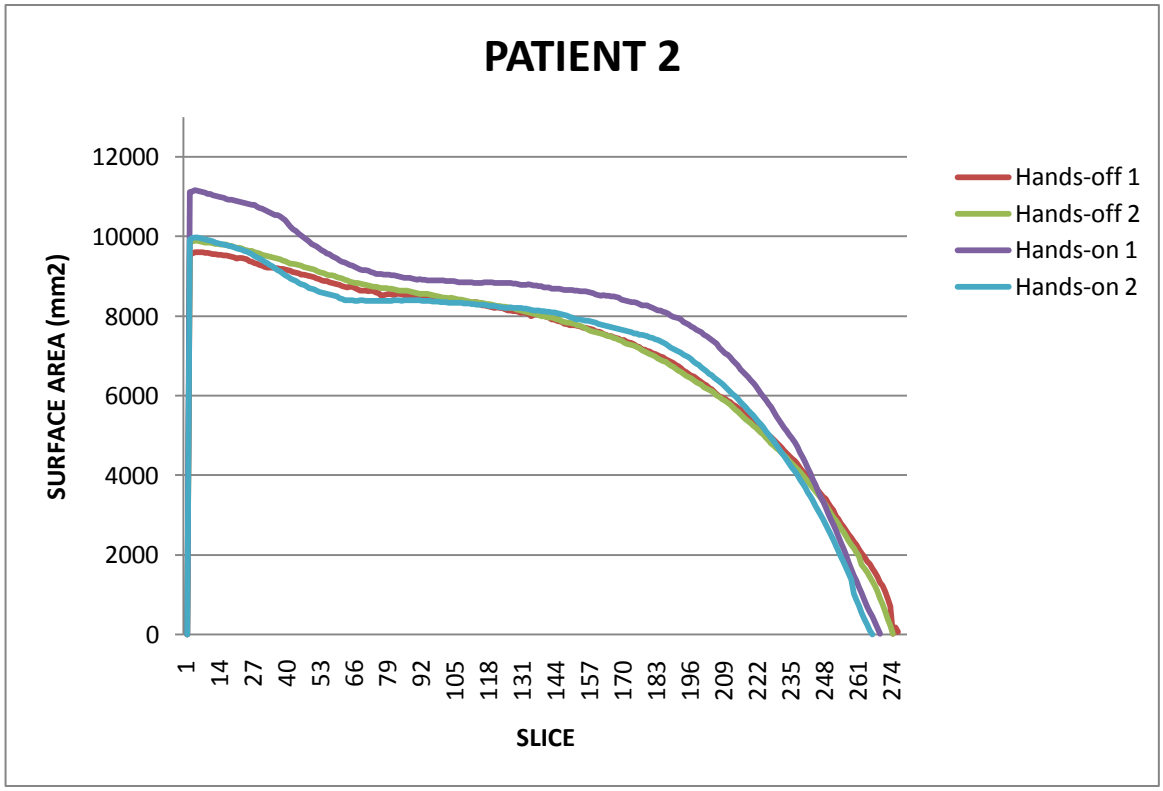

Figure 13-16: Cross sectional surface area of the residual limb, amputee 2

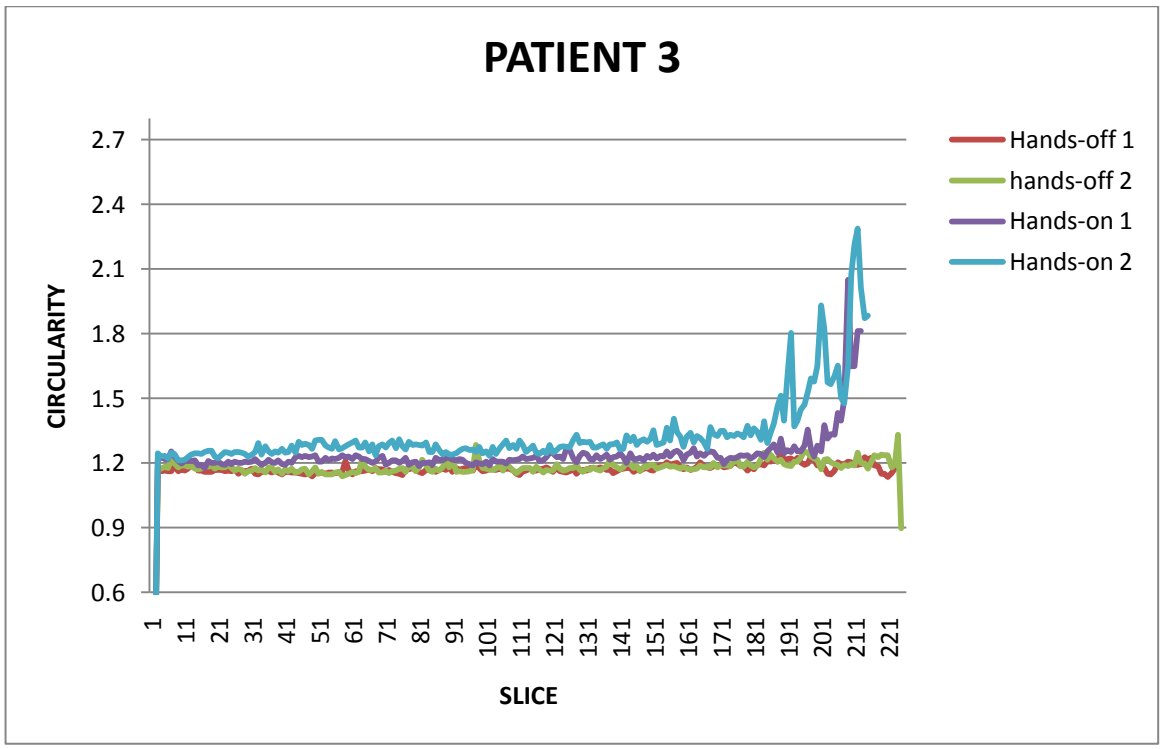

Figure 13-17: Circularity of transverse cross-section of the residual limb, amputee 3

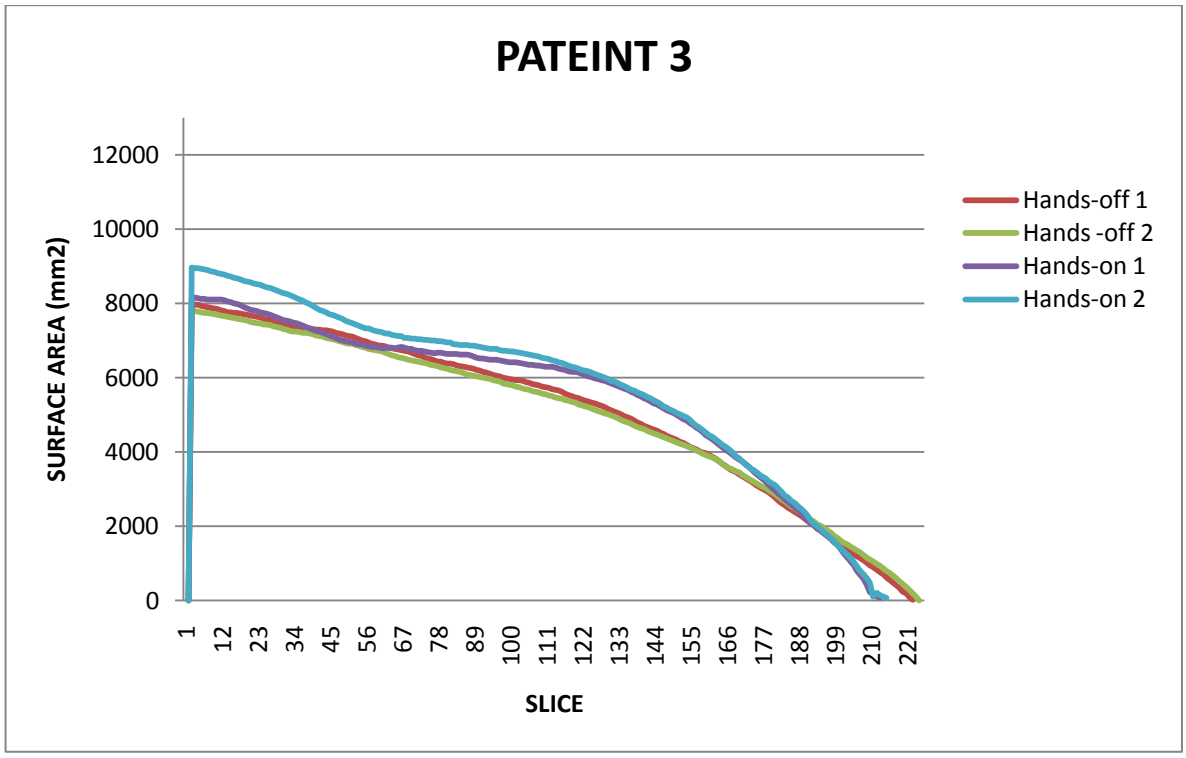

Figure 13-18: Cross sectional surface area of the residual limb, amputee 3

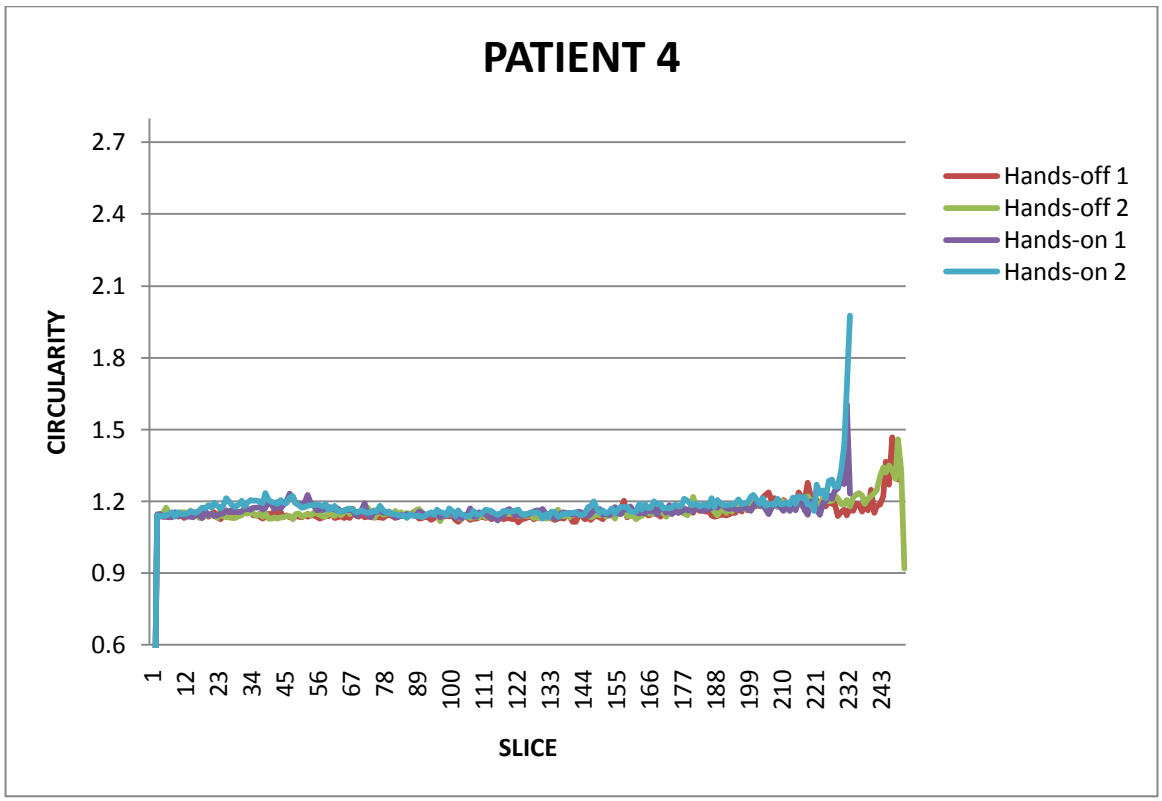

Figure 13-19: Circularity of transverse cross-section of the residual limb, amputee 4

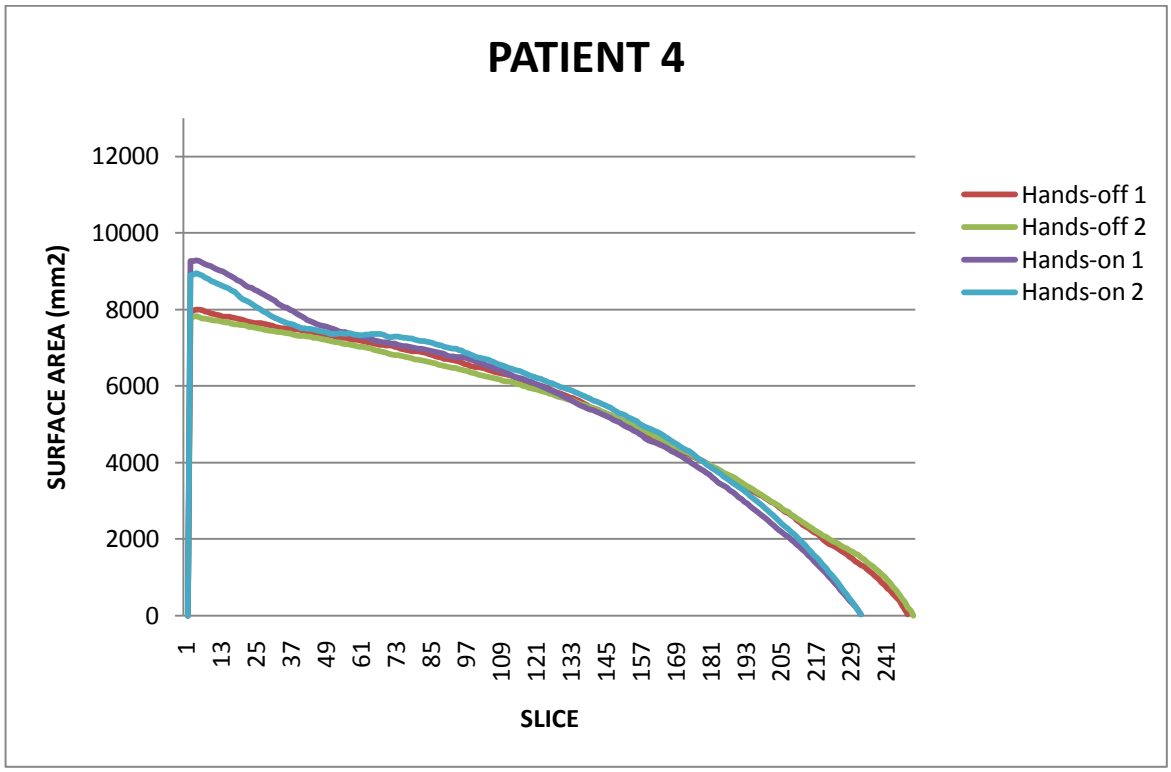

Figure 13-20: Cross sectional surface area of the residual limb, amputee 4

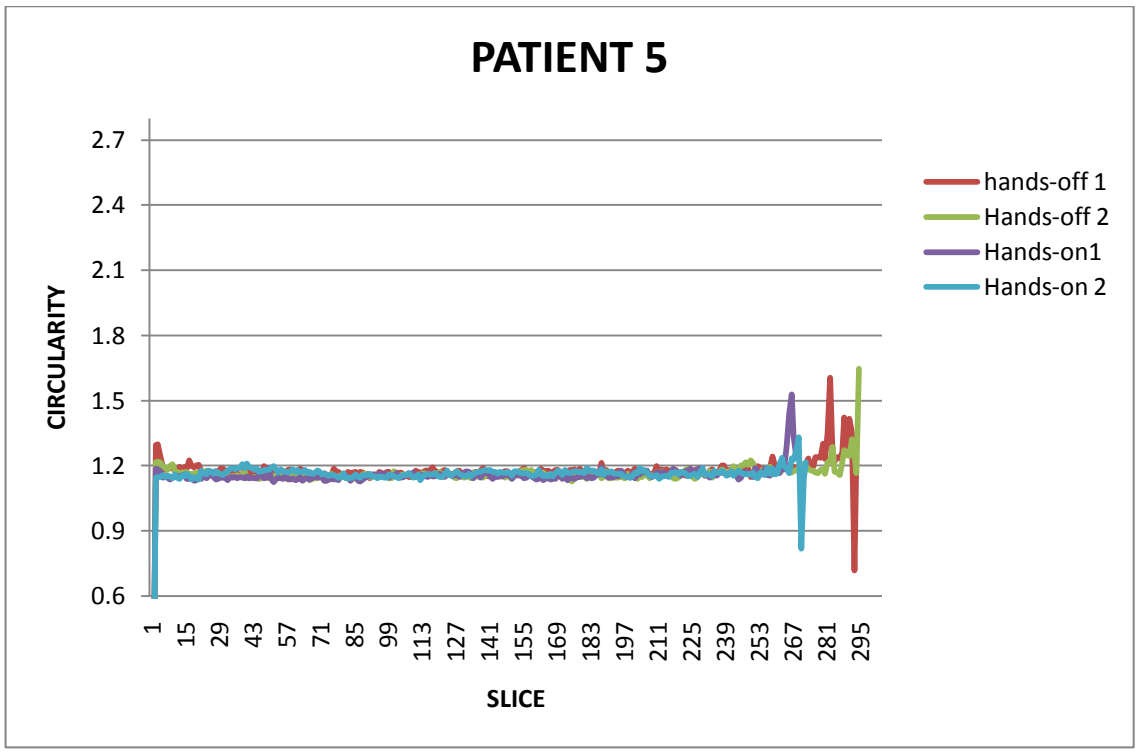

Figure 13-21: Circularity of transverse cross-section of the residual limb, amputee 5

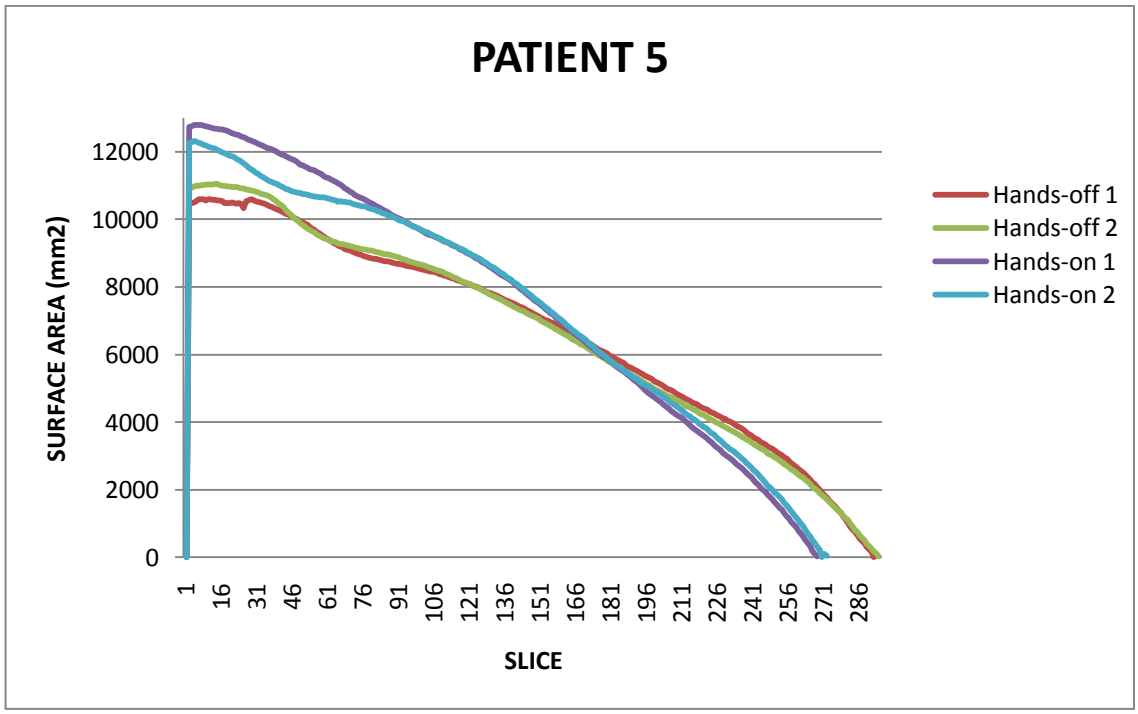

Figure 13-22: Cross sectional surface area of the residual limb, amputee 5

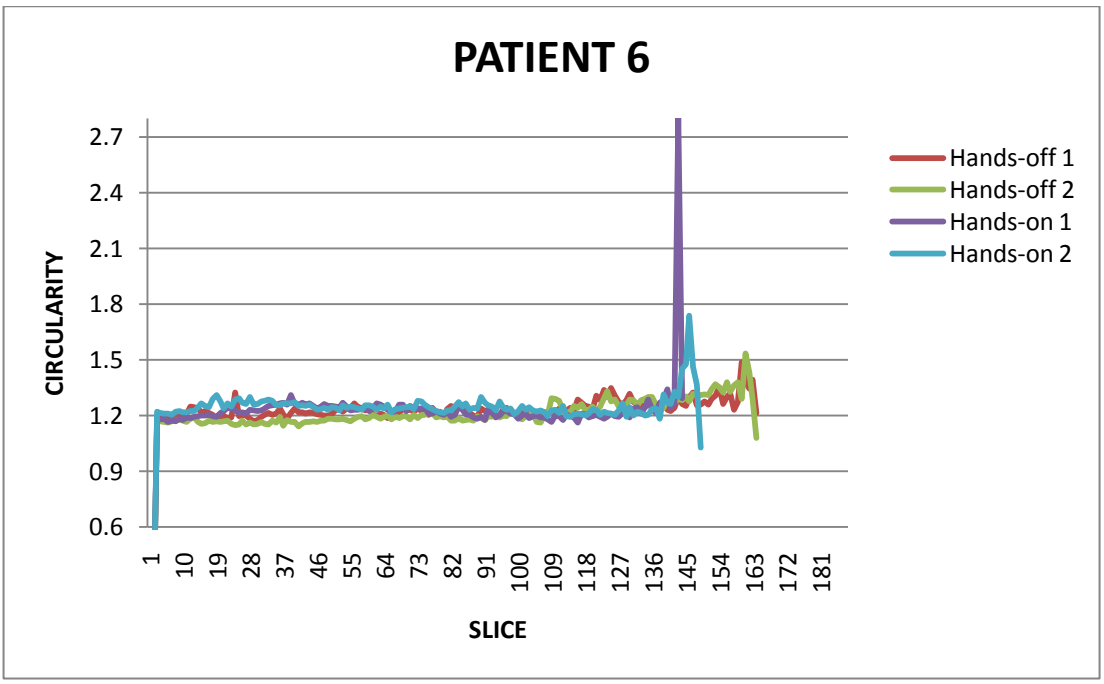

Figure 13-23: Circularity of transverse cross-section of the residual limb, amputee 6

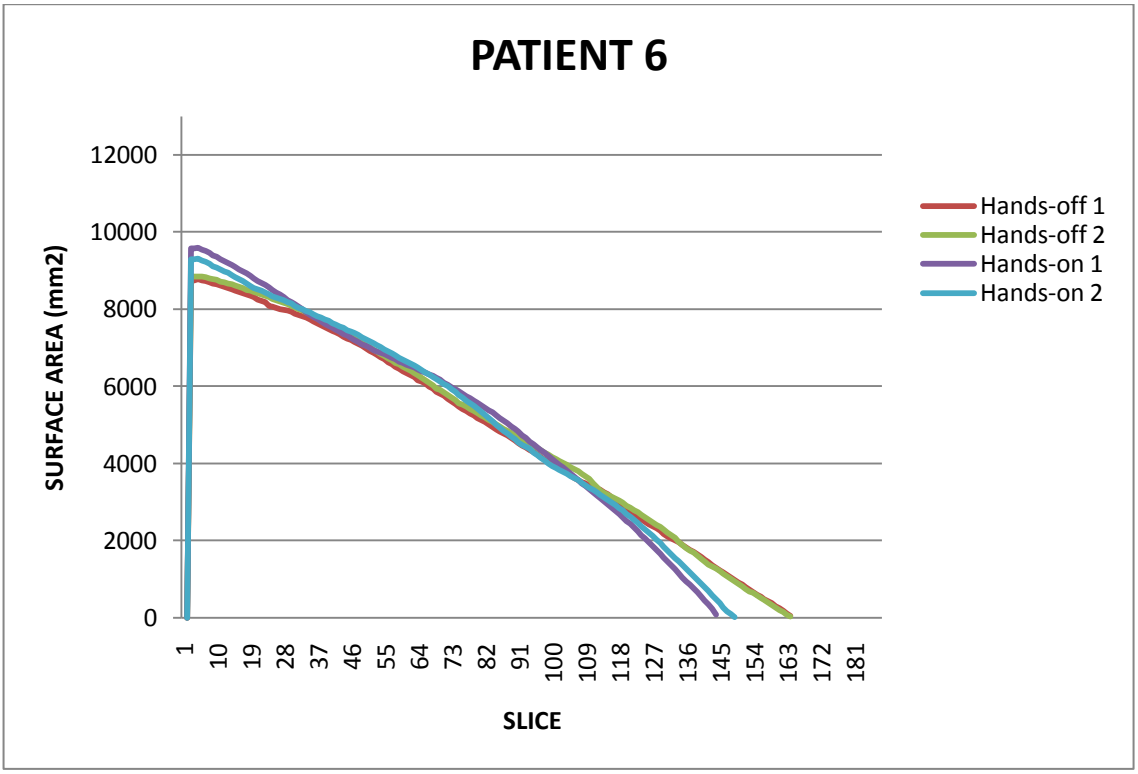

Figure 13-24: Cross sectional surface area of the residual limb, amputee 6

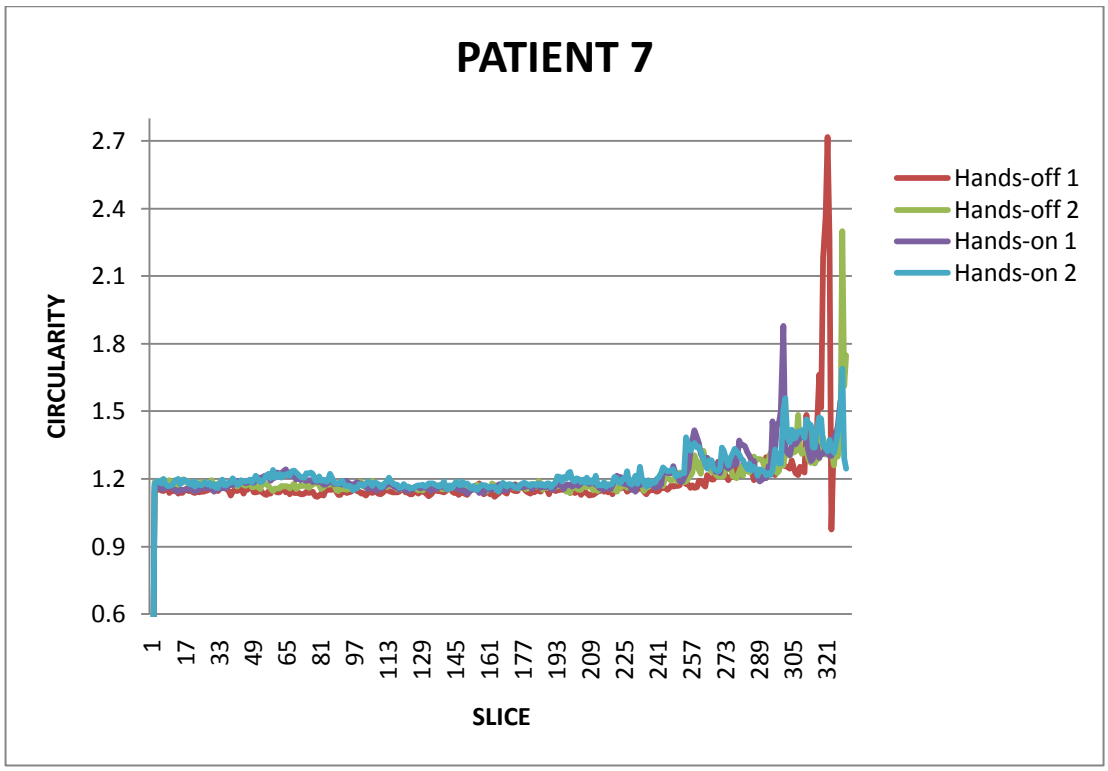

Figure 13-25: Circularity of transverse cross-section of the residual limb, amputee 7

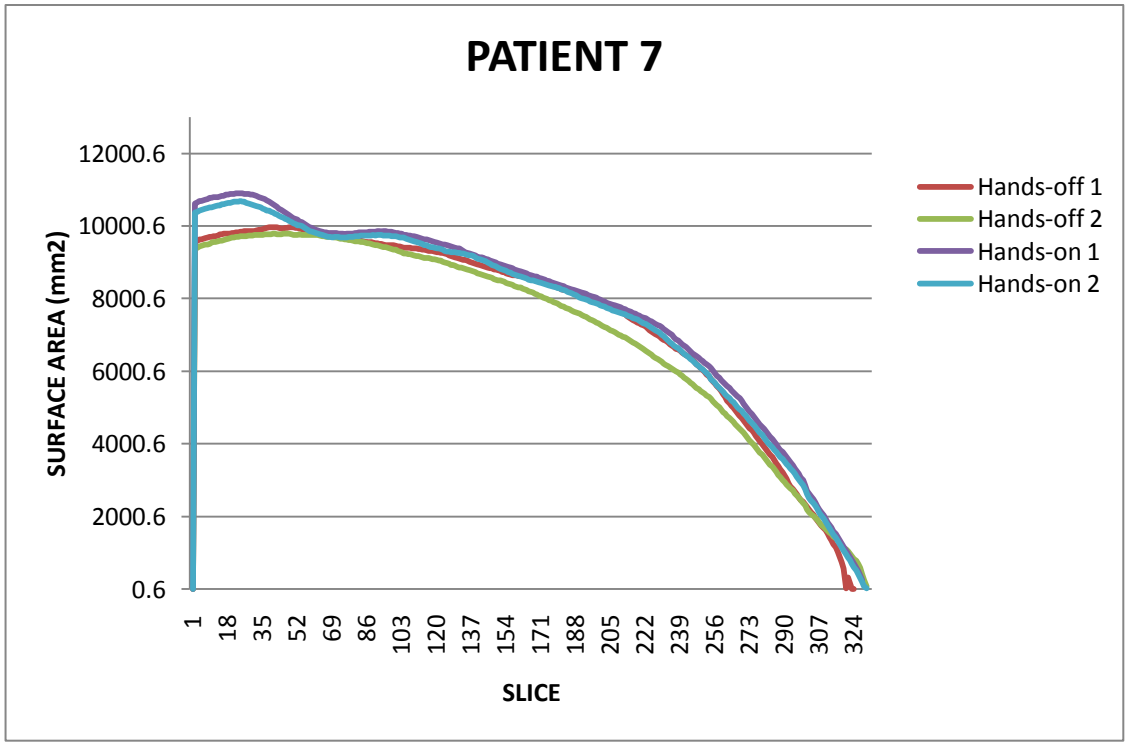

Figure 13-26: Cross sectional surface area of the residual limb, amputee 7

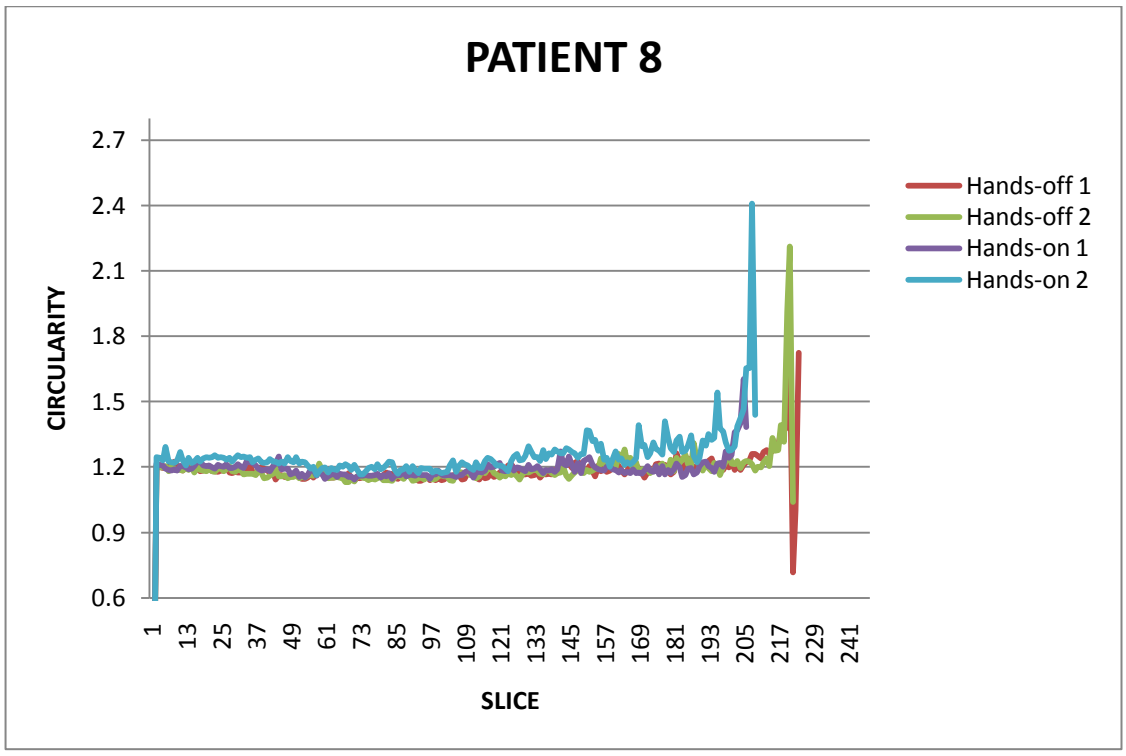

Figure 13-27: Circularity of transverse cross-section of the residual limb, amputee 8

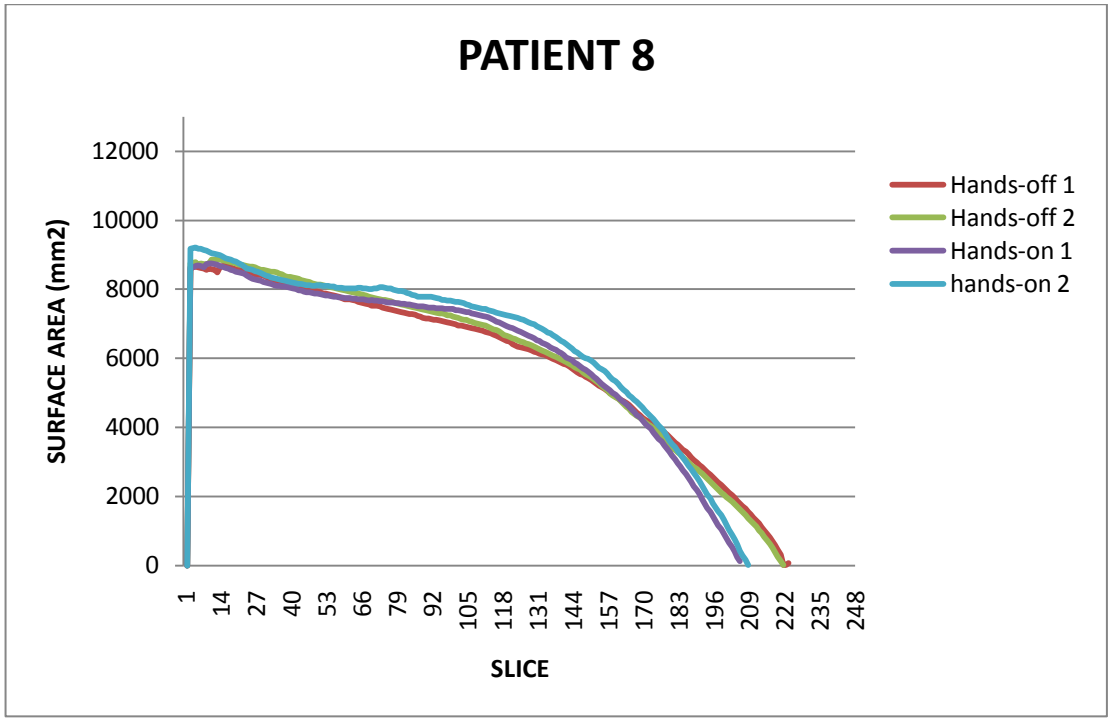

Figure 13-28: Cross sectional surface area of the residual limb, amputee 8

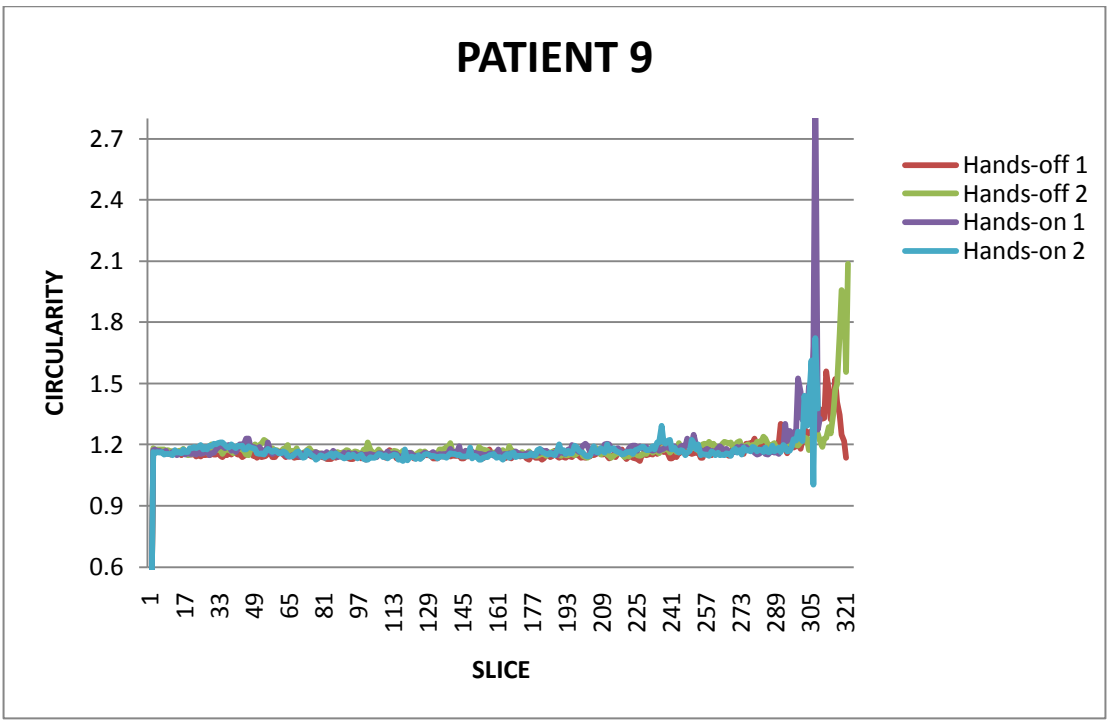

Figure 13-29: Circularity of transverse cross-section of the residual limb, amputee 8

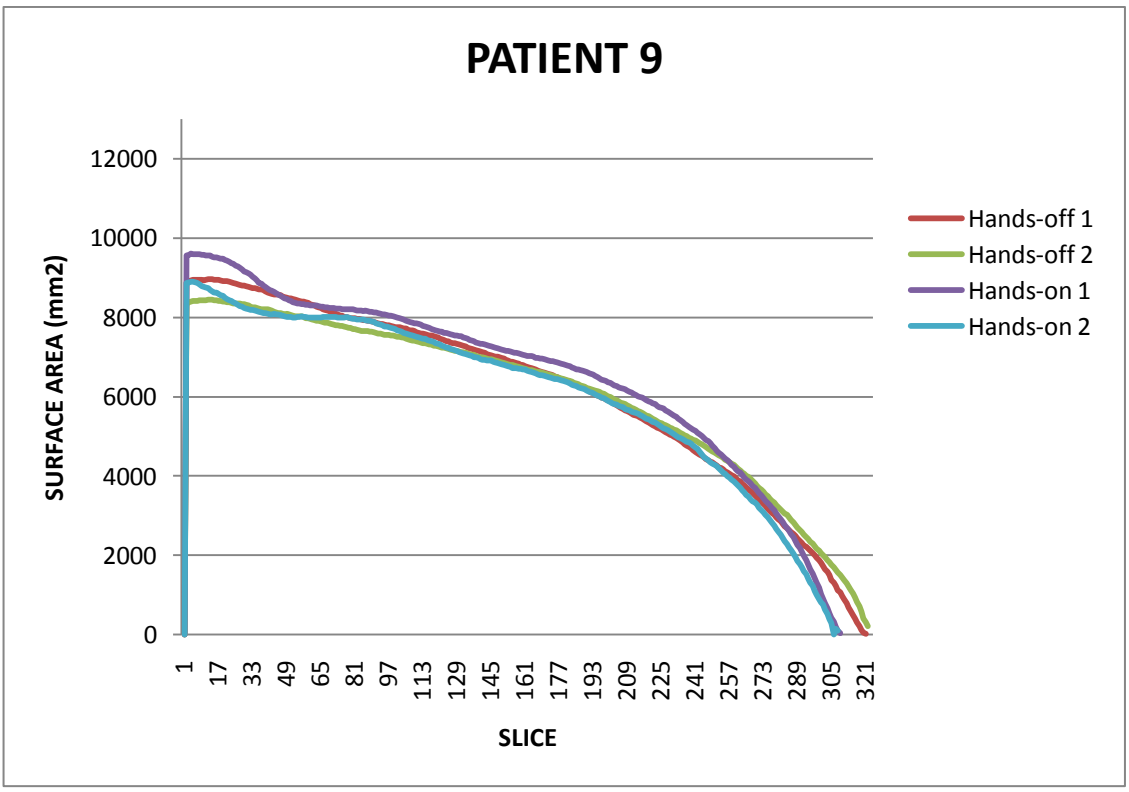

Figure 13-30: Cross sectional surface area of the residual limb, amputee 9

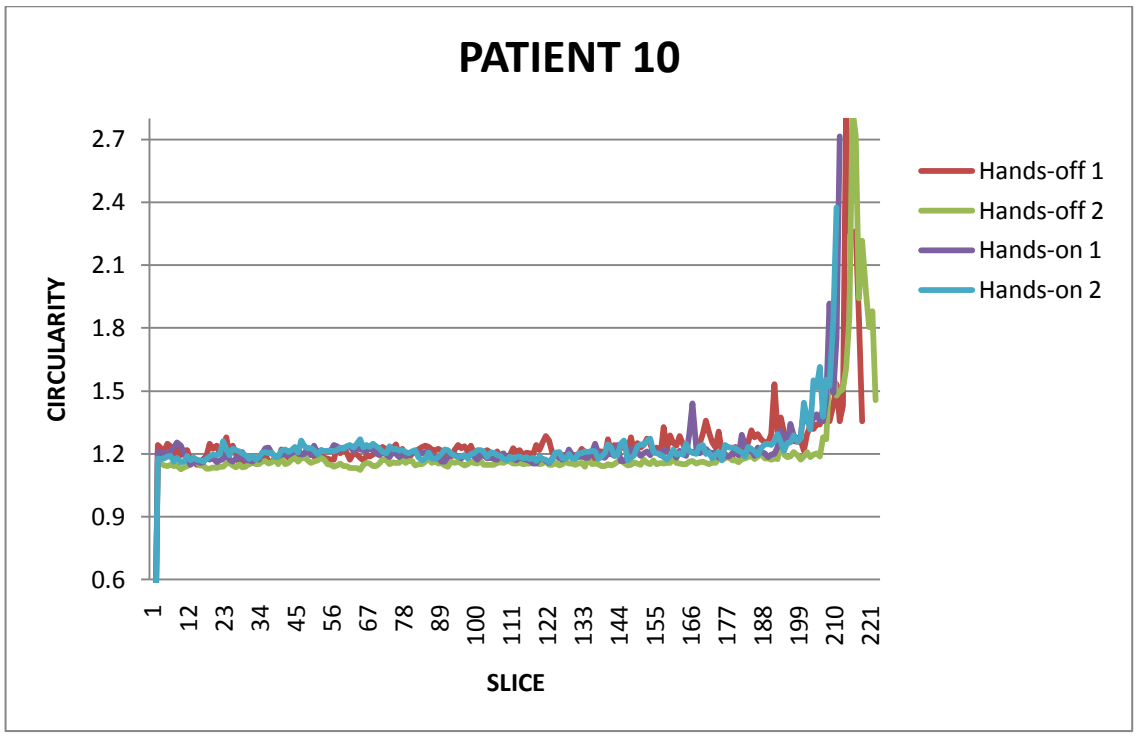

Figure 13-31: Circularity of transverse cross-section of the residual limb, amputee 10

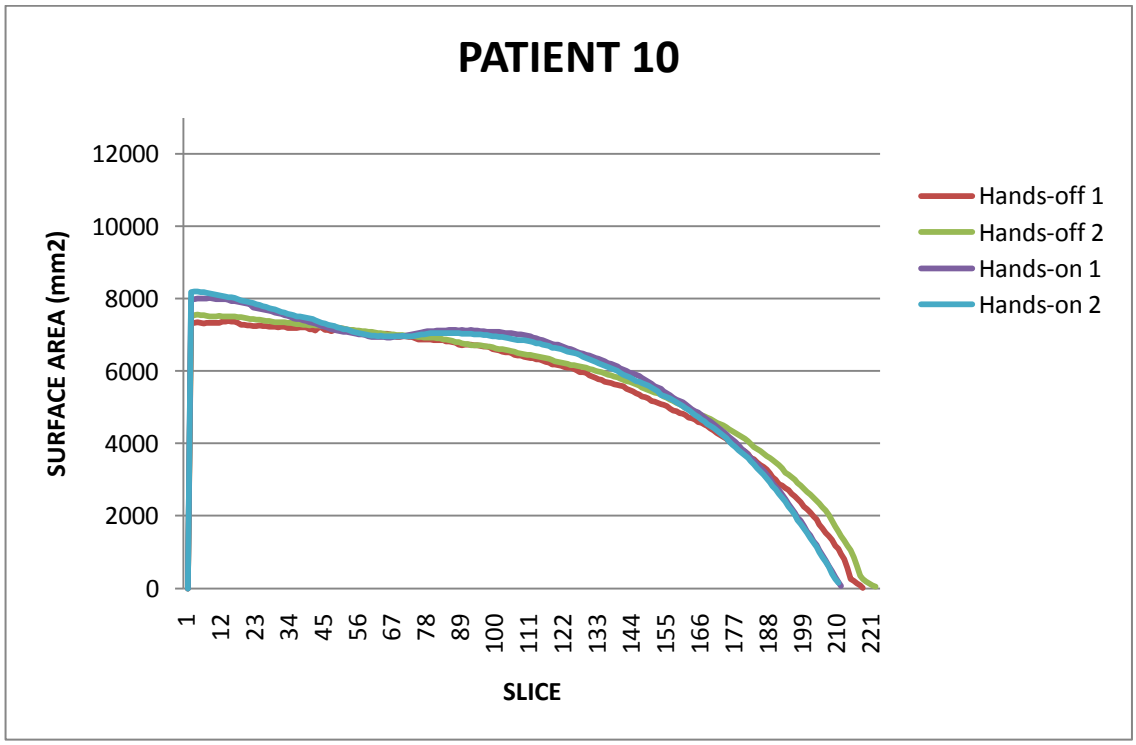

Figure 13-32: Cross sectional surface area of the residual limb, amputee 10

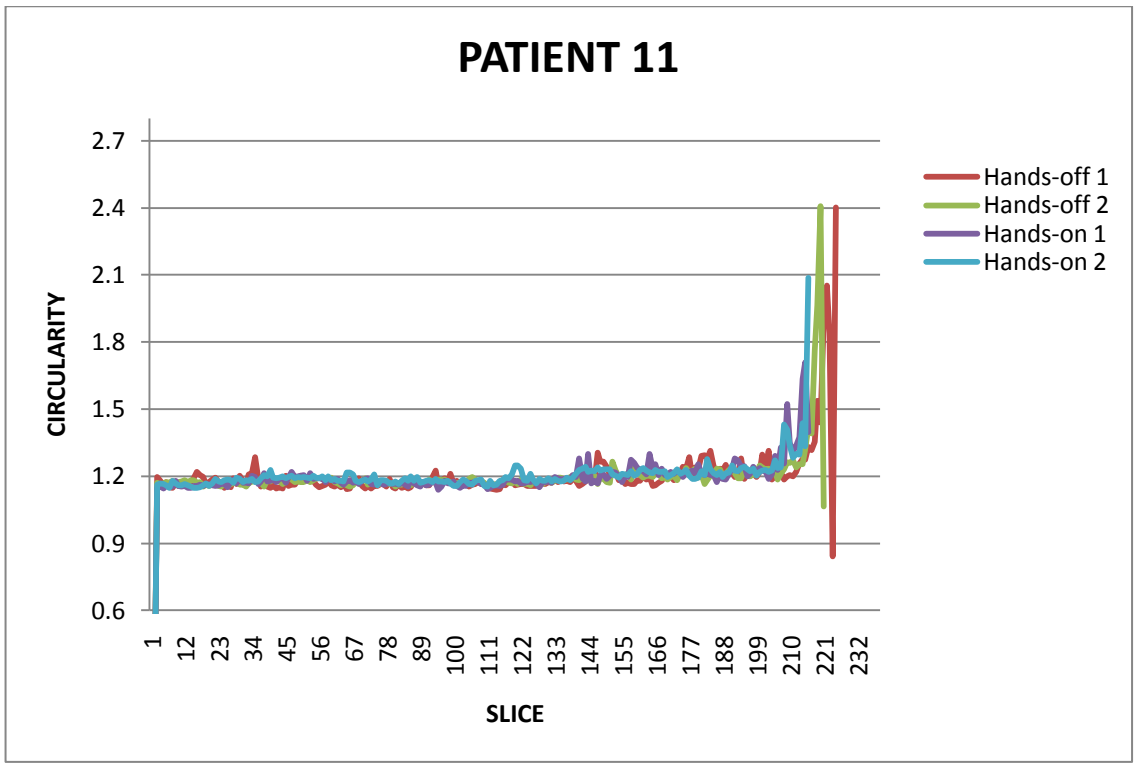

Figure 13-33: Circularity of transverse cross-section of the residual limb, amputee 11

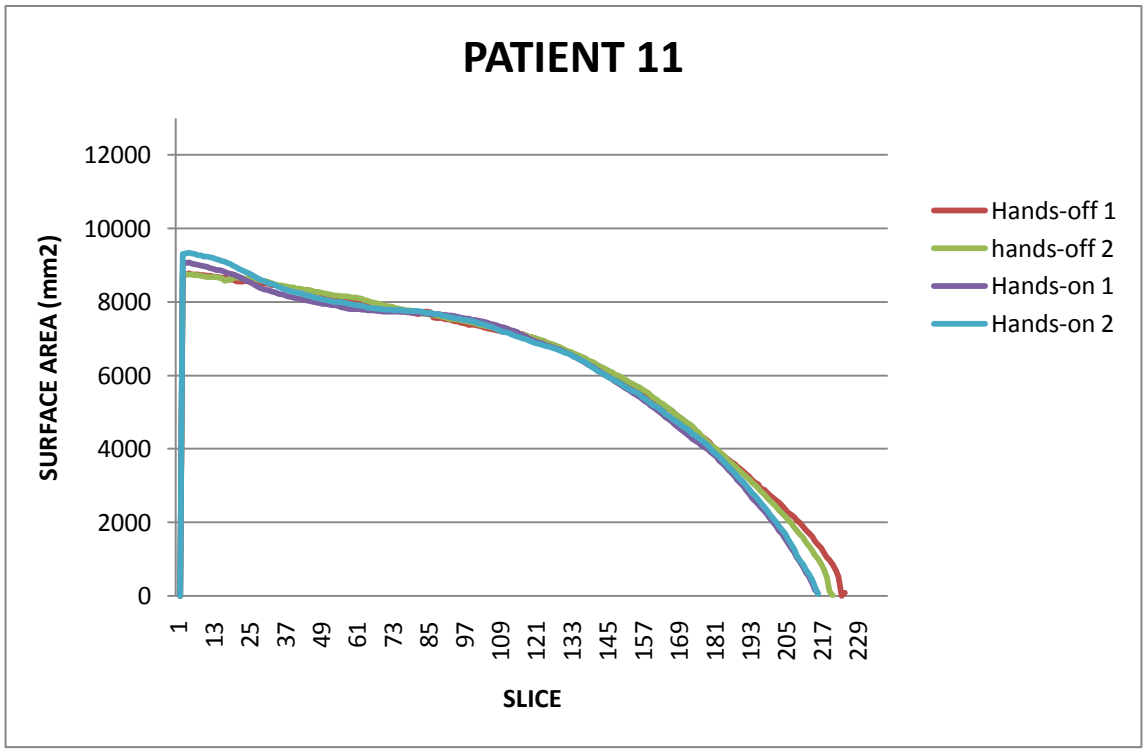

Figure 13-34: Cross sectional surface area of the residual limb, amputee 11

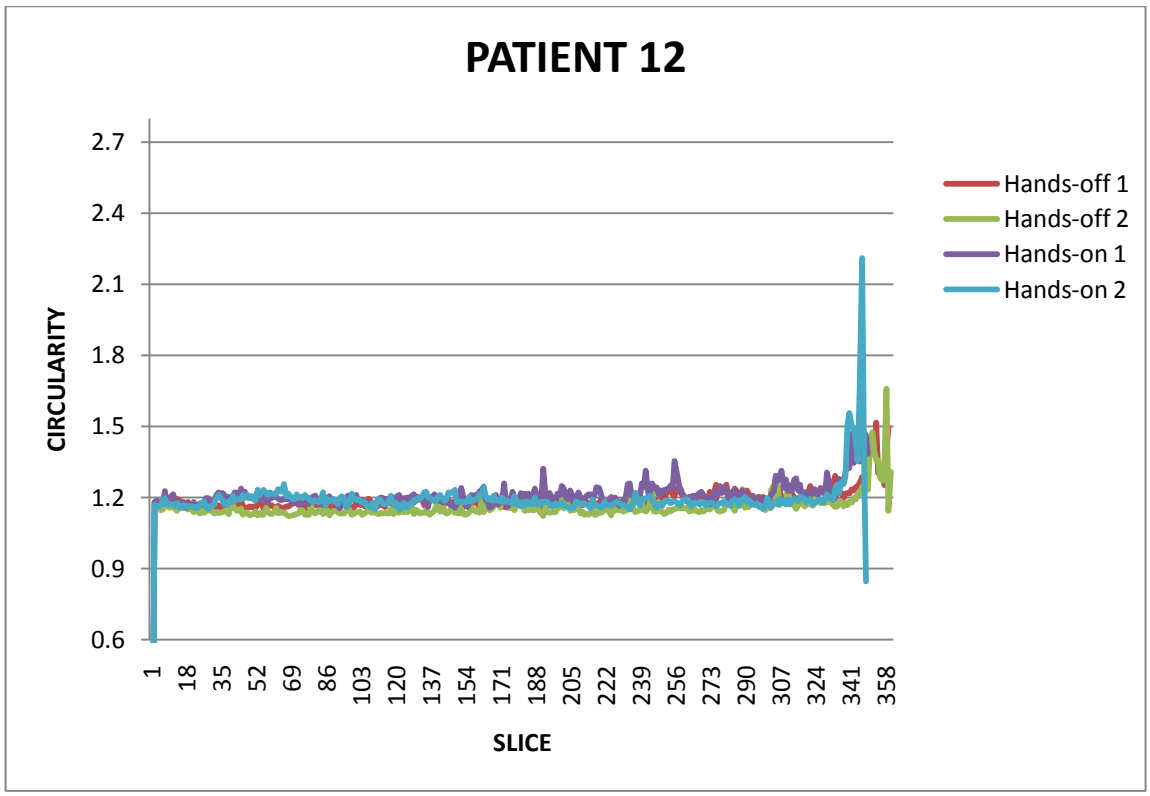

Figure 13-35: Circularity of transverse cross-section of the residual limb, amputee 12

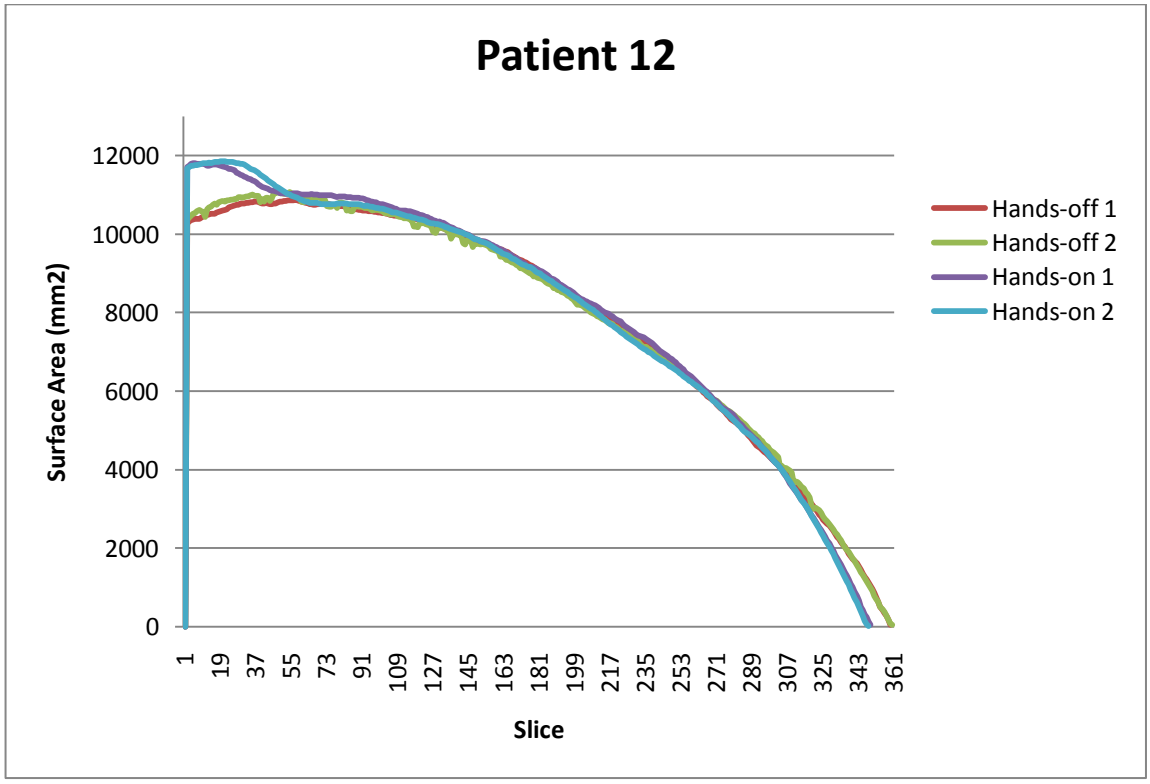

Figure 13-36: Cross sectional surface area of the residual limb, amputee 12

13.4 Research Access Letter

Acute Services Division

Research & Development Directorate
NHS Greater Glasgow and Clyde
The Tennent Institute
WIG, 38 Church Street
Glasgow
G11 6NT

NHS
Greater Glasgow and Clyde

Mr Reza Safari
PhD Student
Curran Building
University of Strathclyde
131 St James Street
Glasgow
G4 0LS

Date 03 April 2009
Your Ref SN08NE446
Our Ref DG/EC/RAL

Direct Line 0141 211 8551
Fax 0141 211 2811
Email: Emma.Cuthbertson@ggc.scot.nhs.uk

Dear Mr Safari

Greater Glasgow and Clyde Health Board, Research Access Letter

On behalf of Greater Glasgow and Clyde I am writing to provide you with a **Research Access Letter (RAL)** to enable you to work on projects and valid until 31st December 2009.

- This letter enables you to undertake research duties and you shall not be deemed an employee of the NHS Greater Glasgow and Clyde.
- You are required to comply with ICH GCP, Research Governance Guidelines, Health and Safety Act, the Data Protection Act and all Policies and Procedures implemented by NHS Greater Glasgow and Clyde.
- In the course of your duties you may have access to confidential information. This information will not be used by you for your own benefit or disclosed to a third party without the consent of the Division.
- This RAL does not come associated with payment for any costs incurred including (but not limited to) travelling expenses, library expenses and hospitality expenses.
- NHS Greater Glasgow and Clyde accepts no responsibility for damage to or loss of personal property, with exception of small valuables handed to their officials for safe custody. You are therefore strongly recommended to take out an insurance policy to cover your personal property.

If you agree to accept this appointment, please sign the slip of acceptance attached to this letter and return it to me. The original copy should be retained by you for future reference.

Yours sincerely

Dr Darren Gibson
R&D Co-ordinator

Enc. Acceptance Slip

Delivering better health

www.nhsggc.org.uk

40389

13.5 R &D Management approval and the University Sponsorship

Acute Services Division

NHS
Greater Glasgow and Clyde

Coordinator/administrator: Darren Gibson/Emma Cuthbertson
Telephone Number: 0141 211 8551
Fax Number: 0141 211 2811
E-Mail: Emma.Cuthbertson@ggc.scot.nhs.uk

R&D Management Office
Western Infirmary
Tennent Institute
1st Floor, 38 Church Street
Glasgow, G11 6NT

03 April 2009

Dr Arjan Buis
Senior Research Fellow
NCPO
Curran Building
University of Strathclyde
131 St James Road
Glasgow
G4 0LS

R&D Management Approval

Dear Dr Buis

Project Title: Socket shape and volume quantification of two distinct different prosthetic concepts by means of the establishment of a reference grid using MRI technology
Chief Investigator: Dr Arjan Buis
R&D Reference: SN08NE446
Protocol no (including version and date): version 2, dated 2nd October 2008

I am pleased to confirm that Greater Glasgow & Clyde Health Board is now able to grant **Management Approval** for the above study.
As a condition of this approval the following information is required during the lifespan of the project:

1. SAES/SUSARS – If the study is a **Clinical Trial** as defined by the Medicines for Human Use Clinical Trial Regulations, 2004 (CTIMP only)
2. Recruitment Numbers on a quarterly basis (not required for commercial trials)
3. Any change of Staff working on the project named on the ethics form
4. Change of CI
5. Amendments – Protocol/CRF etc
6. Notification of when the Trial / study has ended
7. Final Report
8. Copies of Publications & Abstracts

Delivering better health
www.nhsggc.org.uk
40389

081172

01 April 2009

University of Strathclyde
From The Secretary to the University

Dr Arjan Buis
National Centre for Prosthetics and Orthotics

University Sponsorship of Proposed Investigation Involving Human Subjects
Shape capturing consistency of two prosthetic socket concepts

On behalf of the University I advise that pursuant to the University's Code of Practice on Investigations on Human Subjects, and based on the information contained in the ethics application, the University agrees to act as sponsor of the project entitled "Shape capturing consistency of two prosthetic socket concepts" subject to the following conditions;

1. That the University Ethics Committee gives ethical approval for the project.

2. That the project is carried out according to the project protocol.

3. That the project continues to be covered by the University's insurance cover.

4. That the Director of Research and Innovation is immediately notified of any change to the project protocol or circumstances which may affect the University's risk assessment of the project.

5. That the project starts within 12 months of the date of this letter.

As sponsor of the project the University has responsibilities under the Scottish Executive's Research Governance Framework for Health and Community Care. You should ensure you are aware of those responsibilities and that the project is carried out according to the Research Governance Framework.

If you have any queries regarding sponsorship please contact Louise McKean at Research and Innovation.

Yours faithfully

Peter W A West

McCance Building
16 Richmond Street
Glasgow G1 1XQ
Direct line: 0141 548 2001
Facsimile: 0141 553 1521

Secretary to the University:
Peter W A West, OBE
DL MA DUniv DPhil
Email: p.west@strath.ac.uk
Website: www.strath.ac.uk

13.6 Patient Information Sheet

Participants Information Sheet

Measuring socket shape and volume of two different types of prosthetic sockets

Invitation to Participants:

You are being invited to take part in a research study conducted as a part of PhD qualification. Before you decide, it is important to understand why the research is being done and what it will involve. Please take time to read the following information carefully and discuss it with friends and relatives. You can also contact us if there is anything that is not clear or if you would like more information. Take time to decide whether or not you wish to take part.

What is the purpose of the study?

The way your artificial limb is fitted to your limb is an important factor in the comfort you might experience during use. The first step in manufacturing an artificial limb is to capture the shape of your amputated limb using plaster of Paris. At the moment there are two methods available to the prosthetist. However, it is not known which method produces a more consistent shape. To understand which method is better we plan to use magnetic resonance imaging (MRI) to obtain detailed images of your shin bone relative to the plaster cast.

Why have I been chosen?

This study requires twelve unilateral below-knee amputees who have been using their prosthesis for at least 6 months.

Do I have to take part?

No. It is purely voluntary. If you decide to participate, you will be given this information to keep and asked to sign a consent form. You can withdraw at any time and without the need to give an explanation. The decision to withdraw, or a decision not to take part, will not affect the standard of care you receive.

What will happen to me if I take part?

An appointment will be arranged for you at the neurology department of the Southern General Hospital in Glasgow at a convenient time for yourself and researcher. During this session a prosthetist will cast your limb four times, twice for each plaster casting method. After each application of plaster bandage you will be asked to lie in the MRI machine for 10 minutes whilst an image is taken. After each imaging your cast will be removed and you can rest for 15 minutes. Then another plaster cast, using the other casting method will be applied by the same prosthetist and images will be taken with the MRI machine. This sequence will be followed until all four scans are completed. The entire process estimated to take up to four hours in total. Due to the high cost of MRI scanning and to make each session more efficient we will involve two participants in each session, i.e. while you are being scanned the other person will being cast and visa versa.

Expenses and payments

You will be paid £19 per session and travelling expenses will be covered. If travelling by car, 40 pence per mile will be paid plus parking fee. If you travel by public transport, expenses will be covered providing receipts are available.

What do I have to do?

After you decide to take part in the study and sign the consent form, you will be sent a timetable for which you can chose the best time slot to suit you. We will send you a letter confirming your appointment and where to come.

What are the possible disadvantages and risks of taking part?

MRI is a safe imaging method and there are no known hazards to the participant, when safety protocols are followed. Because the MRI has a very strong magnetic field it is important that no metal objects will be present in the room where the machine situated.

Therefore, an extensive MRI safety questionnaire and examination by the MRI staff to ascertain that there are no hazards to you will be performed.

You will be positioned in the MRI machine as illustrated below.

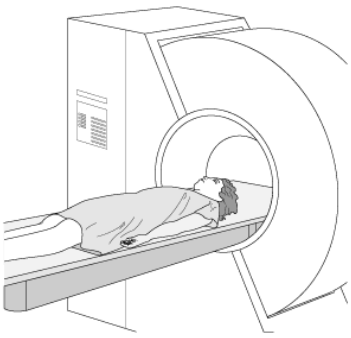

There might be a potential problem with participants who have a fear of being in an enclosed space. In the case of those who get into the magnet and then feel uncomfortable you can simply press an alarm button, given to all participants, at which point the MRI staff immediately remove you from the scanner.

The MRI also produces a loud “clicking” noise which can become uncomfortable if your ears are unprotected. For this reason all participants are provided with either earplugs or sound reducing 'headphones', which will bring the noise level down to acceptable levels.

What are the possible benefits of taking part?

The benefit of taking part would be to enhance the understanding of socket design and in the long term improve socket fit for a wider amputee population.

The only possible benefit to you personally would be in the unlikely event that the obtained MRI images of your leg would show an abnormality, with the potential to allow early intervention or treatment. If there is a suggestion of an abnormality then hardcopies of the images with the patient details removed will be produced and sent to an independent specialist who is blinded to the identity of the volunteer. If an abnormality is then confirmed, you will be informed by the researcher and advised to contact your GP.

What will happen if I don't want to carry on with the study?

You have the option to withdraw at any stage of the trial. If relevant data has already been collected through MRI scans, this will continue to be analysed, and used in the outcomes of the study. If you do not wish any data to be used in this study then all data relating to you will be destroyed.

Will my personal data obtained during this study be kept confidential?

All information which is collected about you during the course of the research will be kept strictly confidential. Any information about you which leaves the hospital/surgery will have your name and address removed so that you cannot be recognised from it.

If you need further information regarding the research please contact:-

Dr. Arjan Buis

NCPO
Curran Building 131 St James' Road
Glasgow, G4 0LS
Scotland, UK
Phone (+44) 141-548 3116
Fax (+44) 141-552 1283
e-mail: Arjan.buis@strath.ac.uk

Reza Safari

NCPO
Curran Building 131 St James' Road
Glasgow, G4 0LS
Scotland, UK
Phone (+44) 141-548 3434
Fax (+44) 141-552 1283
e-mail: m.safari@strath.ac.ukDr. Arjan Buis

If you need further information regarding the University ethical aspects of the research please contact:-

Dr Jo Edwards

Policy Officer

University of Strathclyde

0141 548 5909

jo.edwards@strath.ac.uk

13.7 Consent Form

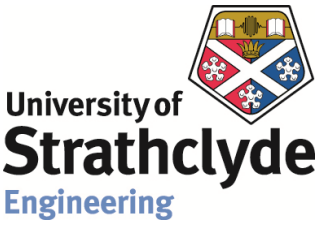

CONSENT FORM

Research Project: Socket shape and volume quantification of two distinct different socket concepts by means of MRI

PARTICIPANTS NAME……. DATE OF BIRTH…….

To be completed by the patient

☐ I confirm that I have read and understand the information sheet dated.....for the above study. I have had the opportunity to consider the information, ask questions and have had these answered satisfactorily.

☐ I understand that my participation is voluntary and that I am free to withdraw at any time without giving any reason, without my medical care or legal rights being affected.

☐ I understand that I will be informed in the unlikely event that a significant abnormality is found.

☐ I understand that I am free to withdraw from the study at any time, without having to give a reason and without affecting my medical care.

☐ I agree to take part in the above study.

Name of Patient	Date	Signature
_____	_____	_____
Name of Person taking consent	Date	Signature (if different from researcher)
_____	_____	_____
Researcher	Date	Signature
_____	_____	_____

(When completed, 1 for patient; 1 (original) for researcher site file; 1 to be kept in medical notes)

13.8 Patient Invitation Letter

Invitation to participate in a study to investigate Socket shape and volume quantification of two distinct different socket concepts by means of MRI

You are invited to participate in a research study which will be conducted in the Southern General Hospital. The objective of the research project is to compare two below-knee socket designs, namely PTB and ICECAST, in shape and volume using Magnetic Resonance Imaging (MRI). We are looking for persons with below-knee amputation who have been using prosthesis for more than 6 Months and have a residual limb with no blister or skin problem. A patient information sheet relating to the study is enclosed with this letter.

Your presence will be required on one session, lasting approximately 4 hours. Your travel costs will be reimbursed and you will also receive a modest fee for your efforts.

If you are interested in participating in this project and your answer to all question on MRI safety checklist (next page) is NO please contact the following researchers in a week from receiving this letter.

Dr. Arjan Buis

NCPO
Curran Building 131 St James' Road
Glasgow, G4 0LS
Scotland, UK
Phone (+44) 141-548 3116
Fax (+44) 141-552 1283
e-mail: Arjan.buis@strath.ac.uk

Reza Safari

NCPO
Curran Building 131 St James' Road
Glasgow, G4 0LS
Scotland, UK
Phone (+44) 141-548 3434
Fax (+44) 141-552 1283
e-mail: m.safari@strath.ac.uk

13.9 MRI Safety Checklist

If your answer to any of following is **YES** please **DO NOT** reply to this invitation.

Do you have or ever had?

A cardiac pacemaker or defibrillator or internal pacing wires

An operation on your heart

A brain aneurysm clipped or treated

A plate in your skull

Any operation in your head

A vascular clamp, coil or stent

An artificial heart valve

A bladder implant

An insulin or infusion pump

An ear implant

A pain relief implant

Any electronic implants (e.g. Neurostimulator)

Any other implants or prostheses

Metal has entered your body from an industrial accident or through military service

An eye injury or attended an eye department or had eye surgery

Working on milling or drilling machines or in the shipyards where metal may have entered your eyes

Any artificial joints or screws or pins or plates for broken bones

Suffer from fits or blackouts

Had any surgical operations in the last six weeks

Had a spinal fracture

Have permanent eye-lining

Have a contraceptive diaphragm

Have breast implant

Are you pregnant?